Biophysical and cellular insights into the membrane insertion mechanism of CLIC1

Alexandra Christina Hendry

A thesis submitted for the degree of Doctor of Philosophy

University of Kent

Department of Biosciences

2021

Foreword

Declaration

The work presented in this thesis is original and was conducted myself (unless stated otherwise), under the supervision of Dr José Luis Ortega Roldán. All sources of information have been acknowledged by means of references. None of this work has been used in any previous application for a degree.

This research was funded by a Vice Chancellor's Scholarship from the University of Kent.

Acknowledgments

To my PhD supervisor Jose, thank you for choosing me to join your lab and giving me this incredible opportunity. I am so grateful for the endless support, guidance and for every single thing you have taught me from the minute I have stepped into the CLIC1 adventure. Thank you for all the patience, amazing positivity and for filling me with all the confidence and skills to be a researcher, plus the many laughs! You provided so many learning and training experiences for me and I can never thank you enough for letting me be part of this really fascinating project.

To Lorena, for being the most amazing mentor as I nervously started in the lab. Thank you for making me laugh every step of the way and teaching me all the tips and tricks you know, turning me into a proper scientist and teaching me the word 'turbid'. Thank you both for the endless support through all hurdles no matter how large, I could never have made it without you.

To everyone who has been a part of the Ortega lab past and present I thank you for all the help, chat and putting up with me and my singing; Joe P, Bradley, Gina and Gloria. To Gary for imparting his wisdom of the NMR, for Diego teaching me all he knows about, so many things, Joe for being my PhD buddy and of course to Encarni for being the loveliest post-doc, motivating me every step of the way and letting me live with you while in Spain! You have all made my experience so fun and I thank you so much.

To Ana & Salva of the University of Granada for letting me be part of their lab for a month, teaching me all they know and helping me get some great data.

To Becky and Davey of my current lab, thank you so much for the patience and support you have given me whilst writing up my thesis. I appreciate it beyond words and love being part of your lab.

To all the lovely people in Bioscience here at Kent that have been part of my journey here thank you for all the chats and smiles. Special mention to Campbell for his advice and help whilst applying for my PhD and to Ian for the constant help and chats while doing my microscopy and to all the Fenton lab, especially Nikki & Max for imparting their cellular wisdom.

Of course, thank you to all my incredible family, for all the words of encouragement and many cups of tea. The biggest thank you to my Mum and Dad, who have been there every step of the way, always telling me to go for it and for providing me with all the tools to get here. For all the 'Come on keep goings' and hugs. I am forever thankful for everything you have done for me! To my best friends Lic, Ash & Abi for the endless "You are nearly there's" and keeping me going.

And finally thank you to my rock, my biggest cheerleader Callum, the support you have given me is indescribable and quite simply I could have never done it without you. I thank you for all the help and always will.

A special mention to Niken Pam, who I miss dearly and so wish she was completing her PhD alongside me right now.

Publications

Zec, N., Mangiapia, G., Hendry, A. C., Barker, R., Koutsioubas, A., Frielinghaus, H., … Moulin, J. F. (2021). Mutually beneficial combination of molecular dynamics computer simulations and scattering experiments. *Membranes*, *11*(7). https://doi.org/10.3390/membranes11070507

Medina-Carmona, E., Varela, L., Hendry, A. C., Thompson, G. S., White, L. J., Boles, J. E., … Ortega-Roldan, J. L. (2020). A quantitative assay to study the lipid selectivity of membrane-associated systems using solution NMR. *Chemical Communications*. https://doi.org/10.1039/d0cc03612a

Varela, L*., Hendry, A. C*., Medina-Carmona, E., Cantoni, D., & Ortega-Roldan, J. L. (2019). The membrane insertion of soluble CLIC1 into active chloride channels is triggered by specific divalent cations. *BioRxiv*, 638080. https://doi.org/10.1101/638080

Posters & Presentations

Collaborative Computing Project for NMR UK National conference, Virtual, 2020
"The membrane insertion of soluble CLIC1 into active chloride channels is triggered by specific divalent cations"
Alex Hendry, Lorena Varela-Alvarez, Encarni Medina-carmona, Diego Cantoni and Jose L.Ortega-Roldan

London NMR forum at Francis Crick Institute, London, 2019
"Combining NMR, biophysics and microscopy to understand the membrane insertion mechanism of CLIC1"
Alex Hendry

Collaborative Computing Project for NMR UK National conference, Kent, 2018
"Towards the mechanism of CLIC1 membrane insertion: CLIC1 oligomerisation"
Lorena Varela-Alvarez, Alex Hendry, Shahid Mehmood and Jose L. Ortega-Roldan

Abstract

Chloride intracellular channel 1 (CLIC1) is a human protein expressed in the cytosol that has a remarkable feature – it can transition into an active chloride channel in nuclear, endoplasmic reticulum or plasma membranes. This metamorphic nature makes CLIC1 a potential drug target as overexpression of the membrane channel form in cells is implicated in neurodegenerative disease progression and tumour proliferation especially in cancers with poor prognosis such as glioblastomas. The mechanism of CLIC1 activation and membrane insertion, as well as the oligomerisation state and structure of the channel, still remain elusive, therefore my PhD focuses on deciphering more information about how and why CLIC1 forms a chloride channel.

Combining biophysical and microscopy techniques we have discovered that, upon binding to divalent cations Ca^{2+} and Zn^{2+}, CLIC1 relocalises and inserts into the plasma membrane to form an active chloride channel in both in vitro and in vivo experiments. Previous literature heavily implicates the role of cysteine oxidation in CLIC1 channel formation but the use of solution NMR studies confirmed that both the soluble and membrane bound forms of CLIC1 are in the same oxidation state, further supporting the hypothesis divalent cations are the trigger for this translocation from a cytosolic globular protein to integral membrane chloride channel.

The identification of the molecular switch that promotes CLIC1 membrane insertion is a significant discovery as it provides a model that can enable mechanistic studies of CLIC1 translocation and structural investigation of the channel form, known to

have clinical relevance. Additional research focused on how CLIC1 interacts with divalent cations in a cellular environment aiming to elucidate information about the conformational changes the protein undergoes in vivo.

Table of Contents

List of Figures

List of Tables

Acronyms

AB	Beta-amyloid
AKT	Protein kinase B
BSA	Bovine serum albumin
CaCC	Calcium activated channels
CD	Circular dichromism
cDNA	Complementary deoxyribonucleic acid
CFTR	Cystic fibrosis transmembrane conductance regulator
CHO	Chinese hamster ovary
CLIC1	Chloride intracellular channel 1
CNS	Central nervous system
DAPI	4',6-diamidino-2-phenylindole
DDM	N-dodecyl-B-D-Maltoside
DHAR	Dehydroascorbate reductase
DIDS	Dihydro-4,4’-diisothiocyanostilbene-2,2’-disulphonic acid
DMEM	Dulbecco's modified eagle medium
DMPC	1,2-dimyristoyl-sn-glycero-3-phosphocholine
DNA	Deoxyribonucleic acid
DTT	Dithiothreitol
EDTA	Ethylenediaminetetraacetic acid
ELISA	Enzyme linked immunosorbent assay
ERK	Extracellular signal-regulated kinase
FBS	Fetal bovine serum
GABA	Gamma aminobutyric acid
GB1	Protein G B1 domain
GBM	Glioblastoma
GFP	Green fluorescence protein
GSH	Glutathione
GST	Glutathione S-transferase
GSTO	Omega glutathione S-transferase
HAH1	Human antioxidant copper chaperone

HEPES	4-(2-hydroxyethyl)-1-piperazineethansulfonic acid
HPLC	High performance lipid chromatography
IAA94	Indanyloxyacetic acid
ICP-MS	Inductively coupled plasma mass spectrometry
ILV	Isoleucine Valine
ITGa3	Integrin subunit alpha 3
ITgav	Integrin subunit alpha V
ITGB1	Integrin subunit beta 1
LAMP	Lysosomal-associated membrane protein
LB	Luria broth
MAPK	Mitogen activated protein kinase
MST	Microscale thermophoresis
NMR	Nuclear magnetic resonance
NPPB	5-nitro-2-(phenylpropylamino)-benzoate
OSCC	Oesophageal squamous cell carcinoma
PBS	Phosphate buffered saline
PC	Phosphatidylcholine
PCR	Polymerase chain reaction
PDB	Protein database
PE	Phosphatidylethanoamine
P-ERK	Phosphorylated extracellular signal kinase
PI	Phosphatidylinositol
PIPES	Piperazine-N,N'-bis(2-ethanesulfonic acid)
PMA	Phorbol-12-myristate-13-acetate
PTM	Post translation modification
RNA	Ribonucleic acid
ROS	Reactive oxygen species
SAXS	Small angle X-ray scattering
SDS	Sodium dodecyl sulfate
SEC-MALS	Size exclusion chromatography-multiangle light scattering
shRNA	Short hairpin ribonucleic acid

SOCC	Store operated calcium channel
SOD	Superoxide dismutase
STS	Sodium tanshinone sulfonate
TB	Terrific broth
TBS	Tris buffered saline
TCEP	Tris(2-carboxyethyl)phosphine
TEM	Transmission electron microscope
TEV	Tobacco etch virus
TLR	Toll like receptor
TMD	Trans-membrane domain
TPEN	N,N,N',N'-Tetrakis(2-pyridylmethyl)ethylenediamine
VRAC	Cell volume regulated anion channels
ZnPT	Zinc pyrithione

Chapter1: Introduction

1.1 The Chloride intracellular channel family

1.1.1 Discovery of CLICs

CLICs, the chloride intracellular channels, are a large family of proteins found to share an unusual feature of transitioning from cytosolic to an integral membrane chloride channel. Seven paralogues of CLIC proteins have been discovered, CLIC1-CLIC6 (Figure 1.3) (Berryman & Bretscher, 2000; Duncan et al., 1997; Friedli et al., 2003; Heiss & Poustka, 1997; Nishizawa et al., 2000; Qian et al., 1999; Valenzuela et al., 1997), with additional spliced variations of the channels such as CLIC5b a spliced variation of CLIC5 (Landry et al., 1987).

CLIC1, the human chloride intracellular channel 1, was found via screening of a monocytic cell line cDNA library and was found to be homologous to p64, a bovine chloride channel protein (Valenzuela et al., 1997). Small molecular inhibitors targeting chloride channels discovered a protein localised to both apical and intracellular membrane with a clear role in chloride channel activity, yet cloning revealed a protein sequence unlike other integral membranes, and sequence homology led to the discovery of CLIC1, first named nuclear chloride ion channel (NCC27). Localisation of transfected CLIC1 was found to be mainly nuclear but also cytoplasmic and in the nuclear and plasma membranes (Valenzuela et al., 1997). CLIC1 was found to be ubiquitous through human tissue and was found to be highly conserved across species (Valenzuela et al., 2000).

1.1.2 CLICs homology in other organisms

All members of the CLIC family are found to be highly conserved throughout vertebrates, with over 50% sequence homology to each other (Rao et al., 2017). Different organisms have been identified to possess different numbers of the protein family, such as birds and lizards both lacking CLIC1 (Littler et al., 2010). An ancient chordate CLIC protein has been identified to be highly homologous to all vertebrate paralogues suggesting this family of protein have evolved from this common ancestor (Littler et al., 2010). The protein encoded by the exc-4 gene in C. elegans was found to be an ortholog of human CLICs, demonstrating the conservation of these proteins in invertebrates also and when knocked out disrupted the formation and maintenance of the worm's membrane (Berry et al., 2003). Four homologs of CLIC were also found in plants, glutathione S-transferase (GST) proteins found to contain cysteine residues in the active site named dehydroascorbate reductases (DHAR1-4) (Dixon et al., 2002) and one in both drosophila and bacteria, with the ion channel bacterial stringent starvation protein A (SspA) first identified in *Escherichia coli* (*E. coli*) (Rao et al., 2017) and the drosophila ortholog (DmCLIC) shown to localise to the cardiac mitochondria (Ponnalagu, Gururaja Rao, et al., 2016).

1.1.3 Focusing research on CLIC1

The first protein characterised in this large family of proteins is CLIC1 and subsequently the protein my research concentrates on. The reasoning for this focus on this protein is the protein has been characterised the most of all the members of the CLIC family yet so much is still unknown of how this protein inserts as an active chloride channel even though it was first characterised in 1997 (Valenzuela et al.,

1997). In addition, the clinical relevance of this protein is clear, through its association of high tumorigenicity of cancer cells and progression of neurodegenerative disease which will be discussed in further detail in this chapter and highlights this protein as a clear candidate for research that could have therapeutic significance.

1.2 Structure of CLIC1

1.2.1 CLIC1 is a member for the glutathione S-transferase family.

CLIC1 was found to be one of six paralogues, belonging to the Glutathione S-transferase (GST) superfamily. GSTs are mainly cytosolic proteins, with human GSTs divided into 6 different classes; alpha, mu, pi, omega, theta, and zeta (Townsend & Tew, 2003), with the more abundant classes identified as alpha and mu GSTs (Dourado et al., 2008). Glutathione S-transferases are detoxifying cytosolic proteins that catalyse the conjugation of glutathione to electrophilic substances (Sheehan et al., 2001). The N-terminal domain tends to be conserved between classes of GSTs, as it contains the catalytic residue that interacts with the thiol group of glutathione. Structural comparison of many classes of GST revealed despite having low sequence homology, the structures share two distinct protein domains, with the N domain of four beta sheets and three alpha helices, generating a thioredoxin like fold (Sheehan et al., 2001). Functions of these proteins include isomerisation of maleylacetoacetate, (Fernández-Cañón & Peñalva, 1998) binding bilirubin and carcinogens (Litwack et al., 1971) and regulation of stress kinases (Adler et al., 1999); (Dulhunty, Gage, Curtis, Chelvanayagam, & Board, 2001).

Comparison of the amino acid sequences between members of the GST family and CLIC1 reveals CLIC1 is related to this superfamily, (Dulhunty et al. 2001; Harrop et al. 2001), with the percentage homology depending on the class of GST (Figure 1.1). CLIC1 is also found to include an all alpha helical C domain which is typical of GSTs (Littler et al., 2004), and an intact glutathione binding site (Harrop et al. 2001).

However CLIC proteins differ from classical GSTs by containing a self-activating cysteine, cys24, in their active site, rather than activation of the thiol group in the glutathione that binds the enzyme (Harrop et al. 2001; Littler et al. 2010).

Furthermore GSTs are known to be dimeric while CLIC1 was crystallised as a monomer (Harrop et al. 2001).

1.2.2 Omega GSTs

One class of GSTs, Omega GSTS (GSTO), is of particular interest when discussing CLIC1, as these proteins share the most homology (Figure 1.1). CLIC1 is found to closely resemble this omega class of GST proteins (Dulhunty et al., 2001), with 24% sequence homology shown, CLIC1 and GSTO display homology at the C domain of the proteins in particular (Figure 1.1).

Omega GSTS are cystosolic proteins found to convert reactive alpha-haloketones to nontoxic acetophenones in cells (Board & Anders, 2007), and human GSTO (GSTO1-1) was found to be ubiquitously expressed and demonstrates gluthathione-dependent thiol transferase and reductase activities. Omega GSTS share the canonical GST fold but in contrast to other mammalian GSTS, GSTO1-1 appears to have an active site cysteine that can form a disulphide bond with glutathione (Board et al., 2000).

1.2.3 Crystal structure of monomer and dimer

A monomeric crystal structure of CLIC1 is structurally homologous to glutathione S-transferase (Harrop et al. 2001), recognised as 1K0O in the protein database (PDB), was identified and found to dimerise under oxidation conditions (Goodchild et al.,

2009; Littler et al., 2004). Cytosolic CLIC1 is believed to have enzymatic activity and the structure of the soluble form has been identified; a completely helical C domain with a highly negatively charged proline rich loop region and a 90 residue N domain of four stranded B-sheets and three alpha helices (Harrop et al. 2001). Furthermore, the crystal structure of a completely helical dimer showed oligomerisation through the two N domains of the monomer, with complete structural arrangement forming disulphide bonds between Cys24 and Cys59 (Littler et al., 2004).

The structures are highly conserved between CLIC1 and GSTO1-1, PDB 1EEM (Figure 1.1) (Board et al., 2000), and while investigating the relationship between CLIC1 and the GST omega proteins a conserved motif Cys-Pro-Phe was found in the glutathione binding site (Figure 1.1), with the site's structure closely resembling glutaredoxin; containing a redox active cysteine that forms a disulphide bond with glutathione (Harrop et al. 2001). Various studies hypothesise that cysteine 24, in the glutathione(GSH) binding site, is the catalytic residue in CLIC1 that reduces the disulphides (Al Khamici et al., 2016; Harrop et al., 2001; Littler et al., 2004). However differences in structure are seen between GSTO and CLIC1 in the loop between Pro147 & Gln164 at the foot of the molecule and helix 9's position at the carboxyl-terminal (Figure 1.1) (Harrop et al., 2001). It is important to note that Omega GST proteins do not insert into the membrane like CLIC1 (Dulhunty et al. 2001), with alpha helix 1 in GSTO found to not have as high helical propensity as the same helix in CLIC1 (Stoychev et al., 2009). Any structural differences could point to necessary features of CLIC1 for insertion.

A

```
GSTA1_HUMAN      MAE----------KP-------KLHYF--NARGRMESTRWLLAAAGVEFEEKFIKSAEDL 41
GSTM1_HUMAN      --M----------PM-------ILGYW--DIRGLAHAIRLLLEYTDSSYEEKKYTMGDAP 39
GSTO1_HUMAN      MSGESARSLGKGSAPPGPVPEGSIRIYSMRFCPFAERTRLVLKAKGIRHEVININLKNKP 60
CLIC1_HUMAN      MAEEQ--------PQVELFVKAGSDGAKIGNCPFSQRLFMVLWLKGVTFNVTTVDTKRRT 52
                                                .    :*   .  .:

GSTA1_HUMAN      --DK--LRND---GYLMFQQVPMVEIDGMKLVQTRAILNYIASKYNLYGKD--------- 85
GSTM1_HUMAN      DYDRSQWLNEKFKLGLDFPNLPYLIDGAHKITQSNAILCYIARKHNLCGET--------- 90
GSTO1_HUMAN      -----EWF----FKKNPFGLVPVLENSQGQLIYESAITCEYLD------EAYPGKKLLPD 105
CLIC1_HUMAN      -----ETV----QKLCPGGQLPFLLYGTEVHTD-TNKIEEFLEA-VLCPPRYPKLAALN- 100
                                    :* :  .

GSTA1_HUMAN      -IKER----ALIDMYIEGIADLGEMILLLPVCPPEEKDAKLALIKEKIKNRY---FPAFE 137
GSTM1_HUMAN      -EEEK----IRVDILENQTMDN--HMQLGMICYNPEF--------EKLKPKY---LEELP 132
GSTO1_HUMAN      DPYEKACQKMILELFSKVPSLVGSFI----RSQNKEDYA-------GLKEEFRKEFTKLE 154
CLIC1_HUMAN      -PE---SNTAGLDIFAKFSA----YI----KNSNPALND-------NLEKGLLKALKVLD 141
                           :::  :        :                    ::      :  :

GSTA1_HUMAN      KVL-----------KS-----HGQDYLVGNKLSRADIHLVELLYYVEEL-DSSLISSFPL 180
GSTM1_HUMAN      EKL-----------KLYSEFLGKRPWFAGNKITFVDFLVYDVLDLHRIF-EPKCLDAFPN 180
GSTO1_HUMAN      EVL----------------TNKKTTFFGGNSISMIDYLIWPWFERLEAMKLNECVDHTPK 198
CLIC1_HUMAN      NYLTSPLPEEVDETSAEDEGVSQRKFLDGNELTLADCNLLPKLHIVQV------------ 189
                 : *                      :: **.::  *  :   :   .

GSTA1_HUMAN      LKALKTRISNLPTVKKFLQPGSPRK----PPMDEKSLE-----EARKIFRF--------- 222
GSTM1_HUMAN      LKDFISRFEGLEKISAYMKSSRFLP----RPVFSKMAV-----WGNK------------- 218
GSTO1_HUMAN      LKLWMAAMKEDPTVSALLTSEKDWQGFL--------ELYLQNS----------PEACDYG 240
CLIC1_HUMAN      -------------------VCKKYRGFTIPEAFRGVHRYLSNAYAREEFASTCPDDEEIE 230


GSTA1_HUMAN      ----------  222
GSTM1_HUMAN      ----------  218
GSTO1_HUMAN      L---------  241
CLIC1_HUMAN      LAYEQVAKALK 241
```

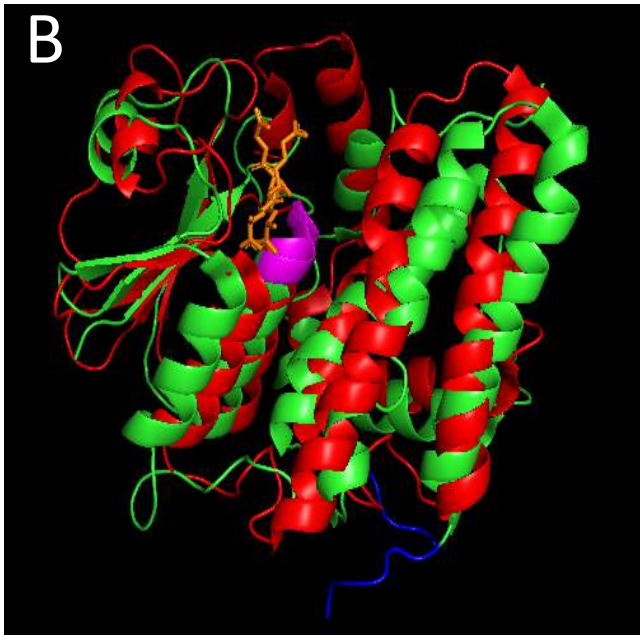

Figure 1.1 – Sequence homology map between glutathione-S-transferases and CLIC1. A) Proteins compared are Human Glutathione S-transferase A1 (GSTA1), Glutathione S-transferase Mu1 (GSTM1), Glutathione S-transferase Omega-1 (GSTO1) and CLIC1. Alignments were generated using the Clustal Omega server. "*" denotes identical residues in all sequences, ":" denotes conservative substitutions and "." denotes semiconservative substitutions. The residues are coloured according

to chemical properties; red – small hydrophobic, blue – acidic, purple – basic and green – hydroxyl/sulfhydryl/amine. The sequence alignment displayed sequence homologies for CLIC1 of 16.57%, 15.48% and 23.96% to GSTA1, GSTM1 and GSTO1 respectively.
B) Pymol superimposition of OGST1-1 (red) and CLIC1 (green) structures, with glutathione binding site for both molecules shown (orange).
Structural differences in foot loop region(blue) and shared conserved Cys-Pro-Phe motif at the active site (magenta) are both shown on pymol and by black boxes in sequence homology (Board et al., 2000; Harrop et al., 2001).

1.3 CLIC1 forms an active chloride channel

1.3.1 CLIC1 chloride conductance

Electrophysiological experiments testing the chloride conductance of CLIC1 have shown untreated CLIC1 mediates chloride conductance in lipid bilayers (Harrop et al., 2001; Warton et al., 2002), and cell membranes (Tonini et al., 2000; Valenzuela et al., 1997; Warton et al., 2002), however it is unclear through what process CLIC1 transports the chloride ions. CLIC1 was shown to have active chloride channel activity in chinese hamster ovary (CHO) cell membranes, both plasma and nuclear (Tonini et al., 2000; Valenzuela et al., 1997, 2000), with slow conductance kinetics hypothesised to be assembly of subunits to form a channel of high conductance with fast kinetics (Warton et al., 2002). Similar channel conductance was seen in CHO membranes to Phosphatidylcholines (PC) lipid bilayers (Warton et al., 2002) and electrophysiological characteristics between channels in the nuclear membrane and plasma membrane were indistinguishable (Tonini et al., 2000).

1.3.2 Membrane localisation of the CLIC1 channel.

The proven ability of CLIC1 to form a chloride channel is clear and the different membrane this protein inserts into in the context of a mammalian cell have been investigated. CLIC1 has shown to localise to the plasma membrane of different mammalian cells, for instance in Chinese hamster ovary (CHO) cells (Warton et al., 2002), human macrophage (Tang et al., 2017) and microglial cells (Milton et al. 2008). However the plasma membrane is not the only membrane in cells CLIC1 can form an active channel in, with the protein shown to include the nuclear localisation signal KKYR (Gururaja Rao et al., 2018), and outer nuclear envelope CLIC1 channel

activity seen (Valenzuela et al., 1997). Furthermore to endoplasmic reticulum localisation (Ponnalagu, Rao, et al., 2016), the mitochondrial membrane is associated with CLIC1 channel formation as shown in human osteoblastic cells (Yang et al., 2009). These studies prove CLIC1 localisation is not limited to the plasma membrane and CLIC1 has the suitability to localise to many intracellular membranes to form an active chloride channel.

1.3.3 Importance of other chloride channels in mammals.

Chloride channels are of vital importance in mammalian cells with most cell types being able to demonstrate that chloride ions are actively transported across the membrane to maintain electrochemical equilibrium. For instance chloride ions in epithelial cells control fluid secretion by allowing passive diffusion of the ions out of the cell (Duran et al., 2009), and neuron channels permeable to chloride ions can reduce neuron maturity and excitability when activated by the neurotransmitter y-aminobutryic acid (GABA) (Ben-Ari et al., 2007). There are many forms of characterised chloride channels besides the CLIC proteins, all of which can be activated via different mechanisms; those include calcium activated channels (CaCC), cAMP activated channels such as the cystic fibrosis transmembrane conductance regulator (CFTR), cell volume regulated anion channels (VRAC) and ligand gated channels such as those described above controlled by GABA. Chloride ions can be pumped into the cell via Na/K co-transporters and effluxed via cotransporters or sodium dependent, carbonate exchange channels. This extensive network of different chloride channels shows the importance of the intricate control of chloride

ions concentration within a cell and highlights how the CLIC family may play a role and presents the question by which mechanism is their activity controlled.

When chloride channels malfunction there can be severe implications within cells than can lead to disease phenotypes. For example, defects of the CFTR range from impaired protein synthesis, reduced plasma membrane expression, abnormal gating or conductance of the channel, to incorrect folding of the protein, which can all lead to cystic fibrosis, a fatal lung disease (Mall & Hartl, 2014). Myotonia congenita, a genetic defect in the skeletal muscle ClC-1 chloride channel causes progressive muscle dysfunction throughout the human body (Jeng et al., 2020). CLIC1 is no exception to this rule, however it is the upregulation of the protein that is heavily implicated in disease as sections below will describe.

1.4 The mechanism of CLIC1 channel insertion

1.4.1 Channel configuration of CLIC1

The configuration of CLIC1 as a membrane channel remains unsolved, however experiments that used antibody tagged CLIC1 saw a reduction in chloride conductance activity, with the amino terminal exposed extracellularly and the carboxyl group facing inwards (Tonini et al., 2000). Experiments investigating CLIC1s channel conformation so far have revealed the protein spans the membrane an odd number of times with the C terminus on the cytoplasmic side, with a putative transmembrane domain; the redox active site of the N domain (Figure 1.2) (Harrop et al. 2001). This transmembrane domain contains a positively charged C terminus and is hypothesised to be disrupted to allow the protein to form a channel.

1.4.2 Structural rearrangement to form the chloride channel

The structural information of how CLIC1 oligomerises and changes structural conformation is limited and an area of research my PhD sought to investigate. Helix 1 and beta-strand 2 of the monomeric structure of CLIC1 (Harrop et al. 2001) is hypothesised to undergo complete structural rearrangement to form the transmembrane helix.

The N domain of the protein has highly conserved residues of GST proteins for the glutaredoxin-like binding site; such as the Cys-Pro-Phe/Ser-Ser/Cys motif in helix1 (Figure 1.1, 1.2 & 1.3), a proline at position 65 and aspartate at residue 76 and the cysteine at position 24 is likely to be the reactive thiolate (Harrop et al. 2001). Conserved sequences of transmembrane helices were compared to CLIC1 and the protein was found to contain the typical pattern; 10 non-polar central amino acids

with seven surrounding residues with more polar characteristics and a highly conserved phenylalanine at position 26 and 41 (Figure 1.2) (Harrop et al. 2001). This putative transmembrane helix is hypothesised through sequence analysis (Figure 1.3) of all CLIC proteins, to be between Cys24 to Val46, helix1 and B-strand2 in the soluble structure, with Arg29 and Lys37 thought to line one face of the helix (Figure 1.2) (Harrop et al. 2001). In C. elegans a conserved 55-amino acid sequence allows CLIC homolog, EXC-4, to translocate from the cytosol to the lumenal membrane and deletion of the beta-sheet 2 resulted in strong cytosolic localisation within the worms (Berry et al., 2003). Mutations of CLIC1, in both cysteine residues at position 24 and 59 (Figure 1. 2), were found to prevent oligomerisation of the protein from monomer to dimer in gel filtration experiments compared to wild type CLIC1 (Littler et al., 2004) and mutation of the highly conserved leucine 46 in helix a1 also shows disruption of membrane localisation in C. elegans (Berry et al., 2003) Trp35 is also proposed to lie in the putative transmembrane domain of CLIC1 and quenching studies revealed the monomer, both oxidised and reduced, to be more accessible to the aqueous phase than the oxidised dimer, however in the presence of lipid a reduction in accessibility to the aqueous phase was only seen with the oxidised monomer and dimer. The data implies Trp35 is located deep within the bilayer (Goodchild et al., 2009).

Due to the sequence of the transmembrane domain(TMD) residues in CLIC1, the soluble structure is hypothesised to contain a hydrophobic surface patch, interestingly not found in Omega GST proteins (Harrop et al. 2001).

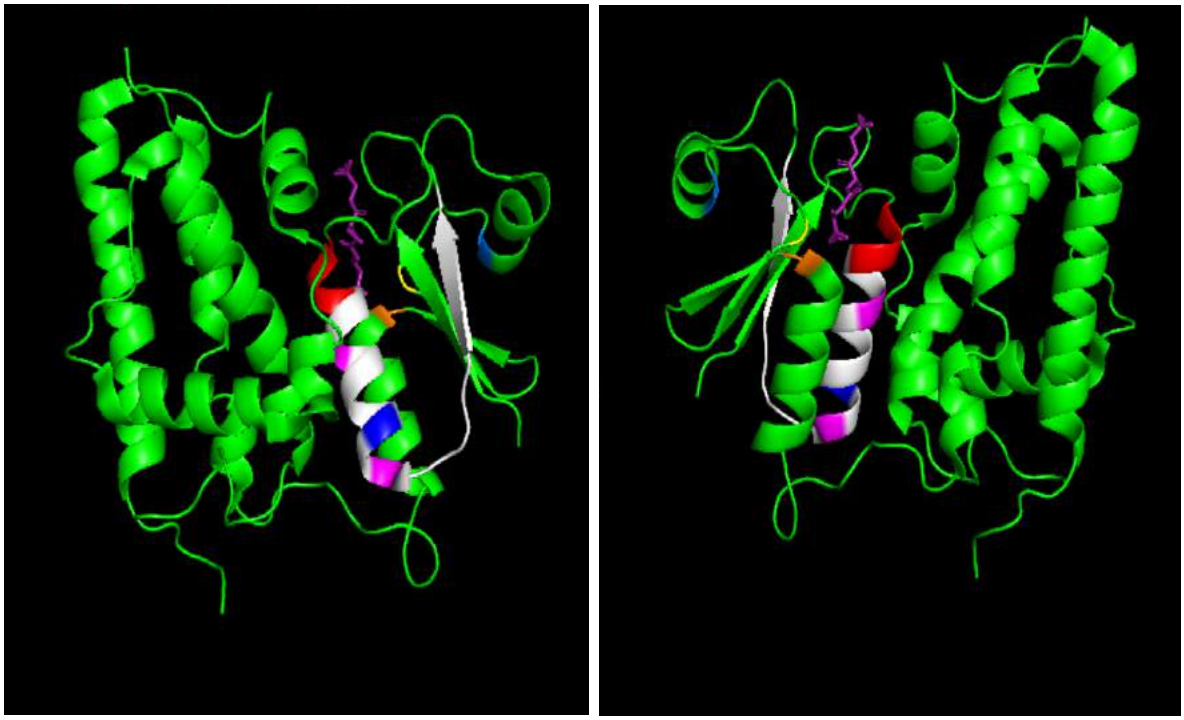

Figure 1.2 – Two views of the Pymol structural model of monomeric CLIC1 with key residues hypothesised to be involved in conformational change into the chloride channel highlighted. Putative transmembrane domain (white), including conserved CYS-PRO-PHE motif (red). Key residues of importance are as follows; Arg29 & Lys37 (Pink), Trp35 (Blue), Pro65 (Yellow) and Cys59 (Light blue). Bound glutathione (GSH) is shown in purple.

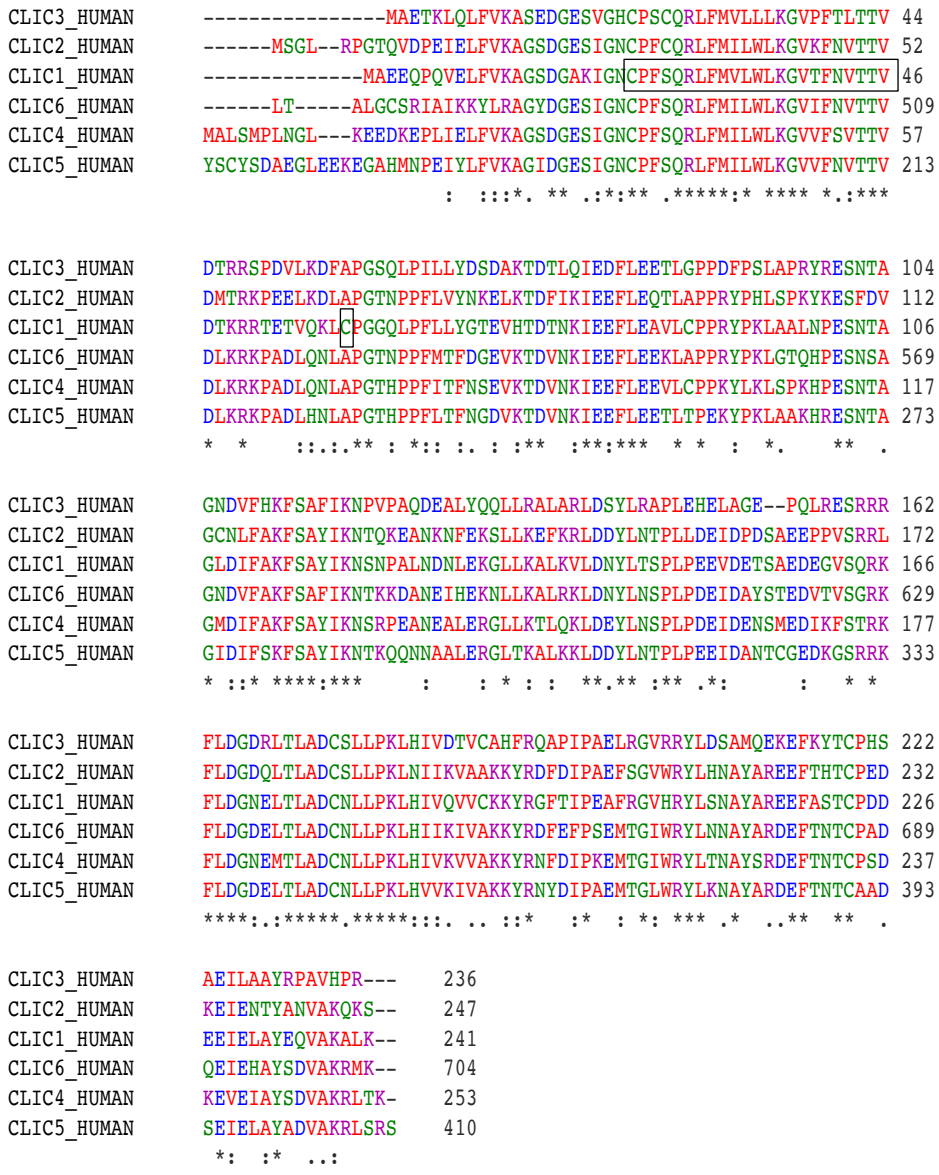

Figure 1.3 – Sequence homology map between members of the CLIC family, CLIC1-CLIC6. Putative transmembrane domain and hypothesised reactive Cys59 are highlighted by a black box. It is important to note CLIC5 and CLIC6 have an additional N-terminal domain to the other CLIC proteins (Littler et al., 2010)**.** Alignments were generated using the Clustal Omega server. * denotes identical residues in all sequences, : denotes conservative substitutions and . denotes semiconservative substitutions. The residues are coloured according to chemical properties; red – small hydrophobic, blue – acidic, purple – basic and green – hydroxyl/sulfhydryl/amine

The sequence alignment displayed sequence homologies for CLIC1 of 60.17%
50.85%, 66.39%, 62.66% and 61.83% for CLIC2, CLIC3, CLIC4, CLIC5 and CLIC6 respectively.

1.5 Trigger for CLIC1 membrane insertion

1.5.1 Oxidation triggers CLIC1 channel formation

Various studies have linked the oxidation of CLIC1 monomer with oligomerisation of the protein to a dimer, and therefore hypothesises the role of oxidation in insertion to the membrane (Figure 1.4).

Gel filtration of the recombinantly expressed protein saw a predominantly monomeric solution of the protein with some dimer present and after incubation with H_20_2 a shift in the equilibrium towards dimer was seen, with reducing conditions to the original solution making no difference (Littler et al., 2004).

Electrophysiological studies showed chloride conductance of monomer and oxidised dimer samples of protein and an increase in percentage of channel activity with untreated monomer and dimer samples compared to reduced channel formation and a lack of channel activity with either oligomer of CLIC1 with reducing agent DTT (Littler et al., 2004).

Further experiments were carried out investigating the role of oxidation on the protein. Vesicle sedimentation assays looked at how effectively the monomer and dimer bound to membrane and it was clear when monomer was treated with H_20_2, shifting equilibrium to dimer, a higher percentage of CLIC1 bound to the vesicles. However, when measuring initial binding of an oxidised dimer against monomer of CLIC1, the oxidised dimer demonstrated less binding to the membrane (Goodchild et al., 2009). A similar pattern of results is observed with bromide quenching studies of Trp35, where the oxidised monomer shows the greatest interaction with the membrane (Goodchild et al., 2009).

A model for how CLIC1 inserts into the membrane was generated from these experiments, showing oxidation as the key for dimerisation, which can promote membrane docking of the dimer for then, through an unknown mechanism, insertion of the protein into the membrane before oligomerisation as a channel (Figure 1.4). This has been the hypothesised method of CLIC1 insertion throughout many years of literature (Littler et al., 2010).

1.5.2 CLIC1 insertion may be more complex than just oxidation of the protein

There are still many unknowns with how CLIC1 oligomerises and forms a channel and there are some concerns to be raised around the data already in literature. Oxidation is implied to be essential for transition of CLIC1 from monomer to integral channel form by Littler (Littler et al., 2004), but upon further investigation the data implies instead that the soluble monomer in non-reducing conditions has the potential for channel activity while oxidation leads to dimer formation, which is seen in the crystallised structural model. Other studies of CLIC1 also see insertion of the protein, even in buffer containing the reducing agent TCEP (Valenzuela et al., 2013). The dimerisation of the GST proteins also show little resemblance to the oxidised dimer of CLIC1 (Littler et al., 2004) and the second cysteine shown to be essential for dimerisation Cys59 is not conserved in other CLIC proteins (Littler et al., 2004) (Figure 1.3). As Cys59 is not found in the other members of the CLIC family, these proteins must dimerise via a different mechanism and could question whether Cys59 is essential for the dimerisation of CLIC1 either. More recently, other possible triggers for CLIC membrane insertion has been explored, which are discussed below.

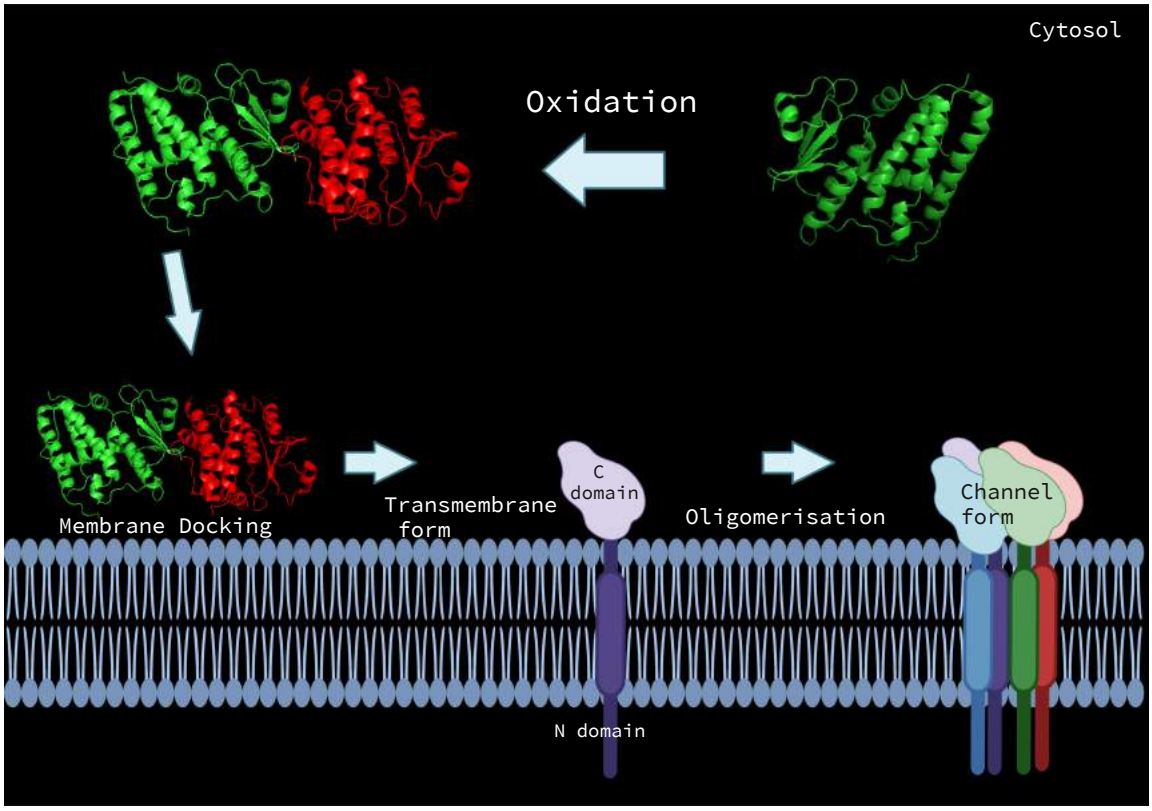

Figure 1.4 – Hypothesised membrane insertion model for CLIC1. Model shows dimerisation of the protein upon oxidation, allowing the protein to interact with the membrane before an unknown mechanism causes CLIC1 insertion and oligomerisation. (Littler et al., 2010)

1.5.3 Low pH is the trigger for channel formation

pH was perceived to be implicated in the structural rearrangement of CLIC1, with hypothetical pH sensor residues proposed. Mutations in both Glu85 & Glu228 of the protein was demonstrated to decrease the conformational stability of the protein but the structure of the protein was found unchanged (Cross et al., 2015). Rapid hydrogen exchange experiments indicated the proteins core structure remains unchanged at both low and neutral pH but conformationally becomes more flexible. Domain 1 of the protein, consisting of alpha helices 1-3 and beta sheets 1-4, was found to be less stable than domain 2 made of helices 4-10. Alpha helix 1, part of the putative TMD, is found to be intrinsically stable so likely retained in the membrane

structure, while beta strand 2 has propensity to form a helix. Alpha helix 1 was found to become partially unfolded in an acidic environment exposing a hydrophobic surface, which could suggest a lower energy barrier for membrane insertion at a low pH (Stoychev et al., 2009).

Electrophysiological studies showed that at lower pH the time taken to see a small conductance of chloride channel activity decreased (Warton et al., 2002), and acidic pH was shown to increase the open channel probability of SspA in *E. coli* (Rao et al., 2017).

In addition, CLIC1 was first cloned from macrophages (Valenzuela et al., 1997) and in these cells a physiological link between CLIC1 and pH was discovered. Resting macrophages had punctate cytoplasmic CLIC1 localisation, while activation of the macrophages for phagocytosis resulted in CLIC1 insertion into the phagosomal membranes (L. Jiang et al., 2012). During phagosomal maturation, acidification of the phagosome interior usually occurs as it is required for microbicidal capabilities (Hackam et al., 1999). However when CLIC1 is knocked down in mice there is a resultant defect is phagosomal acidification and consequences of this elevated pH include decreased phagosomal proteolytic activity (L. Jiang et al., 2012).

1.5.4 Lipid composition can affect CLIC1 insertion

Active channels have been shown to form in lipid bilayers; phosphatidylcholine (PC) lipids with cholesterol (Goodchild et al., 2009; Littler et al., 2004; Valenzuela et al., 2013), as well as CHO mammalian cell membranes, which are made up predominantly of PC.

The lipid environment, and the percentage of cholesterol was thought to play a role and studies carried out in lipid bilayers demonstrated a higher chloride conductance as the percentage of cholesterol in the membrane was increased. Pre-incubation of the protein in the absence of cholesterol also decreased the channel conductance, indicating a potential role of cholesterol in CLIC1 forming a channel. The protein was also shown to change structural orientation in the presence of cholesterol by inserting within phospholipid acyl chains of the phospholipid monolayer (Hossain et al., 2017).

1.5.5 Divalent cations interaction with ion membrane channels

My research will explore the different triggers for membrane insertion and concentrate on the novel hypothesis of divalent metal binding. Some of the insertion assays of CLIC1 into a membrane channel in literature were carried out in the presence of calcium and other divalent cations. Furthermore calcium signalling has previously been implicated in the exocytosis of CLIC1 in secretory vesicles from mammalian cells (Thuringer et al., 2018) and CLIC1 knock out in lung cancer cells affected intracellular basal calcium and ROS levels, suggesting some interplay between the intracellular metal levels and the protein (J. R. Lee et al., 2019). Calcium activated chloride channels have also been identified (Berg et al., 2012); such as chloride channels found in excitable mammalian cells that are activated by an increase in intracellular calcium concentration (Large & Wang, 1996).

Zinc has also been shown to have a modulatory effect on the formation of ion channels; including potassium, sodium and calcium channels (Noh et al., 2015). Some examples include the ability of zinc to change the opening of potassium channels in

mammalian cells (Anumonwo et al., 1999), the competitive inhibition of store operated calcium channel (SOCC) calcium channels (Gore et al., 2004) and the activation of epithelial sodium channel activity by zinc (Sheng et al., 2004). In regards to chloride channels, zinc signalling has been shown to modulate the voltage gated ClC-0 channel cloned from an electric fish (Chen, 1998).

1.6. The role of CLIC1 in cancer

1.6.1 CLIC1 regulates the cell cycle

CLIC1 is hypothesised to have a role in cell cycle regulation. Different experiments provide evidence for this, with CLIC1 chloride channel activity in CHO cells changing throughout cell cycle progression with the highest activity when the cells had a round phenotype (G2/M phase) and were undergoing mitosis. In comparison cells had very low channel conductance when in the G1/S phase of the cell cycle (Valenzuela et al., 2000). Treatment of cells with inhibitors of CLIC1 conductance have been shown to arrest the cell cycle (Peretti et al., 2018; Valenzuela et al., 2000), indicating that CLIC1 conductance is vital for cell cycle progression, not just a product of the process (Valenzuela et al., 2000). It is hypothesised during mitosis the nuclear envelope disassembles and this may release the nuclear localised CLIC1 into the cytoplasm, allowing for more insertion of the protein into the plasma membrane (Figure 1.5) (Valenzuela et al., 2000).

In oesophageal sarcoma cells, CLIC1 was silenced and it was shown that the cells transfected with the protein were in higher number at the sub-G1 phase compared to control cells, providing more evidence for the role of CLIC1 in cell cycle management and the proliferation of cancer cells (Kobayashi et al., 2018).

1.6.2 CLIC1 expression in cancer cells

Clinicopathological correlation with CLIC1 expression is seen in many cancer forms. Higher CLIC1 expression was seen in patients in later stages of Gastric cancer (B. P. Li et al., 2018) and high grade ovarian cancers had higher CLIC1 levels compared to low grade tumours (Yu et al., 2018). In addition higher expression of CLIC1 saw shorter

overall survival and progression free rates in ovarian cancer compared to patients with lower CLIC1 expression, therefore leading to poorer prognosis in patients with higher levels of CLIC1 (Yu et al., 2018). Staining of lung adenocarcinoma cells also displayed a correlation between CLIC1 expression levels and T staging of tumours with staining seen in the nucleus and cytoplasm of the cancer cells (Wang et al. 2011) and high expression of CLIC1 in the lung adenocarcinoma led to a statistically different reduced 5 year overall survival rate compared to low expression tissue (Wang et al. 2011). Again CLIC1 expression was shown to be significantly different in different stages of the cancer, in this case pancreatic cancer. In pancreatic cancer the average overall survival time in patients with CLIC1 expression was significantly lower than in those patients without (Lu et al., 2015) and differences in positive CLIC1 expression are seen in the histological grade and tumour size of pancreatic cancer patients with poorly differentiated tissues and the largest tumours having the highest expression of the protein (Jia et al., 2016). Furthermore, there was also clear correlation with patient survival time with those that survived less than 1 year having significantly higher CLIC1 expression and those patients who were CLIC1-negative having significantly higher average survival times (Jia et al., 2016).

CLIC1 protein expression differed in histological grades of oral squamous carcinomas (OSCC), with large tumour size positively correlated with CLIC1 expression. The mean survival time in CLIC1 positive cancer patients was also significantly lower than those who were negative for CLIC1 (Xu et al., 2018) ELISA assays were performed in patients with OSCC which revealed CLIC1 expression was significantly higher in these patients compared to the blood of healthy controls, with the highest levels seen in patients with late stage cancer. After treatment with resection and chemotherapy the levels

of CLIC1 in the plasma were statistically lower (Xu et al., 2018). Healthy tissue of patients with merkel cell carcinoma were shown to express lower levels of the CLIC1 protein compared to the cancerous cells (Stakaityte et al., 2018).

Immunohistochemical staining of many cancer tissues revealed clear cytoplasmic, nuclear and plasma membrane localisation of CLIC1 with the localisation varying between cancer type and the grade of the tumour with no identifiable pattern (Feng et al., 2019; Jia et al., 2016; Kobayashi et al., 2018; Lu et al., 2015; Nesiu et al., 2019; Qu et al., 2016; Xu et al., 2018; Zhang et al., 2015).

CLIC1 is a clear risk factor for many types of cancer and can be used as a biomarker for disease prognosis, the protein levels also seem to correlate with tumour size and highlight the role of the protein in cancer growth.

1.6.3 CLIC1 & tumour growth

CLIC1 expression levels are shown to correlate with differences in tumour growth rates in many different cancer types. For instance, two human pancreatic cell lines revealed that the downregulation of CLIC1 inhibited viability of the cells over time and the number of colonies decreased compared to the control cancer cells (Lu et al., 2015). Oral squamous cell carcinoma (OSCC) cells with CLIC1 knocked down and overexpressed, displayed significantly decreased and increased cell viability respectively compared to control cancer cells (Feng et al., 2019) and oesophageal squamous cell carcinoma cell lines were shown to express CLIC1, with silencing of CLIC1 resulting in significantly lower cell numbers after 72 hours growth (Kobayashi et al., 2018) In an ovarian carcinoma cell line a knockdown for CLIC1 by short hairpin

RNA (ShRNA) lentiviral transfection, saw significantly slower cell growth against an empty vector control (Qu et al., 2016).

Furthermore when studying tumour growth models in mice, gastric cancer (B. P. Li et al., 2018), OSCC (Feng et al., 2019) and ovarian cancer cells lines (Qu et al., 2016) all revealed slower growth and smaller tumour mass when CLIC1 had been silenced compared to control cancer cells. Together, these many examples of cancer cell lines reveal the positive correlation of CLIC1 with enhanced tumour growth.

1.6.4 Metastasis and invasion correlation with CLIC1

Due to the positive correlation of CLIC with later stage cancer cells and large tumours, the role of the protein in metastasis and invasion of cancer cells was investigated. It was shown if CLIC1 is silenced in pancreatic cancer cell lines, their invasive abilities significantly decrease (Lu et al., 2015) and high levels of CLIC1 expression in renal cancer cells invading the surrounding tissue as well as in cells within the blood vessels associated with the tumours (Nesiu et al., 2020). Wound-healing motility and cell invasion assays in various cancers cells showed slower closure of the wound, less migration and inhibition of cell invasion when CLIC1 expression was reduced. This shows CLIC1 has a clear role in metastasis in cancer cells (Feng et al., 2019; R. K. Li et al., 2012; Yue et al., 2019).

Two different gallbladder carcinoma cell lines inoculated into BALB/c nude mice had notable differences in incidences of metastasis to the liver, as well as significantly different cell invasion and motility abilities in vitro. To investigate the differences in metastatic ability, they looked at differences in protein expression and found CLIC1

as one of the proteins upregulated in the cell line more able to metastasise. In addition the highly metastatic cell line was successfully transfected to silence CLIC1 where a reduction in invasion and migration abilities were observed compared to the unmodified cell line (Wang et al. 2009).

Silencing and overexpression of CLIC1 in merkel cancer cells saw a significant decrease and increase in cell motility respectively. Higher CLIC1 levels were also seen in patients with cancer cells that had metastasised than those whose cancer's had not (Stakaityte et al., 2018).

1.6.5 CLIC1 & angiogenesis

Tumour growth depends on many factors including angiogenesis, the formation of new vascular network growth to supply oxygen and nutrients (Nishida et al., 2006).

CLIC1 was shown to promote angiogenesis in an oral squamous carcinoma model, with overexpression of the protein and knockdown of the protein increasing and decreasing endothelial cell tube formation respectively (Feng et al., 2019).

Furthermore endothelial migration, cell growth, branching morphogenesis, capillary-like network formation, and capillary-like sprouting were all found to reduce in human endothelial cells when CLIC1 was downregulated (Tung & Kitajewski, 2010).

The ability of CLIC1 to regulate endothelial cells is also linked with reactive oxygen species (ROS), with endothelial cells treated with H_2O_2 displaying enhanced CLIC1 expression and when the protein is inhibited with IAA94 (Indanyloxyacetic acid 94), ROS production in the cells is reduced (Xu et al., 2016). In addition to this, flow cytometry revealed key integrins needed for angiogenesis, such as B1, A3, AVB3 and AVB5, were regulated by CLIC1 (Tung & Kitajewski, 2010).

1.6.6 Focusing on CLIC1 in glioblastoma cells

One cancer type CLIC1 is well characterised in is glioblastoma multiforme (GBM), a high grade IV form of cancer with poor prognosis, which is why CLIC1 has such clinical relevance. CLIC1 is found to be overexpressed in glioblastoma cells compared to healthy tissue (Setti et al., 2013) with protein levels significantly correlated with poor prognosis and shorter overall survival in patients (Wang et al. 2012).

Furthermore, when CLIC1 is inhibited or silenced in glioblastoma cells, the cells were found to have reduced cell growth, viability, self-renewal ability and tumourigenic capacity. Together this reveals the importance of CLIC1 in cancer progression, particularly in glioblastomas (F. Barbieri et al., 2018; Peretti et al., 2018; Setti et al., 2013).

In the search for therapeutics against glioblastoma growth, CLIC1 was found to be a direct target of metformin, a widely available medication used for diabetes mellitus treatment, in human glioblastoma cells. Treatment of GBM cells with this drug resulted in antiproliferative effects and a reduction in glioblastoma cell invasiveness (F. Barbieri et al., 2018; Gritti, Würth, Angelini, Barbieri, Pizzi, et al., 2014). The mechanism of how metformin's inhibition of CLIC1 activity results in reduced GBM cancer progression was investigated. Metformin was shown to arrest the cells in the G_1 phase of the cell cycle (Gritti, Würth, Angelini, Barbieri, Pizzi, et al., 2014) which further supports the role of CLIC1 in cell cycle regulation as previously described (Valenzuela et al., 2000). Cell cycle arrest of GBM cells in the G_1 phase was also achieved by inhibition of CLIC1 by another inhibitor, IAA94, and in particular function of CLIC1 as a membrane channel was found to be crucial for glioblastoma cell cycle

progression (Peretti et al., 2018). Targeting therapeutics against the membrane channel form of CLIC1 could reduce glioblastoma growth rates in clinically ill patients.

1.7 Interaction of CLIC1 in cells

1.7.1 CLIC1 cell signalling in the cancer phenotype

The interaction of the CLIC1 protein in mammalian cells is ill-defined and literature proves the protein to have complex mechanisms of interactions, many of which could be regulated by CLIC1 expression in cancer diseased states. The following are possible hypotheses for how CLIC1 affects the cancer cell phenotype (Figure 1.5).

Apoptosis of cancer cells could be regulated by the expression of CLIC1 with apoptotic protein Bcl-2 down regulated in gastric cancer cells lines when CLIC1 was silenced (B. P. Li et al., 2018), and knockdown in squamous cell carcinoma cells had upregulated apoptosis rates with higher caspase 3 & 9 protein expression (Feng et al., 2019). Flow cytometry was used to measure cell cycle kinetics and it revealed in mouse hepatocarcinoma cells when CLIC1 expression is reduced the number of cells at G2/M increase and the number of apoptopic cells decrease compared to control (Li et al. 2012).

In liver cancer cells, CLIC1 expression was found to be a potential target of a microRNA, specifically miRNA-124, which is found to be significantly downregulated in several types of cancer and acts as a tumour suppressor (Yue et al., 2019). When liver cancer cells were transfected for overexpression of miR-124, CLIC1 expression was significantly decreased, and when CLIC1 was knockdown in liver cancer cells the tumour suppressor effects of miR-124 were reversed, suggesting the interaction of CLIC1 with miR-124 has a role to play in liver cancer metastasis (Yue et al., 2019). A hypothesis is CLIC1 is overexpressed in a cancer cells, so less tumour suppression is seen with the reverse seen in healthy tissue as CLIC1 is at lower levels so miR-124 can acts as a tumour suppressor.

The role of CLIC1 in epithelialmesenchymal transition is also hypothesised with key factors in this process found to change expression levels when CLIC1 levels are reduced or overexpressed in cancer cells (Feng et al., 2019). Identifying signalling pathways for CLIC1 regulation is also of interest and mitogen activated protein kinase (MAPK) signalling is found to be regulated by CLIC1 (Figure 1.5). The MAPK pathway is a complex signalling mechanism, composed of at least three families; extracellular signal-regulated kinase (ERK), Jun kinase (JNK) and p38 MAPK, found to regulate proliferation, differentiation and development of cells (Wei & Liu, 2002). Downstream signalling molecules of the MAPK pathways, matrix metalloproteinases MMP-2, MMP-9, MMP-13 and phosphorylated extracellular-signal-regulated kinase (P-ERK) protein levels were positively correlated, while JUN mRNA levels were negatively correlated with CLIC expression in tumour cells (Feng et al., 2019; Kobayashi et al., 2018; Xu et al., 2018). Matrix metalloproteinases are found to help breakdown the extracellular matrix in cancer cells so could aid tumour cell migration and angiogenesis (Quintero-Fabián et al., 2019), ERK expression is known to be essential for cell development but when overactive can enhance cancer development and progression (Y. Guo et al., 2020), while JUN signalling is known to control cell proliferation, survival and transformation in both agonistic and antagonistic manners (Shaulian, 2010). Further signalling pathways in cells are correlated to CLIC1 expression. When CLIC1 was silenced in these oesophageal cancer cells the mRNA levels of toll like receptor 2 (TLR2) and Myeloid differentiation primary response 88 (MYD88) were measured and were found to increase, both upstream targets of MAPK (Kuriakose et al., 2019). The silencing of CLIC1 led to increased phosphorylation of (c-Jun N-terminal kinase) JNK but decreased the

phosphorylation of ERK, and indicated the TLR and JNK pathways are involved in the regulation of cancer cells of CLIC1 (Kobayashi et al., 2018).

Annexin7, (ANXA7) a calcium dependent phosholipid binding protein, was show to be upregulated In mouse hepatocarcinoma cells when CLIC1 expression was downregulated (Figure 1.5). The in vitro data was reaffirmed with xenograph mice models that revealed a higher expression of CLIC1 in mice injected with hepatocarcinoma cells with ANXA7 knocked down (Zhang et al., 2015). This could indicate an interplay between this protein, divalent cation binding and CLIC1 to regulate the membrane fusion process. CLIC1 expression was also linked to chemosensitivity in oral squamous carcinoma cells, there was a significant increase in sensitivity of CLIC1-knockdown cells to cisplatin compared to the control and cells with CLIC1 overexpressed (Feng et al., 2019).

Furthermore, it was found that CLIC1 was actually secreted from cancer cells, with higher levels of CLIC1 in the secretome compared to healthy tissue (Singha et al., 2018). This could indicate cell to cell signalling involving CLIC1 and further evidence confirms this, with CLIC1 found in extracellular vesicles transferring between glioblastoma and endothelial cells increasing the levels of CLIC1 in these cells (Figure 1.5) (Thuringer et al., 2018).

1.7.2 CLIC1 interacts with cytoskeleton to aid migration and proliferation

CLIC1 has been shown to colocalise and change expression levels in correlation with different components of the mammalian cell cytoskeleton and the extracellular matrix, that could explain how the protein can aid migration and proliferation in tumour cells (Figure 1.5).

The interaction between integrins and CLIC1 has also been characterised with increased levels of ITGav & ITGB1 in cancer cells where CLIC1 is silenced (Feng et al., 2019). Integrins are a family of proteins responsible for attachment and migration of cells on extracellular matrix and in cancer have been shown to regulate tumour growth, angiogenesis and metastasis (Jin & Varner, 2004). Furthermore GeneMANIA was used to look for signalling interactions between CLIC1, MAPK and Integrins and it was hypothesised CLIC1 was in the same signalling network as ITGav, ITGa1, ITGa3, ITGB1, EKR, AKT1 and p38 (B. P. Li et al., 2018).

The interaction of CLIC1 with the cytoskeleton has also been investigated with CLIC1 colocalisation seen with cytokeratin20, an component of intermediate filaments in merkel cell carcinoma cells which is used to recognise the cancer cells in tissue (Stakaityte et al., 2018). Regulation of CLIC1 channel activity was also correlated with cytosolic F-actin, which was found to have an inhibitory effect on the protein's activity, and this modulation could play a key role in the cell proliferation effects of CLIC1 (Singh et al., 2007). CLIC1 has also been shown to be vital for cytokenesis in cell division to occur, hypothesising the protein interacts with CLIC4, acting as a plasma membrane-actin anchoring complex (Kagiali et al., 2020). Further research is needed into how these cellular interactions with CLIC1 specifically lead to regulation of cell division or proliferation and if they are upregulated in cancer cells.

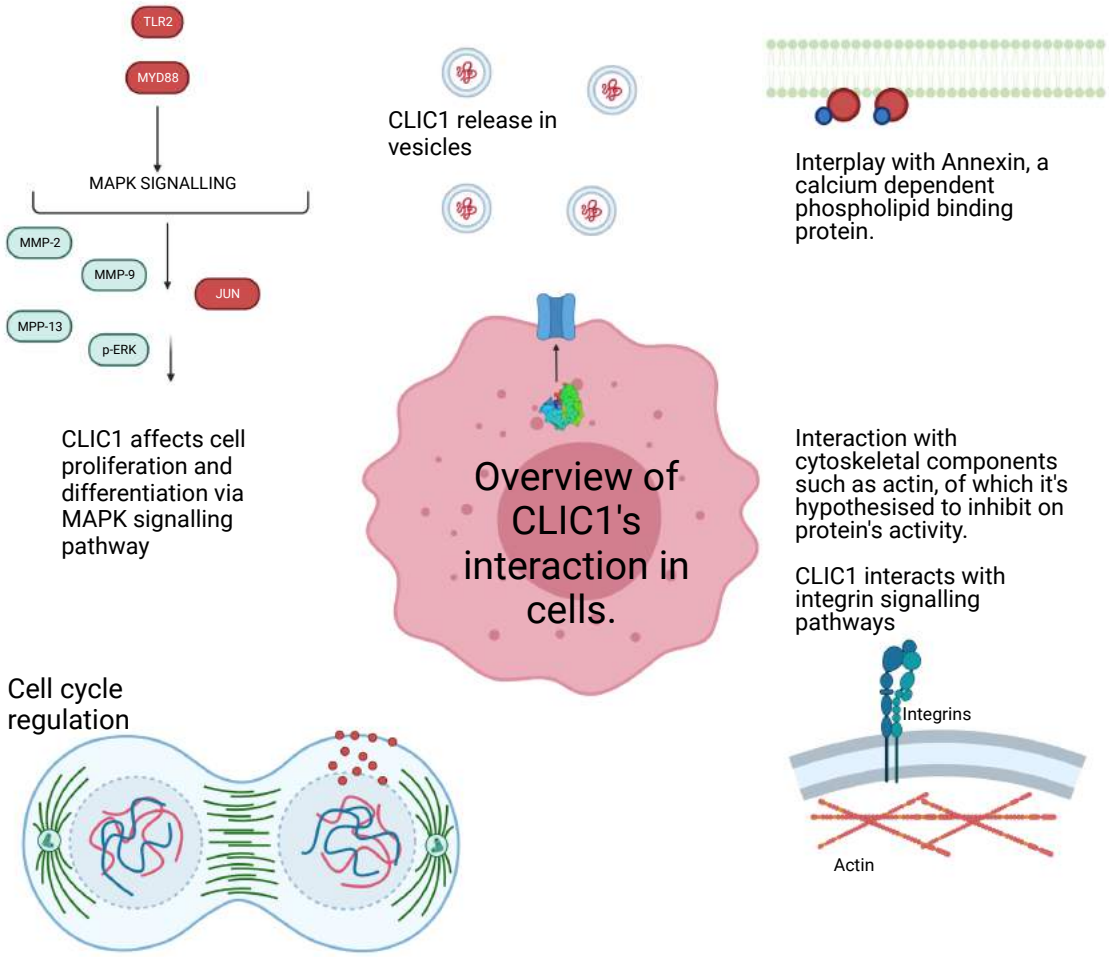

Figure 1.5 – Summary of hypothesised interactions of CLIC1 in cells. CLIC1 is hypothesised to leave the nucleus and insert into the plasma membrane in mitosis thus regulating the cell cycle at different stages. CLIC1 expression is shown to affect the upstream and downstream signalling molecules in the MAPK pathway involved in cell proliferation and differentiation. Molecules positively correlated with CLIC1 are shown in green and negatively shown in red. CLIC1 has been shown to be released from cells via extracellular vesicles, which could aid cell to cell communication. CLIC1 has also been shown to regulate calcium binding protein annexin7 and has links to regulating integrins and actin filaments, which could aid control of cell proliferation, migration, and angiogenesis.

1.8 CLIC1 in other diseases & therapeutic applications

1.8.1 CLIC1 in heart conditions

Immunohistochemical staining revealed CLIC1 in atherosclerotic plaques of aorta tissue sections, with a significantly higher protein expression found in tissue from mice fed a high fat, cholesterol rich diet than a normal diet. Experiments investigating the relationship of CLIC1 with heart disease reveal evidence for a clinical therapy for cardiovascular disease, tanshinone IIA sodium sulfonate (STS), working to regulate endothelial dysfunction by downregulating CLIC1 (Zhu et al., 2017). Furthermore an upregulation of CLIC1 is seen in human atrial tissue from patients suffering from rheumatic mitral valve disease (Y. Y. Jiang et al., 2017). Overexpression of CLIC1 in endothelial cells has also been associated with accelerated atherosclerotic plaque formation (Xu et al., 2016).

1.8.2 CLIC1 & neurodegenerative disease

Alzheimer's Disease is characterised by B-amyloid (AB) plaques surrounded by astrocytes and reactive microglia, AB activates the microglia to produce ROS by NADPH oxidase and this oxidative stress causes neurodegeneration and it is shown that the AB plaques upregulates the chloride current in microglia by upregulation of CLIC1 (Novarino et al., 2004). In addition, the protein translocates to the membrane during microglia activation by AB and inhibition of CLIC1 reduces microglial-mediated neurotoxicity (Milton et al., 2008; Novarino et al., 2004). Furthermore CLIC1 protein was revealed to increase during neurodegenerative disease progression in monocytes from patients with AD, with an increase in plasma membrane CLIC1 in the neuropathological central nervous system (CNS) compared to healthy patients

(Carlini et al., 2020). Furthermore this provides another physiological background for the interplay between ROS and CLIC1.

1.8.3 CLIC1 & inhibitors

Pharmaceutical chloride channel inhibitors effects on conductance of CLIC1 have been tested. Indanyloxyacetic acid (IAA94), a known chloride channel inhibitor, was found to reversibly block chloride conductance of the CLIC1 channel in CHO cells (Tonini et al., 2000; Valenzuela et al., 2000) and in lipid bilayers of PC and cholesterol (Warton et al., 2002). Due to IAA94's effectiveness at reducing CLIC1 channel activity it has been used to study the effect of CLIC1 inhibition in cancer cell lines (F. Barbieri et al., 2018; Peretti et al., 2018; Setti et al., 2013).

The diabetes drug metformin has also been used as a direct inhibitor of CLIC1 in glioblastoma cells as previously described. Other cancer forms have trialled this therapeutic with gallbladder cancer cell lines displaying reduced viability over time when treated with metformin (Liu et al., 2017). The specificity of metformin was proven further by treatment of CLIC1 with IAA94 or silencing of the protein prior to metformin treatment, as it reduced the effectiveness of the drug with a smaller decrease in gall bladder viability and colony formation seen. In addition overexpression of CLIC1 saw increased sensitivity to metformin and demonstrates CLIC1 as a clear target for the drug in cancer cells (Liu et al., 2017).

Other channel inhibitors have been investigated for their action to inhibit CLIC channels and 5-nitro-2-(phenylpropylamino)-benzoate (NPPB), dihydro-4,4'-diisothiocyanostilbene-2,2'-disulphonic acid (DIDS), and phloretin were all found to inhibit the chloride current in cardiac myocytes (Malekova et al., 2007).

1.8.4 CLIC1 used for cancer therapeutics

The use of CLIC1 to initiate the immune response as a form of immunotherapy has also been investigated in mice. The N domain of CLIC1 has previously been fused with a tuberculosis heat shock protein and in a CLIC1 dependent mechanism was able to activate the immune response to increase cell lysis of ovarian cancer cells (Yu et al., 2017).

In addition, the overexpression of CLIC1 in the cancer tissue compared to healthy tissue presents a tumour biomarker than can be used for prognosis of these cancer types and the overexpression of the channel form of the protein in these cells can provide a novel target for therapeutics, with limited impact on healthy cells.

1.9 Aims of the project

The overall aim of this project is to elucidate the mechanism of how CLIC1 inserts into the membrane to form a chloride channel and what triggers the protein to make this conformational change. In addition to this, we sought to study this change of localisation of the protein in the context of cancer cells.

Aims:

1. Purify and study the oligomerisation state of soluble CLIC1 and measure insertion into lipids.
2. Verify and understand the trigger of CLIC1 insertion into lipids.
3. Study the insertion of the protein in the context of cancer cells.
4. Use the novel structural technique of In-cell NMR to try and elucidate more information about the conformational changes involved in the membrane insertion mechanism of CLIC1.

CHAPTER 2: Recombinant expression and purification of CLIC1

2.1 Introduction

CLIC1 is one of 7 paralogues within the chloride intracellular family that are structurally homologous to the omega class of the glutathione S-transferases (Harrop et al., 2001). Existing as both a globular cytosolic protein and an integral membrane channel, CLIC1 is poorly understood structurally as a channel. However recombinant expression and purification of the soluble form allows study of the cytosolic protein and structural changes when membrane insertion is triggered.

As previously introduced, the overexpression of CLIC1 in the membrane channel form is known to aid tumour proliferation in various forms of cancer (Ding et al., 2015; Ma et al., 2012; Nesiu et al., 2020; Setti et al., 2015; Ulmasov et al., 2007; Zhao et al., 2015). This highlights the importance of studying the protein for potential therapeutic applications, and recombinant expression and purification of the protein is a necessity for this.

The first recombinant expression carried out in *Escherichia coli* (*E. coli*) was the synthesis of the hormone Somastatin (Itakura et al., 1977). The original method for recombinant expression involved generating cDNA libraries using reverse transcriptase to find the target gene and then insert into the bacterial cells to replicate the desired DNA product. Since then the field of molecular cloning has greatly improved with the invention of the polymerase chain reaction (PCR) in 1987 (Mullis & Faloona, 1987), which allowed fast, high volume production and amplification of nucleic acid sequences in vitro. The combination of this cloning and

PCR technology has allowed for the recombinant expression of the protein of interest, CLIC1, within this project.

Expression and purification systems often need to be optimised to the specific protein, from which organism to use for the expression system, what affinity tag to use for purification, and which vector to select.

There are many different organisms to choose from for recombinant protein expression, from mammalian cells, most commonly CHO cells (Geisse et al., 1996), yeast cells such as Pichia pastoris or Saccharomyces cerevisiae (Bill, 2014), routinely used lepidopteran insects cells (Cérutti & Golay, 2012), or filamentous fungi such as Aspergillus species (Fleiner & Dersch, 2010).

Using a bacterial expression system, in particular *E. coli*, was selected for this project, as *E. coli* systems are known for their low cost, high productivity and fast speed of growth (Terpe, 2006), with some *E. coli* expression systems known to be able to produce recombinant proteins up to 80% of their dry weight (Demain & Vaishnav, 2009).

Post translation modifications (PTMs) must be considered when selecting the organism for recombinant expression. PTMs of CLIC1 are not well characterised, CLIC4 has been hypothesised to undergo S-nitrosylation to regulate translocation of the protein (Kagiali et al., 2020). This could be relevant to CLIC1 as S-nitrosylation is the covalent attachment of a nitrogen monoxide group to a thiol side chain of a cysteine (Hess et al., 2005), and cysteines particularly Cys24 & 59 have been implicated in the dimer formation of CLIC1 (Littler et al., 2004). Futhermore S-nitrosylation has been shown to play an important role in many protein dynamics and cellular signalling and can be regulated by redox reactions (Hess et al., 2005),

which could link to the evidence of the oxidation of CLIC1 being involved in translocation and channel formation (Goodchild et al., 2009; Littler et al., 2004). Based on in-silico predictions from the amino acid sequence of CLIC1, it is hypothesised CLIC1 also possesses PTMs such as myristoylation, glycosylation and phosphorylation near the C-terminal or transmembrane domain but little is known how these modifications regulate the protein (Gururaja Rao et al., 2018). Non-glycosylated proteins are typically produced in *E. coli* expression systems due to the advantages described above, and due to little being known about glycosylation of CLIC1 more complex and costly systems that can glycosylate proteins such as yeast, insect or mammalian cells (Demain & Vaishnav, 2009) were not required and *E. coli* was selected as the recombinant system. Furthermore, CLIC1 had previously been shown to insert into membranes of *E. coli*, demonstrating the bacteria's suitability for expressing correctly folded protein to form a channel (Varela et al., 2019).

In addition *E. coli* recombinant expression is a much simpler protocol than, for instance, insect cells which require viral infection for protein production (Agathos, 1991). NMR is a major tool used for our research and in order to carry out these experiments isotopic labelling of the protein is required and this is known to be easily achieved in *E. coli* with well established, cost effective and efficient methods (M. Cai et al., 1998). Furthermore, CLIC1 had previously been successfully purified in *E. coli* systems (Valenzuela et al., 1997) and it was the logical choice to attempt purification of this protein for our research.

In order to study the insertion of CLIC1, and to gain further structural information of the protein as an integral membrane channel, the protein needs to be expressed and purified in high yields. Recombinant expression of CLIC1 has been successfully

carried out in previous experiments with various vectors used for molecular cloning. Initial attempts to recombinantly express CLIC1 saw use of the GST fusion protein vector system, pGEX, to create a fusion of GST and CLIC1 which was then separated by thrombin digestion of the cleavage site between the proteins (Harrop et al., 2001; Tulk et al., 2000; Valenzuela et al., 1997; Warton et al., 2002). Examples of other vectors used for the successful expression of CLIC1 into *E. coli* include pET28a vector (Goodchild et al., 2011; Khamici et al., 2015) and pHIS-8, a modified pET-28a(+) vector with an N-terminal octahistidine tag and a thrombin cleavage site (Singh & Ashley, 2006).

Consequent to the use of various vectors, different chromatography methods have been used for the purification of CLIC1. Glutathione agarose was used to purify CLIC1 within the pGEX vectors with a GST affinity tag, using streptavidin-agarose to remove the thrombin (Harrop et al., 2001; Valenzuela et al., 1997; Warton et al., 2002). Nickel chromatography was used for CLIC1 vectors containing His-tags (Goodchild et al., 2011; Khamici et al., 2015).

Glutathione S-transferase tags were first used to express and purify parasitic polypeptides in 1988 (Smith & Johnson, 1988), and as mentioned have been used regularly to purify CLIC1. However, they are known to have disadvantages, including inclusion body formation with high expression levels (Kimple et al., 2013), and can often require the removal of contaminants that co-purify (Thain et al., 1996).

Instead, alternative chromatography tags were investigated for CLIC1 purification, including polyhistidine tags known to be successful for CLIC1 purification previously. Polyhistidine tags were first used to purify recombinant galactose dehydrogenase

by immobilised metal affinity chromatography (Lilius et al., 1991), and have since been used for purification of many proteins, due to their small size and charge of tag that easily binds to metal ions like Ni^{2+} (Kimple et al., 2013).

Advantages of other tags were explored and the use of strep tags binding to strep-tactin resin beads were known to bind with optimal affinity and allow the protein to stay folded during purification (Kimple et al., 2013).

Further purification with gel filtration was routinely used from the first purifications of CLIC1 (Harrop et al., 2001; Valenzuela et al., 1997), and size exclusion chromatography in combination with quasi-elastic light scattering was used to reveal a molecular weight of 32 +/- 4 kDa (Tulk et al., 2000). It is also important to note CLIC1 expression is seen with the use of various *E. coli* strains; XL-blue (Tulk et al., 2000), HB101s (Valenzuela et al., 1997), and BL21s (Goodchild et al., 2011; Littler et al., 2004; Stoychev et al., 2009) to name a few.

In this chapter the recombinant expression and purification of soluble CLIC1 with and without a fluorescent GFP label is described in detail and all factors discussed in this introduction results in successful purification of CLIC1 in both vectors.

2.2 Methods

2.2.1 Molecular cloning of CLIC1 into pWaldo vector

The gene encoding human CLIC1 was recloned into the pWaldo-d vector to generate CLIC1 with a C-terminal GFP tag. Primers were designed to insert the Human CLIC1 gene (HsCD00338210 from the plasmid service at Harvard medical school) into the pWaldo-GFPd_PepTSt vector (D. E. Drew et al., 2001; Solcan et al., 2012). PCR was carried out to amplify both the CLIC1 fragment and the vector independently according to Gibson assembly (New England Biotech) instructions and transformed into DH5alpha competent cells for DNA replication. The DNA was extracted and purified using a miniprep kit (Qiagen) from overnight cultures of the DH5alpha, growing with kanamycin antibiotic selection for the vector. The purified DNA was sent for sequencing (Eurofins genomic sequencing) and the insertion of CLIC1 into the pWaldo vector (D. E. Drew et al., 2001) was confirmed.

2.2.2 Protein expression tests

The gene for human CLIC1 has been previously cloned into a pASG vector (IBA) in Dr Jose Ortega-Roldan's laboratory with a N-terminal Twin strep tag. Both this construct and the CLIC1-GFP construct generated, as described above, were subsequently used for protein expression. CLIC1 in both the pWaldo and pASG vectors were transformed into C43 competent cells and Shuffle T7 *E. coli* expression cells (New England biolabs) for recombinant expression. CLIC1-pWaldo was additionally transformed into Origami (DE3) expression cells (Novagen). Transformed colonies were selected for growth in either LB or richer media TB. Once OD_{600} of ~0.7 was reached, 1 mM IPTG was added for induction, and the temperatures post reduction were regulated

depending on the sample. At 3 hours and 24 hours post induction, a sample of each growth was taken, and for fair comparison the OD_{600} was taken and the equal number of cells were calculated for each SDS gel sample. Each sample was boiled after addition of sample buffer (10% w/v SDS, 10 mM DTT, 20% v/v Glycerol, 0.2 M Tris-HCL, pH 6.8 and 0.05% w/v Bromophenolblue) and urea, all to aid lysing of the cells. The samples were then run on a 12% Tris-glycine SDS gel and stained with Coomassie blue for detection of the protein bands.

2.2.3 Protein expression and purification

Once optimal expression conditions were identified through expression tests, CLIC1 in both vectors were transformed and recombinantly expressed in *E. coli* C43 competent cells (Lucigen) with antibiotic selection. Growth was undertaken at 37°C until the cells reached an OD_{600} of ~0.7, and induction was then carried out with 1 mM IPTG at 30°C overnight. The cells were harvested by centrifugation at 4000 rpm and resuspended in lysis buffer; 150 mM Tris 50 mM NaCl 1 mM EDTA pH 7.4. Sonication was used to lyse the cells, with the soluble and membrane fraction separated by ultracentrifugation at 117734 g. Purification of both fractions was carried out independently using Strep-Tactin XT or nickel affinity chromatography for CLIC1 in both the pASG and pWaldo expression vectors respectively. Gel filtration into either 20 mM HEPES 20 mM NaCl pH 7.4 buffer or 20 mM Potassium Phosphate 20 mM NaCl pH 7.4 buffer was carried out using a Superdex200 Increase column (GE). Tris-glycine SDS gel electrophoresis was performed at 200 V and stained using Coomassie blue to verify the size of the purified protein.

2.2.4 Fluorescence assays

Intrinsic tryptophan protein fluorescence of the tryptophan residue in CLIC1 (Figure 2.1), was recorded by excitation at 280 nm and emission was measured between 300 nm to 400 nm and excited at 395 nm for emission between 400 nm to 500 nm for the GFP-labelled samples, using a Varian Cary Eclipse fluorimeter. For the GFP fluorescence assay small growths were prepared from glycerol stocks of Pwaldo CLIC1-GFP in C43 *E. coli* cells, with selection for the construct with Kanamycin. The cells were grown to reach an OD_{600} of 0.7 before induced with 1 mM IPTG and left to grow overnight at 30°C. Cells were harvested by centrifugation at 4000 rpm and sonicated to break the bacterial membranes. An initial fluorescence reading was taken of the cell lysate. The samples were then ultra-centrifuged at 208000 g for 30 minutes at 25°C to separate the membrane and soluble protein. The soluble fraction was extracted from the membrane fraction immediately after centrifugation and the pellet resuspended to similar volume as the supernatant. GFP fluorescence readings were then recorded for both samples with the same protocol as used for initial recordings.

MAEEQPQVELFVKAGSDGAKIGNCPF
SQRLFMVLWLKGVTFNVTTVDTKRRT
ETVQKLCPGGQLPFLLYGTEVHTDTNK
IEEFLEAVLCPPRYPKLAALNPESNTAG
LDIFAKFSAYIKNSNPALNDNLEKGLLK
ALKVLDNYLTSPLPEEVDETSAEDEGV
SQRKFLDGNELTLADCNLLPKLHIVQV
VCKKYRGFTIPEAFRGVHRYLSNAYAR
EEFASTCPDDEEIELAYEQVAKALK

Figure 2.1 – Amino acid sequence of CLIC1. The Tryptophan residue is highlighted in blue.

2.2.5 Circular dichroism

Purified and cleaved CLIC1 was diluted to 20 µM in 20 mM HEPES, 20 mM NaCl pH 7.4 buffer and loaded into a 2 mm cuvette. The spectra were recorded at room temperature, from wavelengths of 260 nm to 210 nm on a JASCO J-715 spectropolarimeter. The resolution was 1 nm, with 1 nm band width and 100 mdeg sensitivity, with a response time of 1 second. The final spectra were an average of 5 scans collected at a speed of 100 nm/min speed.

2.3 Results

2.3.1 Molecular cloning and purification of CLIC1 with GFP tag

To create the desired protein construct of CLIC1 with a GFP Tag, a suitable bacterial expression vector was selected, the pWaldo-GFPd (Solcan et al., 2012) plasmid, formed from a high expression pET28a(+) plasmid, but featuring a T7 Promoter, TEV cleavage site, GFP, His Tag and Kanamycin resistance. This specific vector was chosen due to easy cleavage of the GFP and His tag if needed during purification, using TEV protease, a highly specific cysteine protease generated from the Tobacco Etch virus (TEV) able to cleave the affinity tag from the protein via site specific endoproteolysis (Parks et al., 1994). Furthermore, the location of the GFP (as shown in Figure 2.2) is important due to its location on the C-terminal side of CLIC1. The N terminus of CLIC1 is thought to be implicated in the rearrangement of the protein into the channel form (Singh & Ashley, 2006) and therefore ensured the possibility of the GFP tag interfering with the rearrangement would be minimal. A His-tag is required to purify the protein using nickel chromatography and the kanamycin resistance is for bacterial selection during the recombinant expression growth process.

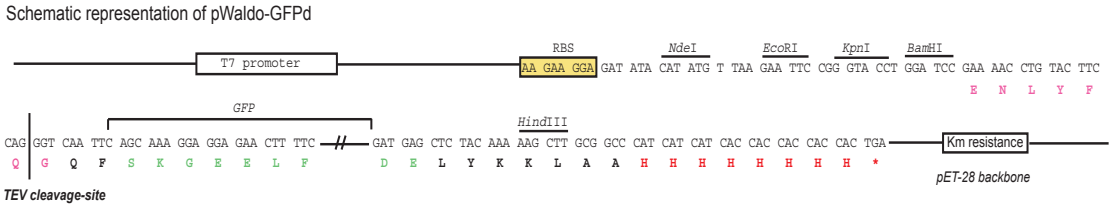

Figure 2.2 – Schematic of the pWaldo vector. Vector used to introduce a C-terminal GFP tag to the CLIC1 protein, including a His tag, TEV cleavage site and Kanamycin antibiotic resistance (D. Drew et al., 2006).

Gibson assembly PCR was used to successfully introduce the CLIC1 protein into the vector and this was confirmed by sequencing revealing the correct sequence of DNA bases for CLIC1 inserted into the pWaldo vector, Figure 2.3 shows the exact construct generated. Transformation into competent *E. coli* cells such as C43s, selected due to their known effectiveness at recombinantly expressing large membrane proteins even when toxic (Miroux & Walker, 1996), allowed growth of the CLIC1-GFP protein construct. After nickel chromatography the protein was run on an SDS gel to check the correct molecular weight of the product, as seen in Figure 2.4, CLIC1-GFP was successfully purified.

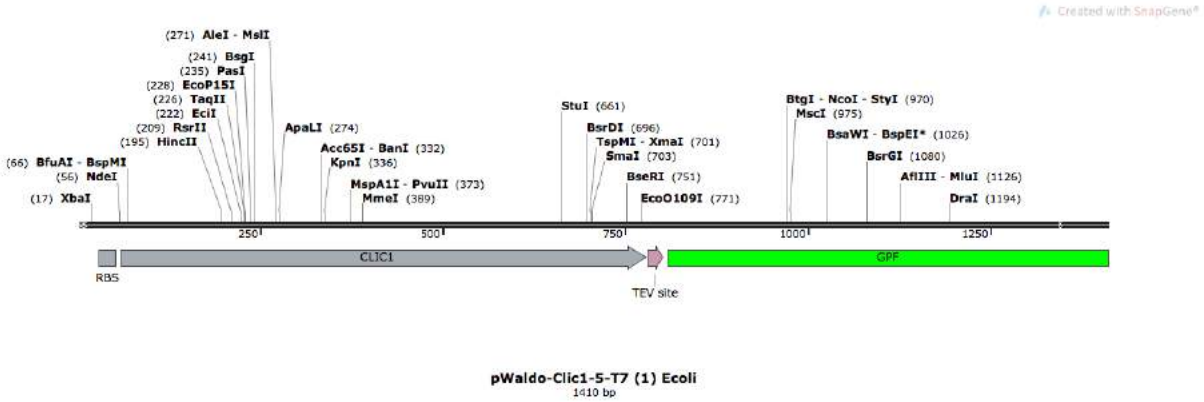

Figure 2.3 – Schematic of CLIC1 inserted into the pWaldo-GFPd Vector. The TEV cleavage site and GFP are located at the C terminus of the protein. This construct was used to fluorescently label CLIC1 and was confirmed by DNA base sequencing.

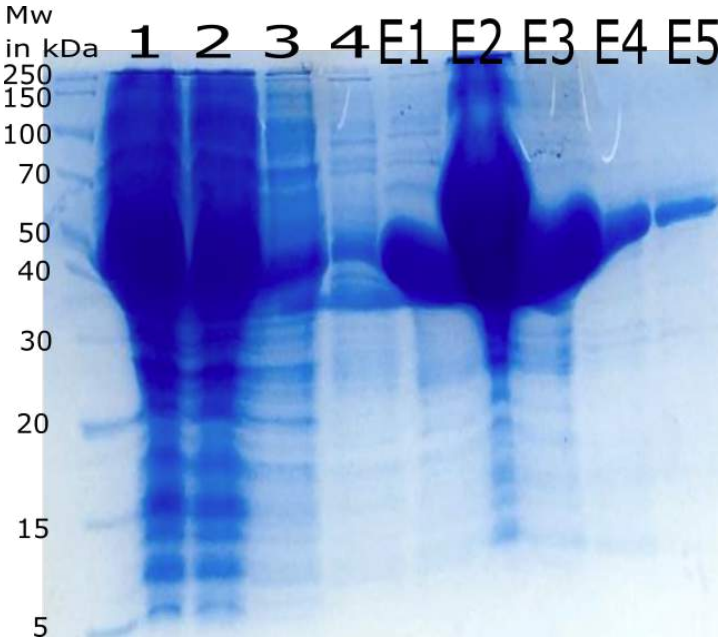

Figure 2.4 – Tris glycine SDS gel of soluble CLIC1-GFP protein purified by nickel purification column. 1 = Sample one, 2 = Flow Through, 3 = Wash one, 4 = Wash two, E1-E5 = Elutions of purified CLIC1-GFP. The protein can be seen at 56Kda.

2.3.2 Optimal CLIC1-GFP bacterial expression in C43 cells

Purification of proteins requires the best growth conditions using the optimal competent cell line, induction temperature and media for each specific expression system. Small scale growths were carried out for CLIC1-GFP in BL21 cell line C43s, as expression of CLIC1 in the pASG vector had been optimised in this cell line previously in the laboratory (Varela et al., 2019).

Expression for the pWaldo construct of CLIC1-GFP showed expression in the C43 cell line with clear bands forming at the correct molecular weight, 56 kDa, for all samples. However, the expression test (Figure 2.5) allowed direct comparison of the construct in both LB and TB media and the results show increased protein expression in LB media. In addition, expression of the protein increased as the post-induction temperature is lowered from 37°C. These expression tests gave optimal conditions

for recombinant expression of CLIC1-GFP and subsequently these conditions were used for all growth and purifications throughout the research project.

2.3.3 CLIC1 expression is not enhanced with competent cells that induce disulphide bond formation.

SHuffle T7 express cells are known to promote folding of proteins via disulphide bonds and Origami competent cells contain mutations in glutathione reductase and thioredoxin reductase to help enhance correct disulphide bond formation (Sigma Aldrich). Both of these cell lines were used in small scale expression tests for CLIC1 in both the pASG vector but also labelled with GFP as the competent cells promoting disulphide bond formation were of interest to see if protein could be purified in a higher oligomerisation state or the enhanced stability would increase protein yield. At two induction temperatures, 30°C and 37°C, both SHuffle and Origami cells, produce only faint expression bands at 27 kDa for unlabelled CLIC1 or the dimer at 54 kDa. However, in the Origami cells two very clear bands can be seen at higher molecular weights but at approximately 64 kDa & 120 kDa, which are incorrect molecular weights expected for soluble CLIC1 dimer and tetramer at 54Kda and 108kDa respectively (Figure 2.5).

A CLIC1-GFP expression test in the SHuffle competent cells also revealed lower protein expression than seen in the BL21 C43 cell lines, revealing these cell lines to have no benefit for CLIC1 expression.

2.3.4 Successful recombinant expression, growth and purification of monomeric and dimeric CLIC1

Firstly, to produce good yields of soluble CLIC1 via recombinant expression in *E. coli*, the pASG vector (IBA) was used and CLIC1 was purified via streptactin chromatography as described in methods. The pASG vector (shown in Figure 2.6), was selected due to the tetA resistance gene to regulate the plasmid promoter to prevent *E. coli* death by production of a cytotoxic protein (IBA). Figure 2.7 shows the successful purification of soluble CLIC1 at the correct molecular weight of 27 kDa. Following cleavage with TEV Protease to remove the chromatography tag and secondary reverse nickel chromatography to remove the protease (Figure 2.8), the soluble CLIC1 protein was further purified with gel filtration chromatography (Figure 2.9). CLIC1-GFP, from the pWaldo vector, was successfully purified to a high yield using nickel chromatography followed by gel filtration chromatography (Figure 2.10).

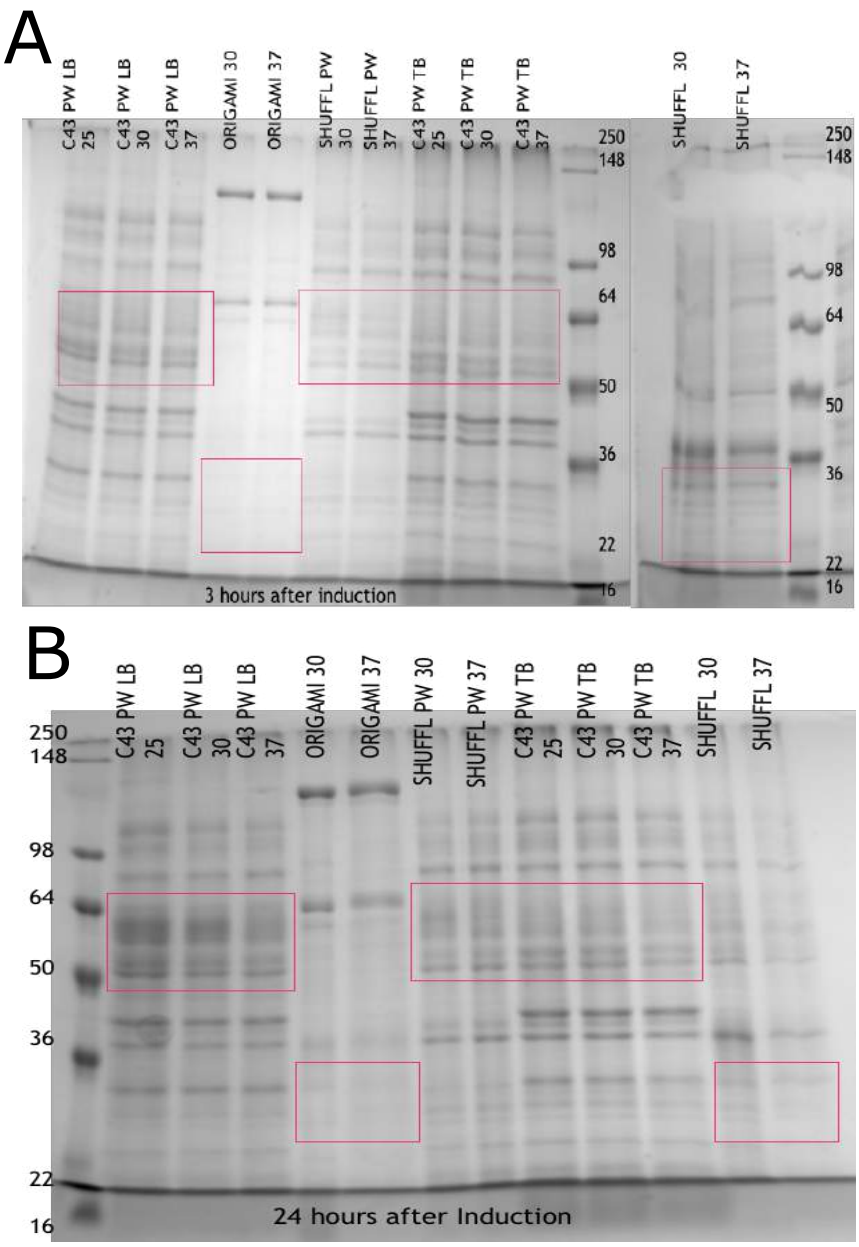

Figure 2.5 – Optimisation of CLIC1 expression. SDS gels of expression tests of CLIC1 with either soluble CLIC1 or C-terminal GFP tagged CLIC1 (PW) in different competent cells; C43s and Origami or Shuffle Cells used to promote disulphide bond formation. Furthermore, different media LB or TB and different induction temperatures were tested to optimise expression. A – Protein expression 3 hours post induction. B – Protein expression 24 hours post induction. Pink boxes represent areas CLIC1 expression was expected in each sample.

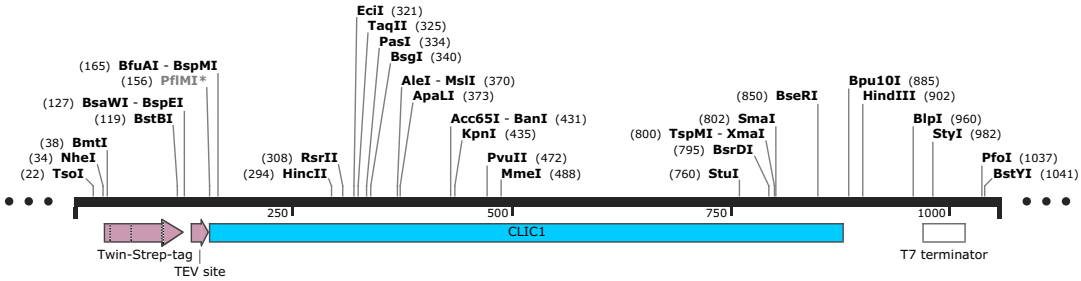

Figure 2.6 – Schematic of pASG vector. The vector includes a Twin-strep tag and TEV protease cleavage site on the N-terminal domain of CLIC1. This construct was used for purification of all unlabelled soluble protein.

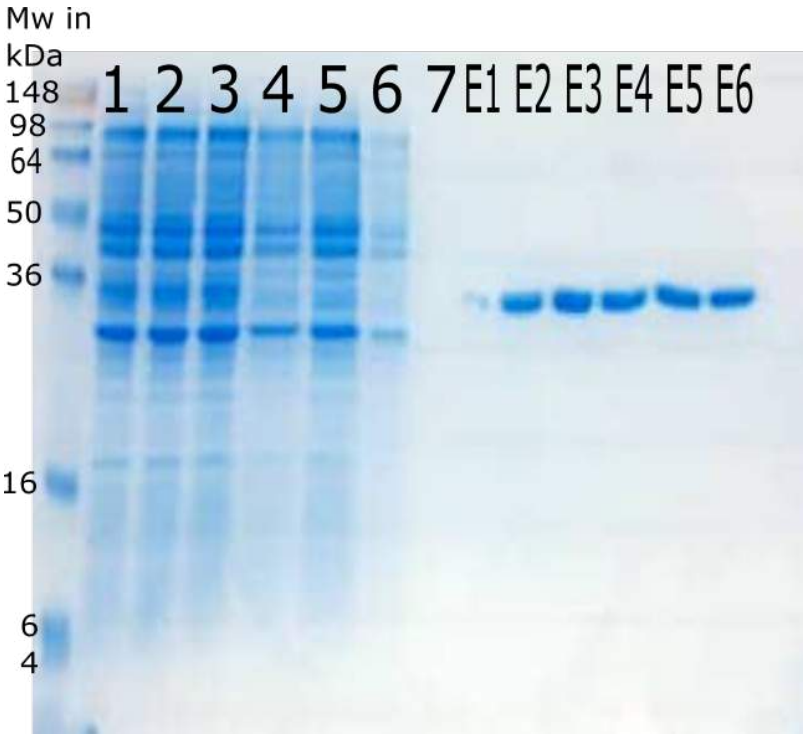

Figure 2.7 – Tris glycine SDS gel of soluble CLIC1 protein purified by streptactin purification column. 1 = Sample one, 2 = Sample two, 3 = Sample three, 4 = Flow through one, 5 = Flow through two, 6 = Wash one, 7 = Wash two, E1-E6 = Elutions of purified CLIC1. The protein can be seen at 27Kda.

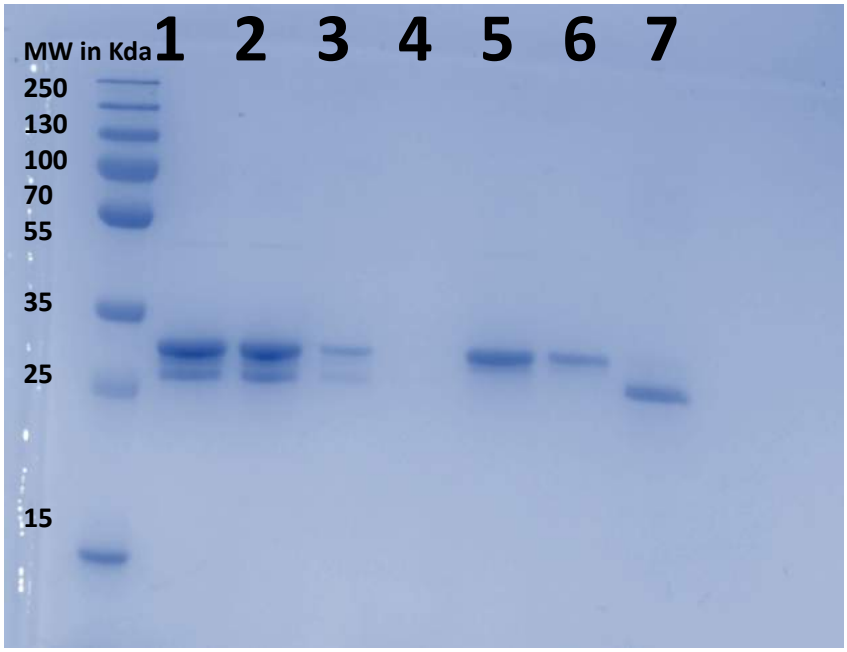

Figure 2.8 – Tris glycine SDS gel of soluble CLIC1 after TEV protease cleavage. 1 – CLIC1 in dialysis buffer after cleavage. 2 – CLIC1 flow through from streptactin column (contains cleaved protein and TEV protease). 3 – Wash through of streptactin column. 4 – Elution of un-cleaved protein. 5 – Flow through from nickel chromatography column (contains cleaved protein only). 6 – Wash through of nickel column. 7 – Elution of TEV protease.

2.3.5 Oligomerisation state of soluble CLIC1.

To further purify and determine the relative yields of protein a gel filtration chromatography system was used. Ultraviolet absorption readings of the protein revealed that protein is produced with growth from both constructs. Size exclusion chromatography revealed that for protein purified from both the pASG and pWaldo expression systems, the majority of the protein is monomeric while dimeric species and possible higher order oligomers are also present in the unlabelled CLIC solution but in lesser quantities to the monomer (Figure 2.9 & 2.10).

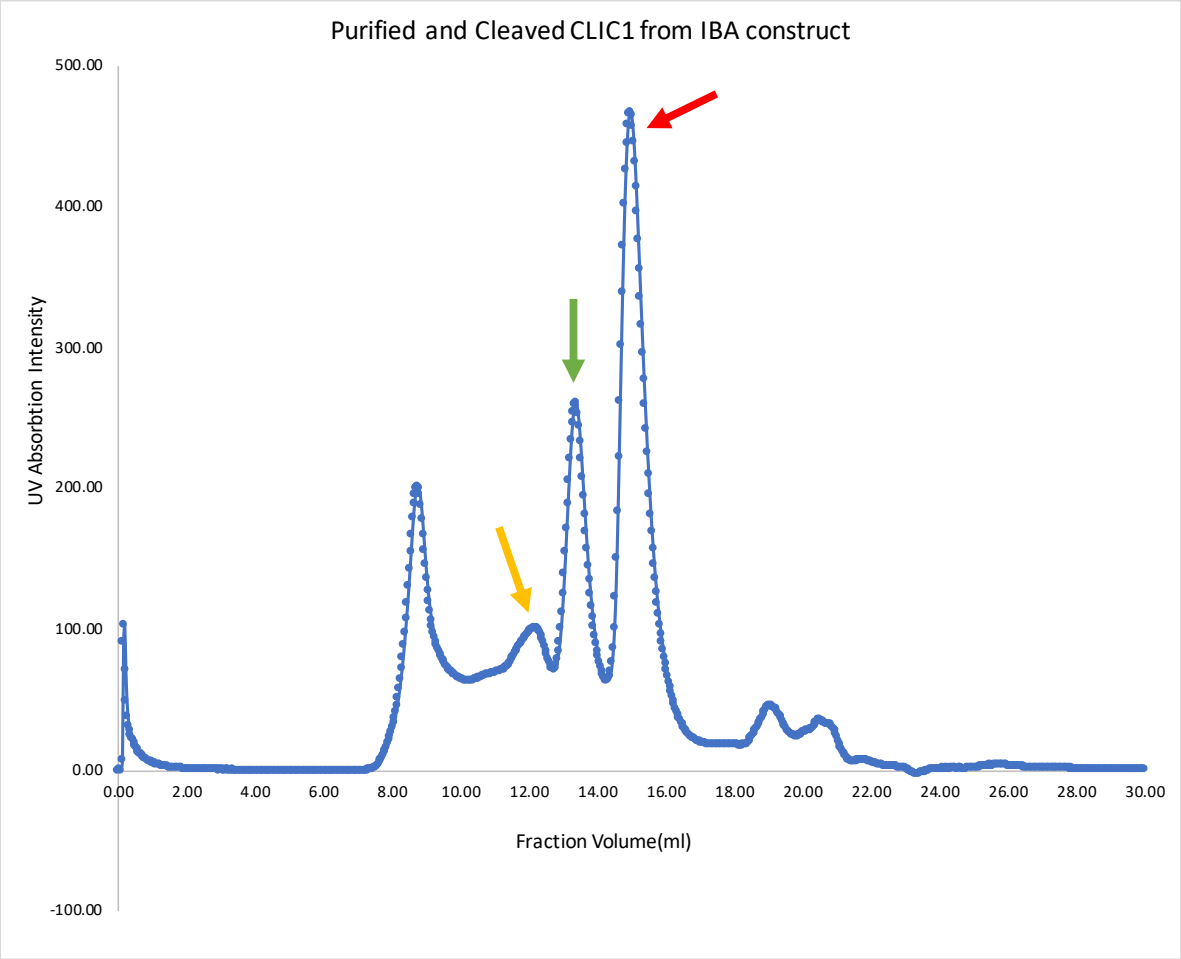

Figure 2.9 – Size exclusion chromatography image of CLIC1 purified from the pASG vector. Red arrow indicates monomers, green arrows indicates dimers and orange arrows indicates higher order oligomers in solution due to the peaks correlating with the molecular weights of each oligomer in fraction volume.

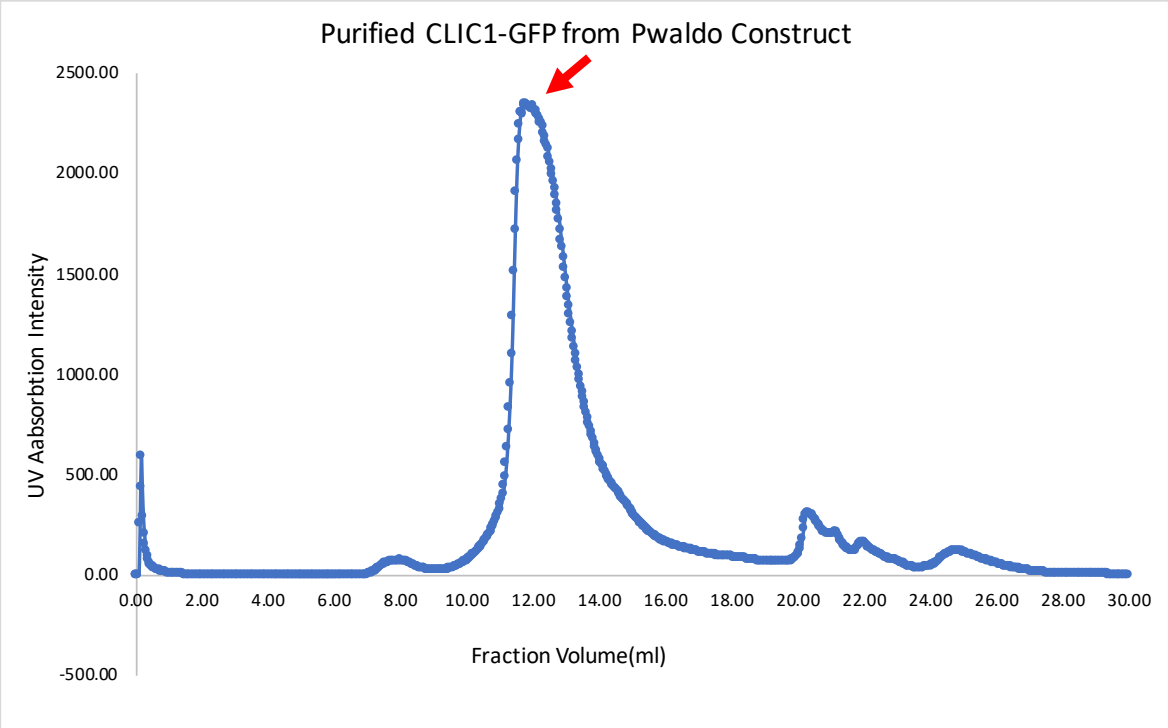

Figure 2.10 – Size exclusion chromatography of GFP labelled CLIC1. Size exclusion chromatography image of CLIC1 purified in the pWaldo vector with a GFP C-terminal tag. Red arrow indicates a peak for at the fraction volume corresponding to a monomeric species. However, the broadness of the peak could incorporate dimeric species.

2.3.6 Detecting CLIC1 protein by Intrinsic tryptophan fluorescence

CLIC1 is known to have one tryptophan residue in its sequence (Figure 2.1), which means intrinsic tryptophan fluorescence can be used to study the protein using a fluorimeter. Preliminary native tryptophan fluorescence readings were carried out on both the protein prepared from the pASG vector and GFP labelled protein expressed from the pWaldo vector (Figure 2.11). It can be seen clearly that for the protein produced in both expression vectors a clear signal is seen within a bell-shaped curve. In addition, both samples of protein show a peak emission of fluorescence around 340 nm. Both spectrums for the unlabelled CLIC1 and CLIC1-GFP produce similar spectrums suggesting a similarly folded protein. These findings

demonstrate that through both means of expression and purification viable protein is produced, in addition CLIC1 purified through these methods can be shown to be folded as a mixture of alpha helices and beta sheets through circular dichroism (CD) (Figure 2.12).

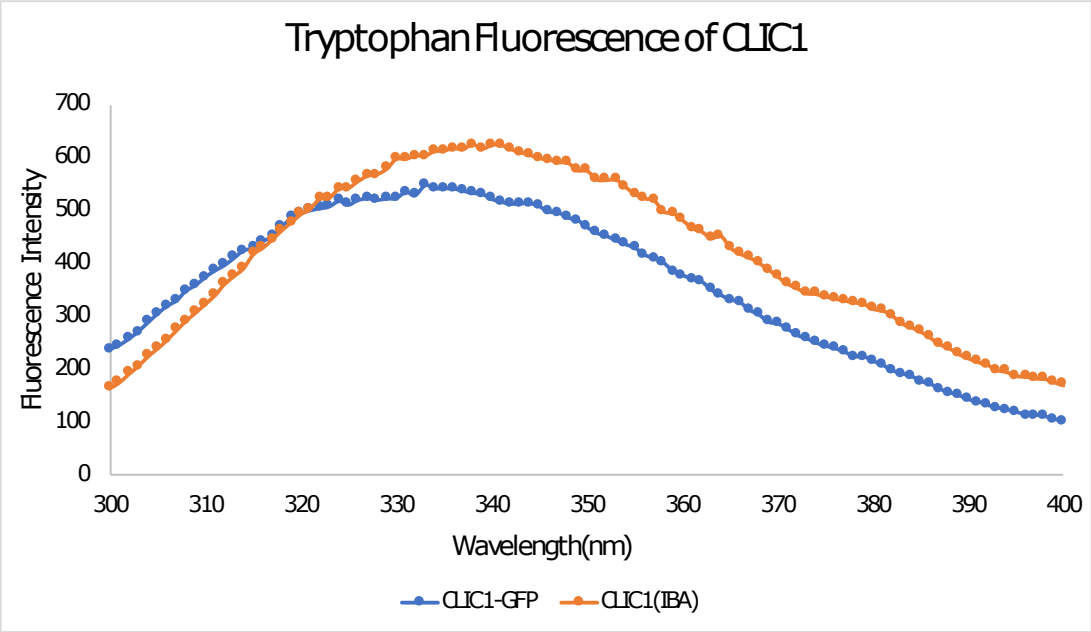

Figure 2.11 – Tryptophan fluorescence signal of CLIC1. Intrinsic tryptophan fluorescence signal of CLIC1 recombinantly expressed in the pASG vector and GFP labelled CLIC1 recombinantly expressed in the pWaldo vector.

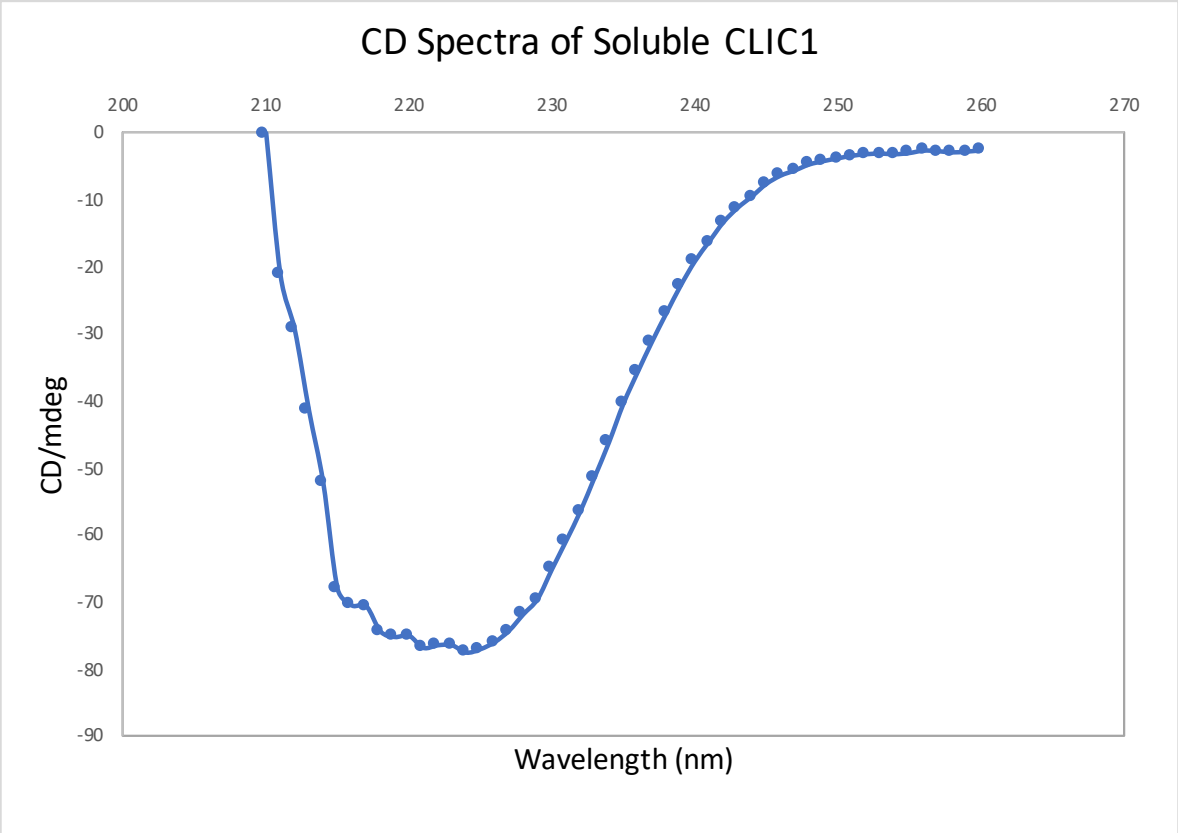

Figure 2.12 – CD spectrum of purified CLIC1. A mix of alpha helices, with known 'W shape' with minima at 222 nm and 208 nm, and 'V' shaped trough of β sheet at 218 nm can be seen (Ranjbar & Gill, 2009). This correlates with the published crystal structure of CLIC1 as a mix of alpha helical chains and pleated β sheets (Harrop et al., 2001).

2.3.7 CLIC1 naturally favours insertion into *E. coli* membranes during recombinant expression.

Detection of the GFP fluorescently labelled CLIC1 within *E. coli* cells allows identification of where CLIC1 naturally resides, whether cytoplasmic or as a membrane channel in a cell, albeit prokaryotic, during recombinant expression. CLIC1-GFP from *E. coli* cell lysate was detected after induction demonstrating effective protein production, before centrifugation to separate the soluble fraction of the cells from the membrane fraction. The soluble fraction shows low GFP fluorescence signal, with the membrane pellet showing high GFP fluorescence

signal.(Figure 2.13) To further confirm the findings the addition of fluorescence intensity of the soluble and membrane fraction approximately totals the fluorescence signal from the initial reading. This shows little protein is lost to the experimental process or to precipitation. Based on the GFP fluorescence readings 80% of protein produced in *E. coli* was found to naturally insert into the membrane (Figure 2.13).

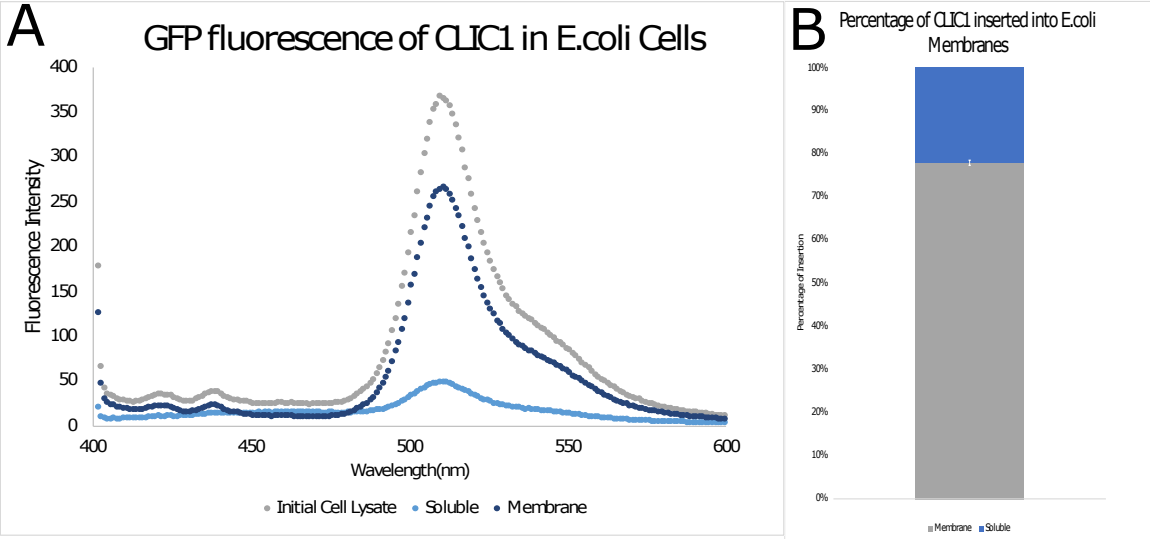

Figure 2.13 – GFP fluorescence intensity of *E. coli* cells induced for expression of pWaldo CLIC1-GFP. A- Fluorescence spectrum of CLIC1-GFP in cell lysate and subsequent soluble and membrane fractions after centrifugation. B- Calculated percentage of protein insertion into the *E. coli* membranes after induction of CLIC1 by measuring GFP in soluble and membrane fractions. N=2

2.4 Discussion

Expression tests revealed that specifically for CLIC1 in both the pASG vector and pWaldo vectors, C43 competent cells provide good yields of the protein, at the correct molecular weight, with the other two cell lines tested showing their unsuitability for producing soluble CLIC1. Unlabelled CLIC1 was successfully purified with high yields using this particular expression vector and purification system. There are a many different affinity tags available for protein purification and it can be difficult to select an appropriate methodology, however the use of streptactin technology can be seen to clearly produce unlabelled CLIC1 efficiently. In addition, the production of unlabelled CLIC1 is essential for experiments studying how CLIC1 is folded, and how this could change when inserting into the membrane, and using this specific vector allowed purification of protein for this purpose, as twin strep tag allows the use of chelating agents and metalloproteins compared to his tags.

Molecular cloning of the DNA for the gene of CLIC1 into the pWaldo vector was shown to be successful by confirmation of the sequence. The suitability of the specific pWaldo vector for recombinant expression of CLIC1 is confirmed with high yields of the protein. This production of this specific vector allowed the formation of a fluorescently labelled protein that provided the ability to study CLIC1 in various ways which could not be done with the pASG vector produced CLIC1. The protein produced was in high yields and was subsequently used for fluorescence assays on a fluorimeter, electroporation tests and microscopy. Nickel chromatography is known to bind the protein with high affinity.

It is important to note that throughout my PhD research the presence of divalent cations, in particular Ca^{2+} and Zn^{2+} have become of importance for CLIC1 insertion into the membrane and in order for thrombin cleavage to be carried out, $CaCl_2$ must be present in the buffer. This means the use of TEV protease instead of thrombin in the purification of CLIC1 has been a huge advantage in preparing protein samples with no divalent cations present.

The high molecular weights of the bands on the SDS gel seen with the Origami cells lines reveal that likely a different protein was expressed in the growth as oligomerisation of CLIC1 is unlikely to produce proteins of these molecular weights, 70 kDa & 120 kDa. Dimers and tetramers promoted by possible disulphide bond formation in CLIC1 would be displayed at molecular weights 54KDa and 108Kda respectively. The formation of disulphide bonds in CLIC1 are implicated to be involved in production of the channel protein (Singh & Ashley, 2006), explaining why these cell types were investigated, as an intramolecular disulphide bond between cysteine-24 and cysteine-59 was shown to be necessary for CLIC1 channel activity (Littler et al., 2004). The SHuffle competent cell line failed to produce good yields of CLIC1 at all. For this reason, C43s were confirmed as the optimal growth conditions for the protein in both the pASG vector and pWaldo constructs. C43s are a mutant strain of BL21s, and furthermore are known for their ability to overcome toxicity associated with recombinantly expressing protein (Dumon-Seignovert et al., 2004). Carrying out expression tests for both constructs were essential in establishing the ideal combination of cell type, media and induction temperature that allowed production of good yields of CLIC1 for all subsequent studies within my PhD.

Purification of the protein was successfully carried out many times throughout my research and high yields are demonstrated by SDS gels with the clear formation of both monomer and dimer when separated by size exclusion chromatography. The use of gel filtration chromatography allowed us to directly compare whether CLIC1 oligomerises differently in the presence of the GFP tag and it is clear that for both constructs the highest ratio of protein is as a monomeric species. In the soluble CLIC1, distinct monomer and dimer species peaks are seen, however with the fluorescently labelled CLIC1, the peak corresponds to monomer but is broad and could encompass the presence of dimers too. Information of the oligomerisation state of the soluble protein can be determined from these experiments and it is clear than in solution CLIC1 expressed from the pASG vector exists as predominantly a monomer with a smaller amount of dimer species, and to an even lesser degree higher order oligomeric species, hypothesised to be tetramers, however this can greatly depend on the initial protein concentration or buffer and for further verification SEC-MALS experiments could be run. This confirms literature findings of CLIC1 oligomerisation, with it known that CLIC1 can transition between the two oligomerisation states of monomer and dimer with higher order oligomers believed to be involved in formation of the channel (Warton et al., 2002). When looking at the oligomeric states of CLIC1 labelled with GFP purified from the pWaldo vector, there is only a distinguishable peak for monomers which could indicate that the presence of the GFP tag shifts equilibrium towards the protein existing solely as a monomer, compared to the unlabelled protein. This could be due to the GFP tag on the C-terminus of CLIC1 stabilising the monomeric form or preventing the formation of a dimer, which may be due to residues on the c-terminus of the protein being

necessary for the binding of two monomers. The N-terminal domain is hypothesised to be the putative transmembrane domain and involved in structural rearrangement to form the integral channel (Littler et al., 2004). Furthermore, as discussed in Section 5.3, placing the GFP tag on the N-terminal domain reduces insertion of CLIC1 into lipids, while the C-terminal GFP tag still shows insertion. This could mean the reduction in dimerisation in the gel filtration spectrum compared to unlabelled CLIC1 doesn't affect the insertion into the lipids.

Tryptophan fluorescence studies formed a basis for much of the research carried out on CLIC1 within the project. Initial tests of intrinsic native tryptophan fluorescence of the purified soluble protein revealed clear bell-shaped signals of CLIC1, even when only one tryptophan residue is present within the protein. Detecting a clear signal for CLIC1 produced in both the pASG vector and pWaldo vectors allowed the development of this assay to investigate insertion into lipids. These experiments also provided the ability to tell of any loss of the protein in different buffer conditions as precipitation of the protein would result in reduction of the fluorescence signal.

In addition to tryptophan fluorescence the pWaldo vector allowed GFP fluorescence studies of the protein and demonstrated the high percentage of CLIC1 purified as a membrane protein compared to a soluble protein when expressed in *E. coli*. The large ratio of membrane protein to soluble protein allowed optimisation of protein yields in each purification, by revealing that by extracting protein from the membrane fraction the yield of soluble protein would increase for each purification. This finding also tells us that this human protein can readily insert into the *E. coli* membranes and the conditions in these cells actively favours the channel formation. These findings led to investigation of the protein within the *E. coli* cells using In-cell NMR and trying

to identify whether this process of insertion is reversible or not, as discussed in Section 5.

Circular dichroism experiments on the soluble protein revealed that the secondary structure of CLIC1 was a mix of alpha-helix and beta-pleated sheets which corelates with the described crystal structure of the protein (Harrop et al., 2001). This indicates that CLIC1 purified through these methods is correctly folded. Furthermore, purification of CLIC1 in *E. coli* has been shown in literature to form active channels (Tulk et al., 2000) and also bind glutathione (Harrop et al., 2001), which shows this bacterial recombinant expression is suitable for producing folded CLIC1.

In conclusion studying and optimising the steps of recombinant expression and purification has allowed successful and efficient production of CLIC1, both unlabelled and fluorescently labelled. Even at the purification stage we have learnt about the oligomerisation state of the soluble protein and how much naturally inserts into a prokaryotic membrane, as well as a high yield of protein purification being essential to the experiments and findings described in later chapters.

CHAPTER 3: CLIC1 insertion into membrane with metals

3.1 Introduction

CLIC1 exists as a globular cytosolic protein, known to be involved in cell cycle regulation and hypothesised to have an enzymatic role for many cellular processes. The protein is also known to take on an integral membrane channel form, shown to transport chloride ions across membranes, whether with unidirectional efflux or influx of the ions remains to be elucidated. The true mechanism of this transition from cytosolic to membrane channel and how CLIC1 reorganises its conformational state to structurally form a channel additionally remains unknown. This chapter provides evidence for the first time that divalent cations, such as Zn^{2+} and Ca^{2+}, are the trigger for the translocation of CLIC1 into intracellular and plasma membranes.

CLIC1 was shown to form a chloride conductive channel in the plasma membrane and nuclear envelope of a mammalian cell (Tonini et al., 2000; Valenzuela et al., 1997), while also found to localise with the endoplasmic reticulum (Ponnalagu, Rao, et al., 2016). CLIC1 that forms these channels was also found soluble within the cell and found to play an active role in regulating the cell cycle (Valenzuela et al., 2000).

The transition into the membrane has been investigated previously, due to the known overexpression of CLIC1 and the membrane form in diseased states, such as cancer cell proliferation and tumorigenicity (Peretti et al., 2015). It has been shown that CLIC1 expression differs, with localisation to the membrane in different proportions to its cytosolic counterpart in different cell types (Ulmasov et al., 2007) so investigating the mechanism of how CLIC1 structure changes to become a channel and what drives CLIC1 channel formation is of clinical interest.

CLIC1 as a soluble protein has been successfully purified on many occasions and crystallography has shown it exists as a monomer in solution (Harrop et al., 2001). Oxidation of the monomer was found to increase insertion into a bilayer (Goodchild et al., 2009) and a dimer crystal structure was also formed upon oxidising conditions and a shift of equilibrium towards dimer was seen in solution (Littler et al., 2004). Vesicle sedimentation assays upon treatment with H_2O_2, saw a higher percentage of CLIC1 bound to vesicles and conductance assays revealed upon oxidation of the protein, the chloride ion channels increased (Goodchild et al., 2009). Oxidation has since been perceived as the trigger for CLIC1 insertion into the membrane. Cysteine 24 has been implicated as a key cysteine residue which upon oxidation could initiate dimerisation of the protein by forming an intramolecular disulphide bond with the non-conserved cysteine 59 (Littler et al., 2004).

However, the literature proves to be contradictory, with lots of evidence for pH involved in the CLIC1 mechanism for membrane association, in particular lowering the pH to around 5.5 triggers the change in the protein conformation needed to insert as a channel. Alpha helix 1 of the putative transmembrane domain of CLIC1 was shown to become more flexible and partially unfolded in an acidic environment exposing a hydrophobic surface, this implies the protein can insert more readily in a low pH (Stoychev et al., 2009). In addition, electrophysiology studies show chloride channel activity was seen quicker with the protein at lower pH than neutral pH and the rate of CLIC1 interaction with liposomes was shown to increase at pH 6.5 compared to pH 7.4 (Warton et al., 2002). Chloride efflux assays were also shown to have the highest efflux rate at pH 5 and decreased towards neutral pH, interestingly increasing as the pH increases from neutral to pH 9 (Tulk et al., 2002).

A third factor thought to be involved in CLIC1, is the addition of cholesterol. Cholesterol has previously been implicated in aiding pore channel formation of bacterial toxins (Palmer, 2004) and increasing cholesterol composition in the membrane was found to increase CLIC1 conductance as a channel (Valenzuela et al., 2013). However, it is clear even in the presence of lower concentrations or in the absence of cholesterol, CLIC1 membrane conductance can still be seen. This leads to evidence suggesting a cholesterol independent mechanism for CLIC1 insertion into the membrane exists while higher cholesterol composition is preferential (Valenzuela et al., 2013).

The following chapter describes a methodology designed to test CLIC1 insertion into lipids based upon measuring intrinsic tryptophan fluorescence. This is a powerful tool which does not affect the protein and can quantify the amount of protein once split into a soluble supernatant and lipid membrane fraction. The same methodology was used to test various buffer conditions and stimuli for CLIC1 membrane insertion. Divalent cations such as magnesium, calcium and zinc were found to be the trigger for such insertion.

3.2 Methods

3.2.1 Purification of CLIC1 and C24 mutant

Protein purification of both CLIC1 and the mutant, with a mutation in cysteine 24 from cysteine to an alanine, here purified according to the methodology described in section 2.2.3. Both constructs contained streptactin chromatography tags and were purified into 20 mM sodium phosphate, 20 mM NaCl pH 7.4 buffer for initial experiments and into 20 mM HEPES, 20 mM NaCl pH 7.4 for all experiments using divalent cations.

3.2.2 Fluorescence Assays

Thin films of Asolectin (Sigma Aldrich), a lipid extract from soybean, DMPC (Avanti), a synthetic phospholipid and DMPC + PE (Avanti) were prepared by solubilisation of the lipids with chloroform, dried under a nitrogen stream and solubilised in HEPES or phosphate buffer. Intrinsic native tryptophan fluorescence was recorded by excitation at 280 nm and emission was measured between 300 nm to 400 nm and GFP fluorescence was recorded by excitation at 395 nm for emission between 400 nm to 500 nm for the GFP-labelled samples, using a Varian Cary Eclipse fluorimeter. 10 µM CLIC1 was incubated with 1:300 molar ratio of Asolectin/DMPC/PC + PE and initial fluorescence was recorded. All initial experiments were incubated at room temperature, and later experiments at 30°C due to increased insertion seen at this temperature compared to room temperature experiments. Optimisation of insertion of CLIC1 was investigated using different conditions, such as lowering the pH of the buffer, the addition of H_2O_2 or DTT at varying concentrations, or the addition of divalent cations such as Zn^{2+}, Ca^{2+}, Mg^{2+} and Cu^{2+}. The samples were then

ultra-centrifuged at 208000g for 30 minutes at 25°C to separate the membrane vesicles and soluble protein. The soluble fraction was extracted from the membrane fraction immediately after centrifugation and the pellet resuspended to similar volume as the supernatant. Fluorescence readings were then recorded for both samples with the same protocol as used for initial recordings. The percentages were calculated from the average reading of the fluorescence spectra for the membrane fraction against the total protein recorded from the sum of the soluble and membrane fractions together. All fluorescence intensities were normalised to the initial recordings with the buffer and lipid background subtracted.

3.2.3 Vesicle fluorescence microscopy

The formation of giant unilamellar vesicles were generated using a protocol adapted from (Manley & Gordon, 2008; Veatch, 2007). The vesicles were made using asolectin lipid thin films, prepared as described above, in 50 mM HEPES 50 mM NaCl pH 7.4. 1 mM Nile red lipophilic stain (ACROS Organic) was mixed with 2 µl/cm^2 of 1 mg/ml lipid before application to two ITO slides, which was then dried under vacuum for 2 hours. The lipids were then rehydrated using 100 mM Sucrose, 1 mM HEPES pH 7.4 buffer and 10 Hz frequency sine waves were applied to the lipids for 2 hours. The consequential liposomes were then recovered and diluted into 100 mM glucose, 1 mM HEPES pH 7.2 buffer. The liposomes were incubated with 90 nM CLIC1-GFP and either treated with 0.5 mM $ZnCl_2$ 0.5 mM $CaCl_2$ or left untreated. After incubation at room temperature for ten minutes, the samples were placed in an 8 well Lab-Tek Borosilicate coverglass system (Nun) and microscopy was performed with a Zeiss

LSM-880 confocal microscope using 488 nm and 594 nm lasers. All images were processed with Zen Black Software.

3.2.4 MST & channel activity assay

Both experiments were performed by other members of the Ortega Roldan laboratory and were carried out per methods described in (Varela et al., 2019).

3.3 Results

3.3.1 Investigating CLIC1 insertion into the membrane via intrinsic tryptophan fluorescence

A methodology (Figure 3.1) was designed to investigate the triggers for CLIC1 insertion, where the intrinsic tryptophan fluorescence of CLIC1 was measured in both a soluble fraction and in a membrane vesicle fraction to see how much of the soluble CLIC1 could insert. Different buffer conditions were applied to investigate the reported triggers of membrane insertion such as oxidation state of the protein and pH.

3.3.2 CLIC1 tryptophan fluorescence shifts in the presence of lipids

Intrinsic protein fluorescence was used to quantify the concentration of CLIC1, and a shift in fluorescence was observed when asolectin lipids were added, from a maximum intensity of 340 nm to 350 nm (Figure 3.2). It is important to note the overall decrease in fluorescence intensity is due to the dilution of the sample when adding the lipid, as the methodology is highly sensitive to change in concentration of protein. This observed shift in the maximum intensity peak of tryptophan fluorescence in the presence of lipids, could indicate an interaction between the lipid and the protein. Asolectin lipids were selected as CLIC1 has previously been reported to confer chloride permeability into this specific lipid composition (Tulk et al., 2000, 2002) as well as the membrane of mammalian cells (Valenzuela et al., 1997), in addition to asolectin being a cost-effective eukaryotic membrane model.

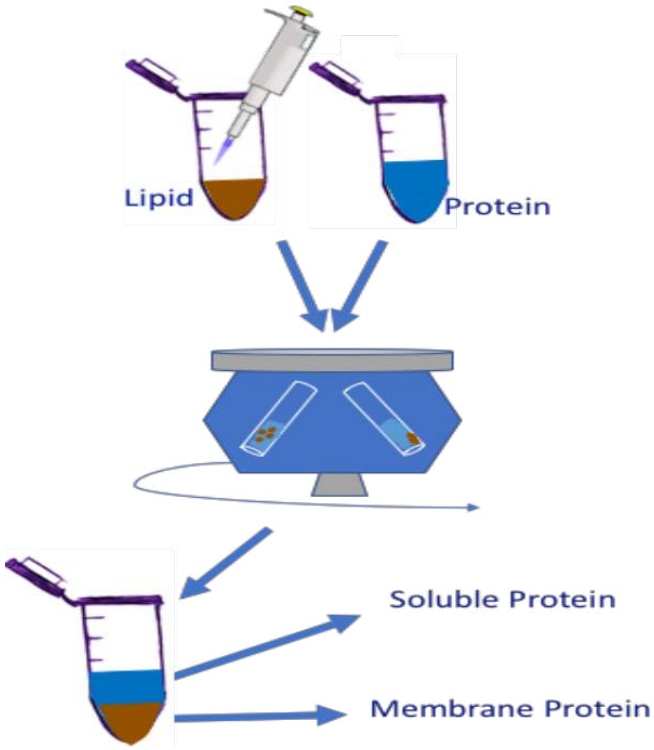

Figure 3.1 – Diagram of the protocol used to measure CLIC1 membrane insertion. Representation of methodology to investigate the insertion of soluble CLIC1 into lipids. The soluble protein and lipid are mixed, with different buffer conditions, they are then centrifuged to pellet the lipids. Immediately after centrifugation the soluble protein is removed as supernatant and the lipids are resuspended to the same volume. Intrinsic tryptophan fluorescence is measured for both the soluble and membrane fraction to detect the degree of membrane insertion.

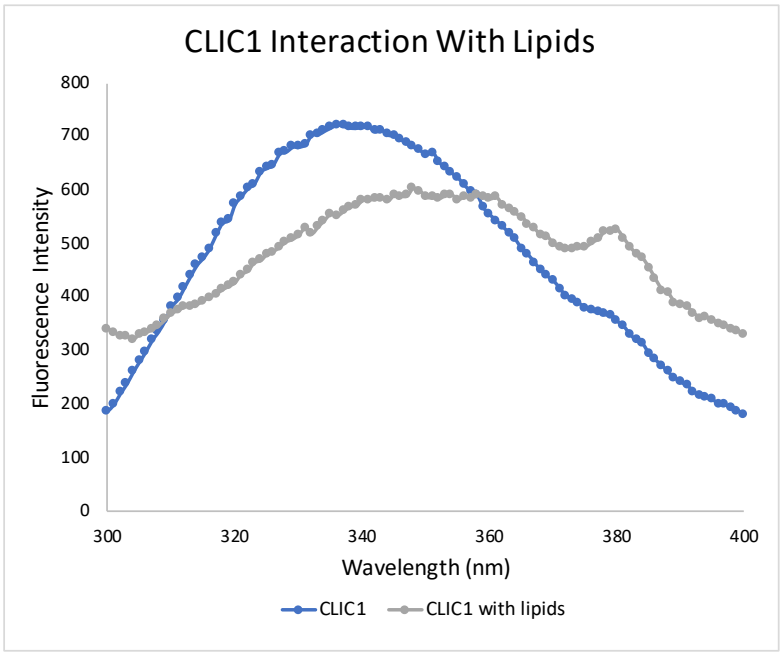

Figure 3.2 – Initial fluorescence readings of soluble CLIC1. Maximum Peak in tryptophan fluorescence emission spectra can be seen for CLIC1 alone and CLIC1 incubated with asolectin lipids.

3.3.3 Initial trials of CLIC1 insertion revealed little insertion into the membrane

The first experiments carried out to study CLIC1 insertion into asolectin membranes saw little insertion when comparing the intensity of the tryptophan emission fluorescence maxima in the membrane fraction to the soluble form. The emission spectra of the soluble fraction in this experiment revealed little protein inserted into these lipids compared to the soluble fraction and further optimisation was required, beginning with changing buffer conditions. This experiment was carried out in pH 7.4 phosphate buffer (Figure 3.3).

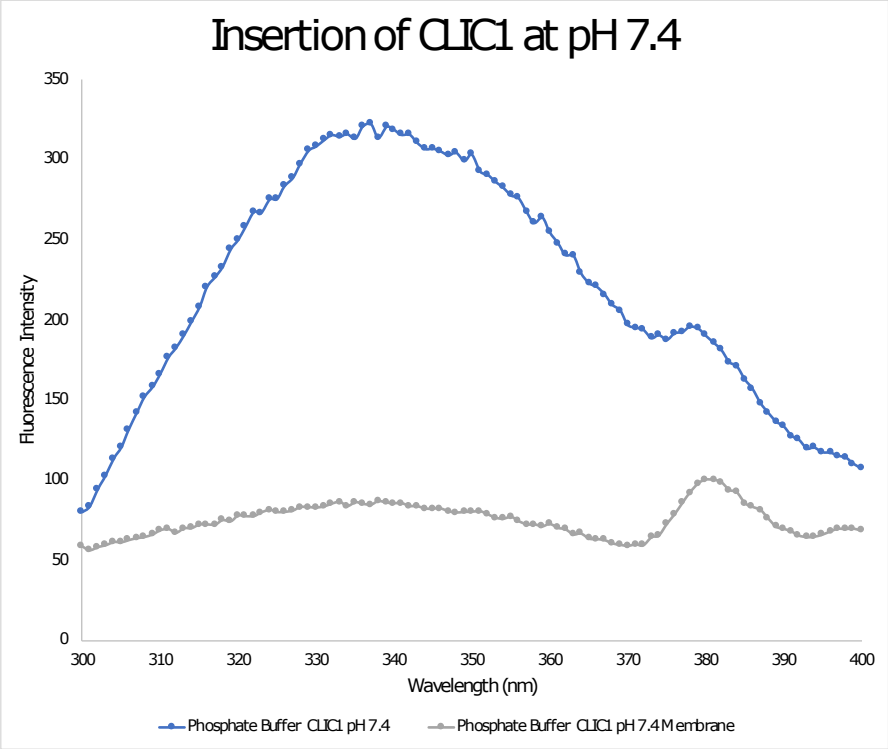

Figure 3.3 – Initial experiment on insertion for CLIC1 into asolectin. The intrinsic tryptophan fluorescence of CLIC1 in both the soluble and membrane fraction of the experiment carried out as detailed in Fig 3.1. This experiment was carried out in sodium phosphate buffer at pH 7.4.

3.3.4 An increase in experimental temperature could aid protein insertion

Two different temperatures were used to also identify whether performing the experiments at a higher temperature could take the lipids above the hypothesised phase transition temperature of the asolectin lipids and improve insertion. The phase transition temperature is the temperature at which a lipid bilayer transitions from an ordered gel phase to a disordered liquid phase (Oldfield & Chapman, 1972), and increasing the temperature from room temperature, ~20°C to 30°C could allow more insertion of CLIC1 due to any conformational change between the lipids within asolectin. The phase transition temperature of temperature of asolectin is ill defined (O'Neill & Leopold, 1982), however the lipid mixture is comprised of mainly PC and PE lipids which have phase transition temperatures ranging from of 0-80°C and 30-90°C respectively (Silvius, 1982). In phosphate buffer at both room temperature and 30°C there is minimal insertion of CLIC1, based on the tryptophan fluorescence spectra of the membrane protein fraction (Figure 3.4). At 30°C there is a marginal increase of a bell-shaped curve of insertion seen for CLIC1 at pH 7.4, however very little protein insertion into the lipids is seen and the spectra appear noisy. Further optimal conditions are needed for the proteins' translocation.

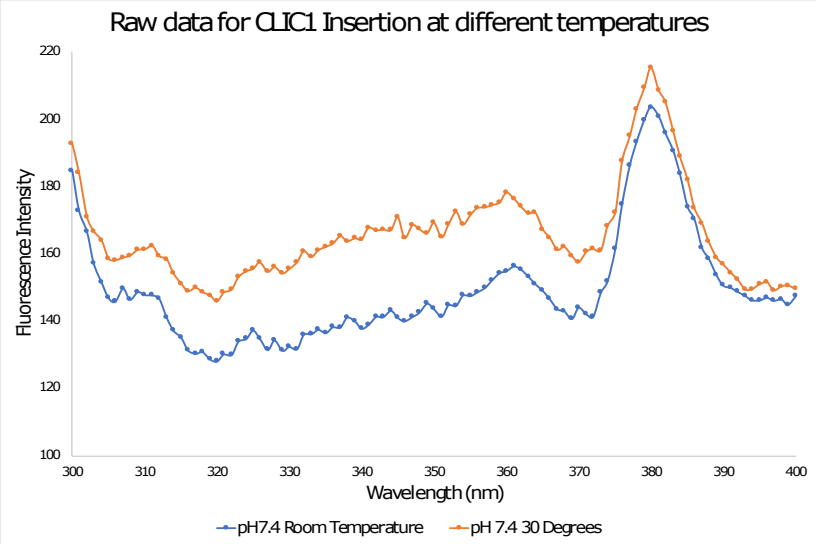

Figure 3.4 – CLIC1 in membrane fraction at varying temperatures. Intrinsic tryptophan fluorescence of CLIC1 showing the insertion into the asolectin lipid membrane fraction, after incubation at different temperatures.

3.3.5 Low pH or oxidation had little or no effect on protein insertion

Oxidation state and pH are thought to be the possible triggers for CLIC1 relocalisation from the cytoplasm to the membrane to form a chloride channel. In order to verify whether low pH and oxidation of CLIC1 did aid insertion, the lipid insertion assay was repeated at low pH 5.5 and with oxidation and reduction of CLIC1, by H_20_2 and DTT respectively, all at 30°C in phosphate buffer. There was no real insertion of CLIC1 into the lipids seen when untreated or with oxidation with H_2O_2 or reduction with DTT (Figure 3.5A). The data further proved to be inconsistent with previous literature as CLIC1 at pH 7.4 and the protein at pH 5.5 failed to insert into the lipids (Figure 3.5B). The lack of insertion can also be seen in Figure 3.5C, where the shape of the fluorescence detected is important in determining whether CLIC1 has inserted into the membrane, a clear gaussian curve for fluorescence is shown when CLIC1 is present, Figure 3.3, but the fluorescence remains flat for all of the membrane fractions whether at low pH or treated for oxidation or reduction. To verify if higher

concentrations of H_2O_2 were needed to see insertion an optimisation with three different concentrations was performed, all in excess molar concentrations to the protein. Little change in CLIC1 insertion into asolectin was seen compared to the control and there was no dose dependent correlation observed (Figure 3.6). These results indicate the optimal insertion conditions for CLIC1 had not yet been deduced and low pH or change in oxidation state are not responsible for the protein's membrane channel formation.

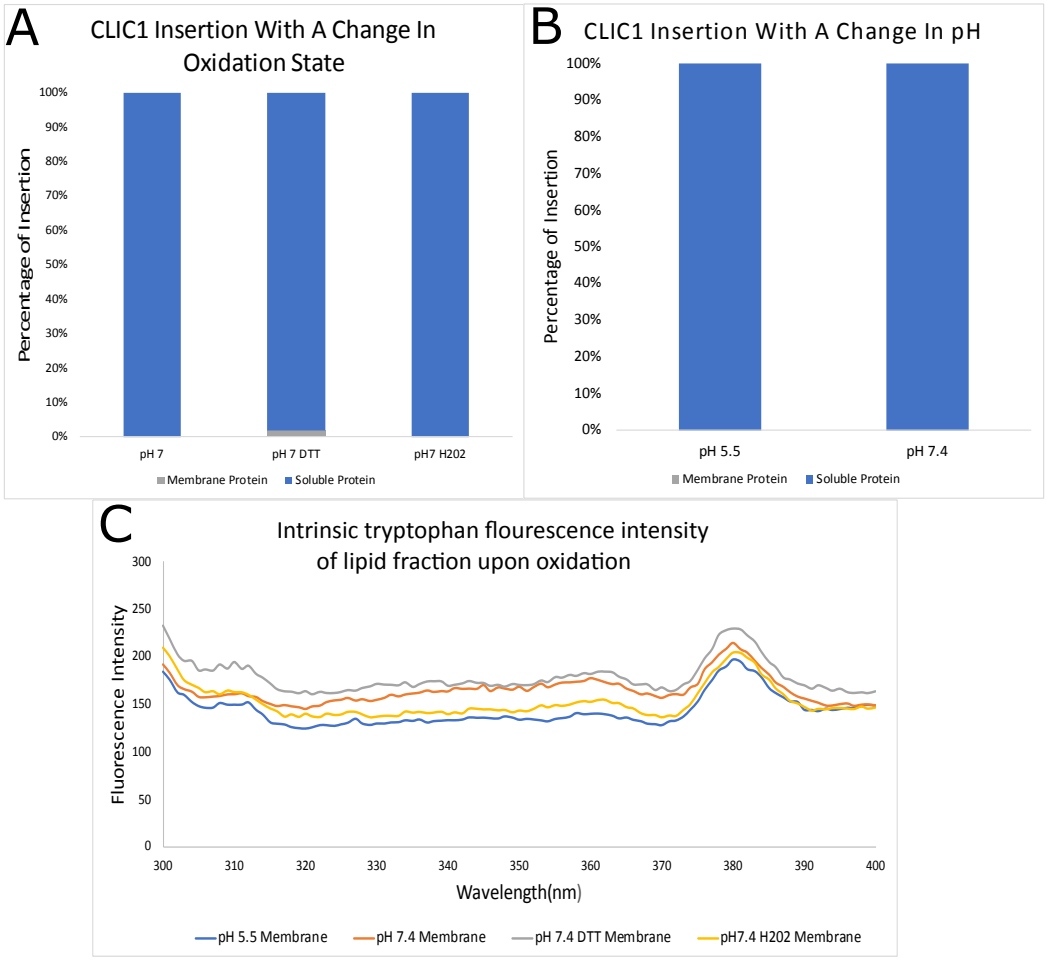

Figure 3.5 – CLIC1 insertion into asolectin lipids when altering the oxidation state and pH. A – The percentage of CLIC1 insertion into the lipid membrane fraction when the protein is oxidised by treatment with 500 µM H_2O_2 and reduced by treatment with 200 µM DTT. B – The percentage of CLIC1 insertion into the membrane fraction at two different pHs, pH 5.5 and pH 7.4. C – Intrinsic tryptophan fluorescence intensity of CLIC1 in the asolectin membrane fractions under these conditions.

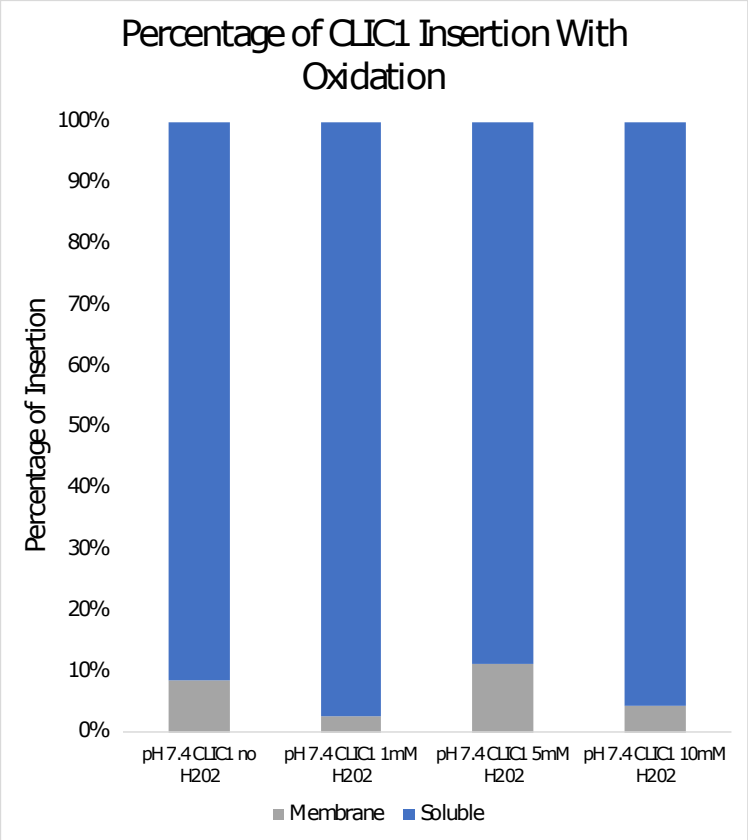

Figure 3.6 – Optimisation of CLIC1 insertion into asolectin membranes with increasing concentrations of hydrogen peroxide. CLIC1 was treated with increasing concentrations of hydrogen peroxide for protein oxidation and the intrinsic tryptophan fluorescence was measured in both the soluble and lipid membrane fraction to quantify percentage insertion in these conditions.

3.3.6 CLIC1 in HEPES buffer showed the first signs of insertion

All previous experiments with little insertion were assayed with CLIC1 in phosphate buffer, however when CLIC1 and the asolectin lipids were used in the tryptophan fluorescence experiment, a clear bell like curve was seen when measuring the fluorescence intensity and the percentage of insertion showed a clear increase (Figure 3.7). This change in buffer allowed CLIC1 insertion to be reproducible in experiments and all following experiments were carried out in this buffer.

The possible hypotheses for differences in insertion seen when CLIC1 was place in HEPES buffer was investigated and divalent cations being freely available to the protein in this buffer but not in phosphate buffer was hypothesised to play a role. Divalent cations have previously been studied in other protein's conformational changes (Manak & Ferl, 2007) and with the knowledge that phosphate buffer is known to form insoluble complexes with divalent cations (Van Wazer & Callis, 1958), while HEPES is known to have very low metal binding affinity, it was deemed the next logical step for insertion factors.

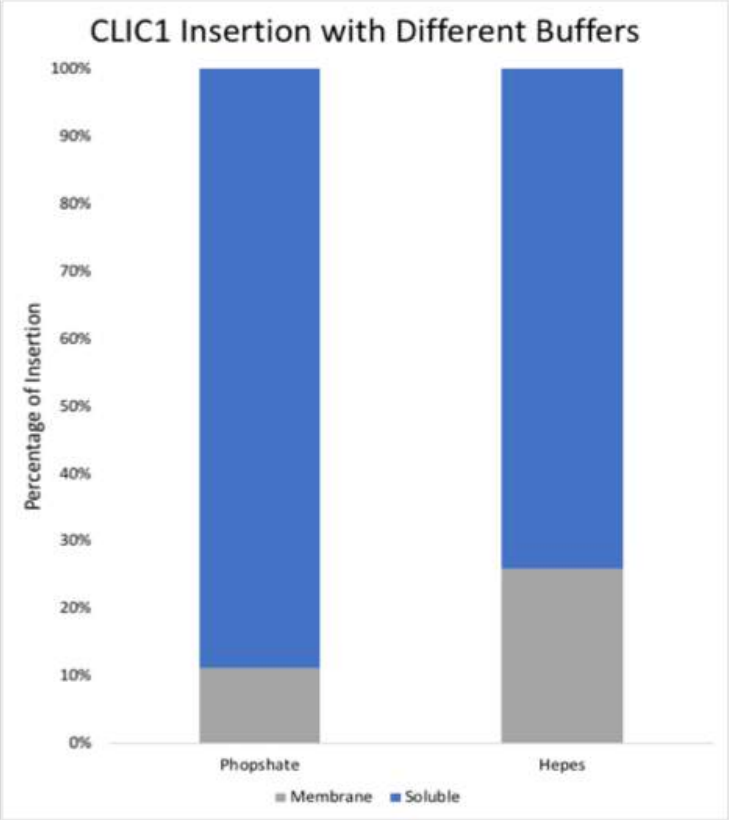

Figure 3.7 – CLIC1 insertion in different buffer compositions. CLIC1 was incubated with lipids in different buffer conditions, 20 mM sodium phosphate, 20 mM NaCl pH 7.4 against 20 mM HEPES, 20 mM NaCl pH 7.4 and the intrinsic tryptophan fluorescence was measured in both the soluble and lipid membrane fraction to quantify insertion in these conditions.

3.3.7 Divalent cations increased CLIC1 insertion

Physiologically relevant divalent cations $Ca^{2+,}$ $Mg^{2+,}$ Zn^{2+} and Cu^{2+} were tested as possible triggers for CLIC1 membrane insertion. The percentage of insertion was found to markedly increase with all divalent cations against the control, clear gaussian fluorescence curves for the membrane fraction were observed, showing for the first time clear CLIC1 insertion into the asolectin lipids (Figure 3.8). The data collected revealed zinc to have the biggest effect on CLIC1 insertion, followed by magnesium and calcium ions, with percentages of insertion as high as 80%, 70% and 40% respectively. The experiment was also attempted with copper but no spectra of CLIC1 could be collected, possibly due to quenching of the tryptophan signal by the copper (Duan et al., 2016; J. C. Lee et al., 2008).

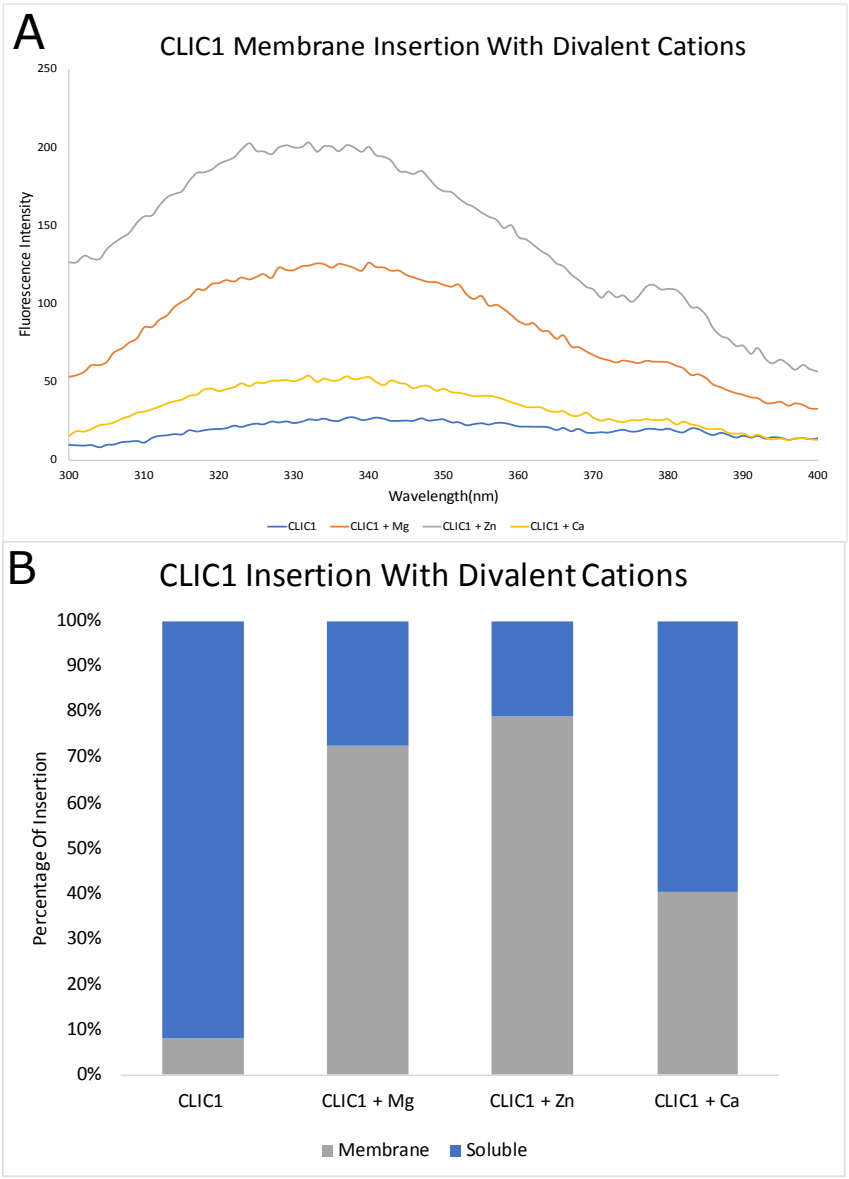

Figure 3.8 – Native tryptophan fluorescence of CLIC1 insertion into asolectin lipids in the presence of (1mM) divalent cations. A – Spectra of intrinsic tryptophan fluorescence of CLIC1 in the asolectin membrane when incubated with 1mM Mg^{2+}, Zn^{2+} and Ca^{2+}. B – Percentage of membrane insertion of total CLIC1.

3.3.8 High concentrations of divalent cations can lead to CLIC1 precipitation

In order to optimise the use of divalent cations for CLIC1 insertion into the membrane, the concentrations of both calcium and zinc ions were assayed with CLIC1 and the total protein in both the soluble and membrane fraction were compared. From the visible eye it was clear that when divalent cations were added

to soluble CLIC1 alone, precipitation formed, yet when the lipids were present before addition of the metals less precipitation occurred. High concentrations of divalent cations saw CLIC1 insert in the membrane but to ensure this was not traded off by loss of majority of the protein the assay was repeated with three ten-fold concentrations of Ca^{2+} and Zn^{2+}.

Total CLIC1 protein from both the soluble and membrane fraction is negatively correlated as the concentration of Zn^{2+} increases, this shows clear precipitation as more metal is present (Figure 3.9). The total protein with increasing concentrations of Ca^{2+}, seems to stay fairly level with slight fluctuations between 1mM and 100mM calcium but unlike with zinc, no clear correlation is seen.

The clear precipitation of CLIC1 in the presence of too high Zn^{2+}, means the concentration of zinc ions in all future experiments was kept at 1 mM or below and always added after the lipids were present. The samples were also visibly checked for clear signs of precipitation as it could decrease the intensity in soluble fractions. Furthermore, any aggregation of the protein that would pellet in the membrane fraction, would not affect the fluorescence intensity recorded in this sample as this protein would no longer display tryptophan fluorescence.

3.3.9 EDTA was shown to significantly reduce insertion of CLIC1 into asolectin

EDTA, a known metal chelator, was shown to significantly reduce the protein in the membrane fraction when measured for intrinsic tryptophan fluorescence, when compared to the protein in HEPES buffer with no treatment (Figure 3.10). This experiment was repeated in duplicate and the difference in insertion was shown to be statistically significant when EDTA was added.

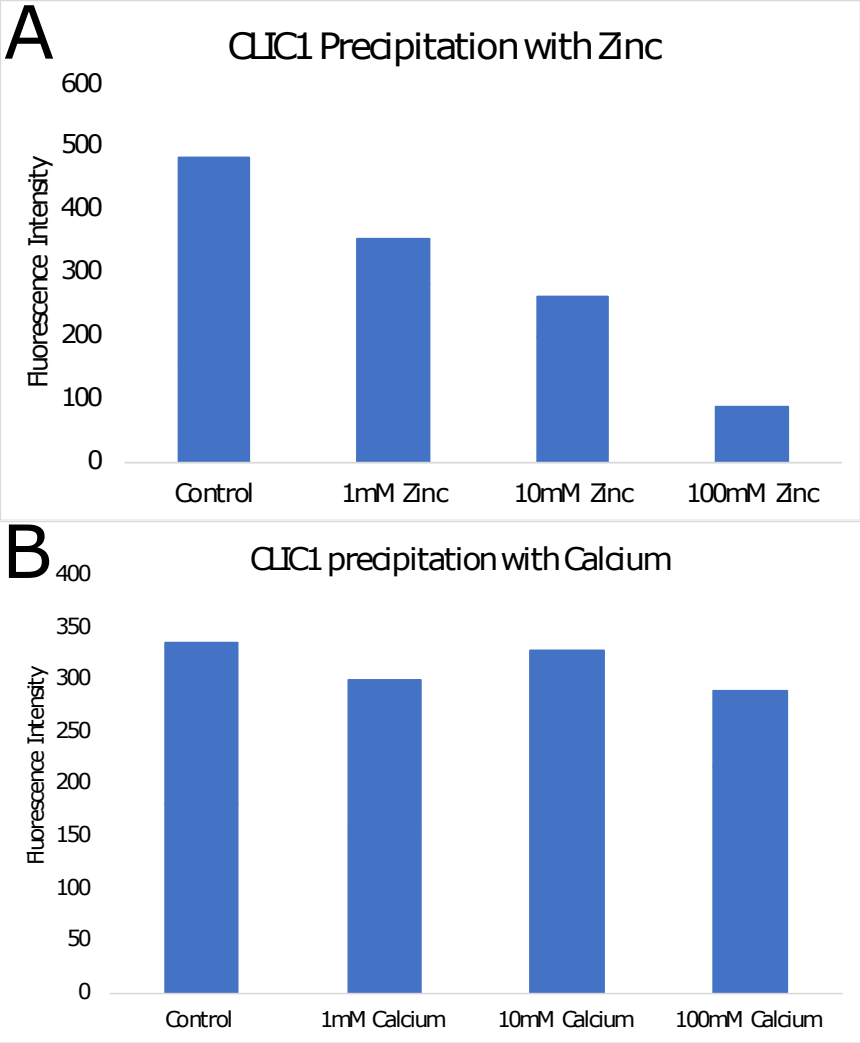

Figure 3.9 – CLIC1 precipitation test with calcium and zinc. The intensity of intrinsic tryptophan fluorescence for total CLIC1 was recorded after performing the fluorescence assay seen in Fig 3.1, under treatment with increasing concentrations of divalent cations. A – Optimisation of the concentration of Zn^{2+}. B – Optimisation of the concentration of Ca^{2+}.

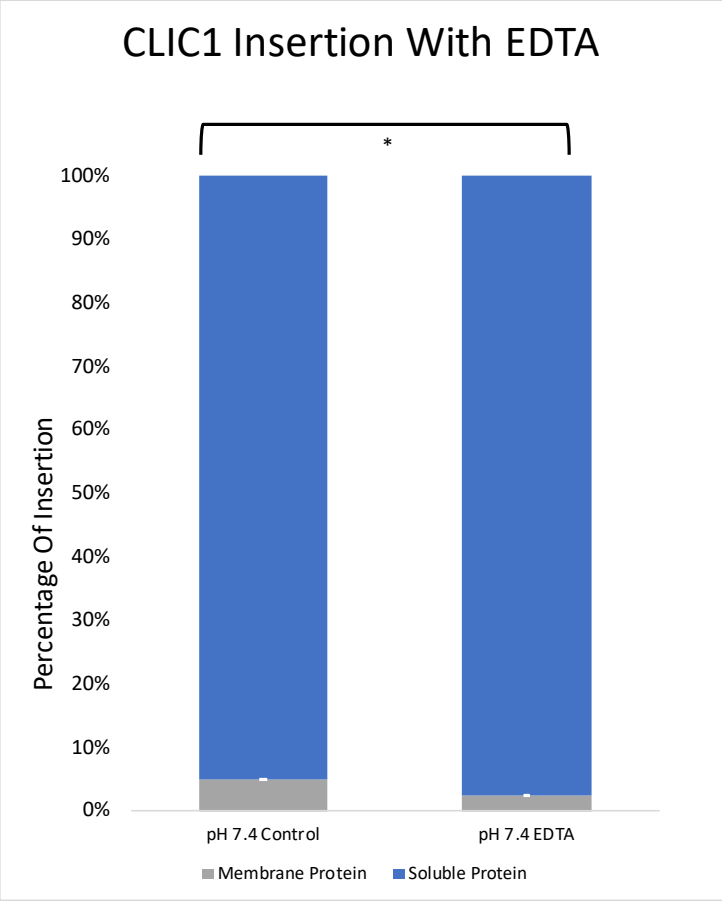

Figure 3.10 – EDTA effect on CLIC1 insertion. Percentage of CLIC1 Insertion into asolectin lipids when treated with 2 mM EDTA compared to a control with no treatment. Statistical analysis Paired T test, * $p < 0.05$ n=3

3.3.10 CLIC1 insertion with divalent cations can be seen in more than one composition of lipids

CLIC1 can be seen to insert into the DMPC and DMPC + PE lipids upon treatment with both calcium and zinc (Figure 3.11), these specific lipids were selected due to CLIC1 chloride conductance shown in asolectin enriched with both PC & PE lipids (Tulk et al., 2002) and upon investigating the lipid selectivity of CLIC1, PC & PE were shown to be the most abundant so the closest to physiological conditions (Medina-Carmona et al., 2020). The insertion of CLIC1 into these lipids showed similar values to insertion into asolectin (Figure 3.8), if not slightly higher values of insertion. This demonstrates

the insertion of CLIC1 into lipids is not limited to one lipid type, asolectin, and the protein insertion could be selective.

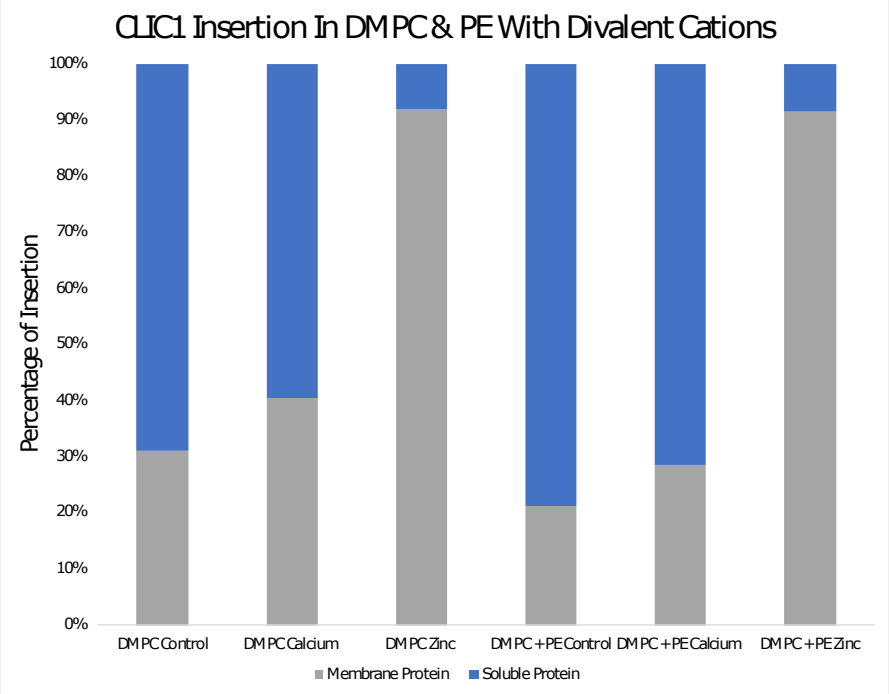

Figure 3.11 – CLIC1 insertion into other types of lipids besides asolectin. The percentage of CLIC1 insertion into the membrane fraction in both DMPC lipids alone and DMPC + PE lipids, treatment with 40 µM divalent cations were used to trigger insertion.

3.3.11 Low pH or reducing conditions did not enhance CLIC1 insertion with divalent cations

CLIC1 insertion with divalent cations was not enhanced with lowering the pH of the buffer, instead the insertion remains unaltered as the pH was lowered to pH 6 the percentage of insertion with no treatment and with zinc were similar to that at pH 7.4. An increase in insertion when zinc is present is still seen for both pHs compared to the control (Figure 3.12).Upon treatment with divalent cations and DTT, to reduce the protein, clear CLIC1 insertion was still seen at both pHs (Figure 3.12).

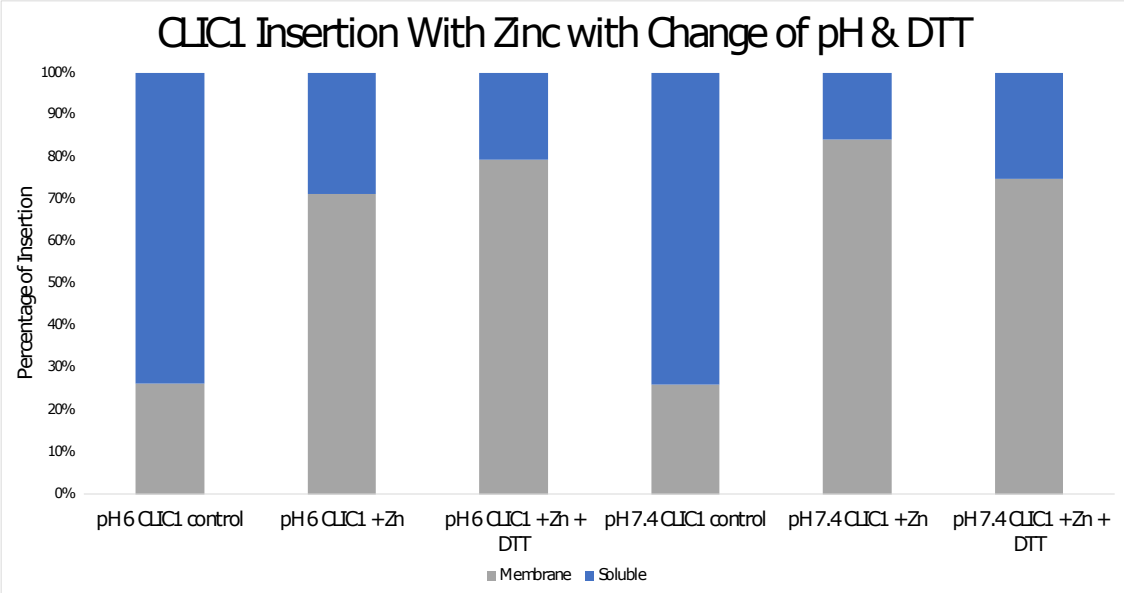

Figure 3.12 – Testing protein reduction and lower pH on the optimised lipid insertion of CLIC1 with Zn^{2+}. pH effect and reduction of the protein with 1 mM DDT on percentage of CLIC1 insertion into asolectin lipids with 30 µM zinc.

3.3.12 Lowering the molar ratio of zinc shows insertion and allows the effect of lowering the pH to be seen more clearly

All previous experiments were carried out in a high excess of divalent cation to protein, instead the excess of zinc was decreased to a molar ratio of 1:50, the same molar ratio used in the latter GUV microscopy experiments (Figure 3.16). First, an experiment testing the insertion of CLIC1 into asolectin with divalent cations was carried out and clear insertion can be seen with all three cations; magnesium, calcium and zinc compared to the untreated control (Figure 3.13). Another experiment at this molar ratio was carried out where CLIC1 insertion was recorded at three different pHs: pH 5.5, pH 6 and pH 7.4. The opposite effect to what was expected from literature was seen (Figure 3.14), as lowering the pH did not enhance CLIC1 insertion, instead lowering the pH was correlated with less insertion in the presence of Zinc. However, all three pHs still displayed clear insertion of CLIC1 into the lipids compared

to no treatment and the results correlated to previous experiments where the divalent cations were added in higher excess. A caveat of this technique combining zinc and low pH when measuring the insertion of CLIC1 is that the low pH can cause the protein to precipitate and this is enhanced in the presence of zinc. However, upon optimisation, it was found if the lipids were already present in the mixture with the protein before addition of any metals, then less precipitation occurred.

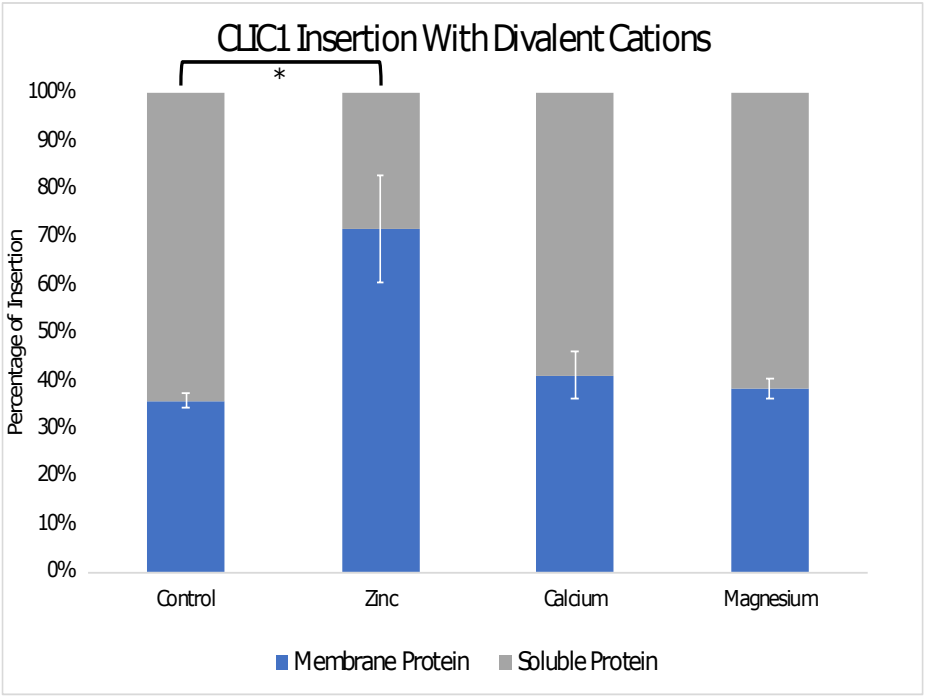

Figure 3.13 – Triplicate assay of divalent cation insertion of CLIC1 into asolectin lipids. Percentage of protein that inserted into the lipid membrane is shown upon treatment with divalent cations. This intrinsic tryptophan fluorescence assay was performed with a molar ratio of 1:50 protein to metal salt. Statistical analysis was performed using a paired T test where * = $p < 0.05$ n=3.

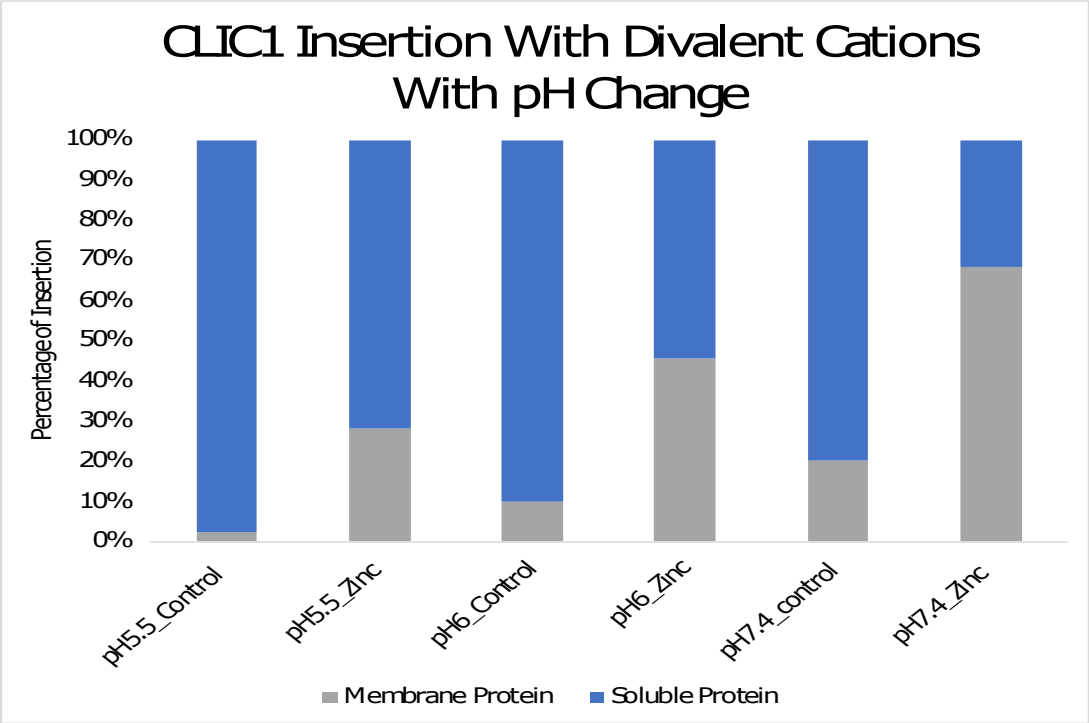

Figure 3.14 – Effect of low pH on CLIC1 insertion into asolectin lipids with optimised insertion conditions with zinc. Intrinsic tryptophan assay performed with a molar ratio of 1:50 protein to Zn^{2+} and percentage of insertion into lipids shown.

3.3.13 Microscopy shows CLIC1 insertion into lipids vesicles

Divalent cations were further confirmed as the trigger for CLIC1 insertion into the lipids by confocal microscopy. CLIC1 with a C-terminal GFP tag, so not to interfere with channel formation, was incubated with giant lipid vesicles labelled with a red dye. When an excess of both calcium and zinc were added into the buffer, clear colocalisation of the CLIC1 protein to the lipid vesicles could be seen. Calcium induced more CLIC1-lipid colocalisation then the control in HEPES buffer alone, and zinc was seen to induce a bigger change in CLIC1 localisation to the lipid vesicles than calcium (Figure 3.15). This was then repeated with lower molar ratios of divalent cation to protein, 1:50, and the same effect was seen, zinc induces a clear localisation

change in the protein, so that it associates with the lipid vesicles more than in the control where no zinc is added (Figure 3.16). pH was also investigated with this method to confirm whether low pH increased the insertion of CLIC1 with zinc. The microscopy images revealed there was very little difference between pH 5.5 and pH 7.4, where treatment of zinc saw lipid colocalisation in both experiments (Figure 3.16). These results correlate with no increase of insertion being seen at low pH with the intrinsic fluorescent experiments.

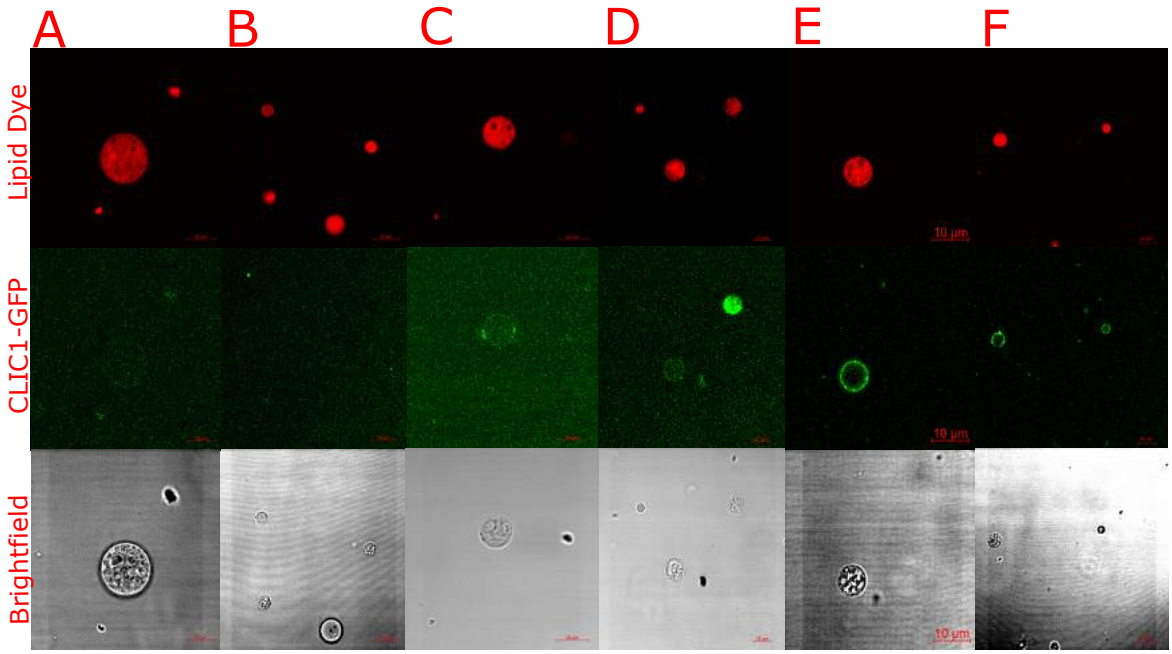

Figure 3.15 – CLIC1 insertion into giant vesicles under treatment with calcium and zinc at pH 7.4. Images of CLIC1-GFP (green) insertion into lipid vesicles (red) are shown with no treatment (A&B), 500 mM Ca^{2+} (C & D) and 500 mM Zn^{2+} (E & F). Brightfield images included to show individual vesicles.

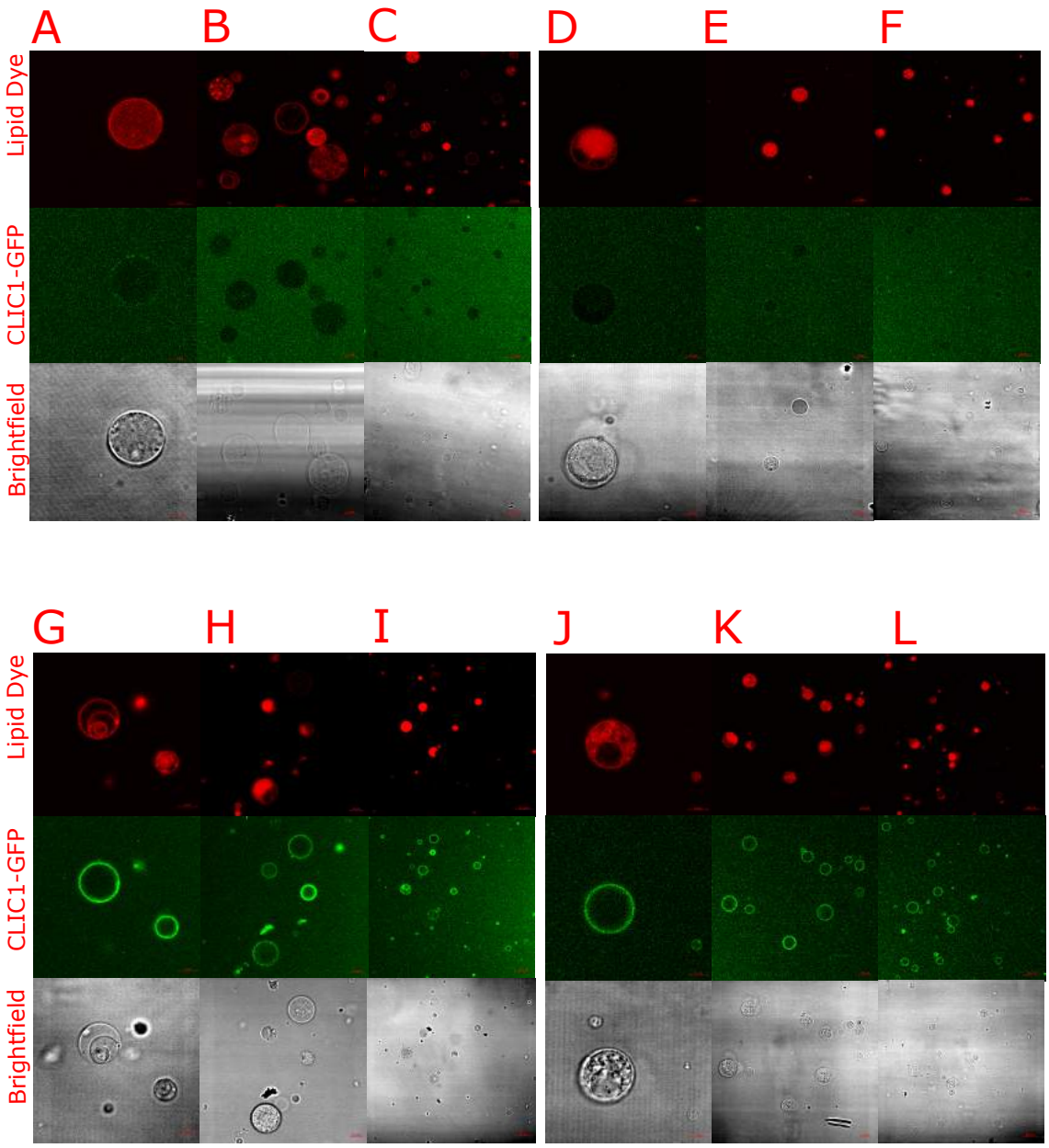

Figure 3.16 – Giant vesicle confocal images of CLIC1 insertion at different pH. Control images of CLIC1-GFP (green) insertion into lipid vesicles (red) at pH 7.4 (A, B & C) against control images at pH 5.5 (D, E & F). CLIC1 treated with 1:50 molar ratios of Zn^{2+} at pH 7.4 (G, H & I) and pH 5.5 (J, K & L). Images of multiple number of vesicles are included for each treatment, alongside brightfield images to correctly identify vesicles.

3.3.14 CLIC1 is shown to directly bind divalent cations

Microscale thermophoresis (MST) experiments were carried out with soluble GFP-tagged CLIC1 with increasing concentrations of Ca^{2+} and Zn^{2+} ligand, they show a dose dependent change in binding affinity (Figure 3.17). These experiments also show a higher affinity for zinc than calcium by CLIC1, which is supported by the lipid fluorescence assays and GUV microscopy and further verify CLIC1 directly interacts with these specific divalent cations.

3.3.15 CLIC1 inserted into the membrane is forming active chloride channels

Chloride efflux assays show an increase in the ion release for CLIC1 in the presence of zinc compared to the protein incubated with EDTA or left untreated (Figure 3. 18). This indicates there is more active CLIC1 channels in the asolectin vesicles in the present of zinc than without and provides further evidence divalent cations are responsible for the insertion of CLIC1 into the membrane to form an active chloride channel.

3.3.16 Mutation of cysteine 24, a key residue implicated in dimerisation with oxidation of CLIC1 does not inhibit membrane insertion

Cysteine 24 is shown in previous literature to be an important residue for CLIC1 dimerisation and consequent oligomerisation for insertion into lipids as a channel, due to its ability to form a disulphide bond with cysteine 59. This dimerization is linked to oxidation of the protein, therefore a mutation in this residue was tested for protein insertion into the membrane. It was shown to still allow for CLIC1 insertion into asolectin lipids, albeit untreated C24A CLIC1 showed decreased insertion to

untreated CLIC1 in other figures, with an increase of insertion seen with the addition of divalent cations, calcium and zinc (Figure 3.19).

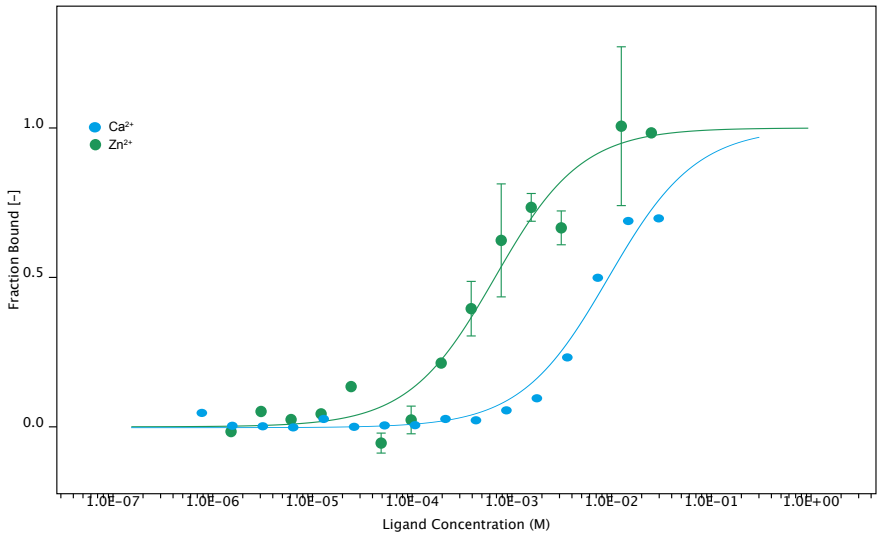

Figure 3.17 – MST experiments of CLIC1 binding to divalent cations Experiments show the amount of protein bound to divalent cations as the ligand concentration is increased. Treatment of CLIC1 was carried out with both calcium and zinc. (These experiments were performed by Dr Jose Ortega-Roldan as part of the laboratory project) (Varela et al., 2019).

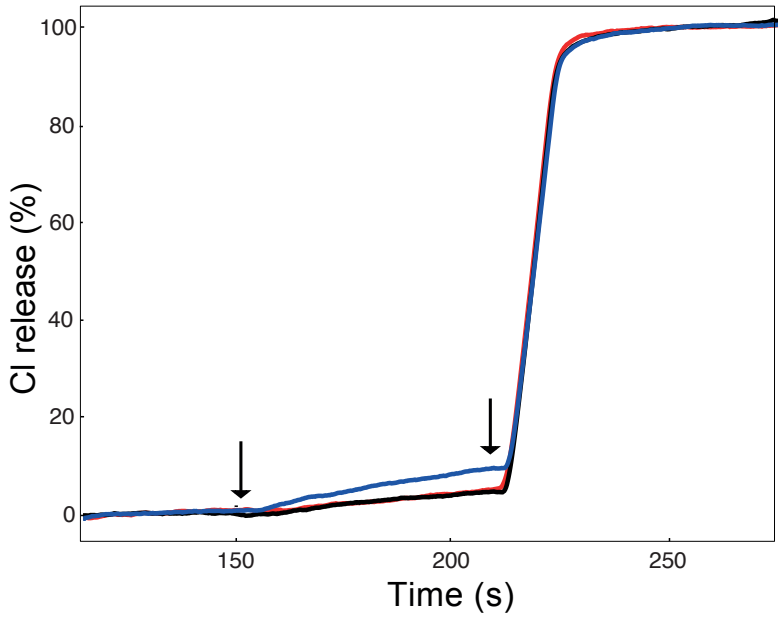

Figure 3.18 – Chloride efflux assays for CLIC1. CLIC1 with EDTA (red) and in the presence of zinc (blue), with a no treatment control (black). All chloride conductance was measured in asolectin vesicles. The first arrow indicates addition of valinomycin, an ionophore used to promote chloride ion transport and the second indicates addition of Triton-x100, a detergent used to break open the vesicles to reach a maximum Cl^- release. (Experiment performed by Dr Lorena Varela-Alvarez as part of the laboratory project) (Varela et al., 2019).

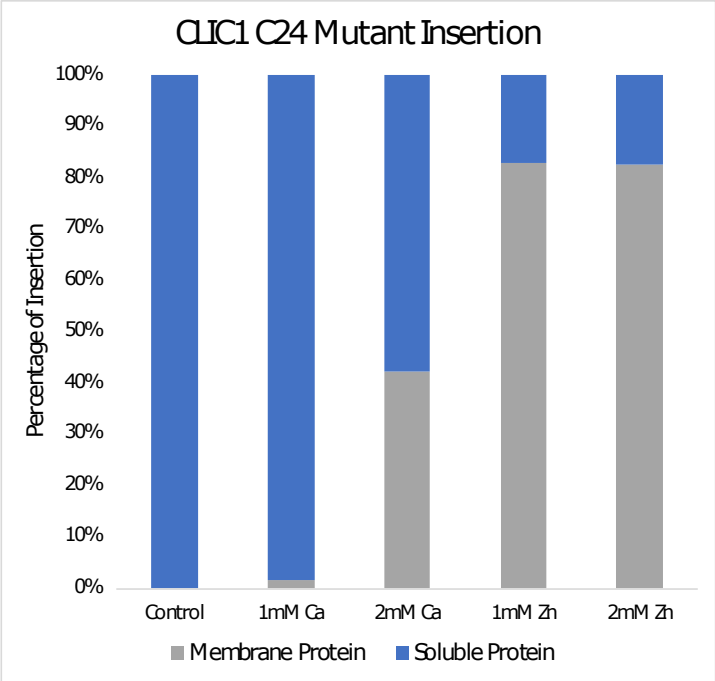

Figure 3.19 – CLIC1 mutant C24A insertion assay using intrinsic tryptophan fluorescence. The percentage of insertion of CLIC1 C24A mutant into an asolectin lipid membrane fraction is shown, different concentrations of both calcium and zinc were used to promote insertion.

3.3.17 Metformin treatment does not inhibit CLIC1 insertion into the lipid membranes

Metformin is a known CLIC1 inhibitor and has been shown to reduce cancer cell proliferation by inhibiting CLIC1 directly. To investigate whether metformin had any effect on insertion into asolectin membrane, the protein was treated with either metformin alone or with divalent cations to induce insertion with metformin.

An inhibition of CLIC1 insertion would be anticipated with the treatment of metformin but this was not seen against a control or with treatment of zinc, instead metformin was seen to increase insertion against the control and made no difference with zinc. Metformin appeared to decrease insertion slightly when CLIC1 was treated with calcium but insertion with metformin + calcium was still increased against

metformin or the CLIC1 control alone, showing insertion of the protein into the asolectin lipids (Figure 3.20).

This data suggests metformin is not an inhibitor of CLIC1 in regards to its insertion into the lipid membrane, however the metals for these experiments were carried out at 2 mM which is high excess to the protein and may counter any effects of the metformin as an inhibitor.

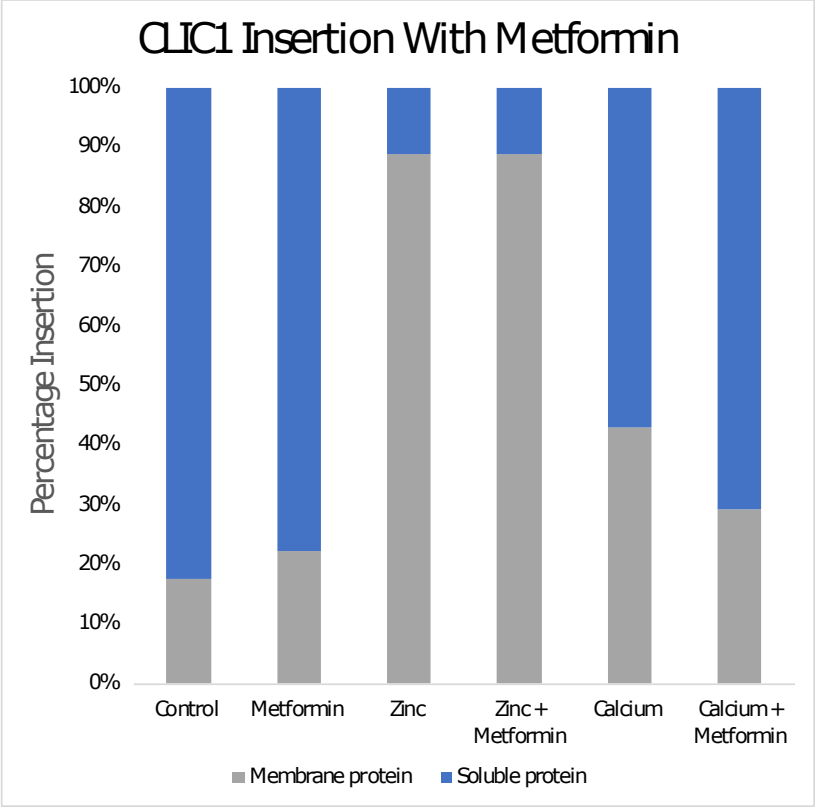

Figure 3.20 – CLIC1 membrane insertion assay using intrinsic tryptophan fluorescence when treated with metformin. The percentage of insertion of the protein into the asolectin membrane fraction is shown in the presence of the inhibitor metformin (3 mM) with and without 2 mM divalent cations used to promote insertion.

3.4 Discussion

The design of intrinsic tryptophan fluorescence assays provided a simple and effective method to visualise insertion of CLIC1 into different lipids under conditions to trigger insertion. The trigger of insertion of CLIC1 has been contradictory in literature for many years with oxidation state, pH and cholesterol all implicated, whether through observing oligomerisation or increased chloride efflux in membranes under these conditions, however this assay provides a clearer method to determine what percentage of the protein is actually inserting into the lipid membranes under these conditions.

Initial experiments testing the hypothesised triggers for insertion of CLIC1, such as oxidation of the protein and lowering the pH of the protein environment, did not reveal any significant changes in CLIC1 localisation and only a small percentage of insertion into the lipids was seen. The conditions tested were the same conditions from literature stating pH 5.5 induces more lipid flexibility, and incubation of the protein with H_2O_2 was enough to induce channel formation, however no CLIC1 insertion into lipids could be seen under these specific conditions.

All experiments were carried out primarily in phosphate buffer and it wasn't until changing the purification step of CLIC1 and tryptophan assay into HEPES buffer that any insertion was identifiable, with a clear increase of fluorescence in the membrane fraction. This change of buffer causing more CLIC1 insertion into the lipids led to the investigation of what difference these buffers could induce. Both buffers were created at the same pH, so no difference was induced by a change in pH. Upon research, phosphate buffer was found to from insoluble complexes with metal cations and cause them to precipitate (Ferreira, Pinto, Soares, & Soares, 2015; Good

& Izawa, 1972), whereas HEPES buffer was one of Good's buffers introduced to have weak binding affinity to metal ions so do not form complexes (Ferguson et al., 1980; Good & Izawa, 1972; Good et al., 1966). This led to the hypothesis metal ions may have a role in CLIC1 insertion into the membrane as a channel.

Insertion assays performed with a range of divalent cations, Mg^{2+}, Ca^{2+}, Zn^{2+} and Cu^{2+}, revealed an increase of insertion of CLIC1 into the lipids in the presence of these ions. The largest change in insertion against the control was visualised in the presence of zinc, but also with calcium and magnesium. Insertion with copper could not be detected using this assay as intrinsic tryptophan could not be detected, this may be due to coppers' proposed ability to quench fluorescence of tryptophan (Duan et al., 2016) or copper's interaction with HEPES buffer (Hegetschweiler & Saltman, 1986) as this interaction could explain the anomalous readings with Cu^{2+} when investigating the metal ions for CLIC1 insertion.

CLIC1 insertion was seen in the presence of metals in all consequent experiments, with increased levels of tryptophan fluorescence compared to controls in just HEPES buffer. These assays were performed with different lipid mixtures, with asolectin used as a eukaryotic lipid mixture, with then PC lipids selected due to their abundance in mammalian membranes. Insertion with zinc and calcium induced insertion in these lipid types also, confirming an increase in availability of these ions in a mammalian cell could trigger insertion into the membranes. Divalent cations have also been previously implicated in proteins' structural changes (Athwal et al., 1998; Manak & Ferl, 2007; Scipion et al., 2018; Stray et al., 2004). Calcium and zinc were focused on in these experiments due to the clear insertion of CLIC1 into the membrane and physiological relevance, on reflection magnesium and other possible

divalent cations could be studied with the same methodology. All experiments were carried out in large excess of divalent cations but even with reducing the molar ratio of metal to protein the same insertion could be seen.

There are clear discrepancies in the literature for the true trigger of CLIC1 insertion into the membrane. Literature heavily focuses upon oxidation to form a CLIC1 dimer and promote insertion into the membrane (Goodchild et al., 2009; Littler et al., 2005), while other literature points towards cholesterol being essential for CLIC1 membrane interaction and insertion (Hossain et al., 2016; Valenzuela et al., 2013). Low pH is also identified as a trigger in literature, stating increased protein flexibility at pH 5.5 promotes CLIC1 membrane insertion (Stoychev et al., 2009; Warton et al., 2002).

Upon closer inspection of the experimental procedures of previous literature where they identify either pH or oxidation state as the trigger for membrane insertion, the protein can actually be found to be purified in the presence of metals such as calcium, with thrombin cleavage being used with $CaCl_2$ present (Goodchild et al., 2009; Harrop et al., 2001; Littler et al., 2004; Valenzuela et al., 1997, 2013; Warton et al., 2002). In addition some of the electrophysiological studies of CLIC1 activity in the membrane show $CaCl_2$ or $MgCl_2$ in the assay buffer (Tonini et al., 2000; Valenzuela et al., 1997). Furthermore CLIC homologs in Drosphila melanoganster and Caenorhabditis elegans (C.elegans), DmCLIC and EXC-4 respectively, were shown to both have a metal ion binding site in the structure of the protein. Electron densities of the structure at this binding site correspond to a bound calcium ion, and demonstrate that the affinity must be high as the only calcium available was from thrombin cleavage during purification (Littler et al., 2008).

In addition, these conditions may be linked as part of complex cell signalling, as low pH could lead to an increased availability of divalent cations such as Ca^{2+} and Zn^{2+} in the cell as signalling molecules. For instance, in neurons a decrease in cellular pH triggered by an influx of calcium ions has been shown to increase intracellular zinc levels (Kiedrowski, 2012). Initiation of the production of reactive oxygen species to create an oxidising environment within a cell is also found to be implicated in literature to the a change in calcium ions and calcium ion signalling has been found to regulate ROS in a cell (Görlach et al., 2015). There could be complex signalling pathways involved in increasing the intracellular metal levels to trigger insertion of CLIC1 into the membrane, which in turn could produce ROS, or ROS induction could cause the intracellular levels of calcium to increase and what we have identified is the downstream cause of CLIC1 insertion.

A residue proposed to be of importance in the oligomerisation of CLIC1 and structural rearrangement for inserting as a channel is cysteine 24 due to its disulphide bond formation under oxidising conditions (Harrop et al., 2001; Littler et al., 2004; Singh & Ashley, 2006). A mutation in this residue of CLIC1 was generated and insertion was tested with the divalent cation treatment. The protein was still seen to insert into the lipid membrane under these conditions, providing further evidence that the hypothesised oxidation model for CLIC1 channel formation is not entirely correct and this residue is not essential for CLIC1 membrane insertion. Contradictory previous literature has also been seen to indicate that this cysteine 24 is not essential for optimal CLIC1 channel activity (Al Khamici et al., 2016).

A final factor implicated to be the trigger for the insertion of CLIC1 into membranes to form active channels is the addition of cholesterol to membranes, providing the

ideal insertion environment for the protein (Valenzuela et al., 2013). Under close inspection all bilayer membranes were prepared with calcium present in the buffer and the addition of cholesterol may just be an example of providing more ideal membrane compositions for the protein, for instance the differences of insertion seen between asolectin and the mammalian lipids.

To complement the intrinsic tryptophan fluorescence experiments the interaction of divalent cations such as zinc was approached from many angles, including investigating whether the metals directly bind the protein. Microscale thermophoresis (MST) experiments revealed CLIC1 has a binding affinity to both calcium and zinc, with the affinity even higher for the zinc ligand. The higher affinity to zinc corresponds to the intrinsic tryptophan studies where CLIC1 insertion is seen with a higher increase with zinc compared to calcium. The differences in the response of CLIC1 to these two metals could be due to the same binding site having different affinities for the two metals, with the binding affinity of zinc being much higher than calcium or due to the fact that the metals bind different sites on the protein and have different mechanisms of action, where the action of zinc happens with a stronger effect. More experiments are needed to investigate this and to deduce the exact binding site of the metals in the protein's structure, mutations in the binding site residues implicated in the drosophila and C. elegans homologs of CLIC1 would be an ideal first mutation site to investigate.

Investigations into whether metals, in particular zinc, lead to oligomerisation of the protein are worth exploring but have so far proved difficult with gel filtration due to the protein precipitating within the column. As shown in Section 2, when purifying CLIC1 a monomer and dimer are clearly shown, and equilibrium shifts towards higher

order oligomers could potentially be seen in the presence of zinc but requires further optimisation. Native mass spectrometry experiments were tried with CLIC1 in the presence of zinc, but unfortunately the metal was found to make the samples unable to run. These are a few of the challenges identified when working with protein with metal in solution. To overcome high levels of precipitation of the protein, adding the metal to the protein was only performed when the lipids were already present and lowering the levels of metals present greatly reduced the amounts of precipitation and aggregation, as shown in the optimisation experiments.

Divalent cations could induce CLIC1 aggregation for different reasons, and in the case of other proteins have been known to cause aggregation (Huang et al., 2020). One of the main reasons for protein aggregation is known to be the exposure of hydrophobic residues (Berrill et al., 2011). The binding to divalent cations could be causing a conformational change which could lead to a more exposed CLIC1 structure which is no longer stable in the soluble buffer conditions. In previous literature the formation of a channel has been linked to the exposure of a large hydrophobic surface forming the dimer interface (Littler et al., 2005), and divalent cations may induce this structural change. Aggregation can also be promoted by disulphide bond formation (Cromwell et al., 2006) and the addition of divalent cations could induce a conformational change which allows for dimerization between the protein monomers, which in turn could promote aggregation. Furthermore, binding of divalent cations to a specific binding site can cause changes to the steric conformation of the protein and cause local structural rearrangement of the molecules which could lead to more aggregation (Berrill et al., 2011).

Due to the above challenges another methodology, confocal microscopy, was used to study CLIC1 insertion with divalent cations further. Formation of the giant vesicles clearly showed elevated insertion of fluorescently labelled CLIC1 in the presence of calcium and an even more distinct change in localisation with zinc. Using microscopy provided strong visual evidence to solidify the theory that the addition of Ca^{2+} and Zn^{2+} is the trigger of CLIC1 insertion into lipid membranes. Section four also details the relocalisation of CLIC1, within a mammalian cell environment, with increased cellular calcium to the cell membranes, providing further evidence that the availability of divalent cations is the necessary trigger for CLIC1 channel formation.

All of the data combined provides evidence that CLIC1 inserts into the lipid membranes but not that the protein there is forming an active channel, therefore experiments studying the chloride ion release into solution was measured in the presence of CLIC1 alone, CLIC1 with EDTA and CLIC1 with zinc. There was a clear increase in chloride ion release when zinc was added to the protein, providing evidence that the protein inserting into the lipid is forming an active chloride channel.

Due to the clinical relevance of CLIC1 channel activity in diseases such as in cancer proliferation or neurodegenerative disease progression (Milton et al., 2008; Peretti et al., 2015), a known inhibitor of CLIC1, metformin was tested in the insertion assay to see if could prevent the insertion of the protein into the lipids when treated with divalent cations. The inhibitor is implicated in literature to act directly on CLIC1 (Gritti, Würth, Angelini, Barbieri, Peretti, et al., 2014) and to slow the progression of glioblastoma growth in clinical patients, however the mechanism is completely unknown. Insertion of CLIC1 into asolectin lipids, when treated with divalent cations

and metformin, was still seen, demonstrating that metformin does not directly inhibit the insertion of the protein into the membrane. This hypothesises that the inhibitor's mechanism of action may be involved in preventing the activity of the channel instead or interacts with the growth of the cancer cell via CLIC1 in a different cell signalling mechanism. More experiments to deduce how and if metformin directly interacts with the protein are needed.

Combined together all the data provides extensive evidence that divalent cations, specifically zinc and calcium are the trigger for CLIC1 insertion into lipid membranes. This finding has importance for many reasons, by deducing how to replicate CLIC1 insertion accurately using these triggers allows the further study of CLIC1 as a membrane channel by being able to form a stable model. This allows experiments to deduce more structural information about the protein as a membrane channel. In addition, identifying divalent cations as the trigger for insertion provides more information into the molecular mechanism of how CLIC1 forms the channel and the first steps in this process. It could also direct further studies into the cellular availability of these divalent cations in diseased states and how this can affect CLIC1 channel formation. Identifying these specific triggers allows for research into potential therapeutics to limit the binding of the divalent cations to CLIC1 but also to study drug binding sites on the channel form of the protein to prevent channel activity in disease states.

CHAPTER 4: CLIC1 relocalisation studies in mammalian cells

4.1 Introduction

The CLIC family of proteins are heavily implicated in diseased states of the human body, with all members contributing to an array of pathologies. CLIC6 is shown to have differential expression in breast cancer cells (Ko et al., 2013), and identified as a diagnostic marker for adenoid cystic carcinoma (Bell et al., 2011). CLIC5 is found to be overexpressed in human cancers such as liver cancer (Flores-Téllez et al., 2015), with heightened activity hypothesised to contribute to leukemogenesis (Neveu et al., 2016), and possible links to vestibular dysfunction and impaired hearing (Gagnon et al., 2006). Increased expression of CLIC4 is linked to endothelial dysfunction in pulmonary arterial hypertension (Abdul-Salam et al., 2019) and neuronal apoptosis (D. Guo et al., 2018), with variant expression shown to modulate different cancer growth (Baolong et al. 2020; Suh et al. 2012; Suh et al. 2007; Suh et al. 2004). CLIC3 was found to be secreted by cancer cells (Hernandez-Fernaud et al., 2017), with significantly increased distribution in mucoepidermoid carcinoma (Wang et al. 2015), and a missense mutation in CLIC2 is implicated in an X-linked intellectual disability due to changes in the protein stability and conformational states (Witham et al., 2011).

CLIC1 is the most characterised member of the CLIC family, including the protein's role and expression in many forms of pathological state. This chapter will focus on exploring the proteins' cellular localisation within the context of disease of which CLIC1 is most heavily implicated; cancer and whether the trigger of divalent cations for membrane insertion in vitro is seen with a in vivo approach.

The role of CLIC1 in cancer progression has been studied in various forms of cancer and has been shown to have significantly higher expression levels in cancerous tissues compared to healthy tissue, such as in ovarian (Yu et al., 2018), gall bladder (Ding et al., 2015), squamous cell carcinoma (Kobayashi et al., 2018) and liver cancer (Yue et al., 2019) to name a few.

In addition to higher expression in cancer cells to healthy tissue, an increase in CLIC1 expression can be seen in higher grade tumours compared to low grade tumours, (Yu et al. 2018) and CLIC1 expression is negatively correlated with overall survival rate (Jia et al., 2016; Lu et al., 2015; Xu et al., 2018). Investigating cancer cell's motility and invasion in response to CLIC1 expression revealed the role of CLIC1 in metastasis (Feng et al. 2019; He et al. 2018; Wang et al. 2009). CLIC1 is also hypothesised to play a role in resistance to current treatments available to treating cancer, such as chemotherapy drugs, as overexpression of the protein is associated with cisplatin resistance (Yu et al., 2018).

Precise cellular pathways that CLIC1 expression could affect have been investigated within cancer tissue. CLIC1 knockdown in gastric cells lead to decreased expression levels of Integrins (ITGa3, ITgav, ITGB1) and reduction of AKT phosphorylation, ERK phosphorylation and p38 phosphorylation (Li et al. 2018), while CLIC1 was shown to regulate the mitogen-activated protein kinase (MAPK)/ERK pathway in prostate cancer (Tian et al., 2014) and the ROS/ERK pathway in colon cancer (P. Wang et al., 2014). The correlation of CLIC1 expression with these pathways besides knowledge of the ability of CLIC1 to control cell volume regulation (Wang et al. 2012) hypothesises the role of CLIC1 in tumour proliferation and metastasis.

CLIC1 expression is also implicated in the ability of cancer cells to undergo angiogenesis, with CLIC1 expression demonstrated to be necessary for capillary-like sprouting and branching morphogenesis in in vitro angiogenesis (Tung & Kitajewski, 2010).

Glioblastomas are tumour cells where CLIC1 expression is highly implicated, consequently the cell type my latter studies of CLIC1 focused on. Immunofluorescence staining of GBM (Glioblastoma) neurospheres, a mix of stem, progenitor and differentiated cells revealed CLIC1 is enriched in the stem & progenitor cell compartment of the neurosphere (Setti et al., 2013). Furthermore, CLIC1 plasma membrane localisation is seen in GBM-derived neurospheres but not in normal human progenitor cells confirming the expression of CLIC1 in the membrane as a phenotype of cancer. To further confirm the role of CLIC1 in cancer proliferation, biguanide-related drugs tested were found to inhibit CLIC1 mediated ion current in glioblastoma which impaired viability, invasiveness and self-renewal (F. Barbieri et al., 2018). One such biguanide drug is metformin, which is currently in phase II clinical trial to investigate how the drug could be repurposed from a treatment for diabetes patients to an anti-tumour agent against glioblastoma, with initial results indicating an increase in median survival of GBM patients from 16 to 20 months and acceptable toxicity (McGill University Health Centre/Research Institute of the McGill University Health Centre, 2015). Furthermore, CLIC1 was shown to be a direct target of metformin in human glioblastoma cells, inducing a G1 arrest of the cell cycle (Gritti, Würth, Angelini, Barbieri, Pizzi, et al., 2014).

The true mechanism of how CLIC1 interacts within the cancer cells to induce these advantageous characteristics for the tumour, such as enhanced metastasis and

angiogenesis still remains unclear and contradictory. Coupled to our in vitro evidence of the change of localisation of CLIC1 based on the level of divalent cations available in the protein's environment, microscopy to visualise the protein within the cancer cells was turned to as a useful technique to deduce further what is really happening to CLIC1 within diseased cells and if the metals are shown to play a role.

The study of CLIC1 localisation in various mammalian cells has successfully been carried out previously using microscopy, with immunofluorescence and immunohistochemical methods combined to study the tissue and subcellular distribution of CLIC1, revealing cell specific results (Ulmasov et al., 2007). Fluorescence microscopy revealed localisation of CLIC1 in the endoplasmic reticulum of neonatal cardiomyocytes, cytoplasm of resting murine peritoneal macrophages (Ponnalagu, Gururaja Rao, et al., 2016) and in peri-nuclear areas of human endothelial cells (Thuringer et al., 2018). The ability of CLIC1 to form invadopodia was shown with phase contrast microscopy, confirming that a knock down of CLIC1 reduced invadopodia formation in endothelial cells, kidney and fibrosarcoma tumour cells (Gurski et al., 2015).

In this chapter, microscopy was therefore turned to as an effective technique to deduce more of CLIC1 behaviour within the context of mammalian cells. HeLa, were selected as the initial cell type of investigation due to being derived from a cervical cancer cell line and their ease to successfully culture. This allowed the study of CLIC1 in a cancer phenotype, but specifically in a cancer not yet implicated in CLIC1 upregulation or membrane expression so any differences induced by metal treatment could be seen. Fluorescently labelling CLIC1 and transfecting the labelled protein into mammalian cells was used as the initial tool to visualise CLIC1 due to

hypothesising the antibody epitope is not known to be suitable to bind to the mammalian channel form of CLIC1, due to the membrane channel's structure still elusive. Transfection resulted in its own challenges due to overexpression of the recombinant protein reducing the viability of the mammalian cells, especially with treatment of metals. Endogenous immunofluorescence staining of CLIC1 was instead optimised and using cell membrane stain, localisation to the membrane of the cells could be confirmed.

Different treatment of the mammalian cells were explored to visualise any change in localisation of CLIC1, from the use of treatments to increase intracellular divalent cations levels such as Zn^{2+} and Ca^{2+} as they are shown as the trigger for CLIC1 insertion in vitro (Varela et al., 2019) to testing the increase of reactive oxygen species (ROS) using H_20_2 and PMA as CLIC1 is hypothesised to insert into the membrane under oxidising conditions (Goodchild et al., 2009; Littler et al., 2004).

Overall, the following chapter shows the optimisation, methods and techniques to allow visualisation of CLIC1 in cancer cells and how this localisation is dependent on cell type but can be triggered by elevating the intracellular metal levels, to reveal CLIC1 membrane localisation as well as phenotypic changes, that could help decipher how CLIC1 enables enhanced proliferation and metastasis in cancer.

4.2 Methods

4.2.1 Molecular cloning of CLIC1 into LAMP1-mGFP vector

Primers were designed to insert the Human CLIC1 gene (HsCD00338210 from the plasmid service at HMS) into the LAMP1-mGFP mammalian expression vector (Falcón-Pérez et al., 2005). PCR was carried out to amplify both the CLIC1 fragment and the vector independently according to Gibson assembly instructions. PCR products for both reactions for the fragment amplification and vector amplification were run on an agarose gel, stained with SYBR safe at 80 volts for 30 minutes and results viewed and photographed under ultraviolet light. The resultant PCR products were then mixed with Gibson assembly mastermix (New England Biotech) and transformed into DH5alpha competent cells for DNA replication. The DNA was extracted and purified using a miniprep kit (Qiagen) from overnight cultures of the DH5alpha, growing with kanamycin antibiotic selection for the vector. The purified DNA was sent for sequencing (Eurofins genomic sequencing) and the insertion of CLIC1 into the mammalian vector was confirmed. SnapGene software was used to produce the Sequence maps.

4.2.2 Maintenance and growth of mammalian cells

The three cell lines used include HeLa, Huh7s and U87 glioblastoma cells, all kindly supplied by laboratories within the university of Kent. The cells were grown from frozen stocks stored in a -80 freezer and were allowed to be passaged at least five times before used for any experiments. All cell types were maintained in DMEM media supplemented with 10% FBS and 1% Penicillin/Streptomycin at 37°C, 95% humidity and 5% CO_2. Cells were washed with phosphate buffered saline (PBS) and

passaged every 2-3 days once around 70% confluent in T-75 flasks. The adherent cells were removed from the flask using trypsin, centrifuged and diluted into fresh DMEM media at a 1/10 dilution for continued growth.

4.2.3 Transfection of CLIC1-GFP into mammalian cells.

Cells were seeded onto autoclaved microscopy slides into a 24-well plate. Hela cells were seeded at 100 000 cells per slide and left to grow and adhere overnight in DMEM media supplemented with 10% FBS and 1% Penicillin/Streptomycin at 37°C, 95% humidity and 5% CO_2. Purified DNA of CLIC1 inserted into the mammalian LAMP1-mGFP vector was diluted into 50 µl of Optimem per well and mixed. Initial transfection experiments saw 500 ng of DNA used per well of cells but was decreased to 400 ng, which all subsequent experiments used. Lipofectamine 2000 was diluted into 50 µl per well and mixed. Both the DNA and lipofectamine in Optimem media were then mixed and left to incubate for 10 minutes at room temperature. Cells were washed with PBS and optimem before 100 µl of the lipofectamine/DNA mixture was added to each well. The cells were then placed back into the incubator and left to undergo transfection overnight at 37°C.

The following day cells were washed with Tris buffered saline (TBS) and treated with $CaCl_2$, $ZnSO_4$, H_2O_2 or Phorbol-12-Myristate-13-Acetate (PMA), depending on the specific experimental investigation, before fixation with 4% formaldehyde for 15 minutes. Cells were then washed 3x with TBS and autofluorescence was quenched with treatment of the cells with 50 mM NH_4Cl in TBS. Three wash steps with TBS were repeated before incubation of the cells for 20 minutes with NucBlu Live Cell Stain (Invitrogen). Slides were then mounted with ProLong Gold Antifade (Invitrogen).

4.2.4 Immunofluorescence assays

All immunofluorescence assays were performed by seeding cells onto sterile microscopy slides within 24 well plates. 24 hours post seeding the cells were washed with TBS, transferred to fresh media, whether DMEM or phosphate free DMEM and treated with $CaCl_2$, $ZnSO_4$, Ionomycin, Zinc pyrithione (ZnPT), metformin or *N*,*N*,*N*',*N*'-Tetrakis(2-pyridylmethyl)ethylenediamine (TPEN) depending on specific experiment, all concentrations are indicated in the results section per individual experiment. The cells were washed with TBS before Fixation with 4% formaldehyde typically one-hour post treatment, with the exception of the ZnPT timed effect on HeLa cells and Ionomycin HeLa experiments with a cell mask where specific time points were selected. Cells were then washed with TBS before incubation for 10 minutes with 0.1% triton in TBS for permeabilization. Any detergent was removed with subsequent TBS washes. In experiments using the membrane cell mask, 15 minutes incubation occurred with CELL MASK deep red plasma membrane stain (Invitrogen) before a blocking step at room temperature with 2% Bovine serum albumin (BSA) for one hour. Experiments requiring no cell mask, saw blocking step immediately after permeabilization washes. A 1:50 dilution of monoclonal mouse CLIC1 antibody (Santa Cruz Biotechnology, clone 356.1) in 2% BSA in TBS was applied to each slide and left at 4°C overnight for the primary incubation step. The cells were washed three times the following day before secondary incubation with a donkey anti-mouse antibody at a 1:1000 dilution (Alexa Fluor 488 (green) or 594 (red) Life Technologies) for one hour at room temperature. Three subsequent washes were followed by 20 minutes incubation with nucleus stain NucBlu Live Cell Stain (Invitrogen) before the slides were mounted using ProLong Gold Antifade (Invitrogen).

4.2.5 Nuclear envelope CLIC1 localisation assay

The cells were prepared with an identical protocol to the immunofluorescence method aforementioned, with an additional permeabilization step before fixation to remove the plasma membrane and cytoplasm. 0.1% triton in cytoskeleton buffer (10 mM PIPES, 300 mM sucrose, 100 mM NaCl, 1 mM EDTA, 3 mM $MgCl_2$ pH7) was applied to the cells for 1 minute before washing with TBS. The protocol then resumed as previously described.

4.2.6 Fluo4 experiments

Both HeLa and U87 cells were counted and seeded at the same cell density into 24 well plates and left to grow overnight. The cells were washed and transferred to fresh media and treated with $CaCl_2$, Ionomycin and metformin and left to incubate for identical times to the corresponding immunofluorescence images. 1x solution of Fluo-4 Direct (Invitrogen) was added to the cells according to the manufacturers protocol. The fluorescence intensity was then imaged to verify intracellular calcium levels.

4.2.7 Microscopy visualisation and image processing

All microscopy, excluding Fluo4 experiments, was carried out on a Zeiss LSM-880 confocal microscope using 405 nm, 488 nm, 633 nm lasers. All images were processed with added scale bars with Zen Black and Zen Blue software. Fluo4 experiments were visualised using a LS620 Etaluma microscope. Contrast and brightness were adjusted equally for all images and pseudo colouring was applied for intensity calibration bar, using ImageJ.

4.3 Results

4.3.1 Molecular cloning of CLIC1 into vector suitable for mammalian transfection with a C-terminal GFP tag.

In order to visualise CLIC1 localisation within mammalian cells, a LAMP1-mGFP mammalian vector (Figure 4.1) was selected that could be used to easily clone CLIC1 with a C-terminal green fluorescent (GFP) tag. Successful recombination of the gene was achieved (Figure 4.1) and this resultant DNA was used to transfect mammalian cells such as HeLa and Huh7s.

4.3.2 Visualising CLIC1 in mammalian cells

Transfection of the fluorescently labelled CLIC1 into HeLa cells revealed preliminary images of the GFP tagged protein (CLIC1-GFP) overexpressed within the mammalian cells and its localisation (Figure 4.2). Initial transformation trials of CLIC1-GFP revealed bright signal of the protein, with the most protein dense region being the nucleus. Cells with no treatment showed diffuse signal for the fluorescently labelled CLIC1 throughout the cytoplasm and demonstrated the successful use of the transfected DNA. However, it is clear the transfection levels for CLIC-GFP in these cell, 500 ng of DNA, was too high (Figure 4.2) and further optimisation of protein transfection was required. A lower concentration of DNA was then used for subsequent transfection and as can be seen (Figure 4.3) there remained clear signal of the CLIC1-GFP, but localisation was much easier identified due to less saturation. These transfection levels, 400 ng of DNA, were seen to be optimal for working with CLIC1 and studying any change in localisation.

4.3.3 Initial treatment of mammalian cells with calcium and zinc, studying CLIC1 localisation.

These initial images reveal treatment of the cell media with both $CaCl_2$ and $ZnCl_2$, indicated a localisation change of CLIC1 with some protein translocating to the plasma membrane (Figure 4.2).

Once transfection was optimised to a level for much clearer identification of CLIC1 localisation, the mammalian cells were treated with $CaCl_2$ and $ZnCl_2$ to reveal a similar change in localisation to the plasma membrane or around the nuclear envelope, with possible endoplasmic reticulum membrane localisation. The control cells show diffuse cytoplasmic localisation of CLIC1. These preliminary images also reveal a change in cell morphology when zinc levels were increased with more filopodia structures identified compared to the control cells (Figure 4.3). Treatment of media with calcium was later shown to increase the intracellular calcium levels compared to control cells (Figure 4.8).

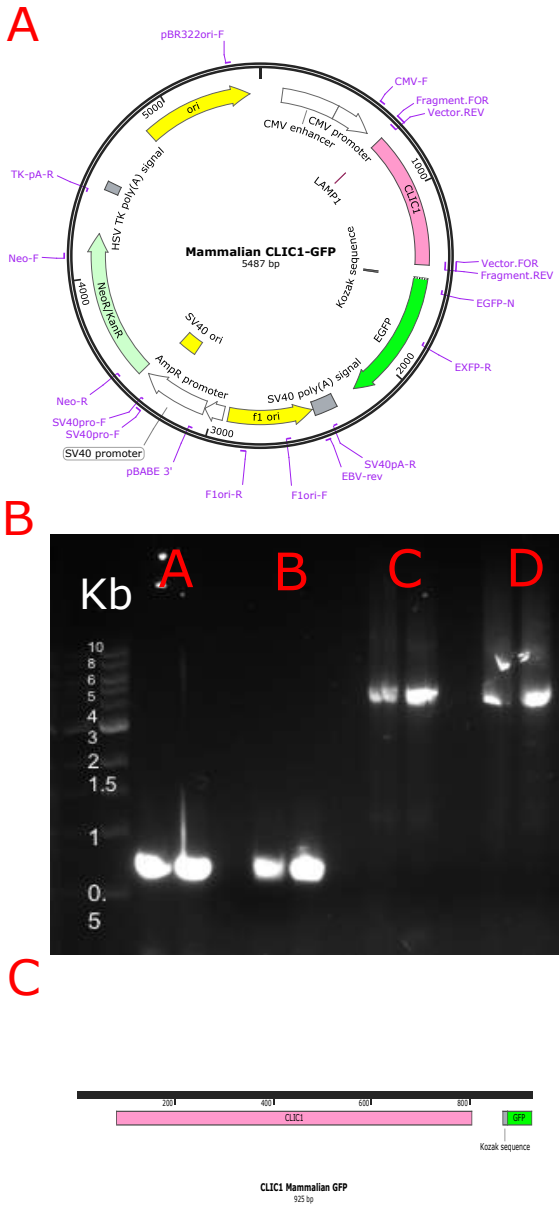

Figure 4.1 - Molecular cloning of CLIC1 gene into vector suitable for mammalian cell transfection. A – Map of Lamp1 vector attaching C-terminal GFP tag to CLIC1 gene. B – Agarose gel for PCR products, A & B lanes showing successful amplification of CLIC1 fragment in two separate PCR attempts. C & D lanes showing successful vector amplification in two separate PCR attempts. C – Map of sequenced DNA with CLIC1 inserted into the plasmid, showing successful cloning through Gibson assembly.

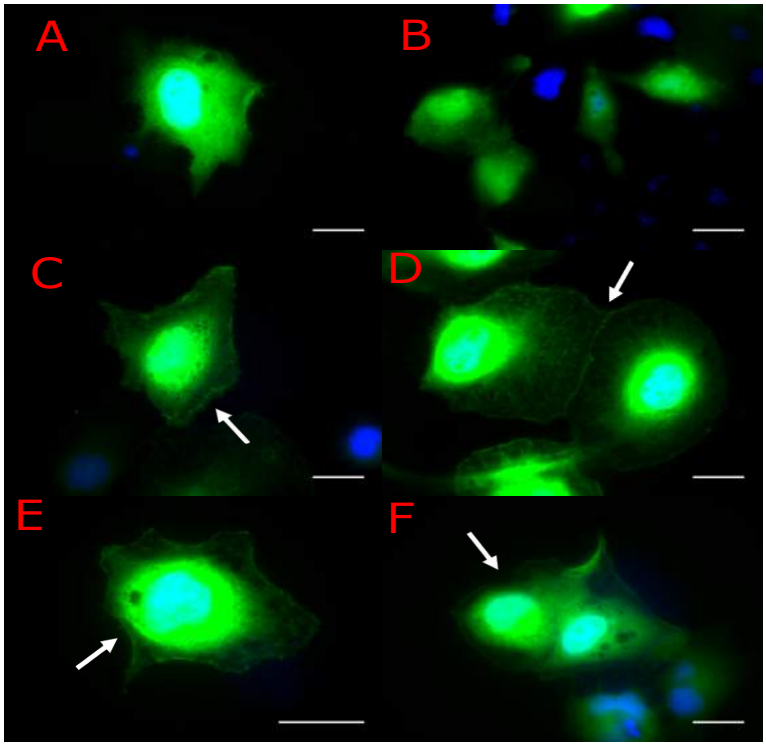

Figure 4.2 - Initial transfection of mammalian cells with CLIC1-GFP under divalent cation treatment to induce CLIC1 membrane insertion. Huh7s with no treatment (A&B), Huh7s treated with 1 mM $CaCl_2$ (C&D) and Huh7s treated with 2 mM $CaCl_2$. Green – CLIC1-GFP, Blue – Dapi nucleus stain. White arrows indicate membrane localisation. Scale bars represent 10 µm.

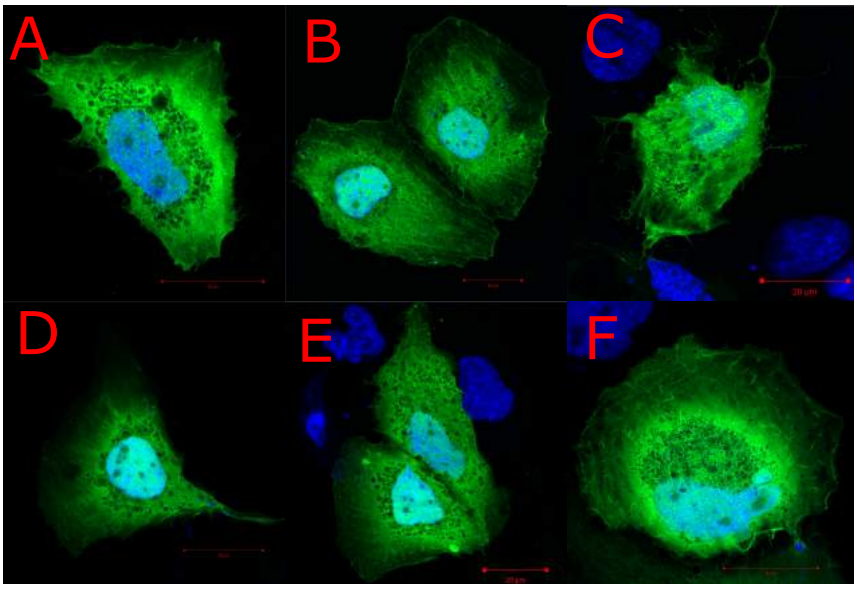

Figure 4.3 – Optimised transfection of CLIC1-GFP into Huh7s to investigate CLIC1 membrane insertion with divalent cation treatment. A & D – Control cells with no treatment. B & E Cells treated with 1 mM $CaCl_2$ and 200 µM $CaCl_2$ respectively. C & F – Cells treated with 1 mM $ZnSO_4$ and 200 µM $ZnSO_4$ respectively. Green – CLIC1-GFP, Blue – Dapi nucleus stain.

4.3.4 Investigating whether ROS in cells leads to membrane localisation

Treatment of mammalian cells with hydrogen peroxide did not appear to lead to any clear membrane localisation when compared to control cells with no treatment, when analysed by microscopy (Figure 4.4). In addition, treatment with metals such as zinc and calcium were directly compared against treatment of the cells to induce reactive oxygen species, such as PMA and H_20_2. Little membrane localisation of CLIC1 was seen with both H_20_2 and PMA treatment alone but when treated with Zinc and PMA/H202 and Calcium with PMA (Figure 4.5), some membrane localisation can be identified, with a similar phenotype to those cells seen with treatment just of metals (Figure 4.3).

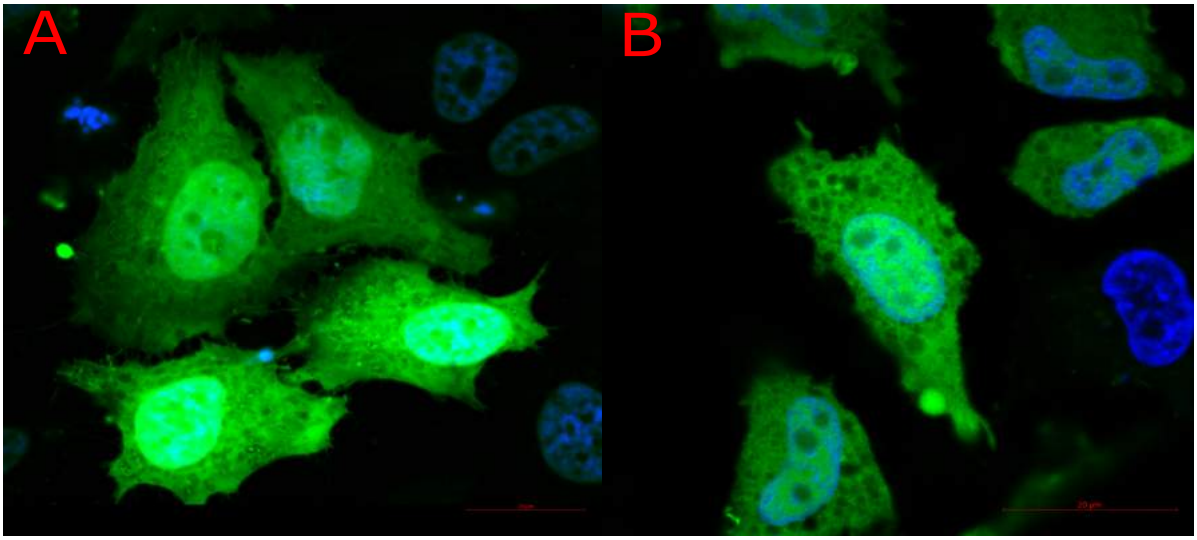

Figure 4.4 – Oxidation of CLIC1-GFP transfected mammalian cells to investigate whether ROS leads to CLIC1 membrane localisation. A – Huh7s treated with 10 mM H_20_2. B – Huh7s no treatment. Green – CLIC1-GFP, Blue – Dapi nucleus stain.

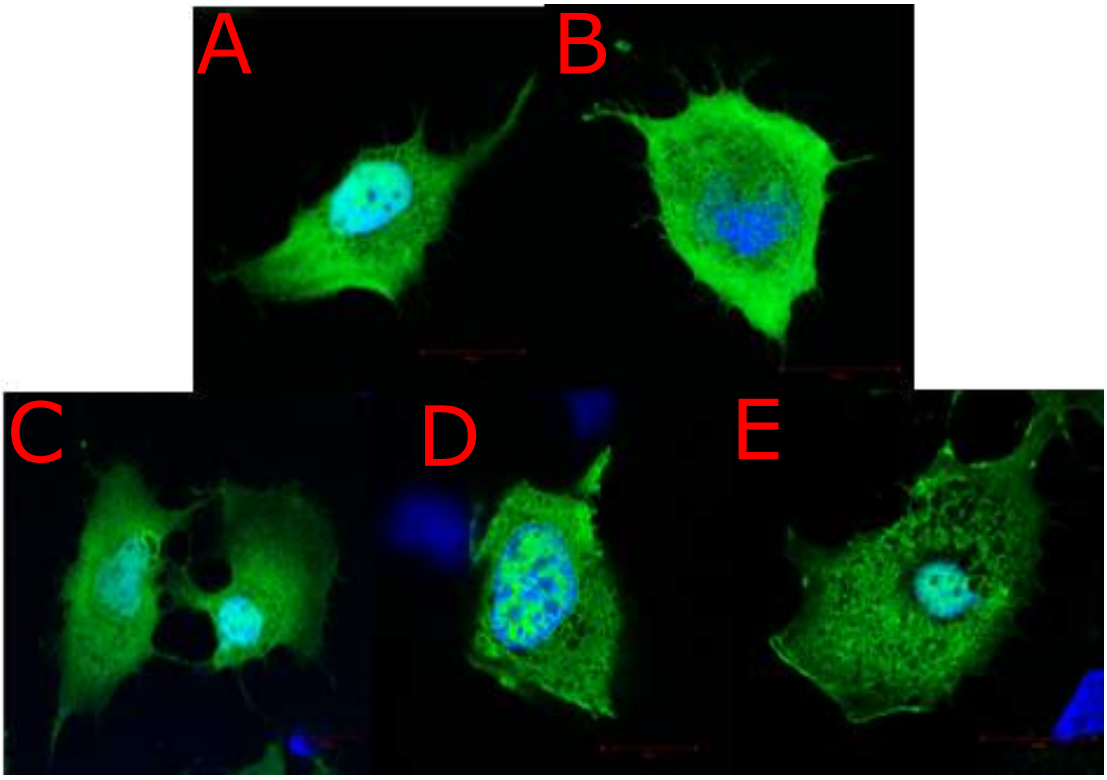

Figure 4.5 – Oxidation of mammalian cells combined with metal treatment to investigate CLIC1-GFP insertion into the membrane. A – Treatment of Huh7 cells with PMA to induce ROS production. B – Treatment with 1mM $ZnSO_4$ and 200nM PMA. C – Treatment with 1mM $CaCl_2$ and 200nM PMA. D – Treatment with H_2O_2. E – Treatment with 10mM H_2O_2 and 1mM $ZnSO_4$. Green – CLIC1-GFP, Blue – Dapi nucleus stain.

4.3.5 Endogenous staining of CLIC1 in mammalian cells

Instead of transfecting fluorescently labelled CLIC1 into mammalian cells the use of immunofluorescence against endogenous CLIC1 was instead explored. Initial attempts show endogenous CLIC1 staining (Figure 4.6) in HeLa mammalian cells and further trials of antibody dilution clarified the optimal concentrations of protein to visualise CLIC1 within the mammalian cells. CLIC1 can be seen with detectable signal in all dilutions but with best seen at the 1/50, with all subsequent experiments using

this dilution (Figure 4.7). Endogenously staining for CLIC1 revealed the protein to be diffuse throughout the cells, with mainly cytoplasmic localisation (Figure 4.6).

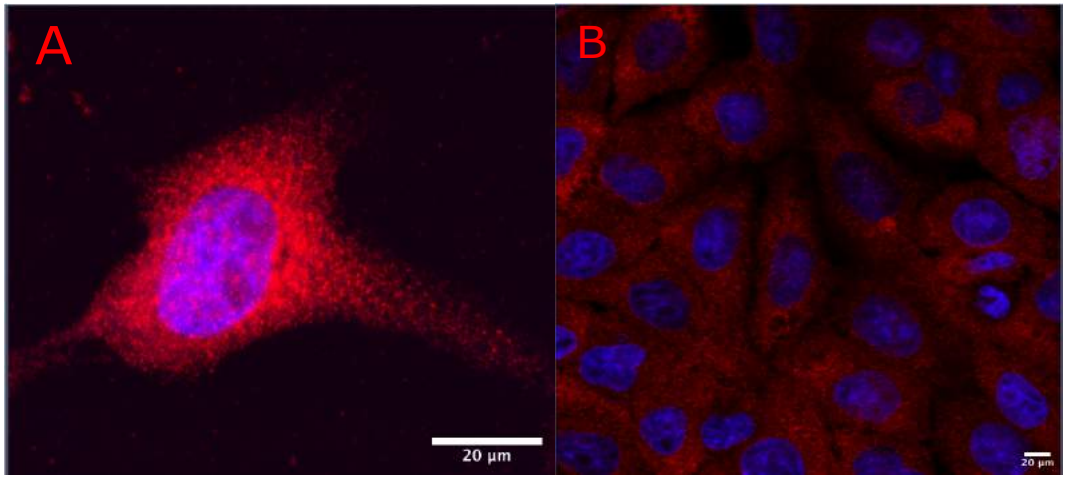

Figure 4.6 – Initial staining of endogenous CLIC1 in mammalian cells. HeLa stained for anti-CLIC1 antibody (red) and DAPI for nucleus staining (blue). A – Single cell. B – widefield.

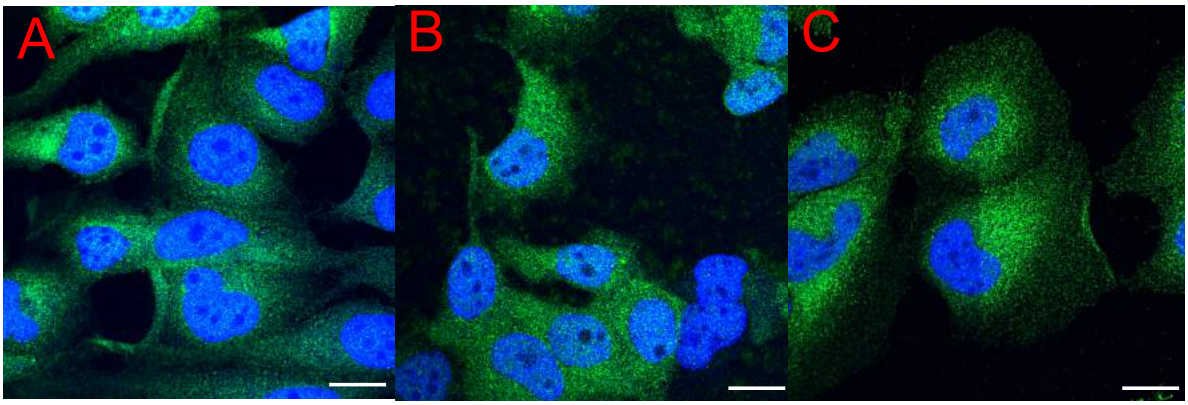

Figure 4.7 – CLIC1 antibody staining optimisation in HeLa cells.
A – 1/300 dilution of antibody. B – 1/200 dilution of antibody. C – 1/50 dilution of antibody. CLIC1 antibody (green) and nucleus staining (blue).

4.3.6 The use of ionophores to raise intracellular metal levels

To more effectively raise the intracellular levels of calcium and zinc rather than adding metal salts to the media, ionophores were used. Ionomycin, a calcium and

zinc ionophore was shown to successfully raise the intracellular calcium levels compared to the control cells and cells in media treated with $CaCl_2$ (Figure 4.8).

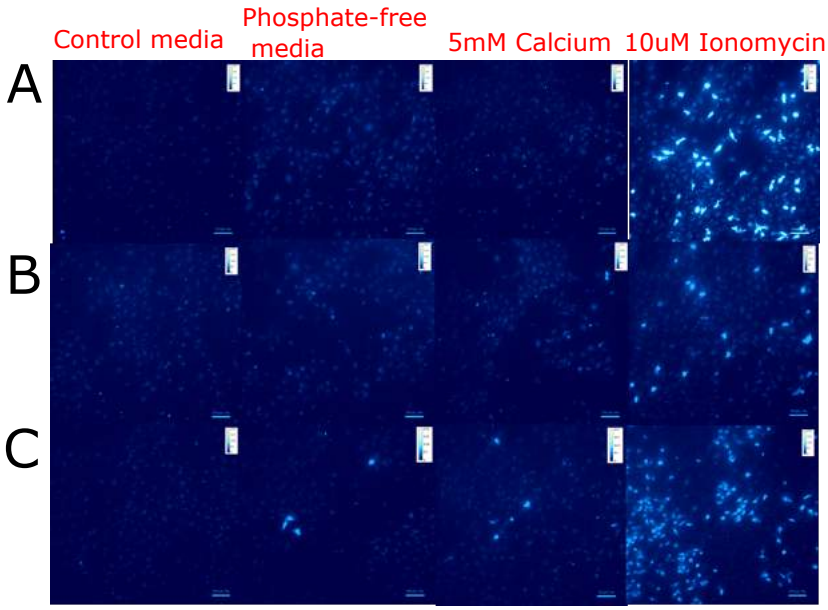

Figure 4.8 – HeLa cells stained with Fluo4 receptor to reveal intracellular calcium levels. Higher colour intensity correlates to higher calcium levels. A, B & C are at 1-hour, 2-hour and 3-hour time points after treatment respectively.

4.3.7 Membrane localisation of endogenous CLIC1 can be detected with immunofluorescent staining, when intracellular calcium levels are raised

To improve detection of the localisation of CLIC1 within the cell and whether it was inserting into the membrane, a membrane cell mask was introduced to the fluorescent microscopy. The red mask can be seen to successfully outline the membrane of the mammalian cells and also stain internal membranes around the endoplasmic reticulum (Figure 4.9 & 4.10). This mask was then combined with the endogenous staining of CLIC1. Clear plasma membrane localisation and colocalization with the membrane mask stain can be seen with both the calcium and ionomycin treatment compared to the control cells, where no treatment is used. More plasma membrane localisation is observed with the ionomycin against media

added $CaCl_2$ (Figure 4.9 & 4.10), which is correlated with increasing the intracellular calcium levels more with ionomycin than when calcium salt is added externally to media (Figure 4.8).

2D images of the cells treated with calcium, help to reveal the change in localisation with a diffuse phenotype in control cells of the protein, to concentrated localisation around the nucleus and plasma membrane when treated to increase intracellular calcium levels (Figure 4.11). The two different time points of visualising CLIC1 localisation in the mammalian cells, 2 hours and 3 hours post treatment reveal that the intracellular calcium levels are raised in the cells treated against the control at both these time points and the cells are still viable. However, there are subtle differences between the two time points, with the most striking effect seen at 2 hours post treatment compared to the 3-hour experiment. This could indicate that CLIC1 relocalisation happens in response to the metals with a peak movement of CLIC1 into the membranes followed by a return back to the cytoplasm, even as calcium levels in the cell remain high.

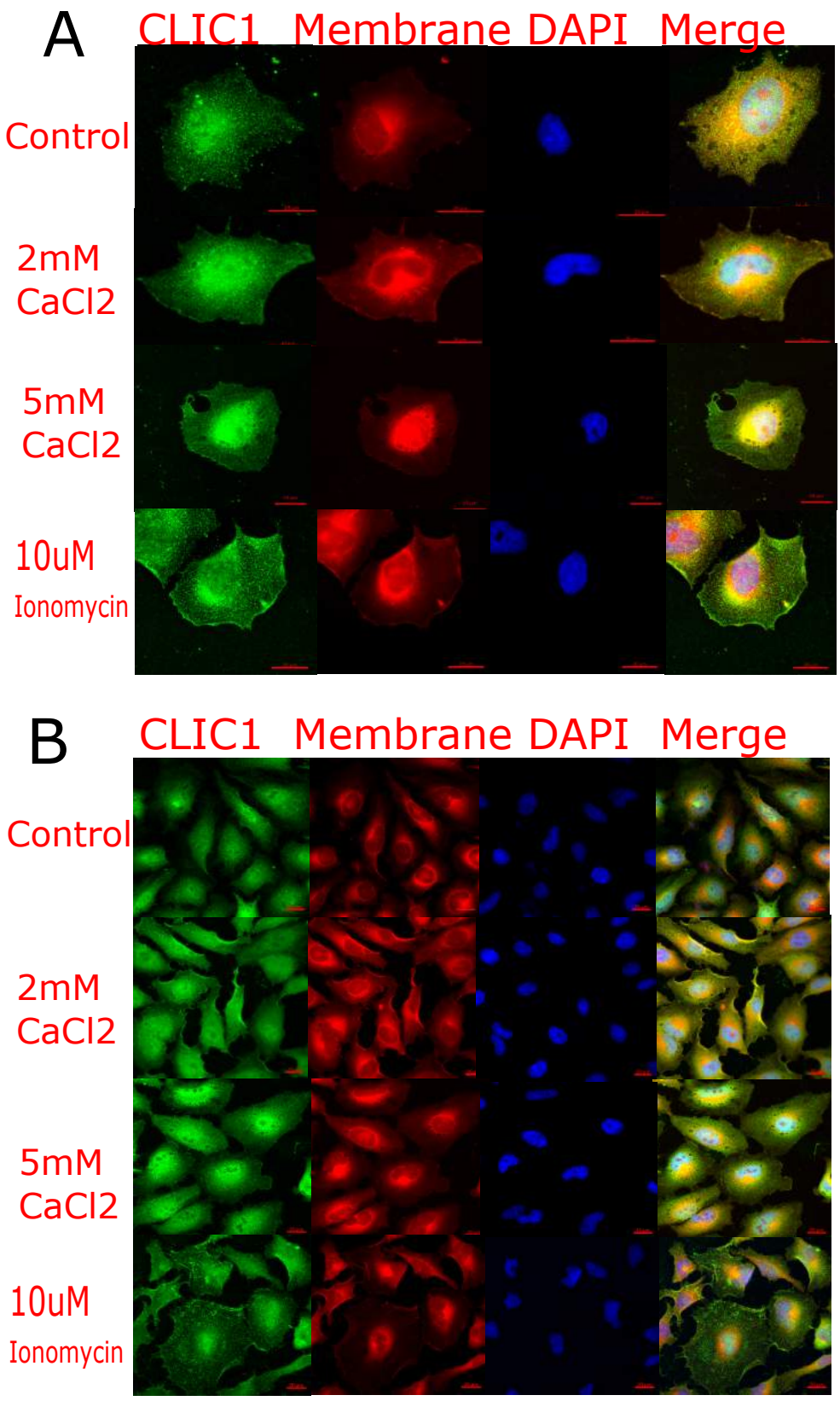

Figure 4.9 – CLIC1 membrane localisation in HeLa cells with increasing intracellular calcium, 2 hours post treatment. CLIC1 antibody (green), membrane mask dye (red) and nucleus staining (blue). A – Single cells. B – widefield images.

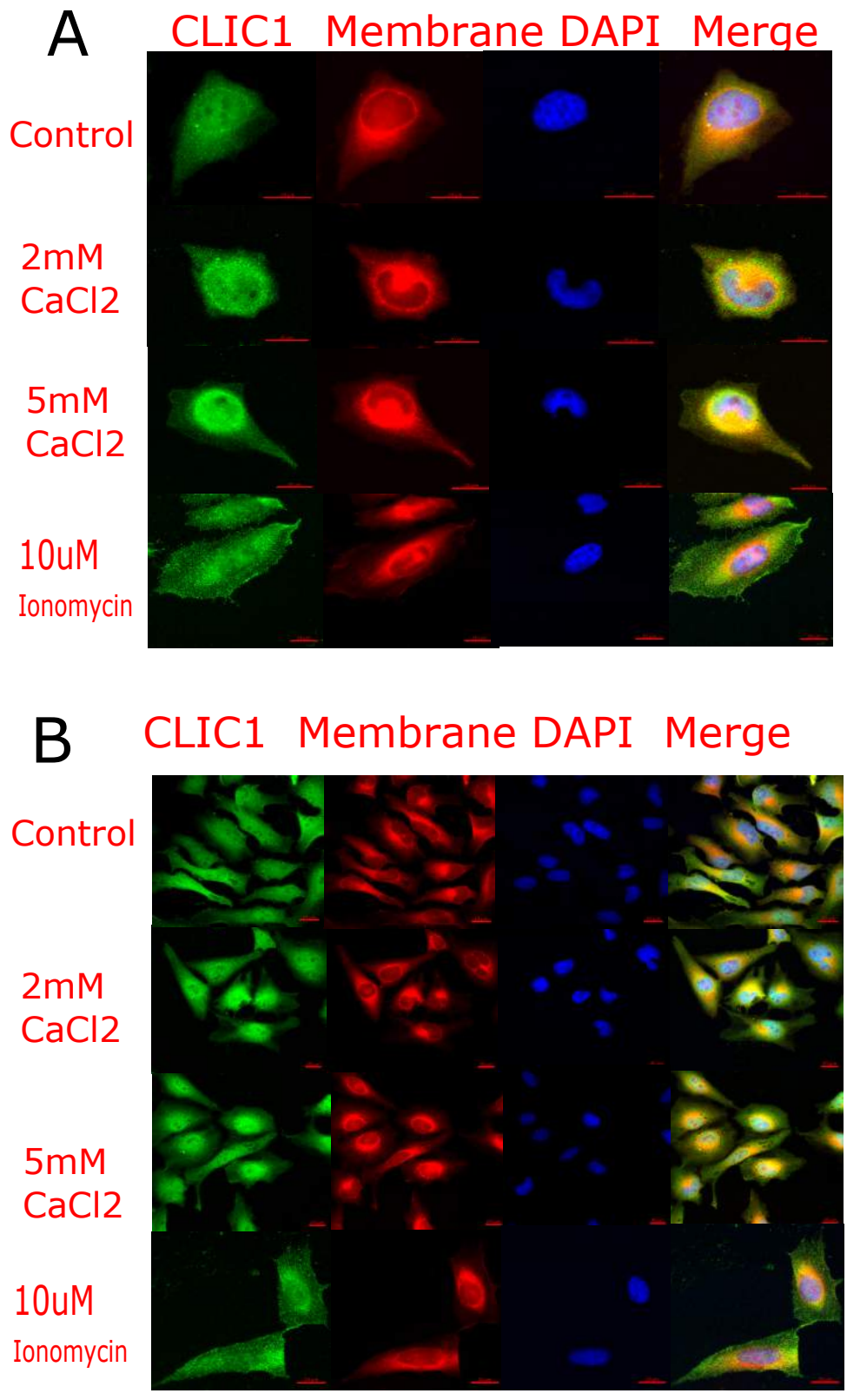

Figure 4.10 – CLIC1 membrane localisation in HeLa cells with increasing intracellular calcium, 3 hours post treatment. CLIC1 antibody (green), membrane mask dye (red) and nucleus staining (blue). A – Single cells. B – widefield images.

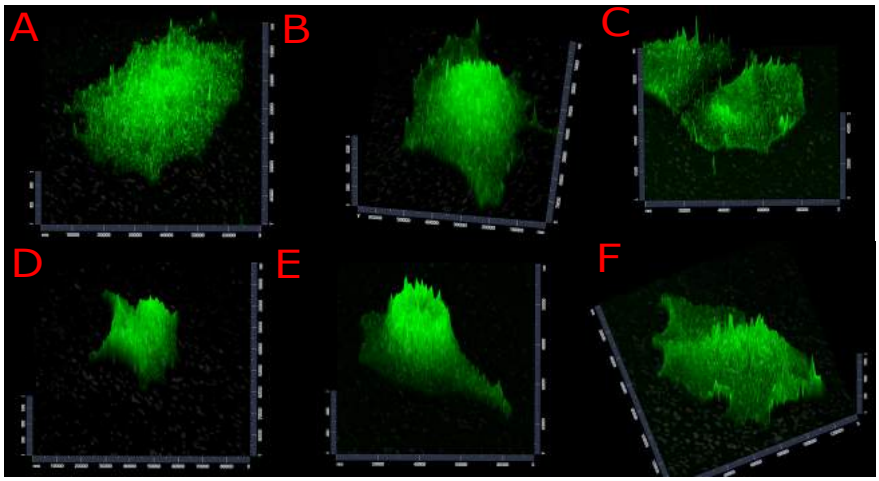

Figure 4.11 – 2D localisation of CLIC1 in HeLa mammalian cells. Mammalian cells treated with antibody against CLIC1 (green). A – Control cell with no treatment at 2 hours post media change. B – Cell treated with 5mM $CaCl_2$ at 2 hours post treatment. C – Cell treated with 10 µM Ionomycin at 2 hours post treatment. D – Control cell with no treatment at 3 hours post media change. E – Cell treated with 5mM $CaCl_2$ at 3 hours post treatment. F – Cell treated with 10 µM Ionomycin at 3 hours post treatment**.**

4.3.8 Localisation of CLIC1 around the nuclear envelope and endoplasmic reticulum changes in response to ionomycin

Treatment of the mammalian cells with strong detergent in a permeabilization step allowed the removal of the plasma membrane and much of the cytoplasm to be able to concentrate on the localisation of CLIC1 immediately around the nucleus (Figure 4.12). When looking at the control cells there appears to be cytoplasmic localisation with little localisation to the nuclear envelope, however when imaging cells with identical detergent treatment but treated with ionomycin to increase intracellular calcium levels, there is nuclear envelope localisation. CLIC1 can be seen lining the nucleus stain and indicates again a change of localisation of the protein within mammalian cells, just by changing the levels of available divalent cations.

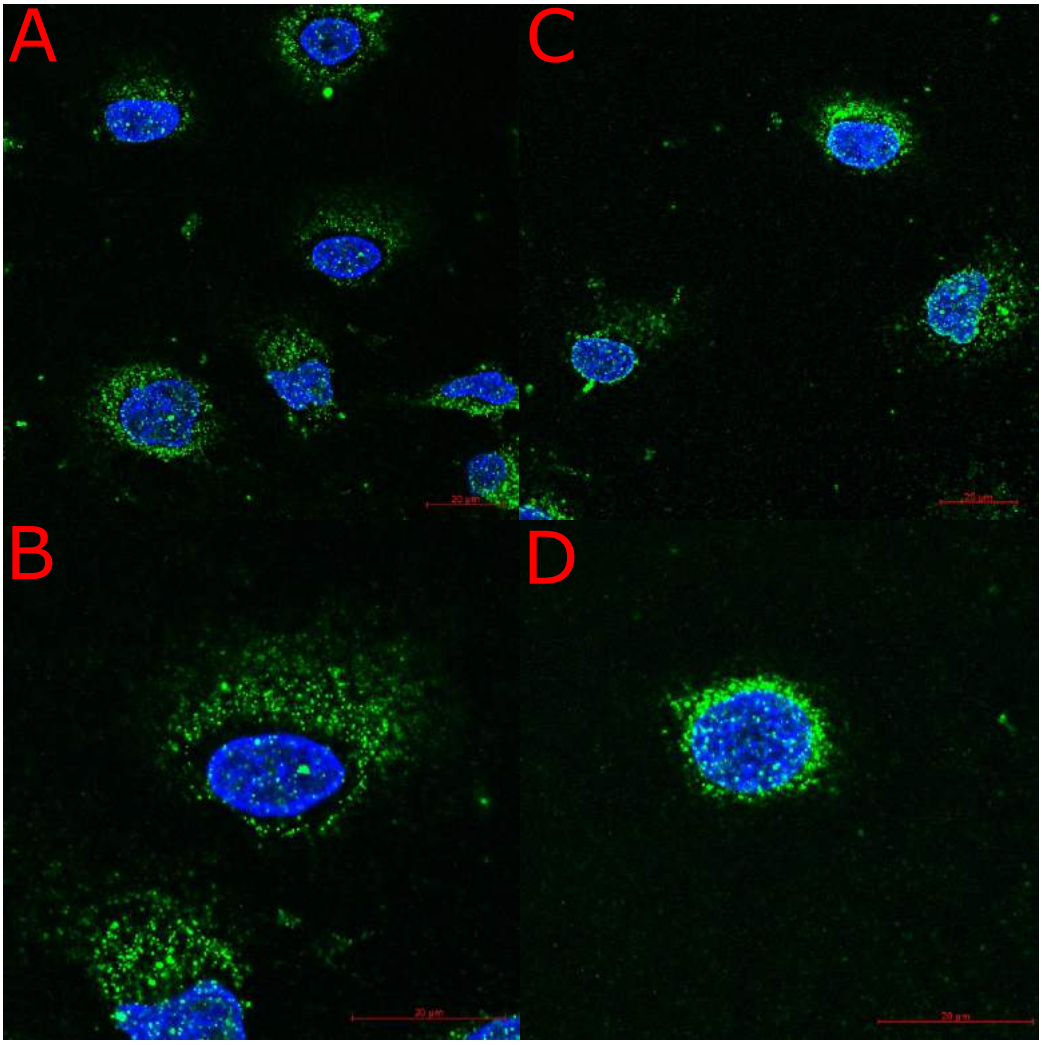

Figure 4.12 – Comparison of CLIC1 localisation around the endoplasmic reticulum and nuclear envelope of HeLa mammalian cells. Cell cytoplasm removed with incubation of detergent, to reveal protein located centrally around the cell nucleus. CLIC1 membrane localisation was induced by an increase in the intracellular level of calcium. A & B – Control cells with no treatment. C & D – Cells treated with 10 µm ionomycin. CLIC1 antibody (green) and nucleus DAPI stain (blue).

4.3.9 Using zinc pyrithione to study the response of CLIC1 to raised intracellular zinc

Increasing the intracellular levels of zinc by adding $ZnCl_2$ or $ZnSO_4$ to the extracellular media proved difficult due to the metals insolubility at neutral pH, instead treatment with ionophore zinc pyrithione (ZnPT) was used to visualise the effect zinc has on endogenous CLIC1 localisation within mammalian cells (Figure 4.13). Treatment with

ZnPT resulted in an abnormal phenotype within the cell compared to a control. Five timepoints were visualised after treatment with the ionophore and the control shows diffuse CLIC1 throughout the cytoplasm at all timepoints, with little plasma membrane localisation of the protein. Upon treatment with ZnPT, there appears to be a difference in CLIC1 localisation seen at the earliest timepoint, with movement towards the nucleus as well as round punctate circles of highly concentrated CLIC1 localised mainly around the plasma membrane of the cells. The effect of the ZnPT treatment also becomes heightened as the time points increase, with more CLIC1 concentrated around the endoplasmic reticulum and nucleus and an increase in the abundance of the unidentified CLIC1 circular objects.

4.3.10 Transmission electron microscopy to investigate source of circular rings of CLIC1

Treatment of mammalian cells with both ionomycin and ZnPT compared to control cells revealed difference in physiological features of the cells that could be detected by a transmission electron microscope (TEM) (Figure 4.14). The high-resolution images show an increased release of cell material from one cell to another with treatment with ionomycin against the control cells and even more so when treated with ZnPT. It is difficult to clarify the exact features of this increased communication between the cells when increasing intracellular metal levels but the images could indicate possible formation of invadopodia or filopodia from the cells or even the release of lipid vesicles to pass signalling molecules to each other.

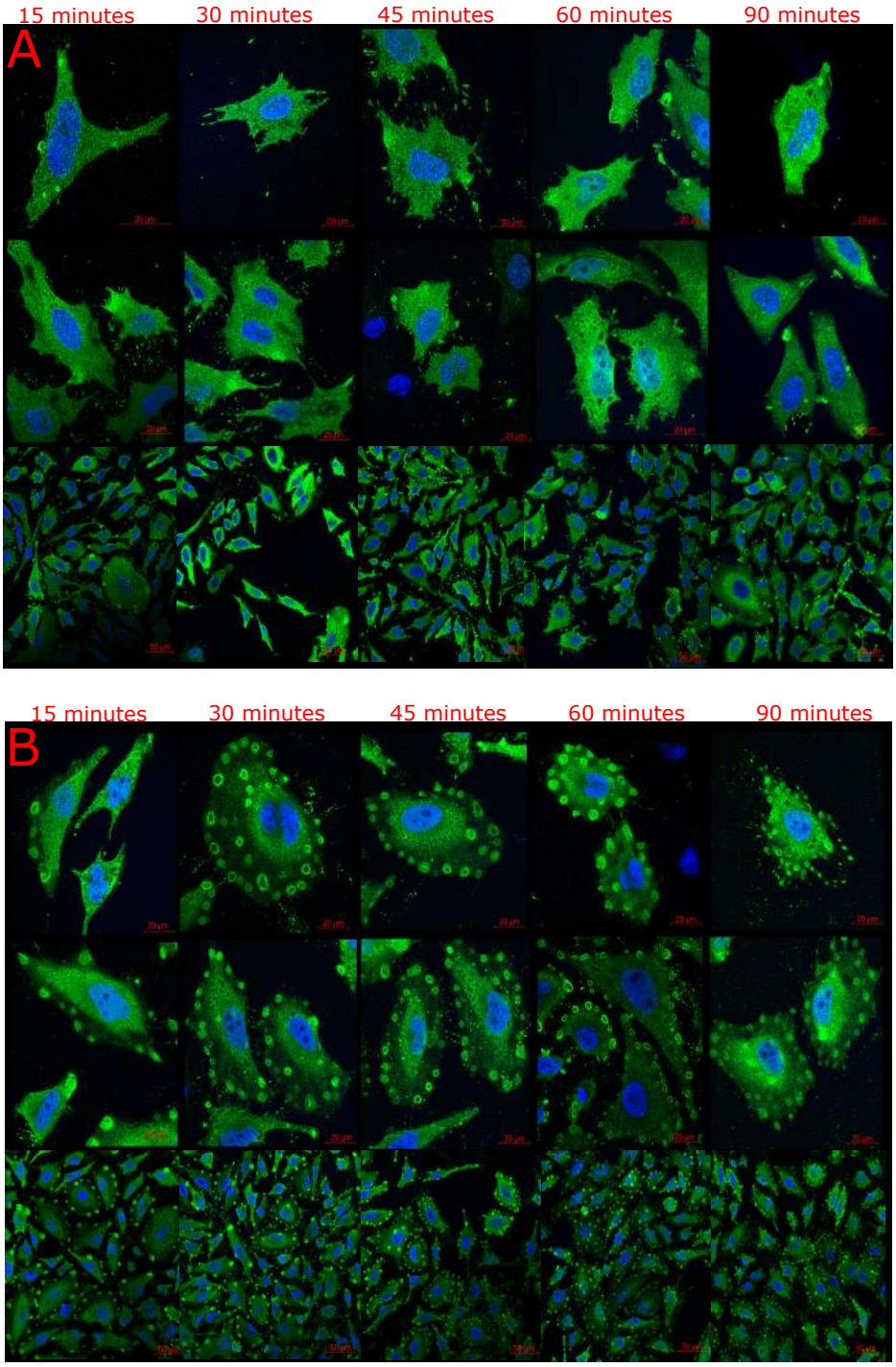

Figure 4.13 – ZnPT treatment panel of HeLa mammalian cells fixed at different time points. Membrane insertion of CLIC1 is investigated by treatment with ionophore Zinc pyrithione to increase intracellular zinc levels. A – Control cells with no treatment fixed at five time points. B – Cells treated with 50 µM ZnPT at the same points for direct comparison. CLIC1 antibody (green) and nucleus DAPI stain (blue).

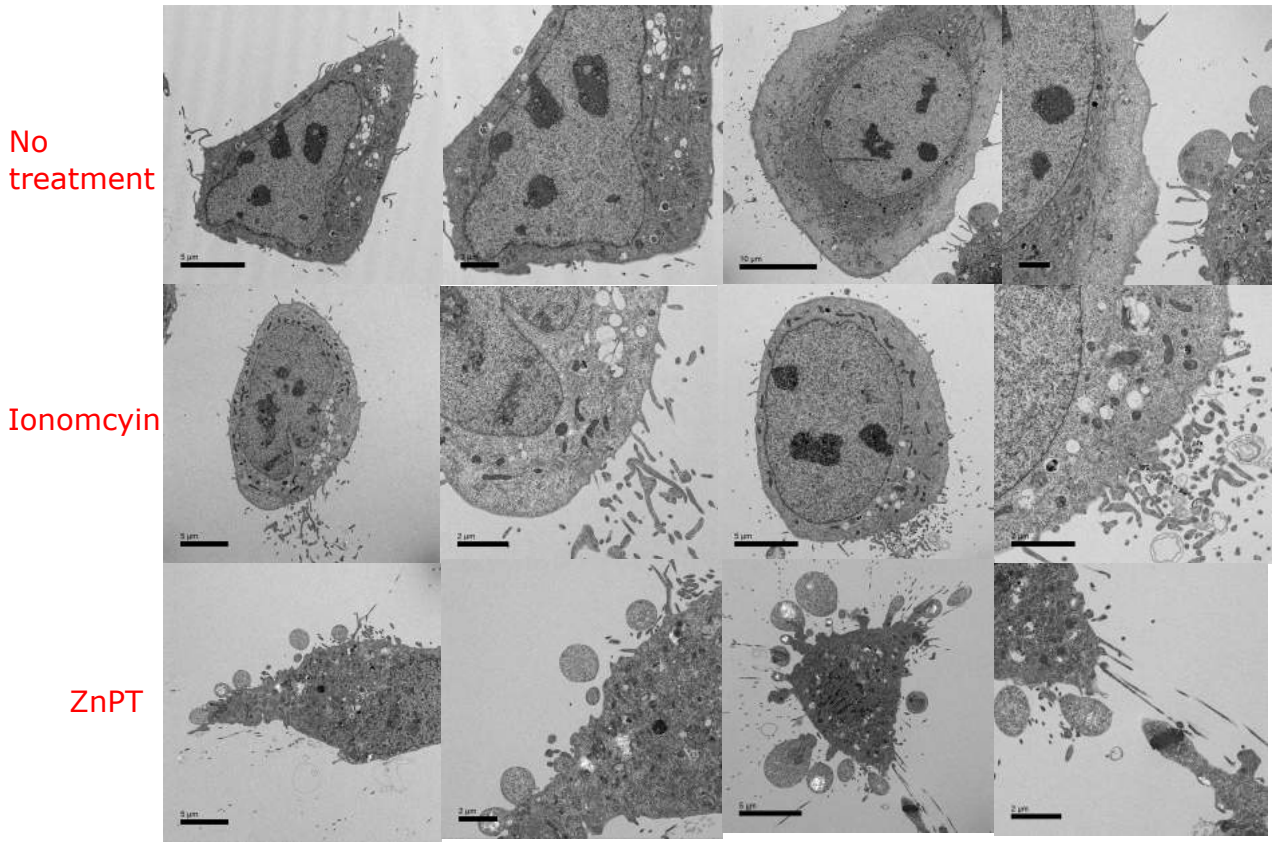

Figure 4.14 – Transmission electron microscope images of HeLa cells with ionophore treatment. The cells are treated with 10 µM Ionomycin and 50 µM ZnPT, the conditions optimised for CLIC1 membrane insertion, to study the effect on the mammalian cells.

4.3.11 Treatment of mammalian cells with metformin, a known CLIC1 channel inhibitor in the presence of raised intracellular calcium and zinc

Mammalian cells were treated with both ionomycin and ZnPT to increase intracellular levels of calcium and zinc, respectively. The usual phenotype, against control cells in both media containing and not containing phosphate, of CLIC1 relocalisation into the plasma membrane and circular CLIC1-rich objects close in vicinity to the plasma membrane, can be seen especially with ZnPT (Figure 4.15).

Treatment of the cells with metformin, a drug shown to specifically inhibit CLIC1 channels, consequently reducing cancer cell proliferation, displayed the expected phenotype of being identical to the control cells, with diffuse localisation of the protein and little membrane insertion. Of interest was CLIC1 in the cells when treated with both ionomycin and metformin as plasma membrane localisation was seen similar to treatment of just ionomycin, so the effect of increasing calcium was not changed by the presence of the inhibitor. Treatment with ZnPT and metformin simultaneously displayed the circular punctate phenotype produced by ZnPT alone so again CLIC1 localisation did not seem to change with metformin.

4.3.12 Metformin does not decrease the intracellular calcium levels

Fluorescent staining of the mammalian cells for intracellular calcium confirms once more the increase in intensity of intracellular calcium upon treatment with ionomycin. Treatment with metformin has little effect on intracellular calcium levels as expected and when the cells were treated with both the ionomycin and metformin, metformin did not decrease the intracellular calcium level increase caused by ionomycin (Figure 4.16).

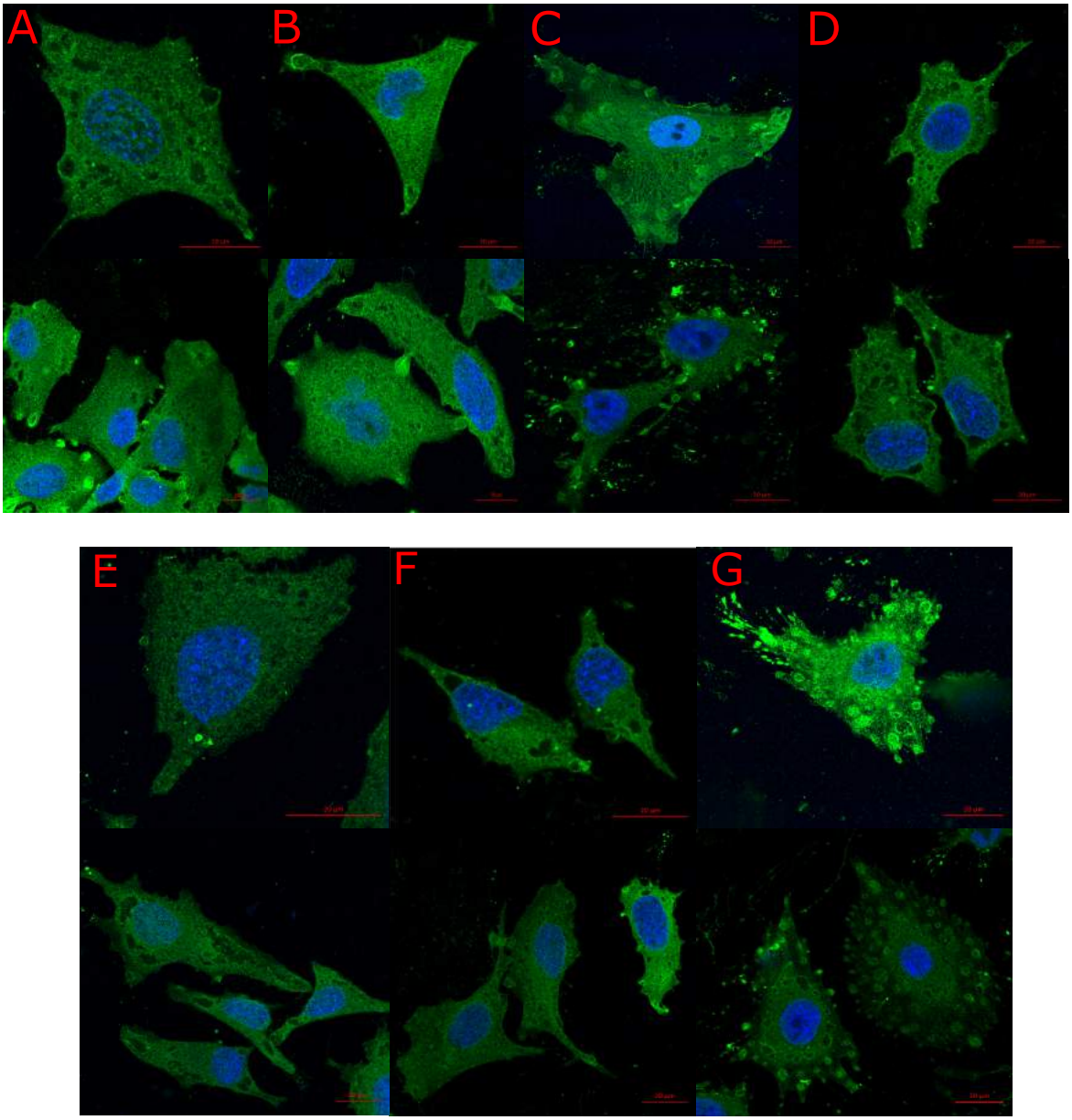

Figure 4.15 – HeLa mammalian cells treatment with ionophores and inhibitor metformin to study CLIC1 localisation. A – Control cells in normal media containing phosphate. B – Control cells in media with no phosphate. C – Cells treated with 50 µM ZnPT. D – Cells treated with 10 µM Ionomycin. E – Cells treated with 1 mM Metformin. F – Cells treated with 10 µM ionomycin and 1 mM metformin. G – Cells treated with 50 µM ZnPT and 1 mM metformin. CLIC1 antibody (green) and nucleus DAP stain (blue).

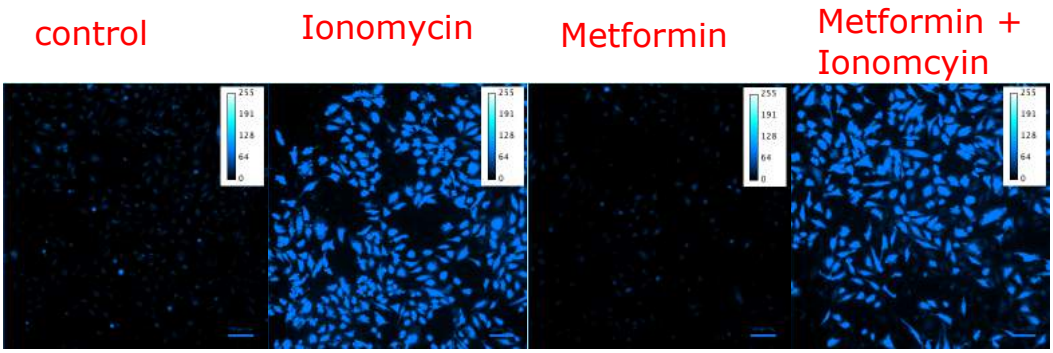

Figure 4.16 – Fluo4 reporter assay to check the effect of metformin on intracellular calcium levels. Hela cells were left untreated as a control or treated with 10 µM ionomycin alone or in combination with 1 mM metformin. Higher colour intensity correlates to higher intracellular calcium levels.

4.3.13 CLIC1 localisation in glioblastoma cells

Endogenous immunofluorescent staining of glioblastoma for CLIC1 reveals the protein is found with high signal throughout all the cell (Figure 4.17). With no treatment of metals there already appears to be plasma membrane localisation with an additional observation of many long processes such as filopodia protruding from the cells, contacting neighbouring cells. These long protrusions are stained brightly with CLIC1 with small circular punctate rings of CLIC1 along their lengths. Little difference is observable between cells grown in normal growth media and media with the phosphate removed, however there are many protrusions observed in the phosphate free media.

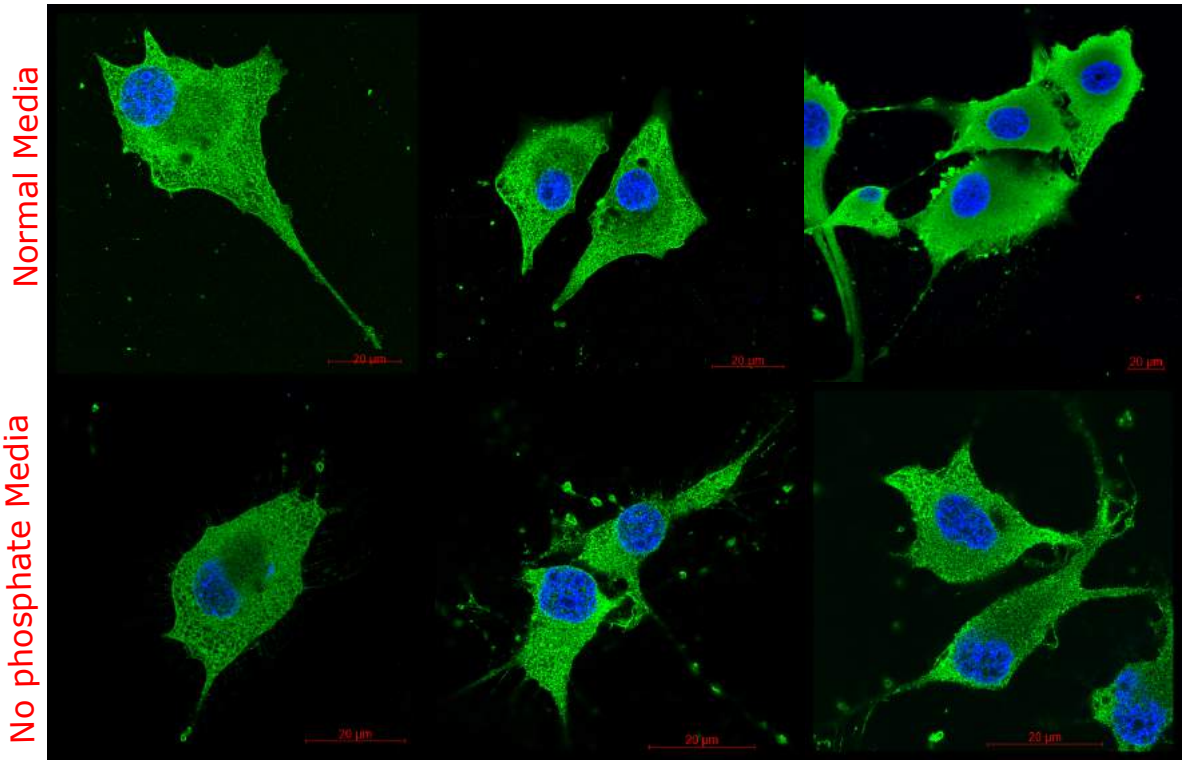

Figure 4.17 – Antibody staining of endogenous CLIC1 in U87 glioblastoma cell line. CLIC1 antibody (green) and cell nucleus DAPI stain (blue) in media with and without phosphate.

4.3.14 Glioblastoma treatment with ionomycin

Due to CLIC1 membrane localisation already being seen with the glioblastoma cells with no treatment, treatment of ionomycin does not give as big a difference in localisation as seen with the other mammalian cells upon treatment (Figure 4.18). However, membrane localisation can be seen all around the circumference of the U87 cells when treated with ionomycin and indicates the same transition from cytosolic to membrane channel is triggered by the increase of divalent cations in U87 cells. The use of TPEN as a metal chelator, seemed to reduce the membrane localisation of CLIC1 and revert the cells to a more diffuse localisation of CLIC1 through the cytoplasm, more similar to control HeLa cells. Furthermore, the bottom panels of Figure 4.17 show the long filopodia from the cells reaching towards each

other for cell-to-cell communication, these protrusions are rich in CLIC1. Ionomycin treatment appears to show longer and more obvious protrusions.

4.3.15 Intracellular calcium levels of glioblastoma

Fluorescent staining of intracellular calcium was carried out on both HeLa and Glioblastoma in direct comparison of the two cell types. There was higher intensity of fluorescence seen in the glioblastoma in both normal and phosphate free media when compared to the HeLa cells. Furthermore, the fluorescence seen with ionomycin treatment of HeLa gave similar fluorescence to the glioblastoma without treatment. Glioblastoma treated with ionomycin had similar fluorescence intensity of the cells to untreated glioblastoma, but it is clear there were fewer cells left to image in the sample (Figure 4.19).

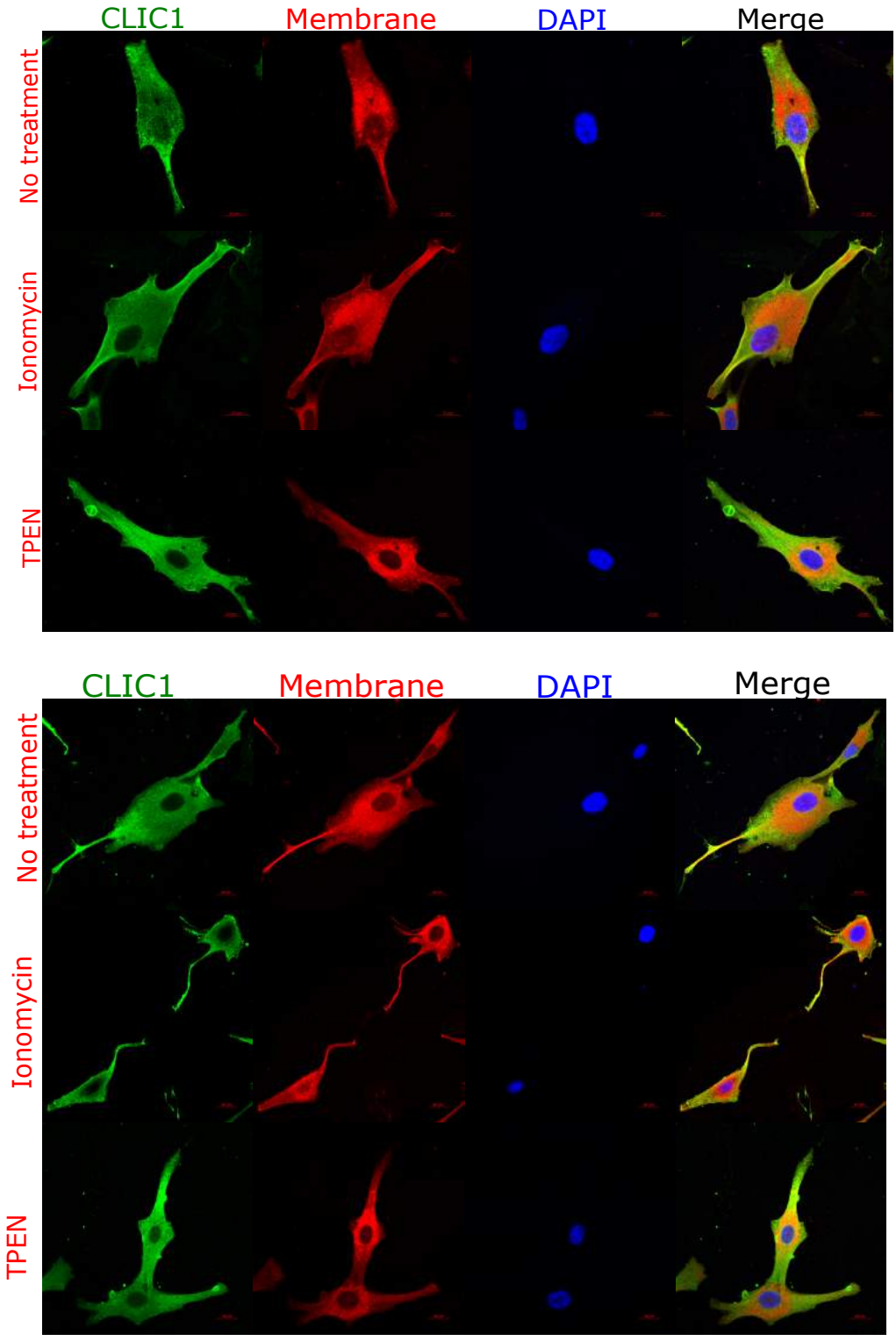

Figure 4.18 – Antibody staining of CLIC1 in U87 glioblastoma cells when treated with 10 µM ionomycin and 10 µM TPEN. Both panels show the same results to display multiple cells. Treatment with ionomycin was used to increase the intracellular calcium level to induce CLIC1 membrane localisation and to study if reducing divalent cations had any effect metal chelator TPEN was used. CLIC1 antibody staining (green), membrane mask dye (red) and nucleus DAPI stain (blue).

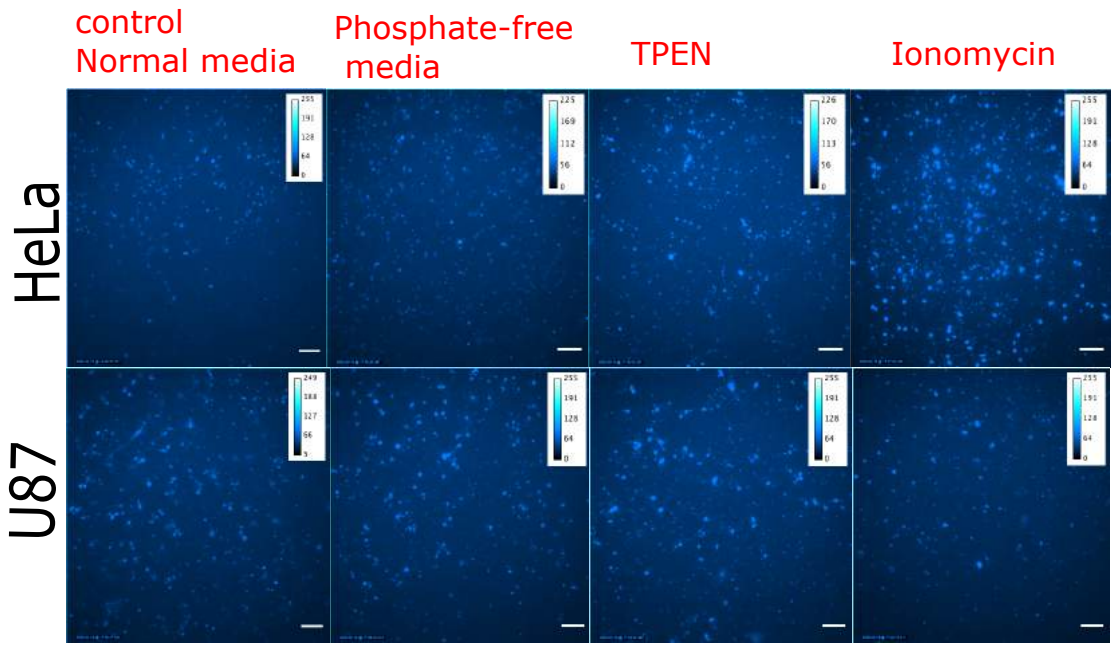

Figure 4.19 – Fluo4 receptor study of both Hela and U87 glioblastoma cells. Right hand panels are shown with treatment of 10 µM metal chelator TPEN and 10 µm calcium ionophore ionomycin. Higher colour intensity correlates to higher intracellular calcium levels.

4.4 Discussion

The trigger that drives CLIC1 into the membrane was found to be divalent cations, in particular calcium and zinc. However, all of the results providing evidence for CLIC1 membrane insertion were carried out in vitro (Section 3). Due to the clinical relevance of CLIC1, with membrane overexpression found to aid cancer progression particularly in glioblastomas, (Gritti, Würth, Angelini, Barbieri, Peretti, et al., 2014; Peretti et al., 2018; Setti et al., 2013) studying the relocalisation of CLIC1 in cancer cells and understanding the response to divalent cations is of importance.

The first mammalian cell type studied were HeLa, as there is no known overexpression of CLIC1 in cervical cancer so any relocalisation of the protein could be identified easily. Transfection of CLIC1 with a fused GFP tag allowed visualisation of the protein within the cells as well as the effect increasing levels of CLIC1 has on cervical cancer cells. An advantage of using the CLIC1-GFP construct to study CLIC1 in mammalian cells is the development of a system where live microscopy could be used to follow the movement of the protein, compared to fixed antibody staining.

The initial transfection of HeLa cells with fluorescently labelled CLIC1 with $CaCl_2$ and $ZnCl_2$ in the media, allowed a change in CLIC1-GFP localisation to be seen, from diffuse in the cytoplasm to centrally located around the nucleus and endoplasmic reticulum but also in the plasma membrane. This provided evidence for the first time that the increase in membrane insertion of CLIC1 with the addition of divalent cations as seen in vitro, as shown in Section 3 (Varela et al., 2019) can be translated into a cellular environment.

Understanding what happens in the cellular environment is of vital importance in understanding the role of CLIC1 in disease progression, with the overexpression of membrane CLIC1 leading to many pathological states.

Hydrogen peroxide treatment proved difficult to visualise and study due to the viability of transfected cells under these conditions. Cells underwent massive stress in the presence of ROS, as literature suggests increasing ROS can lead to cell apoptosis (Simon et al., 2000). We cannot completely rule out that oxidation state does lead to a change in CLIC1 localisation state within cells, as cellular signalling is complex, and ROS could be an upstream target to increased cellular metal levels. Increasing ROS has been shown to be induced by increased calcium levels within cells and increasing ROS can affect intracellular calcium stores (Görlach et al., 2015), while zinc ions are shown to be vital in folding of the superoxide dismutase 1 (SOD1) (Li et al. 2010), a protein vital in protecting human cells against oxidative stress.

Treating cells with two different chemicals inducing ROS production, H_20_2 and PMA, in the cells simultaneously with metals allowed direct comparison against both ROS inducing agents and metals alone. The lack of membrane localisation with ROS species alone but membrane localisation similar to solely metal treatment when both treatments were applied simultaneously, indicates it is the metal levels within the cells that causes CLIC1 to relocate from majority of protein in the cytoplasm into the plasma or internal membranes. The evidence from my microscopy images could be part of a feedback signalling mechanism in the cells, that under certain stress, the intracellular metal levels increase and the protein moves into the membrane.

Literature points to the potential unsuitability of the antibody of CLIC1 (Gururaja Rao et al., 2018) with not knowing if the epitope will show membrane insertion of CLIC1

but the research carried out investigating the relocalisation of CLIC1 with endogenous antibody staining reveals clear membrane localisation. However, it can be discussed whether it is in the membrane channel form of the protein that is being detected by the antibody or rather protein that has docked on the membrane before inserting. The mechanism of exactly how CLIC1 transitions from the cytoplasmic monomer or dimer into higher order oligomeric state remains unclear and if the epitope cannot bind the channel form, it would stand to reason the oligomerisation state of the protein observed in close vicinity of the membrane has not yet adopted the channel structure, or the insertion into the membrane itself makes the epitope inaccessible. However it can also be reasoned that in fact the membrane channel form can be detected by the antibody, as previous studies have also used antibody for membrane localisation studies (Ulmasov et al., 2007) and the above colocalisation studies with a membrane mask, where just the lipids are stained, implies the membrane form itself is being stained for with the immunofluorescent studies.

Relocalisation of CLIC1 into the membrane of the mammalian cells, such as HeLa, with both overexpressed transfected CLIC1 but also endogenous CLIC1, upon the treatment of raised intracellular calcium levels, is a significant finding that shows the divalent cations role in CLIC1 relocalisation to the membrane. Fluo4 reporter experiments verified calcium levels were raised intracellularly by the ionomycin treatment to a higher degree than metal treatment to the media. These results indicate for first time CLIC1 has been shown to relocate within the cell down to this specific divalent cation stimulus and provides more information compared to previous fluorescent microscopy studies where CLIC1 is shown to already be present

in the membrane of certain cell types like glioblastoma. By selecting cells that are not before implicated in CLIC1 overexpression, a model is generated where this change of relocalisation to the membranes of the mammalian cells can be induced. This could have endless uses in deciphering more mechanistic and structural information for the channel form of the protein as a cytoplasmic control can be compared to a membrane channel within the same cell type. Performing invasion and migration assays on this induced phenotype of cell would be of interest, to see if the expression of CLIC1, under metal treatment, in the membrane enhances the tumorigenicity in a cancer not yet correlated with CLIC1.

Throughout my work on CLIC1 within the context of mammalian cells, I have concentrated on looking at cancerous cells, when other disease contexts also implicate higher expression levels of CLIC1, for instance in microglia in neurodegenerative diseases (Novarino et al., 2004). It would be of interest to investigate the localisation of CLIC1 within macrophages and other cell types and see if the same movement to the membrane could be seen, now the treatment for raising intracellular metal levels has been optimised.

Raising cellular zinc levels appeared to induce a strong change in morphology of the cells and localisation of CLIC1, compared to increasing calcium levels. TEM images combined with the specific signalling of CLIC1 in immunofluorescent studies in the ZnPT treated cells indicates that CLIC1 is involved or concentrated in this change of phenotype of the cells. The increase in long processes outreaching from the cells, such as filopodia, seen with treatment of the metals could be indicative of how CLIC1 aids cancer progression. The formation of these filopodia could aid tumour cell migration, invasion of surrounding tissue and metastasis (Arjonen et al., 2011).

Possible explanations for the circular rings of CLIC1 within these images could be the formation of vesicles packed with CLIC1, with localisation around the plasma membrane for release from the cell to be taken in by neighbouring cells. This form of cell-to-cell communication has been characterised previously (Thuringer et al., 2018) and CLIC1 specifically have been hypothesised to pass within these extracellular vesicles to neighbouring cells. Of importance to note is that the absorption of these vesicles is accompanied by intracellular spikes of calcium within the cells and enhanced proliferation, this provides further evidence the levels of divalent cations play a part in how CLIC1 enhances tumorigenicity within cancer cells. Isolation of these vesicles and staining with CLIC1 could help deduce whether the protein is being passed from cell to cell to enhance tumour proliferation.

Another hypothesis involves the enhanced formation of invadopodia or filopodia in the presence of ZnPT, with the circular rings of CLIC1 colocalisation to actin. Circular rings of actin have been visualised previously in the formation of invadopodia (Murphy & Courtneidge, 2011), with a physical appearance similar to the CLIC1 rings seen in the presence of ZnPT. Furthermore CLIC1 has been associated with actin in various experiments (Kagiali et al., 2020; Singh et al., 2007), and invadopodia formation previously (Gurski et al., 2015). Further experiments investigating the colocalization of CLIC1 with this cytoskeletal protein actin within these rings would be of interest into determining how CLIC1 plays a role in enhanced tumorigenicity. The TEM images display lots more protruding objects from the cells with metal treatment, more so with the zinc than calcium, upon investigation these images have lots of resemblance to previous TEM images where invadopodia are identified (Tolde et al., 2010). In addition, it is also key to note that many of these projections from

the cells are towards neighbouring cells so can further confirm the idea of cell to cell communication via these structures. Staining of CLIC1 within the TEM images would be a way to verify this relationship with invadopodia and determine if this concentration of CLIC1 is directly within the abnormal features seen within the TEM images.

The evidence that intracellular metal levels changes the localisation of CLIC1 could indicate the difference between normal healthy tissue and cancerous tissue where CLIC1 plays a role in disease progression and tumorigenicity. Intracellular zinc and calcium levels between cancerous and healthy tissue is unclear with contradictory literature, with increases or decreases in metals against healthy tissue counterparts seen in different cancer types, dependent on the specific kind of tissue. CLIC1 overexpression is also not implicated in all kinds of cells or forms of cancer and the difference in metal levels within in the cells could play a role in the differential action of CLIC1 throughout cancer types.

This is perfectly demonstrated by the different localisation of CLIC1 in glioblastoma cell line U87 with no treatment against the control HeLa cells. There is clear membrane localisation seen with no treatment and large filipodia protrusions towards neighbouring cells, which upon treatment with calcium only become enhanced. Of note is how the filopodia are areas rich in CLIC1 staining, previous experiments report CLIC1 being passed to neighbouring cells via extracellular vesicles and they bud off from these cellular protrusions. These results support the role of CLIC1 as a membrane channel in tumorigenicity and metastasis as glioblastoma tumours are a highly aggressive form of cancer, with poor prognosis. It would be of

interest to downregulate CLIC1 and see if the same filopodia upon treatment of calcium appeared.

These results provide valuable insight into how CLIC1 behaves in different cancer cell types and many future experiments could build upon this knowledge to gain a much more comprehensive knowledge of the role CLIC1 has as both a cytosolic protein but also the integral membrane channel. Future work could include using the transfection models created to visualise CLIC1 with live cell imaging, to treat with the optimal concentrations of ionophores and created a time course of how this CLIC1 relocalisation really happens. Antibody experiments at fixed time points after treatment with calcium, revealed slight differences in membrane localisation so it would be helpful to be able to decipher information on the kinetics on this change of localisation and how long after treatment CLIC1 remains inserted as a membrane channel. Due to the increased protrusions of the cancer cells seen with metal treatment it indicates involvement of cytoskeletal filaments, colocalisation studies with actin and integrins under treatment of the metals would be of interest, additionally due to the involvement of CLIC1 in MAPK signalling pathways. If colocalisation occurs it could reveal key information of how CLIC1 aids tumorigenicity. Performing the ionophore treatment on other cancer cell types could give a wider picture of how CLIC1 can relocate to the membrane in other cancer forms and it would be beneficial to be able to use migration and invasion assays to show a clear change in phenotype in the cancer cells when treated with metals. If an increase in invasion abilities were correlated with increased membrane localisation, due to increased divalent cations, it could further confirm the role of CLIC1 in cancer cell's diseased state.

Investigating the role of metformin, a known CLIC1 inhibitor (Gritti, Würth, Angelini, Barbieri, Pizzi, et al., 2014), on CLIC1 localisation within the cancer cell, allowed determination that the mechanism of action of metformin is not to reduce the intracellular calcium levels and in fact they stay the same to control levels and when treated with ionomycin alongside the inhibitor. Less membrane localisation of CLIC1 was seen with treatment of the drug, indicating the drug could prevent insertion of CLIC1 as a channel but more investigation is needed.

Further clarification of CLIC1 localisation around the nuclear envelope was seen using a detergent removal method of the cytoplasm, similar to a method used by Ulmasov when looking at CLIC1 distribution in many cell types (Ulmasov et al., 2007). This removal of cytoplasm allowed confirmation of CLIC1s localisation to the nuclear envelope, even more so with the addition of intracellular calcium. These images give a clearer picture of the localisation change of CLIC1 due to divalent cation stimuli.

Overall, this chapter uses the powerful tool of microscopy to provide the evidence for CLIC1 translocation to the membrane upon divalent cation treatment in an cellular environment and elucidates key information in the complex puzzle of the role of CLIC1 in the context of disease, these studies allow more knowledge on a potential therapeutic target that could have specific action against cancer cells.

CHAPTER 5: Structural insights into CLIC1 activation mechanism in cells

5.1 Introduction

Studying CLIC1 in the context of the cell is a complex task, with the protein changing conformation from the cytosolic globular protein into a chloride membrane channel the structure is difficult to decipher. Determining any new information in the formation of the chloride channel or how the conformation of the protein within the cell environment is of importance, due to the channel's potential to form a selective drug target.

CLIC1 has previously been purified from bacteria and reconstituted into lipids increasing chloride current (Tulk et al., 2000, 2002; Varela et al., 2019; Warton et al., 2002), demonstrating the protein's ability to form active channels from *E. coli* recombinant expression. The lipids used for these channel formation experiments were often phospholipid mixtures generating artificial membranes (Singh & Ashley, 2006; Tulk et al., 2000, 2002; Warton et al., 2002) or mammalian cell membranes (Tonini et al., 2000; Valenzuela et al., 1997), with little information regarding the activity of CLIC1 in the *E. coli* membranes themselves. CLIC1 chloride conductance was previously tested in bilayers generated with yeast or *E. coli* extracted lipids but little CLIC1 chloride conductance was identified in these studies without the addition of cholesterol (Al Khamici et al., 2016). Native tryptophan fluorescence of CLIC1, as described in section 3.3.1, can be used to determine the insertion of the protein into lipids and this methodology can be applied to investigate whether CLIC1 naturally inserts into the *E. coli* membrane in its purified from. It would be hypothesised CLIC1 can insert into these bacterial lipids upon purification, as *E. coli* membranes are

mainly composed of phospholipids, such as phosphatidylethanolamine, phosphatidylglycerol, and cardiolipin (Sohlenkamp & Geiger, 2016) which correlates to the artificial membranes showing CLIC1 chloride conductance mentioned above. Furthermore the N domain of CLIC1 is hypothesised to form the putative transmembrane domain of the chloride channel (Harrop et al., 2001), and the study of native tryptophan fluorescence could be applied to identify if interfering with the C-terminal or N-terminal regions of the protein could prevent insertion, providing further evidence which region of CLIC1 is necessary for channel formation.

This chapter also discusses the use of nuclear magnetic resonance (NMR) to study CLIC1.

NMR signals are highly sensitive to the chemical environment which allows the effects of buffer composition, pH, and treatment ligands such as metals to be monitored through changes in the protein NMR signals. This technique has the potential for unique information on the structure, interactions, function and dynamics of proteins in a physiological environment, (Stadmiller & Pielak, 2018) which could help elucidate further information about CLIC1.

In-cell NMR is an ever-evolving technique which can study proteins in the context of a cell, providing atomic level structural information but in physiological conditions (Kang, 2019). However the technique has limitations due to the complexity of studying protein in an environment of such macromolecular crowding; the high concentration of other proteins and nucleic acids in the cell cytoplasm can make it difficult to obtain a good quality NMR spectrum of the protein (Luchinat & Banci, 2016; Pastore & Temussi, 2017). The protein undergoes slower tumbling in the crowded cytoplasm compared to in aqueous buffers resulting in general broadening

of the NMR resonances of the protein in-cell compared to in vitro (Luchinat & Banci, 2016).

This technique could provide insight into how soluble CLIC1 looks structurally in the context of a cell and provide clues to its formation of a membrane channel. In cell NMR spectra would allow comparison of the conformation of the soluble form of CLIC1 in vitro and the conformation of the protein in cells, as well as testing any changes in protein conformation upon treatment with conditions hypothesised to be the trigger for the mechanism of protein activation and membrane insertion, for instance oxidation (Goodchild et al., 2009; Littler et al., 2004).

In-cell NMR is best characterised in bacterial cells, with multiple proteins having been successfully studied in *E. coli* cells. One of the earliest examples showed overexpression and isotopic labelling (^{15}N) of small globular proteins, such as the N-terminal metal binding domain of bacterial mercuric ion reductase (NmerA) and human calmodulin in bacterial cells was enough to detect protein signal using heteronuclear NMR and even observe small chemical shifts between in vivo and in vitro samples (Luchinat & Banci, 2017; Serber, Keatinge-Clay, et al., 2001; Serber, Ledwidge, et al., 2001). Solving the structure of proteins in cellulo was demonstrated by the 3D structure of TTHA1718, a heavy metal binding protein from Thermus thermophilus, using *E. coli* cells. The backbone and most side chain NMR resonances were able to be assigned leading to structure calculations that compared highly to previous in vitro structures, demonstrating the capabilities of determining high resolution structures of proteins in more physiologically relevant environments (Sakakibara et al., 2009). Human proteins have also been studied using in-cell NMR in bacterial cells such as superoxide dismutase-1 (SOD1) which allowed the study of

how the protein folds in this prokaryotic cellular environment (Banci et al. 2011). The isotopic labelling process used for in-cell NMR is the same as for the expression of soluble protein for normal solution NMR such as ^{15}N and ^{13}C, however the full purification process is not needed for these experiments which can be an advantage for proteins difficult to purify (Kang, 2019). Eukaryotic cells such as Pichia pastoris can also be harnessed for overexpressing mammalian proteins and in vitro interactions between ubiquitin and RNA in yeast have been confirmed with in-cell NMR studies, furthermore different growth media or changes in metabolic state altered the cellular localisation of the labelled protein allowing spectrum to be obtained in various cellular compartments (Bertrand et al., 2012; Kang, 2019; Majumder et al., 2016). An advantage of using yeast against *E. coli* is not only are they eukaryotic so evolutionarily closer to human cells but they also have a stable cell wall which prevents protein leakage out of the cells (Bertrand et al., 2012). With all experiments studying proteins highly overexpressed it is important to recognise the toxicity this could have on the cells or how such high levels of protein could interfere with normal cell processes.

Micro injection of multiple proteins such as streptococcal protein GB1, ubiquitin and calmodulin into larger cells such as xenopus oocytes successfully generated in-cell NMR spectrum, revealing this techniques potential for studying protein-protein interactions and maturation in cellular conditions (Sakai et al., 2006; Selenko et al., 2006). In addition an advantage to using this cell type and injection is due to their large size the cells allow precise deposition of the protein into the cytoplasm (Selenko et al., 2006) and very few oocyte cells are needed to gain a spectrum (Kang, 2019). This oocyte in-cell model of GB1 protein was tested for paramagnetic labelling

studies which compared an in vitro paramagnetic spectra to an in vivo spectrum and demonstrated even with high molecular crowding of the cellular environment paramagnetic constraints could still be used to determine structural information (B. Bin Pan et al., 2016). This provides a lot of potential for future structural studies in vivo.

In cell NMR in human cells proved even more challenging. Novel methods were used to introduce labelled protein into human cells, such as HeLa cells, using cell penetrating peptides from HIV, covalently linked to the proteins. The peptides used a pyrenebutyrate mediated action and then released the proteins from the peptide by endogenous enzyme activity or autonomous cleavage. This was successfully carried out with three different proteins that obtained high resolution 2D spectra (Inomata et al., 2009).

Another methodology for protein delivery for in-cell NMR was developed by utilising the bacterial toxin streptolysin O (SLO) to form a pore in the cell's plasma membrane allowing large protein molecules to enter the cells, with repair of the pore by the addition of calcium. This was successfully carried out with human embryonal kidney cells and thymosin β4 protein, showing a novel labelled protein delivery method which did not rely on modifying the protein (Ogino et al., 2009).

Comparison of the various methods for achieving in cell NMR is complex as there is far less background signal in injected eukaryotic models compared to overexpression in bacteria but recombinantly expressing and labelling protein outside the cells can be difficult since a high amount of protein is needed for this process. Another methodology was designed to overcome this, a baculovirus system that allows expression of these proteins in eukaryotic cells (Hamatsu et al., 2013). In-cell NMR

was achieved via baculoviral transfection into sf9 insect cells using Protein G domain B1 (GB1), rat calmodulin and human antioxidant copper chaperone (HAH1) as the initial targets. 80% of backbone signals could be seen in cell and many backbone resonances could be assigned in the eukaryotic in cell spectrum of GB1, providing a useful method to bridge the gap between prokaryotic overexpression and inserting purified protein into eukaryotic cells (Hamatsu et al., 2013).

The use of human cells for in cell NMR is the most physiologically relevant and has been achieved in multiple ways. Electroporation of labelled protein into mammalian, including human cells, has also been developed as a method for in-cell NMR. Applying an electric field to the cells allows transient pores to form for the influx of the protein of which the cell can then recover (Chau et al., 2020). Labelled alpha synuclein, associated with Parkinson's disease, translocated into rat neuronal and HeLa cells after the electroporation process and allowed the study of intrinsic structural disorder of this protein within a mammalian cell context (Theillet et al., 2016).

Furthermore in-cell NMR of proteins expressed inside human cells has been achieved via transfection of the protein cDNA into the cells which is then isotopically labelled using growth medium (Banci, Barbieri, Bertini, et al., 2013; L. Barbieri et al., 2016). This process has much higher experimental cost than bacterial or other eukaryotic methodologies and high background signal due to nonspecific isotopic enrichment. However, this technique was able to study maturation of a human protein, SOD1, and folding of a mitochondrial intermembrane space import and assembly protein (MIA40), within human cells (Banci, Barbieri, Bertini, et al., 2013; Banci, Barbieri, Luchinat, et al., 2013). This provides a much more physiologically relevant study of human proteins and gives better insight into true nature of these proteins and how

they interact within the cells which can have huge implications in therapeutics (L. Barbieri et al., 2016; Kang, 2019).

It is important to note challenges with all of these methodologies remain. When isotopically labelling protein within a cellular environment the presence of other molecules or proteins in the cell can lead to complex formation which results in much higher molecular weight targets, which causes rapid relaxation and low signal sensitivity leading to poor NMR spectrum (Kang, 2019). Signals within the NMR can also broaden due to the high viscosity of cell cytoplasm compared to samples in solution of buffer or water, due to slower tumbling of the protein, and it would be difficult to determine if sharp lines on the spectrum were being obtained from a small proportion of extracellular protein. Some experiments sought to combat this by centrifugation and filtration to remove the cells and then measure the supernatant to check it's contribution to the spectrum, and then resuspending the cell pellet to check it restores the spectrum (Serber, Keatinge-Clay, et al., 2001). It was also demonstrated that if the target protein exceeds 20% of the total cellular protein, leakage is likely and checking the supernatant and cell lysate for protein signal to confirm if leakage has occurred is a good control for all in-cell NMR experiments (Barnes & Pielak, 2011).

The protein being in a cell environment can also lead to many unknowns, from potential protein degradation by proteases to ligand binding. This can be overcome by acquiring the spectrum in a short time frame to prevent degradation throughout generation of the spectrum (Kang, 2019).

In terms of scientific advancement in-cell NMR is a new technique of which presents many challenges and is far from optimised for all proteins due to the techniques

complex nature, my PhD sought to try and study CLIC1 using this technique alongside other NMR experiments to determine a close to physiological state of CLIC1 and its unique transition between cytosolic and channel form. The process of how CLIC1 transitions into its membrane-bound state in a cell was previously contradictory with oxidation thought to be the most likely trigger for membrane insertion (Goodchild et al., 2009; Littler et al., 2005) but pH and cholesterol were also implicated (Hossain et al., 2016; Stoychev et al., 2009), however now with all the evidence presented previously (sections 2 & 3) the trigger for CLIC1 membrane insertion is known to be binding of divalent cations (Varela et al., 2019). In-cell NMR methodology could provide further insight into this insertion mechanism, by testing the conformation of the soluble form of CLIC1 in cells and comparing to the in vitro soluble CLIC1 spectrum obtained.

Potential problems highlighted with the in-cell NMR technique is the high background signal from other membrane proteins or components in cells, a possible methodology to overcome some of the poor resolution seen with protein in vivo is the use of selective amino acid labelling. An early demonstration of this for in-cell NMR purposes was ^{15}N labelling the lysine residues of NmerA and human calmodulin to reveal little background signal in these spectrum (Serber, Ledwidge, et al., 2001). Selective methyl labelling was then identified as a more sensitive candidate for in-cell NMR due to the three protons coupled to one carbon nucleus in methyl groups compared to the single proton-amide nitrogen pair. Other advantages to methyl labelling other selective nitrogen labelling is due to the lack of chemical exchange with water and slow relaxation resulting in higher sensitivity (Serber et al., 2004). Selective labelling protocols are constantly under development and have been

successful in generating NMR spectra for large proteins for instance the isotopic labelling of alanine residues of a 306 kDa eukaryotic protein complex using methyl trosy experiments (Isaacson et al., 2007), with isoleucine, leucine and valine (ILV) labelling used for even larger systems such as assignment of a 723-residue enzyme, malate synthase G, and the study of the 670Kd 20S proteasome core particle (Sprangers & Kay, 2007; Tugarinov & Kay, 2003).

This chapter aims to discuss the various experiments performed to visualise CLIC1 in a cellular environment for the first time using in-cell NMR, initially these experiments aimed to study the oxidation state of CLIC1 in cells and deduce the mechanism for membrane insertion.

5.2 Methods

5.2.1 GFP insertion assay with N or C terminal tag

CLIC1 was cloned into a pWaldo-GFP vector, as previously discussed in section 2.2.1, to have a GFP tag located on the c terminus of the protein and in a modified pCold-I vector containing a N-terminal Histidine-tag, followed by a twin-strep tag and a TEV cleavage site. The resultant DNA was transformed into C43 *E. coli* cells for growth. Purification for both the pWaldo-GFP and the pCold-I constructs were carried out as previously described using nickel chromatography. The soluble protein was then incubated with 1mM Asolectin lipids and ultracentrifuged at 117734 g for 30 minutes. A Varian Cary fluorimeter was then used to detect the intrinsic tryptophan fluorescence in the soluble fraction and membrane fraction resuspended to the equivalent volume. The excitation wavelength used was 280 nm, and the fluorescence emission spectra to detect the protein was collected from 300 to 400 nm. 1 mM $ZnCl_2$ was added to both samples to encourage insertion.

5.2.2 *E. coli* membrane fluorescence

In order to detect CLIC1 in the *E. coli* membranes, C43 *E. coli* cells expressing CLIC1 cloned into the pWaldo vector, were grown to a suitable OD600 of 0.7 and then induced with 1 mM IPTG overnight, as per methods for purification in chapter one. The cells were then lysed using sonication and ultracentrifuged at 117734 g for 30 minutes. GFP fluorescence emission spectra were collected for initial cell lysate before ultracentrifugation and then for both the soluble and membrane fraction using an excitation wavelength of 395 nm and emission spectra collected between 400 nm to 600 nm, on a Varian Cary fluorimeter. To investigate reversibility, the

membrane fraction which has been suspended to initial volume in lysis buffer (150 mM TRIS 50 mM NaCl pH 7.4) was treated with 1 mM EDTA and left to incubate before ultracentrifugation again to separate the membrane and soluble protein. The GFP fluorescent readings of theses samples were then taken using the same parameters as described above.

5.2.3 Isotopic ^{15}N & selective methyl labelling of CLIC1

Purification of CLIC1 with isotopic labelling was carried out as described in section 2.3.4 using the pASG vector (IBA), however upon the growth of the cells reaching OD_{600} 0.7 an additional centrifugation step was added at 4000 rpm before resuspension in minimal M9 Media at a 4:1 ratio to the growth in LB media. After resuspension in the M9 media, the cells were grown for one hour at 30°C before IPTG was added to induce protein expression overnight. A similar purification methodology as previously described was carried out. Tris glycine SDS-PAGE gels were run to confirm protein purification (Figure 5.1). For samples just using ^{15}N labelling, $^{15}NH_4Cl$ was as the sole nitrogen source, and selective methyl labelling of methionine was achieved by the addition of isotopic labelled methionine. However, to prepare the ILV samples two precursors, α-ketobutyrate and α-ketoisovalerate were added in addition to the $^{15}NH_4Cl$. For ILV labelling the minimal media was deuterated and the induction time was limited to 8 hours for optimal results as per Turgarinov's protocol (Tugarinov et al., 2006). The minimal media composition is detailed below (Table 5.1).

Table 5.1 – Components of minimal media for isotopic labelling of CLIC1.

Components	Amount added	Ingredients
10 X M9 Salts	100 ml/l	Na_2HPO_4 66g/l (2.H20) KH_2PO_4 33 g/l NaCl 5.5 g/l pH 7.2
1 M $MgSO_4$	1 ml/l	
0.1 M $CaCl_2$	1 ml/l	
1 M Thiamine	1 ml/l	
Trace Metal (100x)	10 ml/l	$FeCl_3$ 0.5 g/l $ZnCl_2$ 0.05 g/l $CuCl_2$ 0.01 g/l $CoCl_2.6H_2O$ 0.01 g/l H_3BO_3 0.01 g/l $MnCl_2.6H_2O$ 1.6 g/l pH 7.0
D-glucose	4 g/l	
$^{15}NH_4CL$	1 g/l	Labels ^{15}N Isotope
13C Methionine	125 mg/l	Only added for ^{13}C labelling of methionine
Alpha keto valerate 3-methyl-^{13}C	120 mg/l	Only added for ^{13}C labelling leucine and valine
2-Keto-3-(methyl-d3)-butyric acid-4-13C,3-d sodium salt	70 mg/l	Only added for ^{13}C labelling of isoleucine
Selective antibiotic	100 ug/ml	For pASG vector = Ampicillin

5.2.4 NMR experiments

For solution state NMR, purified soluble CLIC1 spectra was collected using a 5 mm shigemi NMR tube in a Bruker Avance3 spectrometer operating at a ^{1}H frequency of 600 MHz, while In-cell NMR spectra were collected by centrifugation at 4000 rpm of a 50 ml cell culture, with 200 µl cell slurry then loaded directly into the shigemi tube. Spectra were uniformly collected in the ^{15}N dimension as described in (Varela et al., 2019). The soluble ILV spectra experiments were collected at the MRC Biomedical NMR Centre using a Bruker Avance III 800 MHz spectrometer, with 1H/13C/15N cryoprobe. Experiment parameters for each experiment are detailed below (Table 5.2).

Table 5.2 – Experiment parameters for all NMR spectra shown. SoFast (Schanda & Brutscher, 2005) and TROSY (Pervushin et al., 1997) experiments were used.

Figure	Labelling	Experiment Run	Experiment Parameters
Figure 5.4	^{15}N Soluble CLIC1	^{15}N-SoFast HMQC ^{15}N TROSY	64 scans, 1028 points in direct dimension and 64 increments in the ^{15}N dimension. Relaxation delay of 0.2 s, at 30℃
Figure 5.5	^{15}N Soluble CLIC1/^{15}N in-cell *E. coli*	^{15}N-SoFast HMQC	64 scans, 1028 points in direct dimension and 64 increments in the ^{15}N dimension. Relaxation delay of 0.2 s, at 30℃
Figure 5.6	^{13}C Methionine in-cell *E. coli*	13C-methyl SoFast HMQC	32 scans, 128 increments in the ^{13}C dimension, relaxation delay of 0.2 s, at 30℃
Figure 5.7	^{13}C ILV Soluble CLIC1	Methyl best TROSY	32 scans, 128 increments, 1028 points in direct dimension and relaxation delay of 0.2 s, at 30℃
Figure 5.8 & 5.10	^{13}C ILV CLIC1 in-cell *E. coli*	13C-methyl SoFast HMQC	32 scans, 128 increments in the ^{13}C dimension, relaxation delay of 0.2 s, at 30℃
Figure 5.11	^{15}N in-cell *E. coli*	^{15}N-SoFast HMQC	64 scans, 1028 points in direct dimension and 64 increments in the 15N dimension. Relaxation delay of 0.2 s, at 30℃

5.2.5 ILV in-cell experiments

Once the initial in-cell spectrum had been collected of the ILV labelled CLIC1 in *E. coli* cells, the sample was sonicated to lyse the cells and a spectrum was then collected of the cell lysate by loading it directly into a shigemi tube and collecting the NMR experiments described in table 5.2. The cell lysate was then recuperated and ultracentrifuged at 117734 g for 30 minutes. The soluble fraction of the protein was then collected and similar NMR experiments were acquired. All in-cell experiments were carried out in 20 mM Phosphate, 20 mM NaCl pH 7.4 buffer.

5.2.6 ^{15}N in-cell experiments

For studying the background signal in ^{15}N in-cell NMR for CLIC1, the same protocol was followed as described above for isotopic labelling and a cell slurry loaded into the shigemi tube to collect the labelled protein in-cell. However, for the control experiments the cells were never induced for CLIC1 expression with IPTG and the same spectra were taken with induced cells. Once in cell spectra were collected, the same protocol for lysing the cells and collecting the supernatant spectra was performed as described in section 5.2.5. The supernatant was then incubated with 10 mM EDTA to chelate divalent cations in the sample before collecting the spectra again.

5.3 Results – CLIC1 insertion assays

5.3.1 Evidence to support N terminal involved in structural rearrangement into membrane

Literature on CLIC1 presents a clear case for CLIC1 being able to auto insert into lipid membranes (Tulk et al., 2000; Warton et al., 2002) but initial insertion assays, as described in section 3.3, revealed no insertion was seen without treatment of the protein with divalent cations such as zinc or calcium, identified as the triggers for CLIC1 membrane insertion (Varela et al., 2019). Due to the putative transmembrane domain of CLIC1 hypothesised to be in the N-terminus of the protein (Harrop et al. 2001), the initial tests for insertion were carried out with a GFP tag on either the C-terminal or N-terminal end of the protein to see how this would affect insertion. The percentage of insertion of CLIC1 into the asolectin lipids can be seen to reduce when the tag was present on the N terminus of CLIC1 compared to the C terminus of CLIC1. However, little insertion of CLIC1 into the lipids is seen for both proteins and the spectra obtained are noisy, suggesting further verification is needed to confirm this result (Figure 5.1).

5.3.2 CLIC1 inserts readily into *E. coli* membranes and is not reversible with EDTA

To study how much protein was naturally inserting into the membranes during expression in C43 (BL21s) *E. coli* cells, a GFP labelled CLIC1 construct was used and the CLIC1-GFP levels were measured using fluorescence. As previously shown of the initial cell lysate, 80% of CLIC1 was found to have inserted into the bacterial membranes after centrifugation rather than be in the soluble fraction (Section 2.3.7, Figure 2.13) *E. coli* cells have divalent cations available during the growth of the

protein which could lead to this high proportion of insertion. EDTA, a known divalent cation chelator, was subsequently incubated with the bacterial membranes containing CLIC1 to study whether CLIC1 membrane insertion could be reversed. (Figure 5.2) It was shown that the presence of EDTA could not reverse the lipid insertion process and 100% of CLIC1 remained in the membrane. This study gives meaningful data that CLIC1 can auto-insert into bacterial membranes upon expression as previous studies have focused on recombinantly expressing the protein in *E. coli* before promoting insertion of the soluble protein into pre-prepared phospholipid vesicles (Tulk et al., 2000, 2002) or artificial lipid mono and bilayers (Hossain et al., 2016; Warton et al., 2002).

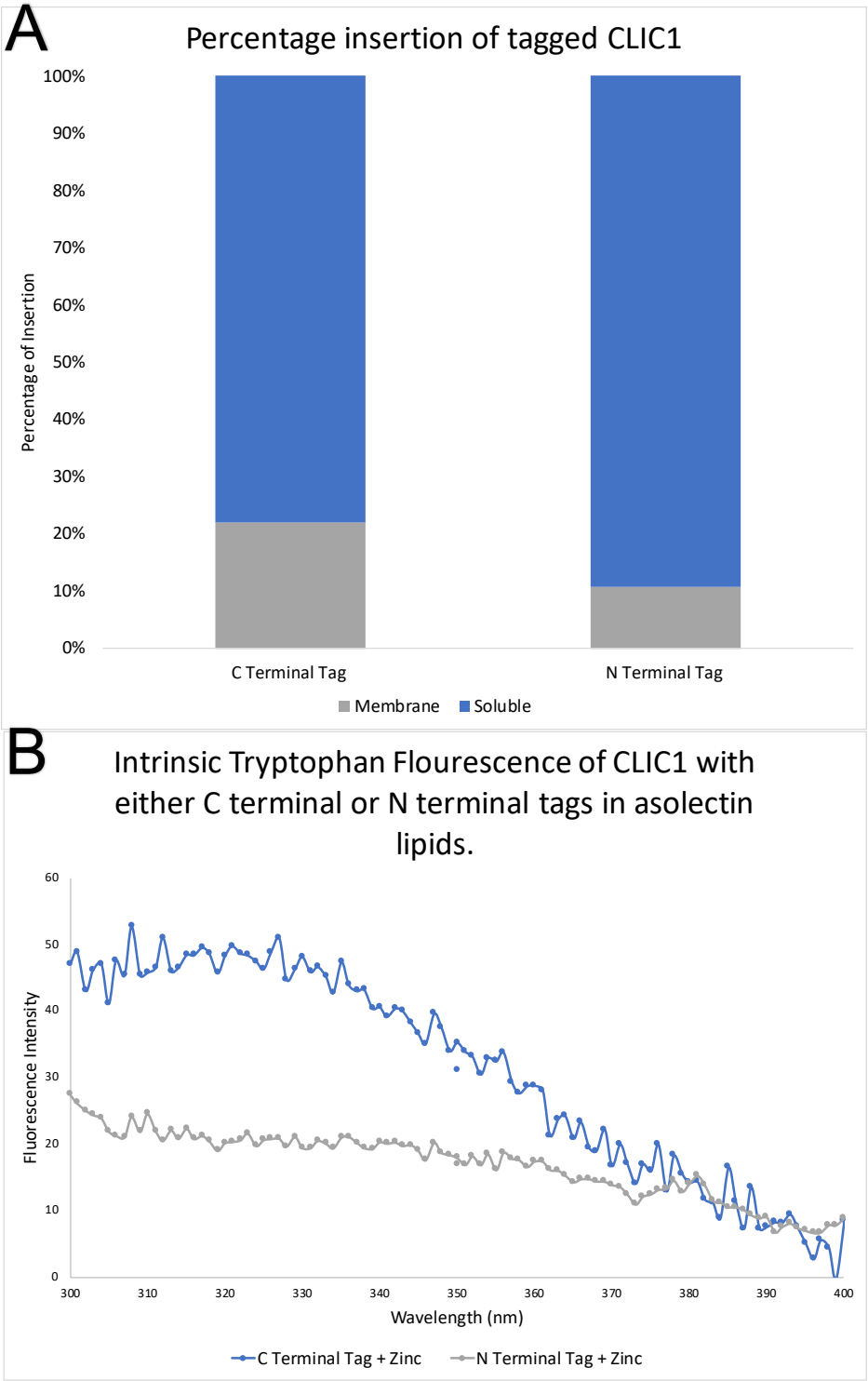

Figure 5.1 – Further evidence for the importance of the N-terminal domain of CLIC1 for membrane insertion. A – Percentage of total CLIC1-GFP fluorescence in both the membrane and soluble fraction for CLIC1 after incubation with asolectin lipids, with the GFP tag located on either the C-terminal or N-terminal domain of the protein. B – Intrinsic tryptophan fluorescence spectrum of CLIC1, with either a C-terminal or N-terminal GFP tag, that has inserted into the asolectin lipid membrane fraction.

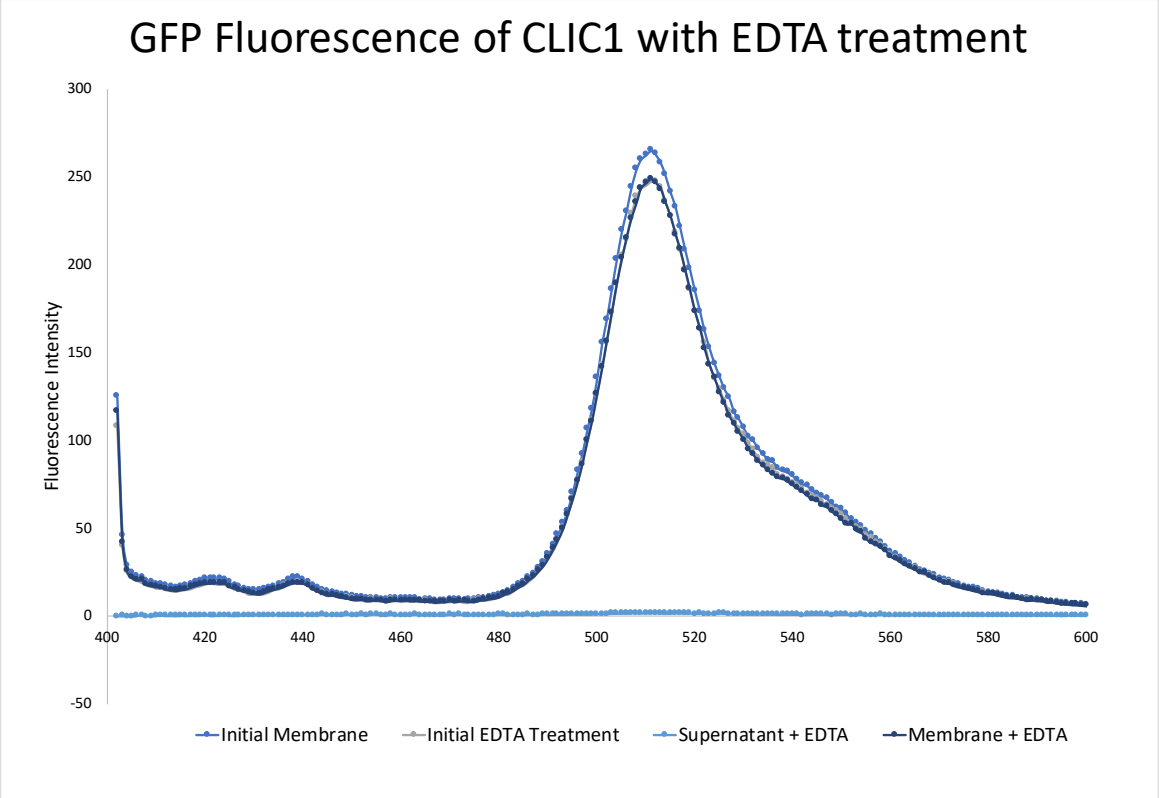

Figure 5.2 - CLIC1 insertion into bacterial cells is not reversible with EDTA.
GFP fluorescence of CLIC1 recombinantly expressed in *E. coli* was separated into soluble and membrane protein, with the initial fluorescence spectra of the membrane fraction shown. The GFP fluorescence of the membrane fraction of CLIC1 incubated with metal chelator EDTA is then shown before centrifugation. The fluorescence of the supernatant and membrane fractions then produced are shown to study whether CLIC1 remains inserted into the membrane after incubation with the metal chelator.

5.4 Results – Studying CLIC1 with NMR

5.4.1 Isotopic labelling of CLIC1

In order to further decipher the structural details of the insertion of CLIC1 into the membrane and how metals interact with the amino acids of the protein, my research turned to using the technique of nuclear magnetic resonance (NMR).To analyse CLIC1 with NMR, isotopic labelling was needed when expressing and purifying the protein, this was first completed with ^{15}N and then more complex labelling by ^{13}C labelling of the methyl groups upon selective residues, for instance on only the isoleucine, leucine and valine amino acids. Successful purification for both labelling techniques can be seen in Figure 5.3 with purified protein in the elution fractions. This protein is shown to have the correct labelling in NMR spectra as discussed later in this chapter.

5.4.2 Studying CLIC1 using NMR

Successful crystallography studies of CLIC1 has revealed the soluble structure of the protein (Harrop et al., 2001; Littler et al., 2004), and how upon oxidation oligomerisation of this protein is seen, which in turn is hypothesised to lead to CLIC1 membrane insertion. As shown in the previous chapters, we have identified Zn^{2+} binding as the trigger for CLIC1 membrane insertion. To test the different membrane insertion mechanisms proposed so far, we attempted to optimise In-cell NMR tools. This methodology could provide details of the protein's state within a cell, and whether oxidation or addition of divalent cations can change the conformation of the

protein in the cellular environment. The first steps taken in this project were to successful isotopically label CLIC1 in its soluble form and investigate the oxidation state of this spectrum , due to the implication of oxidation state triggering the formation of the channel form of CLIC1 (Goodchild et al., 2009; Littler et al., 2004).

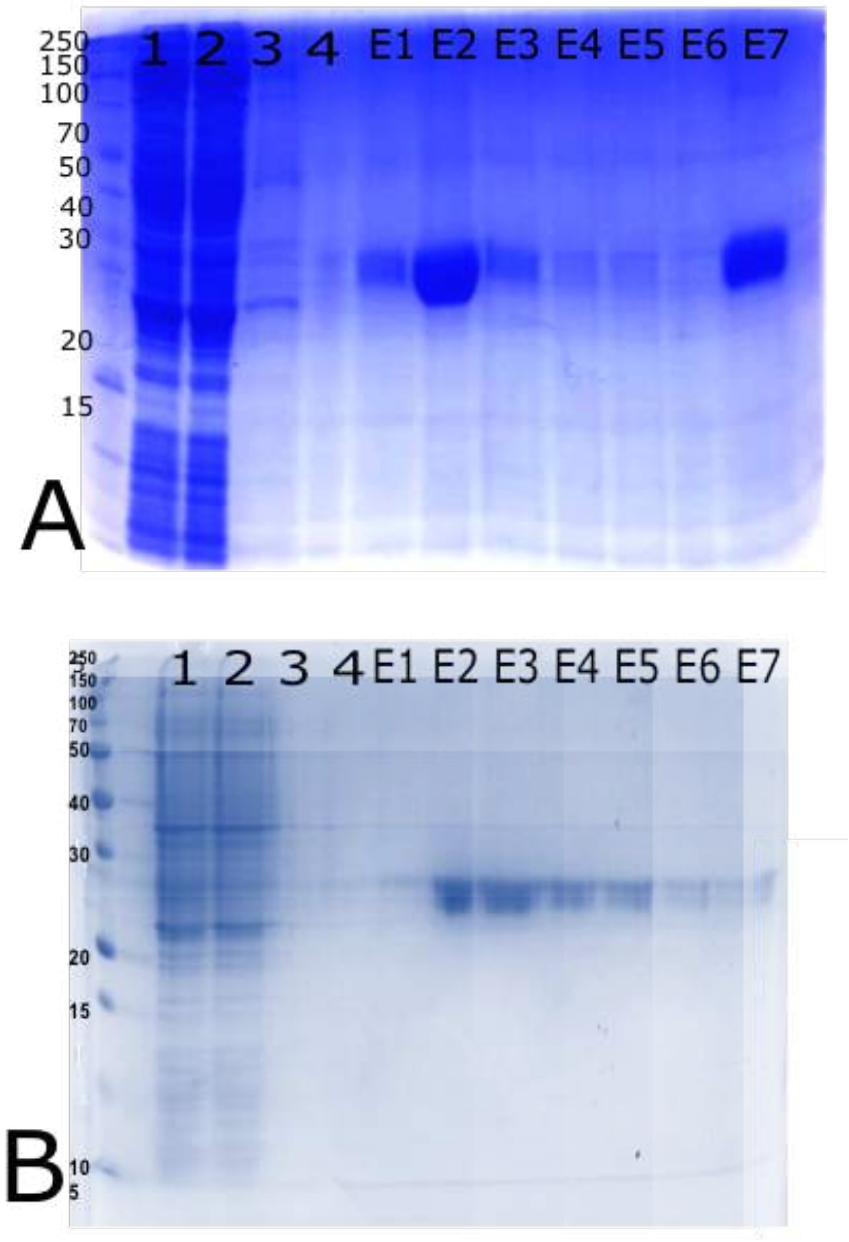

Figure 5.3 – Tris glycine SDS gels of isotopically labelled CLIC1.
Gel of Soluble ^{15}N CLIC1 protein (A) and ^{13}C methyl ILV labelled CLIC1 (B) purified by Streptactin purification column. 1 = Sample one, 2 = Flow through, 3 = Wash one, 4 = Wash two, E1-E6 = Elutions of purified CLIC1, E7 = final elution with excess biotin in Figure A.

5.4.3 CLIC1 inserted into *E. coli* membranes is reduced not oxidised

^{15}N isotopic labelling of CLIC1 allowed the acquisition of an NMR spectrum of the cytosolic form of the protein as seen in Figure 5.4. Due to literature's long standing link between oxidation and the insertion of CLIC1 into the membrane (Goodchild et al., 2009; Harrop et al., 2001; Littler et al., 2005), NMR was also used to investigate any changes in the protein under oxidising conditions. Soluble ^{15}N CLIC1 was recombinantly expressed from *E. coli* and treated with 50 mM H_2O_2. In addition to this, CLIC1 recombinantly expressed in the membrane was solubilised with n-Dodecyl-B-D-Maltoside (DDM) detergent, transitioning the membrane protein form into soluble protein without altering the oxidation state and 2D ^{15}N TROSY or ^{15}N-SOFAST-HMQC NMR spectra of CLIC1 were acquired for all fractions of the protein (Figure 5.4). Chemical shifts for both ^{1}H and ^{15}N were measured to study any changes in CLIC1 as chemical shifts of N-H moieties are highly sensitive to both the structure and dynamics of the protein. Overlay of the spectra in Figure 5.4 revealed that CLIC1 from both the soluble and solubilised membrane fraction were indistinguishable, showing no difference in oxidation state between these proteins. However, when overlayed with the soluble protein that was oxidised with hydrogen peroxide, clear chemical shift differences were seen to both of the untreated protein in many resonances. These results indicate CLIC1 that inserts into the bacterial membranes and soluble CLIC1 are in a reduced state and oxidation is unlikely to be the true trigger for membrane insertion of the protein.

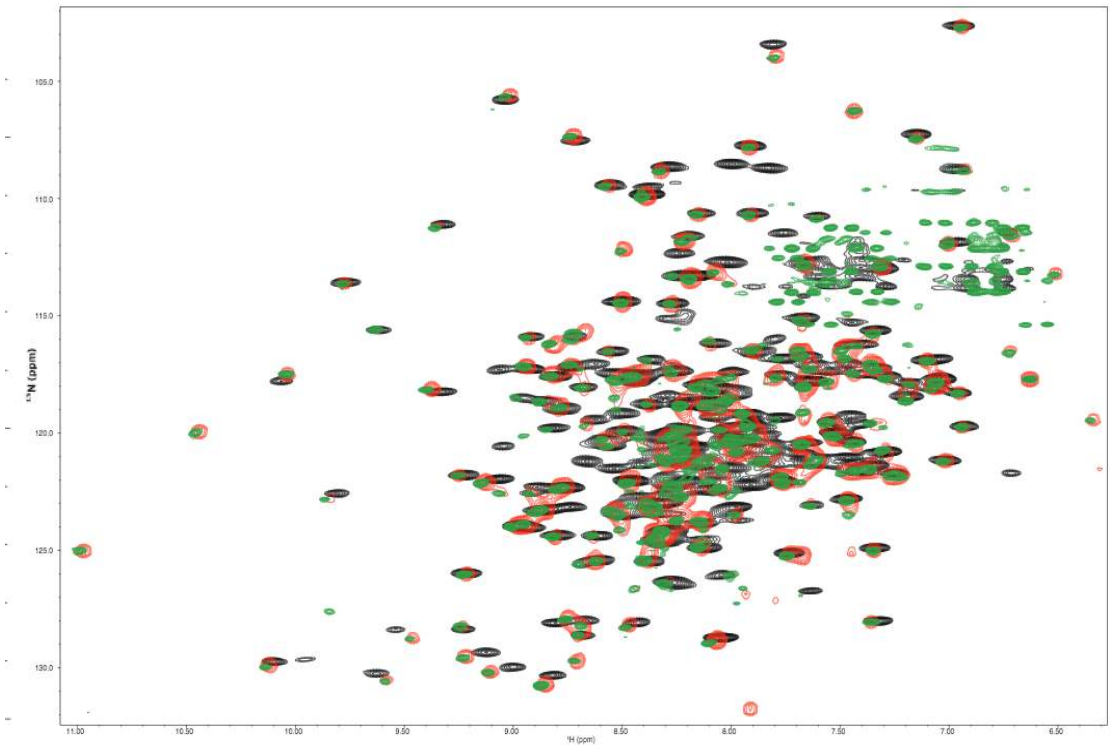

Figure 5.4 – Overlay of ^{15}N Trosy HSQC or SoFAST HMQC spectra of CLIC1. Protein extracted and purified from the *E. coli* membrane fraction (green), or soluble CLIC1 from the cytosol (red) and the soluble CLIC1 oxidised with 50 mM H_2O_2 (black).

5.4.4 First spectrum of CLIC1 in cell

The very first spectrum of CLIC1 was collected by ^{15}N labelling of the protein when recombinantly expressed in bacterial *E. coli* C43 (BL21) cells (Figure 5.5). The red and black spectra correspond to recombinantly expressed and purified ^{15}N labelled soluble CLIC1 in its reduced and non-reduced states, and there is very little differences between these spectrums, backing up the hypothesis that reducing or oxidising the protein is not the real trigger for structural rearrangement or insertion into the membrane. Overlaying the in-cell spectrum of the protein shows for the first time that the protein spectrum can be observed via this methodology as some of the peaks can be distinguished and overlay with the soluble protein. However, the spectrum has very broad peaks that are hard to define so in order to map any

chemical shift changes more optimisation is needed. It is clear the protein in a cellular environment is far more complex than in its purified soluble form due to the large size of the peaks.

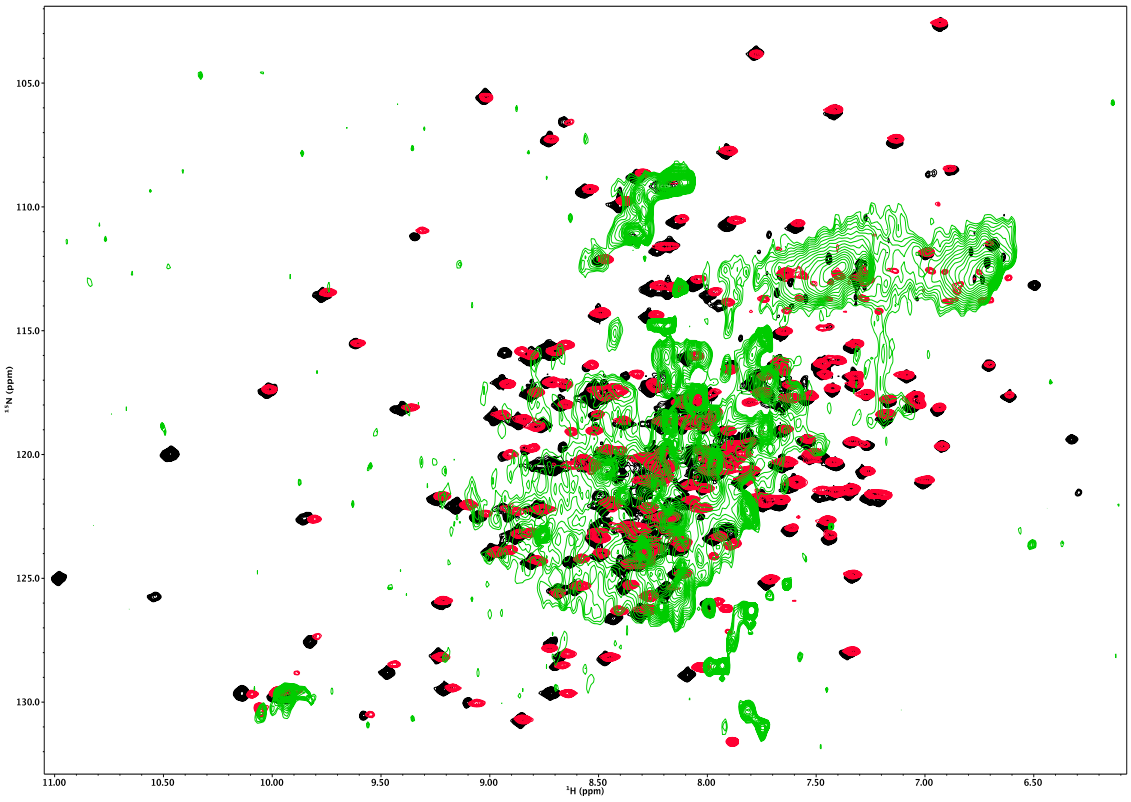

Figure 5.5 – ^{15}N isotopically labelled CLIC1 is shown in bacterial cells.
NMR spectra of soluble CLIC1 is shown reduced with DTT (black) and non-reduced (red) and superimposed with CLIC1 within bacterial cells (green). This spectrum shows CLIC1 in *E. coli* cells for the first time.

5.4.5 Selective methyl labelling in-cell spectrum

In order to obtain an NMR spectrum with better resolution, the labelling of the protein sample was optimised. As previously mentioned, experiments have used the technique of selective methyl isotope labelling to improve NMR spectrum of protein in bacterial cells, as visualising just the methyl groups of select amino acids leads to

less crowding on the spectra so individual peaks can be more readily distinguished. In addition, this type of labelling would alleviate relaxation problems arising from transient complexes formed by CLIC1 in the crowded cytosolic space of cells. The first attempt of selective methyl labelling with CLIC1 was carried out using ^{13}C isotopic labelling of just the methyl groups in methionine residues in CLIC1, of which there is just one in CLIC1 (Figure 5.6). This experiment was carried out as a trial for this labelling technique and the NMR experiments, 13C-methyl SoFAST HMQC, to see if a sharp NMR signal from CLIC1 could be obtained. This allowed for the attempt of further selective methyl labelling but with amino acid residues that are more abundant throughout the protein sequence, such as isoleucine, leucine and valine (ILV) of which there are 7, 30 and 17 residues in CLIC1 respectively. This was carried out with soluble CLIC1 on an 800 MHz spectrometer, of which the spectrum produced has much higher resolution and sharper peaks than previous experiments of CLIC1 on 600 MHz NMR spectrometer. This spectrum shows successful ILV isotopic labelling of the protein and can be used as a reference for comparison with in-cell spectra. With assignment of each of these peaks, ILV labelling could be a very effective method at determining key residues involved in structural rearrangement of CLIC1 from cytosolic protein to membrane channels and these initial spectra collected are an important step for that process (Figure 5.7).

Following successful labelling of the soluble protein, the first in-cell NMR spectrum for CLIC1 using selective methyl ILV labelling was collected (Figure 5.8). There are clear distinguishable peaks within this spectrum, with higher resolution than seen in initial in-cell experiments with ^{15}N labelling (Figure 5.5). Superimposition of the in-cell ILV CLIC1 sample with the soluble ILV CLIC1 spectra (Figure 5.9) shows many

resonances overlay between the spectra so the protein seen in the in-cell spectrum is CLIC1. However, the methyl resonances in the in-cell spectra appear very broad and only enable a qualitative analysis of the results. Furthermore, there are some small chemical shifts differences seen between other peaks in the spectra, which reveal there are chemical environment variations between these samples for CLIC1 and with an assigned spectrum they could be allocated to specific amino acid residues to map any conformational changes. However, the large resonance differences to the left of the in-cell spectrum are not likely to belong to CLIC1 and could arise from scrambling of the labelled precursors.

As described in the introduction, alongside in-cell NMR further experiments should be carried out to improve the information obtained from the technique, therefore the spectrum of the cell lysate from the sample and supernatant after centrifugation of the in-cell ILV sample were taken. The changes seen between these spectra are very slight with good overlay of the resonances, confirming the protein inside the cell can be seen in a similar chemical environment once the cells are lysed and the protein becomes fully soluble again (Figure 5.10). However, the cell lysate and supernatant spectrum have some sharper resonance which could indicate the complexity of the cellular environment, with a crowded and confined space for CLIC1 in the bacteria making it difficult to obtain a high-resolution spectrum. For individual residue peaks there are differences seen between the protein in the lysate and supernatant, which could demonstrate the role partial interactions with the membrane and cellular components have on protein conformation as in the supernatant only the soluble CLIC1 remains. Furthermore, the supernatant spectrum overlays with the in-cell spectrum acquired therefore it does not directly correspond to the soluble ILV

spectrum (Figure 5.7), indicating the cellular environment the protein once was in affects its soluble conformation after. In addition to collecting the supernatant, the role of divalent cations on CLIC1 was tested further with incubation of the soluble CLIC1 from the supernatant with 10 mM EDTA before collecting the spectrum again. The sharpest resonances of all the spectra seen in Figure 5.10 is obtained after treatment with this metal chelator, which indicates by removing the availability of divalent cations the conformation of CLIC1 is altered towards the soluble form. This could be due to the prevention of CLIC1 interaction with any remaining lipids from the cell as less binding of divalent cations is possible, so less CLIC1 is activated to go on to form the membrane channel.

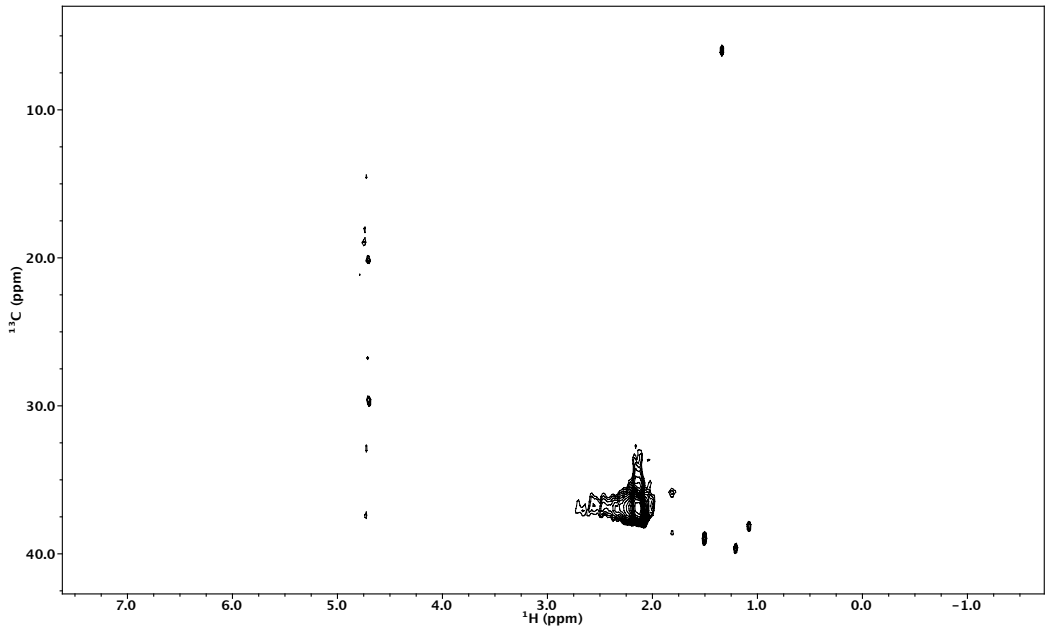

Figure 5.6 – ^{13}C methyl labelling of methionine residues in CLIC1.
Initial ^{13}C-methyl HMQC spectra using Methyl ILV-selective labelling attempt of CLIC1 within a bacteria cell environment.

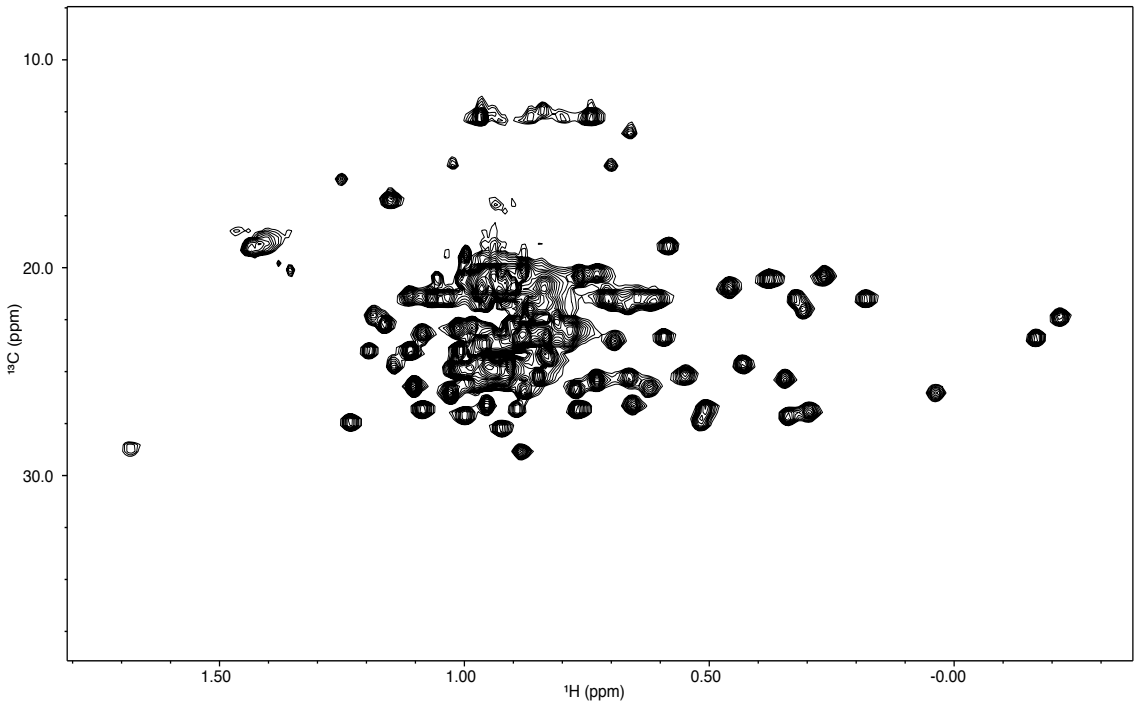

Figure 5.7 – ^{13}C Best TROSY of CLIC1 selectively methyl labelled with ^{13}C in isoleucine, leucine and valine residues. Soluble CLIC1 is shown.

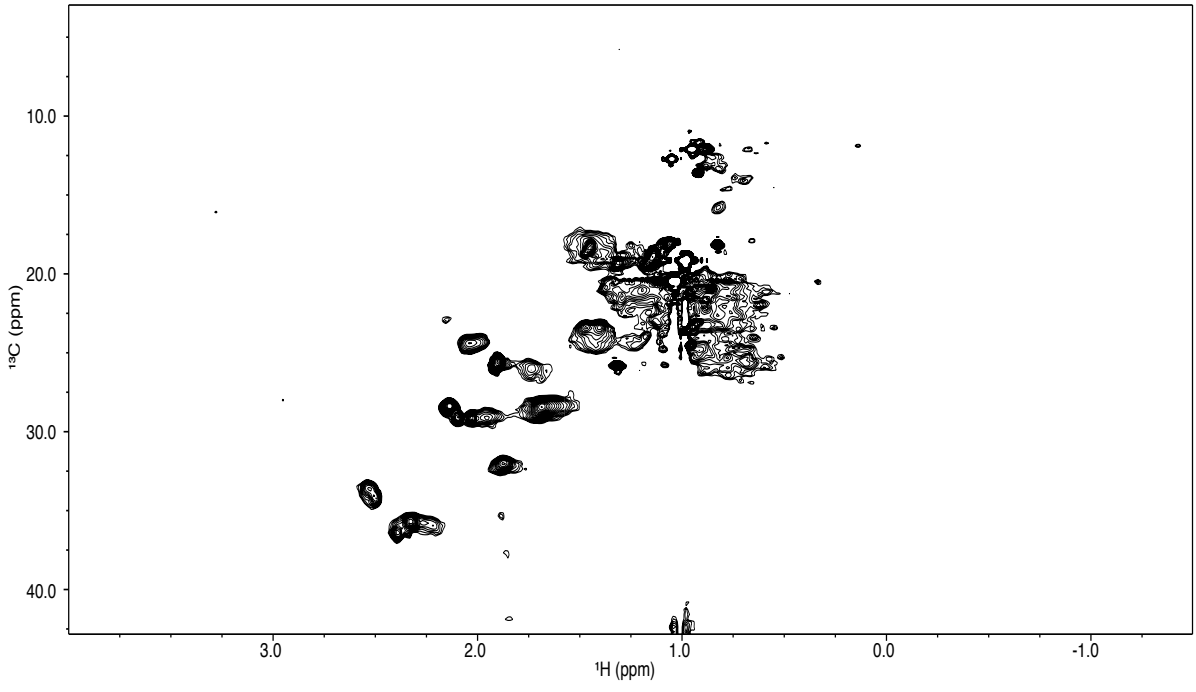

Figure 5.8 – In-cell spectrum of ILV labelled CLIC1 in bacterial cells. Only isoleucine, leucine and valine residues of CLIC1 can be seen.

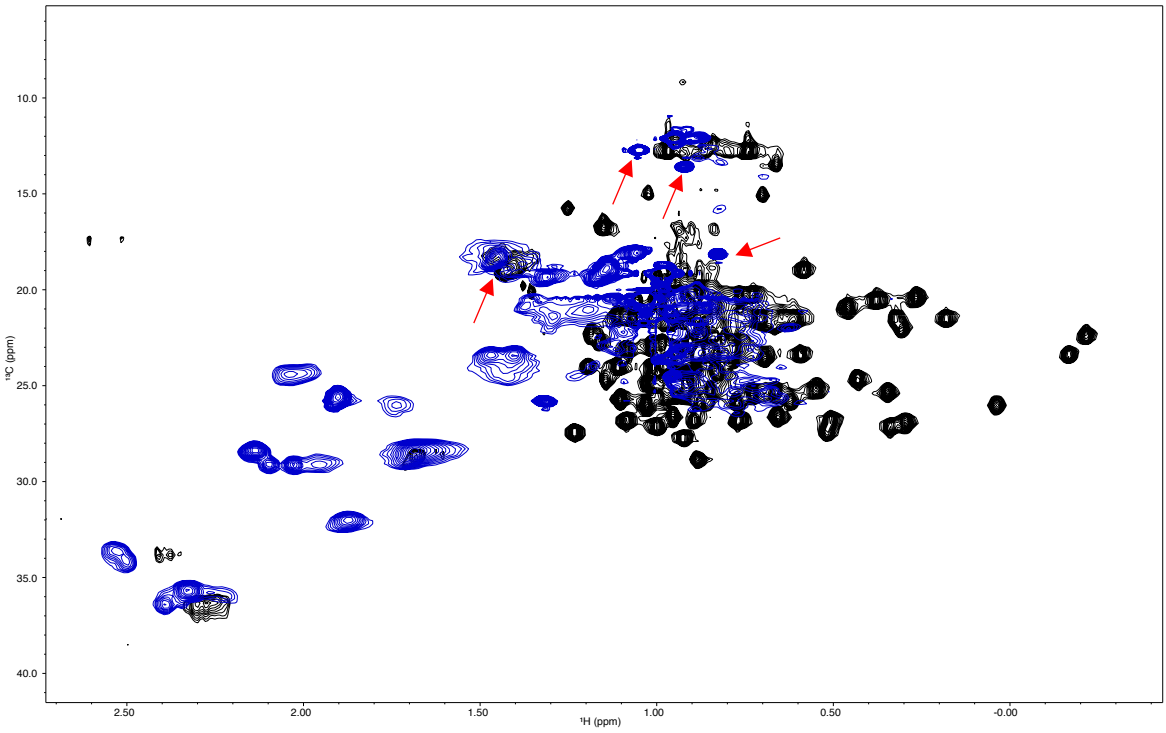

Figure 5.9 – Superimposition of soluble ILV CLIC1 spectrum and ILV CLIC1 in-cell. Soluble CLIC1 spectrum (black) overlayed with CLIC1 in bacterial cells (blue). Red arrows indicate examples of chemical shift changes between the spectra.

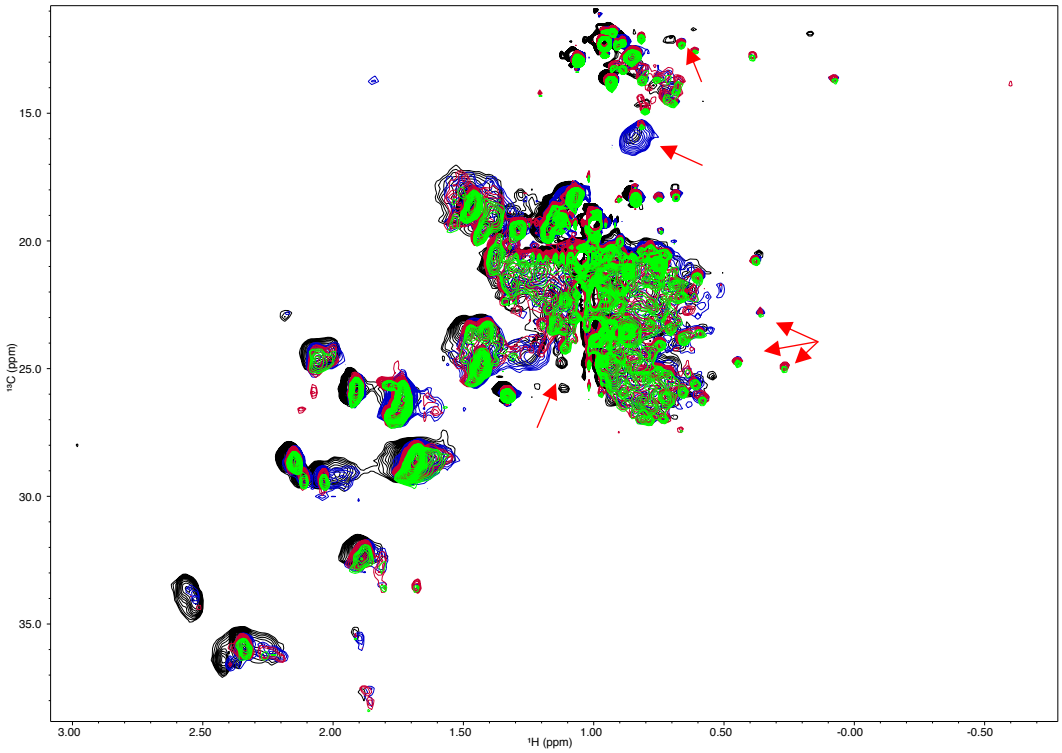

Figure 5.10 – Superimposition of In-cell ILV spectrum of CLIC1 & control experiments. ^{13}C Methyl ILV spectrum of CLIC1 (black) is superimposed with spectrum of cell lysate (blue), supernatant (red) and supernatant treated with 10 mM EDTA (green). Red arrows indicate examples of chemical shift changes seen between spectra.

5.4.6 Optimisation of in-cell NMR for CLIC1

Following the initial bacterial in-cell NMR experiments it was difficult to identify any clear peaks due to such broadness and poor resolution, so another ^{15}N spectrum of CLIC1 in *E. coli* was collected (Figure 5.11B) alongside a spectrum for uninduced cells for subtraction (Figure 5.11A). This allows identification that the labelled peaks that can be seen in the in-cell spectra are due to the specific labelling of CLIC1. In the in-cell NMR spectra from the induced bacterial cells there appears to be stronger signal so more defined peaks for the protein compared to the uninduced sample, which

reveals the signal that we are seeing is due to CLIC1 expression in the cells and that there is a high level of background in the in-cell spectra from other cellular proteins. As discussed earlier, lysing the cells and collecting a spectrum of the supernatant after centrifugation can indicate the conformation of CLIC1 after interaction with cellular components, higher resolution peaks can be identified for both the uninduced and induced samples compared to the in-cell spectra as CLIC1 in no longer experiencing macromolecular crowding in the cells cytoplasm so the resonance resolution is higher (Figure 5.11). Overlaying the in-cell spectra of CLIC1 onto the ^{15}N in vitro spectrum of soluble CLIC1 reveals that for both the in cell and supernatant sample specific resonances overlap with the in vitro protein sample obtained. This provides evidence that CLIC1s conformation changes within the complex cellular environment and the protein that is acquired in these in-cell spectra is in fact CLIC1. Some resonances from the soluble spectra have chemical shifts from the in-cell spectra and this could indicate a change in these specific residues chemical environment when in cell, offering information of CLIC1 structural changes from aqueous buffer to the complex cellular cytoplasm (Figure 5.12). In addition, the differences between peaks seen between the supernatant and soluble lysate spectra, with the supernatant sample acquiring broader peaks, could reveal that partial interaction of CLIC1 with any remaining lipids impacts the proteins conformation so it differs from soluble protein (Figure 5.12). These components of the cell appear to produce a CLIC1 spectra in between the high resolution of the soluble spectra and the broadness of peaks in in-cell samples. This could allow the study of CLIC1 conformational changes with the availability of lipids and how this relates to the protein insertion mechanism.

These experiments provide the basis for further experiments where the uninduced sample is subtracted from the In-cell spectra collected to reveal clearer peaks generated by only the specific protein within the cells or identifying ways to reduce background cellular signal as previously discussed and bridge the gap between the soluble spectra and in-cell CLIC1.

Furthermore, these experiments form the clearest CLIC1 spectrum in-cell yet and provide more information about the protein and how to move forward with this methodology. Being able to successfully identify CLIC1 peaks in these in-cell experiments using the optimisations carried out to date, reveal the protein as suitable for this technique as some proteins can never be visualised using in-cell NMR. With further optimisation, in-cell NMR could elucidate structural information on the CLIC1 protein within the cellular environment and decipher important residues involved in conformational change to form a membrane channel.

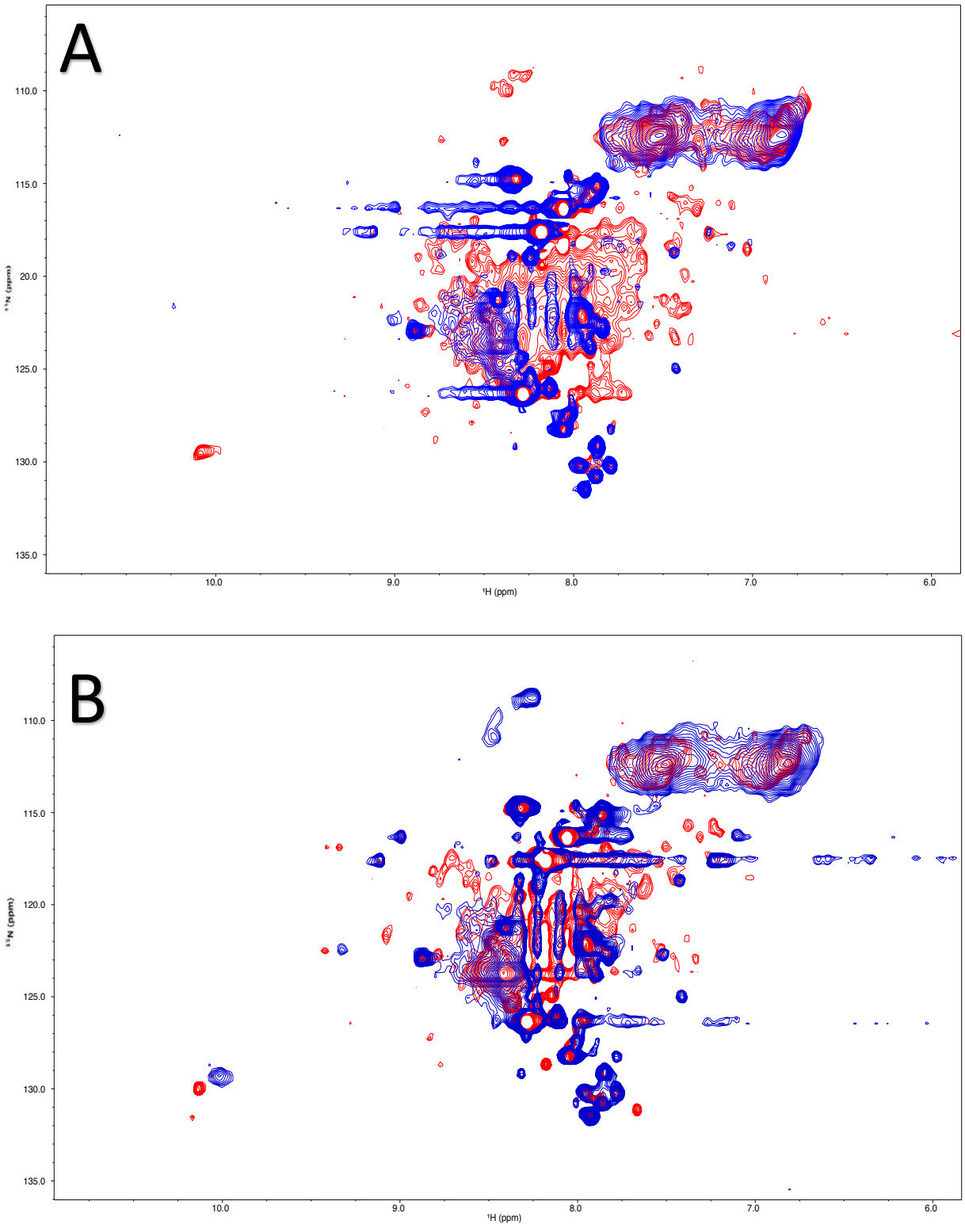

Figure 5.11 – Optimised ^{15}N in-cell NMR spectra of CLIC1. A – Spectra of control bacterial cells with no induction during protein expression. B – Spectra of bacterial cells induced to produce CLIC1. Red – Spectra of protein in supernatant fractions. Blue – Spectra of protein in cell slurry.

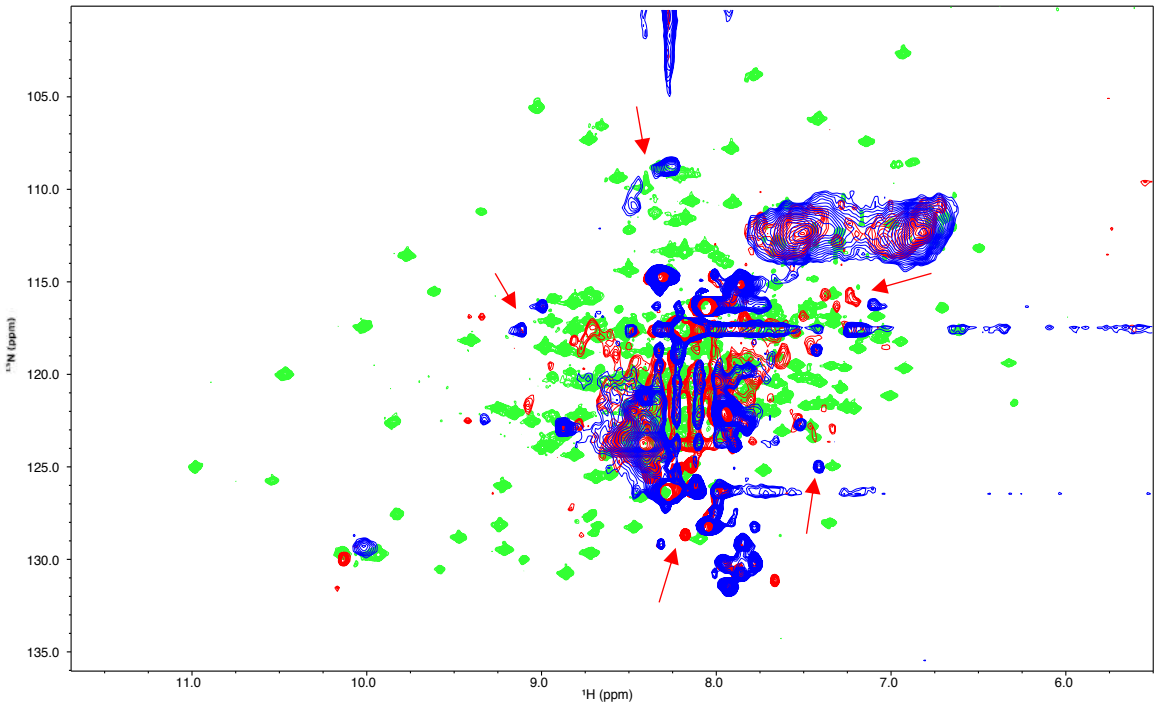

Figure 5.12 – Superimposition of ^{15}N in-cell CLIC1 with ^{15}N soluble CLIC1. Spectra of soluble in-vitro CLIC1 (green) is superimposed with the induced spectra of CLIC1 in bacterial cells (blue), and the spectra of the supernatant of induced CLIC1 (red). Red arrows indicate examples of chemical shift changes between spectra.

5.5 Discussion

The main aim of this chapter was to decipher atomic detail of the protein in a cellular environment and through what mechanism CLIC1 naturally inserts into the membrane.

As described in previous chapters the main hypothesis from literature for CLIC1 insertion into the membrane is oxidation of the protein (Goodchild et al., 2009; Littler et al., 2004), but NMR studies of the soluble protein provide further evidence oxidation is not the true cause, in line with our previous findings that divalent cations trigger CLIC1 membrane insertion. Direct correlation of residue peaks from soluble CLIC1 and the protein extracted from the membrane reveal the membrane form is reduced, as there is clear chemical shift changes against oxidised CLIC1. The protein extracted from the membrane does not have its oxidation state altered at any point, so if the hypothesis of oxidation were true for the insertion of CLIC1 this solubilised protein would match the oxidised sample as disulphide bond formation would show large changes in the spectrum. This leads to the hypothesis other mechanisms are at play for CLIC1 transition into a membrane channel, supported further by a study where no significant difference was found for artificial membrane insertion between reduced and oxidised CLIC1 (Al Khamici et al., 2016). Demonstrating that CLIC1 in the membrane is not oxidised, furthers supports an alternative trigger for the transition from a cytosolic protein into the membrane channel and further supports the hypothesis of divalent cations, as discussed in previous chapters. In addition to this the studies carried out where oxidation was implicated in CLIC1 membrane insertion, divalent cations such as Ca^{2+} were used in the protein purification steps (Littler et al.,

2004). This NMR experiment provides further evidence that oxidation is not the true trigger for insertion.

Investigating how CLIC1 inserts into bacterial membranes further elucidates how CLIC1 forms a channel. The experiments carried out reveals a high percentage of CLIC1 can auto-insert into bacterial membranes throughout recombinant expression. This is of no surprise due to the known selectivity of CLIC1 for phosphatidylethanolamine (PE), phosphatidylcholine (PC) and phosphatidylinositol (PI) lipids (Medina-Carmona et al., 2020), and ability to insert into asolectin lipids, as described in detail in chapter 3.3.7, which is a soybean lipid extract rich in the three aforementioned lipids. The lipid composition of *E. coli* membranes is made of a mix of phospholipids rich in PE and PG and cardiolipin (Epand & Epand, 2009), so CLIC1 can form a channel within these membranes. Interestingly the addition of the metal chelator EDTA did not reverse the insertion of CLIC1 into the *E. coli* membranes, indicating the presence of zinc and calcium within the cells is enough for membrane channel formation and once this transition has occurred it cannot be reversed by removing metals. However, EDTA treatment of soluble CLIC1 removed from bacterial cells was shown to alter the NMR spectrum of the protein, making the resonances sharper than seen in the in-cell, lysate and supernatant samples. Combined with the evidence from insertion of CLIC1-GFP into *E. coli* membranes, this shows CLIC1 ability to bind divalent cations can be reversed to change the protein's conformation in soluble CLIC1, but not once the protein has formed a channel.

Further evidence to support this is MST (Microscale thermophoresis) experiments carried out where CLIC1 was found to bind both calcium and zinc (Varela et al., 2019), implying the binding of these metals is not reversible with EDTA once in channel

formation or the protein has already transitioned into the membrane channel and binding of the metals is no longer a required process, instead it is just the initiation trigger for the cytosolic to membrane transition.

Furthermore, the generation of the CLIC1-GFP construct allows the study of the importance of the C-terminal or N-terminal domain in CLIC1 channel formation. A conserved region in the N-terminal of CLIC1 containing Cys 24, is hypothesised to form a putative transmembrane helix (Harrop et al., 2001) essential to the structural rearrangement of CLIC1 to form an integral membrane channel. By attaching the GFP tag to either the C-terminal or N-terminal domain of the protein allowed the study of the importance of both of these regions in insertion to artificial lipids. Upon comparing the percentage of insertion for both the proteins, it appears by disrupting the N domain with the GFP tag, less CLIC1 inserts into the asolectin compared to the protein with the GFP on the C-terminal domain. However this data requires further repeats to verify the result and determine if the residues 24-46 (Littler et al., 2004) of CLIC1 are really involved in the cytosolic to membrane transition. A more precise methodology to study this would be to introduce mutations in the C-terminal and N-terminal regions of CLIC1 and repeat the intrinsic tryptophan fluorescence insertion assay with these mutants to determine how these domains or specific residues are involved in CLIC1 membrane insertion, such as with Cys24 described in section 3.3.16.

In-cell NMR is a complex technique but can be a powerful tool to determine more knowledge of proteins in their native environment or as close to physiological conditions as possible. This chapter shows for the first time in-cell spectra of CLIC1 collected using NMR and details the various techniques used to try and increase the

resolution of the NMR spectra. Much more optimisation of in-cell NMR is needed for CLIC1 as the peaks remain broad but with assignment of the ILV soluble spectrum peaks could be assigned within the same labelled spectrum within bacteria. Chemical shift changes in any of the ILV peaks could reveal conformational changes in the protein from the soluble cytosolic protein to the membrane channel, of which so little is known. Any changes in the peaks identified in the in-cell NMR spectra could be compared against the in-vitro spectra of CLIC1 and could reveal structural information regarding the mechanism of activation for the protein to transition into a membrane channel. In addition, in-cell NMR experiments obtained with an uninduced sample revealed the high level of background acquired in these experiments and the lysate and supernatant samples reveal the effect the removal of lipids has on the conformational changes of CLIC1 transitioning from an in-cell environment. Optimisation of the controls collected for each experiment to then subtract from the in-cell spectra could help reduce background and improve the spectra of CLIC1 in cell further, this could allow specific chemical shift changes to be mapped between the in-cell and in vitro protein samples and identifying chemical shift changes between the in-cell spectra and cell lysate and supernatant could elucidate conformational information about how CLIC1 partially interacts with the membrane in solution, as spectrum of CLIC1 as a membrane channel cannot be acquired in solution NMR.

All of the in-cell NMR experiments carried out within this chapter were performed in a prokaryotic cell model. The bacterial model is the ideal starting organism for in-cell NMR due to the effective recombinant expression of the protein as described in section 2.3.4, but also due to CLIC1 being shown to form an active chloride channel

after being expressed and purified from bacteria (Tulk et al., 2000). Furthermore, insertion experiments using intrinsic tryptophan fluorescence reveals a high percentage of CLIC1 inserts into the *E. coli* membranes naturally, so it was advantageous to optimise in-cell experiments using CLIC1 purified in the same cells.

Future experiments could focus on in-cell NMR but in mammalian cells. Mammalian cells would be much more physiologically relevant for studying this protein, especially cancer cells due to the overexpression of CLIC1 in this disease cell phenotype (Peretti et al., 2015). Deciphering structural information of the channel could provide further information for therapeutic implications in the future for instance targeted drug design against the channel form as it has been shown inhibition of CLIC1 can slow cancer growth (Gritti, Würth, Angelini, Barbieri, Pizzi, et al., 2014; B. P. Li et al., 2018). One methodology to achieve this would be using electroporation of purified isotopically labelled CLIC1 into the cancer mammalian cells to then run them as in-cell NMR samples. Attempts to electroporate the protein into HeLa cells were carried out, as per (Theillet et al., 2016) method, and spectra of the protein after electroporation without cells present were collected and found to be identical to soluble CLIC1. This reveals CLIC1 to be a suitable candidate for electroporation but any attempts to introduce the soluble protein into the HeLa cells were unsuccessful and no in-cell NMR experiments could be carried out. Future experiments to optimise electroporation or other in-cell NMR experiments using CLIC1 in mammalian cells should be considered to understand more of the protein in a clinically relevant environment.

Furthermore, bioreactors have been identified as a potential way to improve in-cell NMR experiments. The experiments discussed in this chapter were carried out by

loading a cell slurry straight into a shigemi tube for acquiring the NMR spectrum, however this does not control nutrients available and can induce stress on the cells resulting in rapid degradation of the samples. Bioreactors pump fresh media throughout the NMR tube to control both the media temperature and the nutrients and keep the cellular conditions closer to physiological relevant (Kang, 2019). Future experiments using CLIC1 could be performed with a bioreactor and see if the decrease in cellular stress and increase in sample stability improves the spectra acquired.

The further potential for this technique with CLIC1 is obvious, with the possibility of drug screening against the protein to see if any complexes are formed within the cells, similar to extracellular immunosuppressants-protein complexes studied with in-cell NMR previously in human cells (Inomata et al., 2009). In addition in-cell NMR can show endogenous protein interactions from within the cells themselves, as formerly seen with ubiquitin (Inomata et al., 2009).

Furthermore our discovery of divalent cations such as Ca^{2+} and Zn^{2+} driving the translocation of CLIC1 from cytosolic protein to membrane channel (Varela et al., 2019) , as discussed in section 3.3.7, could theoretically be studied in cellulo by either increasing the metals within the cells or adding a chelator such as EDTA to the cells. Studying chemical shift perturbations with the change of metals within a cellular context could reveal the initial states of the activation mechanism of CLIC1.

All in-cell NMR experiments carried out within this chapter form a strong basis for the future study of CLIC1 within a cellular environment using this technique and should continue to be developed to be able to identify peaks which change from the soluble in vitro samples to the in vivo spectra.

Chapter 6: Final Discussion

6.1 Overview

6.1.1 New Hypothesis for CLIC1 membrane insertion

CLIC1 was first cloned in 1997 (Valenzuela et al., 1997), and following its discovery has become a protein of clinical interest due to the ongoing evidence of its role in many diseases such as cancer and neurodegenerative disease progression (Nguyen & Lauto, 2016). Since then literature has pointed to different triggers for membrane insertion such as pH (Cross et al., 2015; Fanucchi et al., 2008; Stoychev et al., 2009), cholesterol (Hossain et al., 2016) and the most cited hypothesis, reactive oxygen species (Averaimo et al., 2010; Goodchild et al., 2009; Harrop et al., 2001). The research in my PhD sought to use this previous knowledge to recombinantly express and purify the protein and produce a model of insertion to study the protein for further conformational and structural information, which could lead to future drug target design. However, upon undertaking research into the protein and how it inserts into the membrane, this research focus shifted.

After successful expression and purification of the protein and the development of an assay where protein insertion could be studied by intrinsic tryptophan fluorescence, the known triggers of insertion of pH and oxidation were extensively assayed with no insertion seen. The buffer change from phosphate to HEPES provided the first evidence another factor was at play before exploring the addition of divalent cations to the protein, of which calcium and zinc ions provided the highest insertion of the protein into asolectin lipids, which was further verified with visual protein insertion into lipid vesicles under a confocal microscope (Varela et al., 2019).

Identifying the highly reproducible trigger of insertion, divalent cations, allowed a new model of CLIC1 translocation to be hypothesised. The new hypothesis for CLIC1 membrane insertion shows CLIC1 in an equilibrium of different oligomerisation sites in solution, from monomer to dimer and higher order oligomeric species, which then binds to divalent cations calcium or zinc. The mix of oligomeric states of CLIC1 in solution was first identified by size exclusion chromatography (SEC) (Section 2.3.5) and further verified by SEC-MALS (multiangle light scattering) which confirmed a non-covalent equilibrium of monomer, dimer and tetramer (Varela et al., 2019) (Appendix). The binding of CLIC1 with the divalent cations is what then promotes association with the lipids and a conformational change that causes CLIC1 to insert as a channel into membrane (Figure 6.1).

Combining the in vitro work with mammalian cells studies allowed the trigger of insertion to be studied within a disease background and seeing the translocation of the protein within cervical cancer cells lines, upon increasing the intracellular calcium levels, provided further evidence the overexpression of CLIC1 in the membrane is regulated by divalent cations. Studying CLIC1 expression within the cell type known to overexpress CLIC1, glioblastoma cells (L. Wang et al., 2012), allowed the clear difference of CLIC1 localisation between cell types to be identified and an increase in cellular protrusions, such as filopodia, to be seen upon an increase in intracellular calcium. This supports the evidence that CLIC1 aids cell proliferation and migration throughout cancer development in a patient (Tian et al., 2014) and performing invasion and migration assays upon these cell types when induced with an increase in divalent cations could cement the link between how CLIC1 inserts into the membrane and how CLIC1 aids cancer progression, as this still remains unclear.

Furthermore, now this basic methodology to study CLIC1 in glioblastoma and other cancer cell types has been developed, the link between divalent cations and CLIC1 channel formation can be investigated in many ways as described below, including testing the trigger for insertion across many different cancer types to see if the translocation is always seen.

Upon discovering that divalent cations are the trigger for the translocation of CLIC1 into the membrane, the possible link to pH or oxidation was investigated further and within the literature that directly points to oxidation, other factors may have affected protein insertion. Oxidation is implied to be essential for transition of CLIC1 from monomer to integral channel form by Littler (Littler et al., 2004), but upon further investigation the data actually implies that the soluble monomer in non-reducing conditions has the potential for channel activity and oxidation leads to dimer formation, which is seen in the crystallised structural model. The crystallised dimer formation was also carried out in HEPES buffer with $CaCl_2$ present (Littler et al., 2004). Other studies of CLIC1 also see insertion of the protein, even when in buffer containing reducing agent TCEP (Valenzuela et al., 2013).

Furthermore the proposed oxidised dimer structure was shown to rely on disulphide bond formation involving two cysteine residues Cys24 and Cys59, but only Cys24 is found conserved in all other CLICs and the proposed dimer structure has no resemblance to other GST dimers (Littler et al., 2004). This poses the question of how the other CLIC proteins translocate into the dimer and insert into the membrane if following this model.

Neither oxidation, pH or divalent cations have to be exclusive in their ability to promote CLIC1 insertion into the membrane, as cell signalling is often complex, and

these different conditions could regulate each other. The mutual interplay between divalent cations and oxidation can be shown as high levels of calcium in the mitochondria are known to have an up-regulatory effect on the production of ROS, with ROS targeting endoplasmic reticulum calcium channels which can increase intracellular calcium release, further increasing ROS in a cyclic mechanism (Görlach et al., 2015). It was shown in human lung cancer cells that when CLIC1 is knocked down there is an increase in intracellular calcium and downstream ROS production which could provide evidence of a feedback mechanism between the protein and these cellular signals (J. R. Lee et al., 2019). In addition overloading of zinc is reported to cause mitochondrial dysfunction in astrocytes leading to enhanced ROS production (R. Pan et al., 2019) and positive feedback cross talk between zinc and ROS were shown during hypoxic-ischemic stress in HeLa cells (Slepchenko et al., 2017). Further investigation of how CLIC interacts with these signalling mechanisms in cell is needed to produce targeted drug therapies.

Studying CLIC1 for more structural information about how the protein translocates into the channel form of the protein was an aim of this project and using in-cell NMR approaches for this, due to the potential of this technique to gather atomic scale data on the protein in its natural cellular state and environment (Luchinat & Banci, 2017). CLIC1 spectra were obtained through this technique in bacterial cells for the first time and using selective methyl labelling techniques the spectra showed more distinct peaks. However, CLIC1 contains 273 amino acids making it a large protein to study using this approach and in a cellular context the protein will be in a complex environment and transitioning between the soluble cytoplasmic structure and the membrane channel so potentially in higher order oligomers in solution, this led to

broad peaks and a spectrum difficult to obtain any structural information out of. Further optimisation of this technique is required to obtain more distinct peaks that can be assigned to specific residues in the protein, but these first steps allow CLIC1 peaks to be acquired in a cellular environment. By producing in-cell NMR spectra of CLIC1 there can be comparison between the in vitro protein and soluble protein within a cell, which allows the study of the trigger for insertion further as the soluble protein can be treated with divalent cations and any chemical shifts can be compared to the spectra collected within a cell. This can provide structural information about how the divalent cations interact with the protein and what is happening naturally in a cellular environment. Future implications of this could be studying the protein in different cellular environments, such as mammalian cells and deciphering if the protein is interacting with the divalent cations within different cancer cell types.

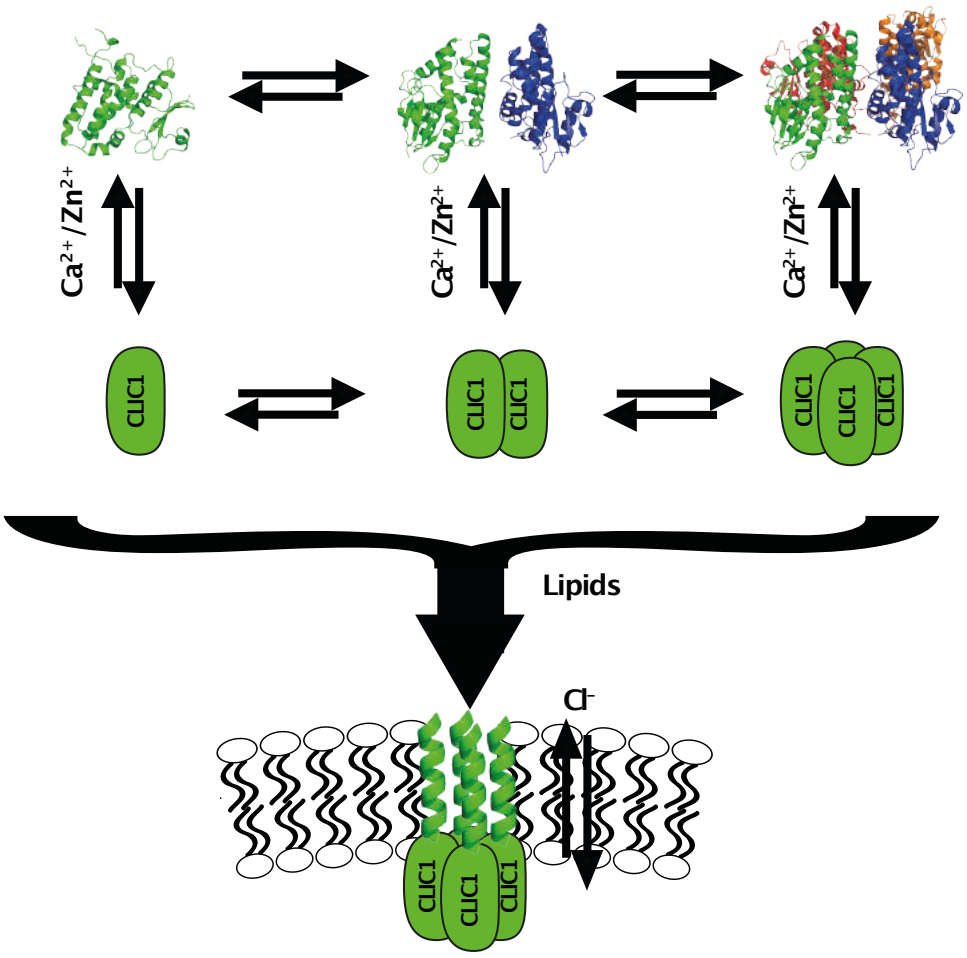

Figure 6.1 – New hypothesised model for CLIC1 membrane insertion. Upon binding of divalent cations calcium or zinc, soluble CLIC1 undergoes a conformational change to insert into the lipid membrane as chloride channel.

6.1.2 Insight into CLIC1 from other divalent cation binding proteins.

The discovery of CLIC1 binding divalent cations for insertion leads to many questions of how exactly metals lead to this lipid interaction. There are other types of protein already known to bind metals and they could provide more insight into how CLIC1 transitions into a chloride membrane channel.

One family of proteins well characterised in calcium interaction is the annexins, phospholipid binding proteins involved in many calcium regulated processes within cells (Monastyrskaya et al., 2007). The structure of annexin was found to be entirely

alpha helical and made of four domains, with three main calcium binding sites identified in domains I, II and IV (Huber et al., 1990; Liemann & Lewit-Bentley, 1995). The calcium binding sites are found in a conserved COOH terminal while the NH_2 terminals are unique to allow for different interactions in the cytoplasm (Monastyrskaya et al., 2007). These proteins are widely distributed throughout species and cell type; for example annexins found in smooth muscle bundles are diffuse in the cytoplasm of relaxed cells, but upon an increase in intracellular calcium during contraction these proteins become membrane associated (Draeger et al., 2005).

Furthermore, different annexin proteins are found to have distinctive lipid selectivity in response to various levels of intracellular calcium elevation and upon activation with calcium can insert into different membranes within a cell such as the nuclear envelope, endoplasmic reticulum, and plasma membrane. This could provide insight into why members of the CLIC family have different distributions within cells for instance CLIC4 and CLIC5 found in the mitochondrial membrane (Gururaja Rao et al., 2020; Ponnalagu, Gururaja Rao, et al., 2016), or CLIC1 and CLIC4 found to have endoplasmic reticulum localisation while CLIC5 does not (Ponnalagu, Rao, et al., 2016).

Another protein found to translocate upon binding to divalent cations is phospholipase A_2, a cytosolic protein that relocates to the golgi, endoplasmic reticulum and nuclear envelope upon stimulation by Ca^{2+} (Glover et al., 1995; Schievella et al., 1995). This protein was found to contain both the calcium binding and phospholipid binding sites in the N-terminal domain of which the crystal structure elucidates how the protein targets hydrophobic head groups of the

phospholipids (Perisic et al., 1998). The knowledge of how these proteins translocate and interact with membranes could help elucidate the mechanism of the insertion of CLIC1 further.

Translocation of proteins to the membrane upon binding of zinc is less well defined and the relocalisation of CLIC1 via zinc activation could provide a novel protein mechanism. However many proteins rely on zinc binding for activation, for instance MG53 (a muscle specific Tripartite motif family protein) which upon an increase in intracellular Zn^{2+} sees translocation of MG53-containing vesicles to acute membrane injury sites for skeletal muscle wound healing (C. Cai et al., 2015). In addition, zinc finger proteins are a group of well characterised transcription factor proteins that bind zinc in coordination with cysteine and histidine residues. These proteins are involved in regulating a wide variety of cellular processes such as DNA repair, cell migration and actin targeting. Zinc finger proteins have also been shown to have a role in cancer progression and metastasis formation, another similarity with CLIC1 (Cassandri et al., 2017; Jen & Wang, 2016).

These few examples of proteins show the role of divalent cations in protein activation and the many cellular signals and functions they can regulate, further investigation into previously characterised proteins that bind either calcium or zinc could help elucidate more about CLIC1, in particular how the protein docks and integrates into the lipid membranes and the structural binding site of the metals.

6.2 Potential limitations

The importance of identifying the trigger for membrane insertion of CLIC1 is clear, by not only providing a way to induce channel formation for study but also providing a target to prevent CLIC1 translocation in diseased state cells. However, there are limitations to the observations made due to the in vitro and in vivo experiments focusing on interaction with the lipids and colocalisation to the membrane, rather than testing the protein always formed active chloride channels within the lipids during these experiments. Furthermore, when drawing conclusions from microscopy it is uncertain how specific the endogenous staining with antibody is to just CLIC1 and unknown if it also binds to other CLICs within the cell environment. Testing the hypothesis of CLIC1 binding to divalent cations within the cell to translocate to the membrane also has limitations as cellular signalling is so complex the addition of metals could have an impact of many different stimuli within the cell which could be aiding CLIC1 membrane insertion via a different mechanism, as introducing the correct controls is complex. Using solution NMR for studying CLIC1 also has limitations as an aim of this study is to identify more structural information about CLIC1 as a membrane channel but when CLIC1 forms a channel in cellulo it can no longer be detected in the solution NMR spectra so all conclusions are drawn from soluble CLIC1 instead. Solid state NMR experiments could be used to further identify more of the structure of membrane inserted CLIC1.

The conclusions drawn provide new insight into the trigger of how CLIC1 inserts into the membrane but need further verification to cement these hypotheses further. Proposed future experiments address these limitations and aim to further prove CLIC1 inserts under the stimuli to form an active channel under divalent cation

binding in both in vitro and in vivo experiments and elucidate more information of how divalent cations causes a conformational change in the protein to insert as a channel and what structure the protein takes in this form.

6.3 Further ideas for CLIC1 research

1. By identifying divalent cations as the trigger for CLIC1 insertion more information needs to be collected on how these metals interact with the protein. Successfully isotopically labelling CLIC1, as shown in Section 5.3.1, provides a tool to study changes in individual amino acid residues of the protein. Assignment of a ^{15}N spectrum of CLIC1 could be used to identify changes within amino acids. Furthermore, a spectrum lowering pH of CLIC1 could detect if any changes were seen in the protein and as show in Section 5.3.3, the membrane extracted form is not oxidised. This technique can be applied to the divalent cations as ^{15}N isotopically labelled CLIC1 can be titrated with zinc, with any amino acid changes identified as concentration of the divalent cation increases. Challenges to this methodology come from precipitation of the protein with divalent cations when no lipid is present and the transformation into higher order oligomer or structural changes cause widening of the residue peaks until they are difficult to isolate in a similar way to the in-cell spectrum collected (Section 5.3.4). With further optimisation of the NMR, treatment of the protein could identify specific amino acids that change their chemical environment and provide structural clues to the protein's transformation into a membrane channel.
2. Assignment of CLIC1 in the NMR spectra collected from the ILV labelled sample of the protein in solution (Section 5.3.4), would allow the peaks of these amino acids to be mapped to the protein structure and with further attempts and optimisation of experimental parameters in in-cell NMR spectrums of ILV labelled protein could provide structural evidence of how

CLIC1 is triggered by divalent cations. Furthermore, once in cell NMR is optimised within the bacterial cells, labelled protein could be electroporated into mammalian cells, specifically the implicated cancer cell lines to study the protein in vivo.

3. Microscale thermophoresis studies have revealed CLIC1 binds to both calcium and zinc, with a higher affinity to zinc (Section 3.3.14) (Varela et al., 2019). Further investigation should be carried out in trying to identify the correct binding site of the metals, due to the potential of specific drug development to block this site to prevent metal binding on the protein. Previously calcium has been found to bind to a CLIC1 homolog in Drosophila melanogaster, when purified with the only source of calcium from thrombin cleavage (Littler et al., 2008), providing further evidence that thrombin cleavage with calcium could have affected oxidation studies with CLIC1 as described in Section 3. The calcium binding site shows close proximity to proline 85, an amino acid conserved in proteins with the GST fold (Littler et al., 2008) and point mutations could be made in CLIC1 to see if calcium binding could be prevented and whether zinc binds to the same site. The intrinsic tryptophan lipid assay, described in Section 3.3.1, could be repeated with the mutant generated to see if membrane insertion could be prevented. Another potential site of mutations could be the other cysteines that are highlighted in literature as important for dimer formation, such as Cys59 (Littler et al., 2004) as three cysteine residues have been identified as sites for zinc binding, involved in channel regulation of chloride channels in human skeletal muscle (Kürz et al., 1999).

4. Following insertion of CLIC1 with divalent cation promotion, it is essential to prove the CLIC1 channels formed have activity. CLIC1 electrophysiology studies have been carried out in asolectin, demonstrating a chloride current is formed from reconstituted CLIC1 into the lipids (Section 3.3.15) (Varela et al., 2019), however in further studies revealed an increased effect of zinc on CLIC1 chloride current upon lowering the pH (Appendix) (Varela et al., 2019). Further studies need to be undertaken to elucidate more of the relationship between CLIC1, zinc and low pH to determine if low pH is required in the cell for gating of the chloride channel and zinc is only needed for channel formation. Furthermore, cell fractionation to distinguish different cellular compartments could be performed with cells left untreated and those with ionophore treatment, and then stained for CLIC1 in various cell compartments using a western blot. This could provide further confirmation of the protein's expression levels and change in localisation upon an increase in divalent cations.
5. Investigate the extracellular vesicle structures generated by the mammalian cells, as seen in Section 4.3.11, especially under stimulation with zinc pyrithione. Isolation of the vesicles from cellular secretion could allow quantification of the number of vesicles produced with additional intracellular divalent cations to see if this increases CLIC1 cell to cell communication for tumour proliferation as described in glioblastoma (Thuringer et al., 2018). The question remains unanswered of why CLIC1 overexpression as a membrane channel leads to disease progression so

research could focus on answering this unknown, for instance looking at how the chloride current affects cancer growth. In addition CLIC1 is linked to invasion and migration of the cancer cells, (B. P. Li et al., 2018) with angiogenesis and invadopodia formation (Gurski et al., 2015) also correlated to the protein. It would be beneficial to carry out invasion and migration assays of the mammalian cells and then treat with calcium or zinc ionophores to see if this treatment increased the cancer progression phenotype.

6. Further expansion of the studies carried out in the cancer cell context, for instance knocking down CLIC1 and seeing if metals still have a proliferative effect on the cancer cells and confirming the chloride current increase generated by CLIC1 within a cell upon induction of higher levels of metals (as seen in Appendix) (Varela et al., 2019). The channel activity of the protein within all the cancer cell lines such as HeLa and glioblastoma could be measured to confirm the protein activity is increased in the presence of increased intracellular metal levels. Live cell imaging could also be used to track fluorescently labelled the movement of CLIC1 upon induction with divalent cations to follow the proteins change of localisation through the cancer cell over time, revealing more about the mechanism of translocation.
7. This project focused solely on CLIC1 and identified divalent cations as the trigger for this protein but there are 6 other members of the CLIC1 family, many correlated with other diseases such as heart conditions, macular degeneration, epilepsy, lupus and many cancers (Gururaja Rao et al., 2018). It would be of interest to investigate divalent cation binding with purification of the other CLIC proteins, as this could provide more information for future

therapeutics for a larger array of clinical diseases than those just correlated with CLIC1 specifically.

8. The idea that divalent cations cause CLIC1 insertion into the membrane leads to the hypothesis that cancer cells have higher availability of these ions for binding to the protein, however, literature is extremely contradictory regarding calcium and zinc levels in tumours. However, CLIC1 is only correlated to certain cancer types where it has been shown to have elevated expression, for instance lung cancer (Ninsontia et al., 2016), gastric cancer (Ma et al., 2012) and glioblastomas (Verduci et al., 2017). Creating a screening of many cancer cell types for their intracellular calcium and zinc levels and compare to CLIC1 expression levels, could help see if the protein's role in tumour progression can be directly correlated to specific cancer types cell signalling. One method to do this could be to use inductively coupled plasma mass spectrometry (ICP-MS) to quantify the metal levels within the whole cells.
9. Investigating CLIC1 further from a structural angle can be aided by the use of divalent cations. Small angle X-ray scattering studies of CLIC1 as a monomer has previously been collected, with dimer formation promoted by the change into HEPES buffer and the addition of divalent cations. The dimer structure cannot be correlated with the published dimer, providing further evidence the hypothesised dimer should be reinvestigated with the new knowledge of the translocation of CLIC1 into the membrane. Native mass spectrometry was also carried out with CLIC1, where a monomeric, dimeric and tetrameric species were identified. An even higher oligomeric species was seen,

potentially a dodecamer and with the addition of lipids the equilibrium shifted further to the higher order oligomeric species. This provides further information about how the protein transforms from a cytosolic globular protein into the unknown structure of a membrane channel. However, this could not be carried out with divalent cations as they made the sample unable to run, as with many techniques the metals can make samples difficult to work with, one due to precipitation of the metal but also to the large effect they have on the protein.

Differential scanning calorimetry studies the thermodynamics of protein unfolding and it could provide structural information about how CLIC1 changes conformation by identifying if the protein unfolds at one temperature of the different domains of the protein such as the putative transmembrane N terminus unfolds differently to the C terminus or whether monomeric species will unfold faster or slower than dimers in solution. Furthermore, gaining secondary structure information about CLIC1 in the presence of metals could be carried out with circular dichroism.

6.4 The impact of this research

Deciphering divalent cations as the trigger for CLIC1 membrane insertion provides the key to developing models to maintain CLIC1 as a channel in the membrane within both in vitro lipids and within living cells. By knowing the trigger and how to stably insert CLIC1 into the membrane, future research can use this to try and decipher more mechanistic information about how this protein inserts as a channel into the membrane but also could aid crystallography studies and other structural techniques to solve the structure of the channel. It also elucidates a physical process to determine how CLIC1 oligomerisation and insertion into the lipids takes place which could reveal the whole mechanism of protein translocation from the cytosolic globular protein into the integral chloride channel. Identifying the trigger for formation of the membrane channel could also help the study of disease progression further and lead to investigations regarding the different availability of divalent cations in cancer cells compared to healthy tissues to study if this affects CLIC1 overexpression and would help to understand the role of CLIC1 in the development of cancer further. The metal induced chloride channel form could aid development of drug therapeutics against cancer proliferation and migration particularly in glioblastomas, a cancer type known to have poor survival rates, with less than 5% of patients surviving 5 years following diagnosis (Tamimi & Juweid, 2017). The development of drugs could focus on divalent cation drug targets or CLIC1 metal binding site inhibitors to prevent translocation of CLIC1 to the membrane in clinically ill patients. In addition, using divalent cations for membrane insertion to gain structural information of the CLIC1 channel conformation could lead to specific drug development against the channel form of this protein only, which could have clinical

impact by targeting only diseased state cells, unlike traditional chemotherapy which has many side effects due to the destruction of healthy cells alongside the cancer cells (Schirrmacher, 2019).

6.5 Conclusion

Overall, this project has sought the use of many varied techniques to understand the mechanistic details of how CLIC1 could lead to diseased phenotypes. By using different angles to investigate the protein's oligomeric state, trigger for translocation into the membrane channel and how these triggers relate to a cellular phenotype, the involvement of CLIC1 in disease physiology has been elucidated further and the different evidence collected for the protein's translocation by divalent cations can provide an invaluable tool to study the membrane channel form.

There is clear potential for many future studies elucidating more of the mechanism of insertion of CLIC1 and how this overexpression of the chloride channel, aided by binding of divalent cations, can lead to disease progression. Just like this project, future studies can combine many integrative techniques to understand this transitionary action of the protein and lead to therapeutic design to specifically target diseased cells. This project provides key findings to be able to study the protein and its role in cancer further.

Bibliography

Abdul-Salam, V. B., Russomanno, G., Chien-Nien, C., Mahomed, A. S., Yates, L. A., Wilkins, M. R., Zhao, L., Gierula, M., Dubois, O., Schaeper, U., Endruschat, J., & Wojciak-Stothard, B. (2019). CLIC4/Arf6 Pathway: A New Lead in BMPRII Inhibition in Pulmonary Hypertension. *Circulation Research*, *124*(1), 52–65.

Adler, V., Yin, Z., Fuchs, S. Y., Benezra, M., Rosario, L., Tew, K. D., Pincus, M. R., Sardana, M., Henderson, C. J., Wolf, C. R., Davis, R. J., & Ronai, Z. (1999). Regulation of JNK signaling by GSTp. *EMBO Journal*, *18*(5), 1321–1334.

Agathos, S. N. (1991). Production scale insect cell culture. In *Biotechnology Advances* 9(1), 9(1), 51-68.

Al Khamici, H., Hossain, K. R., Cornell, B. A., & Valenzuela, S. M. (2016). Investigating sterol and redox regulation of the ion channel activity of CLIC1 using tethered bilayer membranes. *Membranes*, *6*(4), 51.

Anumonwo, J. M. B., Horta, J., Delmar, M., Taffet, S. M., & Jalife, J. (1999). Proton and zinc effects on HERG currents. *Biophysical Journal*, *77*(1), 282–298.

Arjonen, A., Kaukonen, R., & Ivaska, J. (2011). Filopodia and adhesion in cancer cell motility. *Cell Adhesion and Migration*, *5*(5), 421–430.

Athwal, G. S., Huber, J. L., & Huber, S. C. (1998). Biological significance of divalent metal ion binding to 14-3-3 proteins in relationship to nitrate reductase inactivation. *Plant and Cell Physiology*, *39*(10), 1065–1072.

Averaimo, S., Milton, R. H., Duchen, M. R., & Mazzanti, M. (2010). Chloride intracellular channel 1 (CLIC1): Sensor and effector during oxidative stress. In *FEBS Letters*, 584(10),2076-2084.

Banci, L., Barbieri, L., Bertini, I., Cantini, F., & Luchinat, E. (2011). In-cell NMR in E. coli to Monitor Maturation Steps of hSOD1. *PLoS ONE*, *6*(8), 23561.

Banci, L., Barbieri, L., Bertini, I., Luchinat, E., Secci, E., Zhao, Y., & Aricescu, A. R. (2013). Atomic-resolution monitoring of protein maturation in live human cells by NMR. *Nature Chemical Biology*, *9*(5).

Banci, L., Barbieri, L., Luchinat, E., & Secci, E. (2013). Visualization of redox-controlled protein fold in living cells. *Chemistry and Biology*, *20*(6), 747–752.

Baolong, W., Jiqing, Z., Qiongyuan, C., Chaofan, W., Yangxin, L., Xi-Yong, Y., Bin, L., Chun, L., Song-Bai, L., Hui, D., Shuochen, W., Ting, X., David, S., Zhangni, L., Hesham, M. A., Yao-Hua, S., & Jin, Z. (2020). CLIC4 abrogation promotes epithelial-mesenchymal transition in gastric cancer. *Carcinogenesis*, *41*(6), 841–849.

Barbieri, F., Würth, R., Pattarozzi, A., Verduci, I., Mazzola, C., Cattaneo, M. G., Tonelli, M., Solari, A., Bajetto, A., Daga, A., Vicentini, L. M., Mazzanti, M., & Florio, T. (2018). Inhibition of chloride intracellular channel 1 (CLIC1) as biguanide class-effect to impair human glioblastoma stem cell viability. *Frontiers in Pharmacology*, *9*, 899.

Barbieri, L., Luchinat, E., & Banci, L. (2016). Characterization of proteins by in-cell NMR spectroscopy in cultured mammalian cells. *Nature Protocols*, *11*(6), 1101–1111.

Barnes, C. O., & Pielak, G. J. (2011). In-cell protein NMR and protein leakage. *Proteins: Structure, Function and Bioinformatics*, *79*(2), 347–351.

Bell, A., Bell, D., Weber, R. S., & El-Naggar, A. K. (2011). CpG island methylation

profiling in human salivary gland adenoid cystic carcinoma. *Cancer*, *117*(13), 2898–2909.
Ben-Ari, Y., Gaiarsa, J. L., Tyzio, R., & Khazipov, R. (2007). GABA: A pioneer transmitter that excites immature neurons and generates primitive oscillations. *Physiological Reviews*, *87*(4), 1215–1284.
Berg, J., Yang, H., & Jan, L. Y. (2012). Ca2+-activated Cl-channels at a glance. *Journal of Cell Science*, *125*(6).
Berrill, A., Biddlecombe, J., & Bracewell, D. (2011). Product quality during manufacture and supply. In *Peptide and Protein Delivery*, Academic Press pp. 313–339.
Berry, K. L., Bülow, H. E., Hall, D. H., & Hobert, O. (2003). A C. elegans CLIC-like Protein Required for Intracellular Tube Formation and Maintenance. *Science*, *302*(5653), 2134–2137.
Berryman, M., & Bretscher, A. (2000). Identification of a novel member of the chloride intracellular channel gene family (CLIC5) that associates with the actin cytoskeleton of placental microvilli. *Molecular Biology of the Cell*, *11*(5), 1509-21.
Bertrand, K., Reverdatto, S., Burz, D. S., Zitomer, R., & Shekhtman, A. (2012). Structure of proteins in eukaryotic compartments. *Journal of the American Chemical Society*, *134*(30), 12798–12806.
Bill, R. M. (2014). Playing catch-up with escherichia coli: Using yeast to increase success rates in recombinant protein production experiments. *Frontiers in Microbiology*, 5(MAR).
Board, P. G., & Anders, M. W. (2007). Glutathione transferase omega 1 catalyzes the reduction of S-(phenacyl)glutathiones to acetophenones. *Chemical Research in Toxicology*, *20*(1), 149–154.
Board, P. G., Coggan, M., Chelvanayagam, G., Easteal, S., Jermiin, L. S., Schulte, G. K., Danley, D. E., Hoth, L. R., Griffor, M. C., Kamath, A. V., Rosner, M. H., Chrunyk, B. A., Perregaux, D. E., Gabel, C. A., Geoghegan, K. F., & Pandit, J. (2000). Identification, Characterization, and Crystal Structure of the Omega Class Glutathione Transferases *. *Journal of Biological Chemistry*, *275*(32), 24798–24806.
Cai, C., Lin, P., Zhu, H., Ko, J. K., Hwang, M., Tan, T., Pan, Z., Korichneva, I., & Ma, J. (2015). Zinc binding to MG53 protein facilitates repair of injury to cell membranes. *Journal of Biological Chemistry*, *290*(22), 13830–13839.
Cai, M., Huang, Y., Sakaguchi, K., Clore, G. M., Gronenborn, A. M., & Craigie, R. (1998). An efficient and cost-effective isotope labeling protocol for proteins expressed in Escherichia coli. *Journal of Biomolecular NMR*, *11*(1), 97–102.
Carlini, V., Verduci, I., Cianci, F., Cannavale, G., Fenoglio, C., Galimberti, D., & Mazzanti, M. (2020). CLIC1 protein accumulates in circulating monocyte membrane during neurodegeneration. *International Journal of Molecular Sciences*, *21*(4), 1484.
Cassandri, M., Smirnov, A., Novelli, F., Pitolli, C., Agostini, M., Malewicz, M., Melino, G., & Raschellà, G. (2017). Zinc-finger proteins in health and disease. In *Cell Death Discovery*, Nature Publishing Group, 3(1), 1-12.
Cérutti, M., & Golay, J. (2012). Lepidopteran cells: An alternative for the production of recombinant antibodies? *MAbs*, *4*(3), 294–309.

Chau, C., Actis, P., & Hewitt, E. (2020). Methods for protein delivery into cells: From current approaches to future perspectives. In *Biochemical Society Transactions* , Portland Press Ltd, 48(2), 357-365

Chen, T. Y. (1998). Extracellular zinc ion inhibits ClC-0 chloride channels by facilitating slow gating. *Journal of General Physiology*, 112(6), 715-26.

Cromwell, M. E. M., Hilario, E., & Jacobson, F. (2006). Protein aggregation and bioprocessing. *AAPS Journal*, *8*(3), E572–E579.

Cross, M., Fernandes, M., Dirr, H., & Fanucchi, S. (2015). Glutamate 85 and glutamate 228 contribute to the pH-response of the soluble form of chloride intracellular channel 1. *Molecular and Cellular Biochemistry*, *398*(1), 83–93.

Demain, A. L., & Vaishnav, P. (2009). Production of recombinant proteins by microbes and higher organisms. *Biotechnology Advances*, *27*(3), 297–306.

Ding, Q., Li, M., Wu, X., Zhang, L., Wu, W., Ding, Q., Weng, H., Wang, X., & Liu, Y. (2015). CLIC1 overexpression is associated with poor prognosis in gallbladder cancer. *Tumour Biology*, *36*(1), 193–198.

Dixon, D. P., Davis, B. G., & Edwards, R. (2002). Functional divergence in the glutathione transferase superfamily in plants: Identification of two classes with putative functions in redox homeostasis in Arabidopsis thaliana. *Journal of Biological Chemistry*, *277*(34), 30859–30869.

Dourado, D., Fernandes, P., & Ramos, M. (2008). Mammalian Cytosolic Glutathione Transferases. *Current Protein & Peptide Science*, *9*(4), 325–337.

Draeger, A., Wray, S., & Babiychuk, E. B. (2005). Domain architecture of the smooth-muscle plasma membrane: Regulation by annexins. *Biochemical Journal*, *387*(2), 309–314.

Drew, D. E., Von Heijne, G., Nordlund, P., & De Gier, J. W. L. (2001). Green fluorescent protein as an indicator to monitor membrane protein overexpression in Escherichia coli. *FEBS Letters*, *507*(2), 220–224.

Drew, D., Lerch, M., Kunji, E., Slotboom, D. J., & de Gier, J. W. (2006). Optimization of membrane protein overexpression and purification using GFP fusions. *Nature Methods*, *3*(4), 303–313.

Duan, R., Li, C., Liu, S., Liu, Z., Li, Y., Yuan, Y., & Hu, X. (2016). Determination of adenine based on the fluorescence recovery of the L-Tryptophan-Cu2+ complex. *Spectrochimica Acta - Part A: Molecular and Biomolecular Spectroscopy*, *152*, 272–277.

Dulhunty, A., Gage, P., Curtis, S., Chelvanayagam, G., & Board, P. (2001). The Glutathione Transferase Structural Family Includes a Nuclear Chloride Channel and a Ryanodine Receptor Calcium Release Channel Modulator. *Journal of Biological Chemistry*, *276*(5), 3319–3323.

Dumon-Seignovert, L., Cariot, G., & Vuillard, L. (2004). The toxicity of recombinant proteins in Escherichia coli: A comparison of overexpression in BL21(DE3), C41(DE3), and C43(DE3). *Protein Expression and Purification*, *37*(1), 203–206.

Duncan, R. R., Westwood, P. K., Boyd, A., & Ashley, R. H. (1997). Rat brain p64H1, expression of a new member of the p64 chloride channel protein family in endoplasmic reticulum. *Journal of Biological Chemistry*, *272*(38), 23880–23886.

Duran, C., Thompson, C. H., Xiao, Q., & Hartzell, H. C. (2009). Chloride channels: Often enigmatic, rarely predictable. *Annual Review of Physiology*, *72*, 95–121.

Epand, R. M., & Epand, R. F. (2009). Lipid domains in bacterial membranes and the

action of antimicrobial agents. *Biochimica et Biophysica Acta - Biomembranes*, *1788*(1), 289–294.
Falcón-Pérez, J. M., Nazarian, R., Sabatti, C., & Dell'Angelica, E. C. (2005). Distribution and dynamics of Lamp1-containing endocytic organelles in fibroblasts deficient in BLOC-3. *Journal of Cell Science*, *118*(22), 5243–5255.
Fanucchi, S., Adamson, R. J., & Dirr, H. W. (2008). Formation of an unfolding intermediate state of soluble chloride intracellular channel protein CLIC1 at acidic pH. *Biochemistry*, *47*(44), 11674–11681.
Feng, J., Xu, J., Xu, Y., Xiong, J., Xiao, T., Jiang, C., Li, X., Wang, Q., Li, J., & Li, Y. (2019). Clic1 promotes the progression of oral squamous cell carcinoma via integrins/erk pathways. *American Journal of Translational Research*, *11*(2), 557–571.
Ferguson, W. J., Braunschweiger, K. I., Braunschweiger, W. R., Smith, J. R., McCormick, J. J., Wasmann, C. C., Jarvis, N. P., Bell, D. H., & Good, N. E. (1980). Hydrogen ion buffers for biological research. *Analytical Biochemistry*, *104*(2), 300–310.
Fernández-Cañón, J. M., & Peñalva, M. A. (1998). Characterization of a fungal maleylacetoacetate isomerase gene and identification of its human homologue. *Journal of Biological Chemistry*, *273*(1), 329–337.
Ferreira, C. M. H., Pinto, I. S. S., Soares, E. V., & Soares, H. M. V. M. (2015). (Un)suitability of the use of pH buffers in biological, biochemical and environmental studies and their interaction with metal ions-a review. In *RSC Advances*, 5(39), 30989-31003
Fleiner, A., & Dersch, P. (2010). Expression and export: Recombinant protein production systems for Aspergillus. *Applied Microbiology and Biotechnology*, *87*(4), 1255–1270.
Flores-Téllez, T. N. J., Lopez, T. V., Vásquez Garzón, V. R., & Villa-Treviño, S. (2015). Co-expression of Ezrin-CLIC5-Podocalyxin is associated with migration and invasiveness in hepatocellular carcinoma. *PLoS ONE*, *10*(7), e0131605.
Friedli, M., Guipponi, M., Bertrand, S., Bertrand, D., Neerman-Arbez, M., Scott, H. S., Antonarakis, S. E., & Reymond, A. (2003). Identification of a novel member of the CLIC family, CLIC6, mapping to 21q22.12. *Gene*, *320*, 31–40.
Gagnon, L. H., Longo-Guess, C. M., Berryman, M., Shin, J. B., Saylor, K. W., Yu, H., Gillespie, P. G., & Johnson, K. R. (2006). The chloride intracellular channel protein CLIC5 is expressed at high levels in hair cell stereocilia and is essential for normal inner ear function. *Journal of Neuroscience*, *26*(40), 10188–10198.
Geisse, S., Gram, H., Kleuser, B., & Kocher, H. P. (1996). Eukaryotic expression systems: A comparison. *Protein Expression and Purification*, *8*(3), 271–282.
Glover, S., Bayburt, T., Jonas, M., Chi, E., & Gelb, M. H. (1995). Translocation of the 85-kDa phospholipase A2 from cytosol to the nuclear envelope in rat basophilic leukemia cells stimulated with calcium ionophore or IgE/antigen. *Journal of Biological Chemistry*, *270*(25), 15359–15367.
Good, N. E., & Izawa, S. (1972). Hydrogen Ion Buffers. *Methods in Enzymology*, *1972*(24), 53–68.
Good, N. E., Winget, G. D., Winter, W., Connolly, T. N., Izawa, S., & Singh, R. M. M. (1966). Hydrogen Ion Buffers for Biological Research. *Biochemistry*, *5*(2), 467–477.

Goodchild, S. C., Angstmann, C. N., Breit, S. N., Curmi, P. M. G., & Brown, L. J. (2011). Transmembrane extension and oligomerization of the CLIC1 chloride intracellular channel protein upon membrane interaction. *Biochemistry*, *50*(50), 10887–10897.

Goodchild, S. C., Howell, M. W., Cordina, N. M., Littler, D. R., Breit, S. N., Curmi, P. M. G., & Brown, L. J. (2009). Oxidation promotes insertion of the CLIC1 chloride intracellular channel into the membrane. *European Biophysics Journal*, *39*(1), 129–138.

Gore, A., Moran, A., Hershfinkel, M., & Sekler, I. (2004). Inhibitory Mechanism of Store-operated Ca2+ Channels by Zinc. *Journal of Biological Chemistry*, *279*(12), 11106–11111.

Görlach, A., Bertram, K., Hudecova, S., & Krizanova, O. (2015). Calcium and ROS: A mutual interplay. *Redox Biology*, *6*, 260–271.

Gritti, M., Würth, R., Angelini, M., Barbieri, F., Peretti, M., Pizzi, E., Pattarozzi, A., Carra, E., Sirito, R., Daga, A., Curmi, P. M. G., Mazzanti, M., & Florio, T. (2014). Metformin repositioning as antitumoral agent: Selective antiproliferative effects in human glioblastoma stem cells, via inhibition of CLIC1-mediated ion current. *Oncotarget*, *5*(22), 11252–11268.

Guo, D., Xie, W., Xiong, P., Li, H., Wang, S., Chen, G., Gao, Y., Zhou, J., Zhang, Y., Bu, G., Xue, M., & Zhang, J. (2018). Cyclin-dependent kinase 5-mediated phosphorylation of chloride intracellular channel 4 promotes oxidative stress-induced neuronal death. *Cell Death and Disease*, *9*(10), 951.

Guo, Y., Pan, W., Liu, S., Shen, Z., Xu, Y., & Hu, L. (2020). ERK/MAPK signalling pathway and tumorigenesis (Review). *Experimental and Therapeutic Medicine*, *19*(3), 1997–2007.

Gurski, L. A., Knowles, L. M., Basse, P. H., Maranchie, J. K., Watkins, S. C., & Pilch, J. (2015). Relocation of CLIC1 promotes tumor cell invasion and colonization of fibrin. *Molecular Cancer Research*, *13*(2), 273–280.

Gururaja Rao, S., Patel, N. J., & Singh, H. (2020). Intracellular Chloride Channels: Novel Biomarkers in Diseases. *Frontiers in Physiology*, *0*, 96.

Gururaja Rao, S., Ponnalagu, D., Patel, N. J., & Singh, H. (2018). Three decades of chloride intracellular channel proteins: From organelle to organ physiology. *Current Protocols in Pharmacology*, *80*(1), 11.21.1-11.21.17.

Hackam, D. J., Rotstein, O. D., & Grinstein, S. (1999). Phagosomal acidification mechanisms and functional significance. In *Advances in Cellular and Molecular Biology of Membranes and Organelles*, JAI, 5(C), 299-319.

Hamatsu, J., O'Donovan, D., Tanaka, T., Shirai, T., Hourai, Y., Mikawa, T., Ikeya, T., Mishima, M., Boucher, W., Smith, B. O., Laue, E. D., Shirakawa, M., & Ito, Y. (2013). High-resolution heteronuclear multidimensional NMR of proteins in living insect cells using a baculovirus protein expression system. *Journal of the American Chemical Society*, *135*(5), 1688–1691.

Harrop, S. J., DeMaere, M. Z., Fairlie, W. D., Reztsova, T., Valenzuela, S. M., Mazzanti, M., Tonini, R., Qiu, M. R., Jankova, L., Warton, K., Bauskin, A. R., Wu, W. M., Pankhurst, S., Campbell, T. J., Breit, S. N., & Curmi, P. M. (2001). Crystal structure of a soluble form of the intracellular chloride ion channel CLIC1 (NCC27) at 1.4-A resolution. *Journal of Biological Chemistry*, *276*(48), 44993–45000.

He, Y. M., Zhang, Z. L., Liu, Q. Y., Xiao, Y. S., Wei, L., Xi, C., & Nan, X. (2018). Effect of CLIC1 gene silencing on proliferation, migration, invasion and apoptosis of human gallbladder cancer cells. *Journal of Cellular and Molecular Medicine*, *22*(5), 2569–2579.

Hegetschweiler, K., & Saltman, P. (1986). Interaction of copper(II) with N-(2-hydroxyethyl)piperazine-N'-ethanesulfonic acid (HEPES). *Inorganic Chemistry*, *25*(1).

Heiss, N. S., & Poustka, A. (1997). Genomic structure of a novel chloride channel gene, CLIC2, Xq28. *Genomics*, *45*(1), 224–228.

Hernandez-Fernaud, J. R., Ruengeler, E., Casazza, A., Neilson, L. J., Pulleine, E., Santi, A., Ismail, S., Lilla, S., Dhayade, S., MacPherson, I. R., McNeish, I., Ennis, D., Ali, H., Kugeratski, F. G., Al Khamici, H., Van Den Biggelaar, M., Van Den Berghe, P. V. E., Cloix, C., McDonald, L., … Zanivan, S. (2017). Secreted CLIC3 drives cancer progression through its glutathione-dependent oxidoreductase activity. *Nature Communications*, *8*, 14206.

Hess, D. T., Matsumoto, A., Kim, S. O., Marshall, H. E., & Stamler, J. S. (2005). Protein S-nitrosylation: Purview and parameters. In *Nature Reviews Molecular Cell Biology*, Nature Publishing Group, 6(2), 150-166.

Hossain, K. R., Holt, S. A., Le Brun, A. P., Al Khamici, H., & Valenzuela, S. M. (2017). X-ray and Neutron Reflectivity Study Shows That CLIC1 Undergoes Cholesterol-Dependent Structural Reorganization in Lipid Monolayers. *Langmuir*, *33*(43), 12497–12509.

Hossain, K. R., Khamici, H. Al, Holt, S. A., & Valenzuela, S. M. (2016). Cholesterol promotes interaction of the protein CLIC1 with phospholipid monolayers at the air–water interface. *Membranes*, *6*(1).

Huang, J., Ringuet, M., Whitten, A. E., Caria, S., Lim, Y. W., Badhan, R., Anggono, V., & Lee, M. (2020). Structural basis of the zinc-induced cytoplasmic aggregation of the RNA-binding protein SFPQ. *Nucleic Acids Research*, *48*(6), 3356–3365.

Huber, R., Romisch, J., & Paques, E. P. (1990). The crystal and molecular structure of human annexin V, an anticoagulant protein that binds to calcium and membranes. *EMBO Journal*, *9*(12), 3867–3874.

Inomata, K., Ohno, A., Tochio, H., Isogai, S., Tenno, T., Nakase, I., Takeuchi, T., Futaki, S., Ito, Y., Hiroaki, H., & Shirakawa, M. (2009). High-resolution multi-dimensional NMR spectroscopy of proteins in human cells. *Nature*, *458*(7234), 106–109.

Isaacson, R. L., Simpson, P. J., Liu, M., Cota, E., Zhang, X., Freemont, P., & Matthews, S. (2007). A new labeling method for methyl transverse relaxation-optimized spectroscopy NMR spectra of alanine residues. *Journal of the American Chemical Society*, *129*(50), 15428–15429.

Itakura, K., Hirose, T., Crea, R., Riggs, A. D., Heyneker, H. L., Bolivar, F., & Boyer, H. W. (1977). Expression in Escherichia coli of a chemically synthesized gene for the hormone somatostatin. *Science*, *198*(4321), 1056–1063.

Jen, J., & Wang, Y. C. (2016). Zinc finger proteins in cancer progression. In *Journal of Biomedical Science*, BioMed Central, 23(1), 53.

Jeng, C. J., Fu, S. J., You, C. Y., Peng, Y. J., Hsiao, C. T., Chen, T. Y., & Tang, C. Y. (2020). Defective Gating and Proteostasis of Human ClC-1 Chloride Channel: Molecular Pathophysiology of Myotonia Congenita. *Frontiers in Neurology*,

Feb(11), 76.
Jia, N., Dong, S., Zhao, G., Gao, H., Li, X., & Zhang, H. (2016). CLIC1 overexpression is associated with poor prognosis in pancreatic ductal adenocarcinomas. *Journal of Cancer Research and Therapeutics*, *12*(2), 892.
Jiang, L., Salao, K., Li, H., Rybicka, J. M., Yates, R. M., Luo, X. W., Shi, X. X., Kuffner, T., Tsai, V. W.-W., Husaini, Y., Wu, L., Brown, D. a, Grewal, T., Brown, L. J., Curmi, P. M. G., & Breit, S. N. (2012). Intracellular chloride channel protein CLIC1 regulates macrophage function through modulation of phagosomal acidification. *Journal of Cell Science*, *125*(Pt 22), 5479–5488.
Jiang, Y. Y., Hou, H. T., Yang, Q., Liu, X. C., & He, G. W. (2017). Chloride Channels are Involved in the Development of Atrial Fibrillation - A Transcriptomic and proteomic Study. *Scientific Reports*, *7*, 10215.
Jin, H., & Varner, J. (2004). Integrins: roles in cancer development and as treatment targets. *British Journal of Cancer 2004 90:3*, *90*(3), 561–565.
Kagiali, Z. C. U., Saner, N., Akdag, M., Sanal, E., Degirmenci, B. S., Mollaoglu, G., & Ozlu, N. (2020). CLIC4 and CLIC1 bridge plasma membrane and cortical actin network for a successful cytokinesis. *Life Science Alliance*, *3*(2).
Kang, C. (2019). Applications of in-cell NMR in structural biology and drug discovery. *International Journal of Molecular Sciences*, *2*(20), 139.
Khamici, H. Al, Brown, L. J., Hossain, K. R., Hudson, A. L., Sinclair-Burton, A. A., Ng, J. P. M., Daniel, E. L., Hare, J. E., Cornell, B. A., Curmi, P. M. G., Davey, M. W., & Valenzuela, S. M. (2015). Members of the chloride intracellular ion channel protein family demonstrate glutaredoxin-like enzymatic activity. *PLoS ONE*, *10*(1).
Kiedrowski, L. (2012). Cytosolic acidification and intracellular zinc release in hippocampal neurons. *Journal of Neurochemistry*, *121*(3), 438–450.
Kimple, M. E., Brill, A. L., & Pasker, R. L. (2013). Overview of affinity tags for protein purification. *Current Protocols in Protein Science*, *73*, 9.9.1-9.9.23.
Ko, J. H., Ko, E. A., Gu, W., Lim, I., Bang, H., & Zhou, T. (2013). Expression profiling of ion channel genes predicts clinical outcome in breast cancer. *Molecular Cancer*, *12*(1).
Kobayashi, T., Shiozaki, A., Nako, Y., Ichikawa, D., Kosuga, T., Shoda, K., Arita, T., Konishi, H., Komatsu, S., Kubota, T., Fujiwara, H., Okamoto, K., Kishimoto, M., Konishi, E., Marunaka, Y., & Otsuji, E. (2018). Chloride intracellular channel 1 as a switch among tumor behaviors in human esophageal squamous cell carcinoma. *Oncotarget*, *9*(33), 23237–23252.
Kuriakose, S., Onyilagha, C., Singh, R., Olayinka-Adefemi, F., Jia, P., & Uzonna, J. E. (2019). TLR-2 and MyD88-Dependent Activation of MAPK and STAT Proteins Regulates Proinflammatory Cytokine Response and Immunity to Experimental Trypanosoma congolense Infection. *Frontiers in Immunology*, *10*, 2673.
Kürz, L. L., Klink, H., Jakob, I., Kuchenbecker, M., Benz, S., Lehmann-Horn, F., & Rüdel, R. (1999). Identification of Three Cysteines as Targets for the Zn^{2+} Blockade of the Human Skeletal Muscle Chloride Channel *. *Journal of Biological Chemistry*, *274*(17).
Landry, D. W., Reitman, M., Cragoe Jr., E. J., & Al-Awqati, Q. (1987). Epithelial chloride channel. Development of inhibitory ligands. *Journal of General Physiology*, *90*(6), 779–798.

Large, W. A., & Wang, Q. (1996). Characteristics and physiological role of the Ca(2+)-activated Cl- conductance in smooth muscle. *American Journal of Physiology-Cell Physiology*, *271*(2), C435–C454.

Lee, J. C., Gray, H. B., & Winkler, J. R. (2008). Copper(II) Binding to α-Synuclein, the Parkinson's Protein. *Journal of the American Chemical Society*, *130*(22), 6898.

Lee, J. R., Lee, J. Y., Kim, H. J., Hahn, M. J., Kang, J. S., & Cho, H. (2019). The inhibition of chloride intracellular channel 1 enhances Ca2+ and reactive oxygen species signaling in A549 human lung cancer cells. *Experimental and Molecular Medicine*, *51*(7), 1–11.

Li, B. P., Mao, Y. T., Wang, Z., Chen, Y. Y., Wang, Y., Zhai, C. Y., Shi, B., Liu, S. Y., Liu, J. L., & Chen, J. Q. (2018). CLIC1 Promotes the Progression of Gastric Cancer by Regulating the MAPK/AKT Pathways. *Cellular Physiology and Biochemistry*, *46*(3), 907–924.

Li, H. T., Jiao, M., Chen, J., & Liang, Y. (2010). Roles of zinc and copper in modulating the oxidative refolding of bovine copper, zinc superoxide dismutase. *Acta Biochimica et Biophysica Sinica*, *42*(3), 183–194.

Li, R. K., Zhang, J., Zhang, Y. H., Li, M. L., Wang, M., & Tang, J. W. (2012). Chloride intracellular channel 1 is an important factor in the lymphatic metastasis of hepatocarcinoma. *Biomedicine and Pharmacotherapy*, *66*(3), 167–172.

Liemann, S., & Lewit-Bentley, A. (1995). Annexins: a novel family of calcium- and membrane-binding proteins in search of a function. *Structure*, *3*(3), 233–237.

Lilius, G. L., Persson, M. P., Bulow, L. B., & Mosbach, K. M. (1991). Metal affinity precipitation of proteins carrying genetically attached polyhistidine affinity tails. *European Journal of Biochemistry*, *198*(2), 499–504.

Littler, D. R., Assaad, N. N., Harrop, S. J., Brown, L. J., Pankhurst, G. J., Luciani, P., Aguilar, M. I., Mazzanti, M., Berryman, M. A., Breit, S. N., & Curmi, P. M. G. (2005). Crystal structure of the soluble form of the redox-regulated chloride ion channel protein CLIC4. *FEBS Journal*, *272*(19), 4996–5007.

Littler, D. R., Harrop, S. J., Brown, L. J., Pankhurst, G. J., Mynott, A. V, Luciani, P., Mandyam, R. A., Mazzanti, M., Tanda, S., Berryman, M. A., Breit, S. N., & Curmi, P. M. G. (2008). Comparison of vertebrate and invertebrate CLIC proteins: The crystal structures of Caenorhabditis elegans EXC-4 and Drosophila melanogaster DmCLIC. *Proteins: Structure, Function, and Bioinformatics*, *71*(1), 364–378.

Littler, D. R., Harrop, S. J., Fairlie, W. D., Brown, L. J., Pankhurst, G. J., Pankhurst, S., DeMaere, M. Z., Campbell, T. J., Bauskin, A. R., Tonini, R., Mazzanti, M., Breit, S. N., & Curmi, P. M. G. (2004). The Intracellular Chloride Ion Channel Protein CLIC1 Undergoes a Redox-controlled Structural Transition. *Journal of Biological Chemistry*, *279*(10), 9298–9305.

Littler, D. R., Harrop, S. J., Goodchild, S. C., Phang, J. M., Mynott, A. V., Jiang, L., Valenzuela, S. M., Mazzanti, M., Brown, L. J., Breit, S. N., & Curmi, P. M. G. (2010). The enigma of the CLIC proteins: Ion channels, redox proteins, enzymes, scaffolding proteins? *FEBS Letters*, *584*(10), 2093–2101.

Litwack, G., Ketterer, B., & Arias, I. M. (1971). Ligandin: A hepatic protein which binds steroids, bilirubin, carcinogens and a number of exogenous organic anions [6]. In *Nature*, Nature Publishing Group, 234(5330), 466-467.

Liu, Y., Wang, Z., Li, M., Ye, Y., Xu, Y., Zhang, Y., Yuan, R., Jin, Y., Hao, Y., Jiang, L., Hu,

Y., Chen, S., Liu, F., Zhang, Y., Wu, W., & Liu, Y. (2017). Chloride intracellular channel 1 regulates the antineoplastic effects of metformin in gallbladder cancer cells. *Cancer Science*, *108*(6), 1240–1252.

Lu, J., Dong, Q., Zhang, B., Wang, X., Ye, B., Zhang, F., Song, X., Gao, G., Mu, J., Wang, Z., Ma, F., & Gu, J. (2015). Chloride intracellular channel 1 (CLIC1) is activated and functions as an oncogene in pancreatic cancer. *Medical Oncology (Northwood, London, England)*, *32*(6), 616.

Luchinat, E., & Banci, L. (2016). A Unique Tool for Cellular Structural Biology: In-cell NMR. *The Journal of Biological Chemistry*, *291*(8), 3776.

Luchinat, E., & Banci, L. (2017). In-cell NMR: a topical review. *IUCrJ*, *4*(Pt 2), 108–118.

Ma, P. F., Chen, J. Q., Wang, Z., Liu, J. L., & Li, B. P. (2012). Function of chloride intracellular channel 1 in gastric cancer cells. *World Journal of Gastroenterology*, *18*(24), 3070–3080.

Majumder, S., Demott, C. M., Reverdatto, S., Burz, D. S., & Shekhtman, A. (2016). Total Cellular RNA Modulates Protein Activity HHS Public Access. *Biochemistry*, *55*(32), 4568–4573.

Malekova, L., Tomaskova, J., Novakova, M., Stefanik, P., Kopacek, J., Lakatos, B., Pastorekova, S., Krizanova, O., Breier, A., & Ondrias, K. (2007). Inhibitory effect of DIDS, NPPB, and phloretin on intracellular chloride channels. *Pflugers Archiv European Journal of Physiology*, *455*(2), 349–357.

Mall, M. A., & Hartl, D. (2014). CFTR: Cystic fibrosis and beyond. *European Respiratory Journal*, *44*(4), 1042–1054.

Manak, M. S., & Ferl, R. J. (2007). Divalent Cation Effects on Interactions between Multiple Arabidopsis 14-3-3 Isoforms and Phosphopeptide Targets. *Biochemistry*, *46*(4).

Manley, S., & Gordon, V. D. (2008). Making giant unilamellar vesicles via hydration of a lipid film. *Current Protocols in Cell Biology*, *24*(24.3).

McGill University Health Centre/Research Institute of the McGill University Health Centre. (2015). *Metformin, Neo-adjuvant Temozolomide and Hypo-Accelerated Radiotherapy Followed by Adjuvant TMZ in Patients With GBM*. ClinicalTrials.Gov.

Medina-Carmona, E., Varela, L., Hendry, A. C., Thompson, G. S., White, L. J., Boles, J. E., Hiscock, J. R., & Ortega-Roldan, J. L. (2020). A quantitative assay to study the lipid selectivity of membrane-associated systems using solution NMR. *Chemical Communications*, *56*, 11665.

Milton, R. H., Abeti, R., Averaimo, S., DeBiasi, S., Vitellaro, L., Jiang, L., Curmi, P. M. G., Breit, S. N., Duchen, M. R., & Mazzanti, M. (2008). CLIC1 Function Is Required for -Amyloid-Induced Generation of Reactive Oxygen Species by Microglia. *Journal of Neuroscience*, *28*(45), 11488–11499.

Miroux, B., & Walker, J. E. (1996). Over-production of proteins in Escherichia coli: Mutant hosts that allow synthesis of some membrane proteins and globular proteins at high levels. *Journal of Molecular Biology*, *260*(3), 289–298.

Monastyrskaya, K., Babiychuk, E. B., Hostettler, A., Rescher, U., & Draeger, A. (2007). Annexins as intracellular calcium sensors. *Cell Calcium*, *41*(3), 207–219.

Mullis, K. B., & Faloona, F. A. (1987). Specific Synthesis of DNA in Vitro via a Polymerase-Catalyzed Chain Reaction. *Methods in Enzymology*, *155*(C), 335–

350.
Murphy, D. A., & Courtneidge, S. A. (2011). The “ins” and “outs” of podosomes and invadopodia: Characteristics, formation and function. *Nature Reviews Molecular Cell Biology*, *12*(17), 413–426.
Nesiu, A., Cimpean, A. M., Ceausu, R. A., Adile, A., Ioiart, I., Porta, C., Mazzanti, M., Camerota, T. C., & Raica, M. (2019). Intracellular Chloride Ion Channel Protein-1 Expression in Clear Cell Renal Cell Carcinoma. *Cancer Genomics & Proteomics*, *16*(4), 299–307.
Neveu, B., Spinella, J. F., Richer, C., Lagacé, K., Cassart, P., Lajoie, M., Jananji, S., Drouin, S., Healy, J., Hickson, G. R. X., & Sinnett, D. (2016). CLIC5: A novel ETV6 target gene in childhood acute lymphoblastic leukemia. *Haematologica*, *101*(12), 1534–1543.
Nguyen, H., & Lauto, A. (2016). Chloride Intracellular Channel Protein 1 and its Role in Neurodegenerative Disorders and Cancerous Tumors. *Biochemistry & Analytical Biochemistry*, *5*(1).
Ninsontia, C., Phiboonchaiyanan, P. P., & Chanvorachote, P. (2016). Zinc induces epithelial to mesenchymal transition in human lung cancer H460 cells via superoxide anion-dependent mechanism. *Cancer Cell International*, *16*, 48.
Nishida, N., Yano, H., Nishida, T., Kamura, T., & Kojiro, M. (2006). Angiogenesis in cancer. *Vascular Health and Risk Management*, *2*(3), 213–219.
Nishizawa, T., Nagao, T., Iwatsubo, T., Forte, J. G., & Urushidani, T. (2000). Molecular cloning and characterization of a novel chloride intracellular channel-related protein, parchorin, expressed in water-secreting cells. *Journal of Biological Chemistry*, *275*(15), 11164–11173.
Noh, S., Lee, S. R., Jeong, Y. J., Ko, K. S., Rhee, B. D., Kim, N., & Han, J. (2015). The direct modulatory activity of zinc toward ion channels. *Integrative Medicine Research*, *4*(3), 142–146.
Novarino, G., Fabrizi, C., Tonini, R., Denti, M. A., Malchiodi-Albedi, F., Lauro, G. M., Sacchetti, B., Paradisi, S., Ferroni, A., Curmi, P. M., Breit, S. N., & Mazzanti, M. (2004). Involvement of the intracellular ion channel CLIC1 in microglia-mediated β-amyloid-induced neurotoxicity. *Journal of Neuroscience*, 23(24), 5322-5330
O’Neill, S. D., & Leopold, A. C. (1982). An Assessment of Phase Transitions in Soybean Membranes. *Plant Physiology*, *70*(5), 1405.
Ogino, S., Kubo, S., Umemoto, R., Huang, S., Nishida, N., & Shimada, I. (2009). Observation of NMR signals from proteins introduced into living mammalian cells by reversible membrane permeabilization using a pore-forming toxin, streptolysin O. *Journal of the American Chemical Society*, *131*(31), 10834–10835.
Oldfield, E., & Chapman, D. (1972). Dynamics of lipids in membranes: Heterogeneity and the role of cholesterol. *FEBS Letters*, *23*(3).
Palmer, M. (2004). Cholesterol and the activity of bacterial toxins. *FEMS Microbiology Letters*, *238*(2), 281–289,.
Pan, B. Bin, Yang, F., Ye, Y., Wu, Q., Li, C., Huber, T., & Su, X. C. (2016). 3D structure determination of a protein in living cells using paramagnetic NMR spectroscopy. *Chemical Communications*, *52*(67), 10237–10240.
Pan, R., Liu, K. J., & Qi, Z. (2019). Zinc causes the death of hypoxic astrocytes by

inducing ROS production through mitochondria dysfunction. *Biophysics Reports*, *5*, 209–217.

Parks, T. D., Leuther, K. K., Howard, E. D., Johnston, S. A., & Dougherty, W. G. (1994). Release of proteins and peptides from fusion proteins using a recombinant plant virus proteinase. *Analytical Biochemistry*, *216*(2), 413-7.

Pastore, A., & Temussi, P. A. (2017). The Emperor's new clothes: Myths and truths of in-cell NMR. In *Archives of Biochemistry and Biophysics*, Academic Press, 628, 114-122

Peretti, M., Angelini, M., Savalli, N., Florio, T., Yuspa, S. H., & Mazzanti, M. (2015). Chloride channels in cancer: Focus on chloride intracellular channel 1 and 4 (CLIC1 AND CLIC4) proteins in tumor development and as novel therapeutic targets. *Biochimica et Biophysica Acta - Biomembranes*, *1848*(10), 2523–2531.

Peretti, M., Raciti, F. M., Carlini, V., Verduci, I., Sertic, S., Barozzi, S., Garre, M., Pattarozzi, A., Daga, A., Barbieri, F., Costa, A., Florio, T., & Mazzanti, M. (2018). Mutual influence of ROS, PH, and CLIC1 membrane protein in the regulation of G 1 -S phase progression in human glioblastoma stem cells. *Molecular Cancer Therapeutics*, *17*(11), 2451–2461.

Perisic, O., Fong, S., Lynch, D. E., Bycroft, M., & Williams, R. L. (1998). Crystal structure of a calcium-phospholipid binding domain from cytosolic phospholipase A2. *Journal of Biological Chemistry*, *273*(3), 1596–1604.

Pervushin, K., Riek, R., Wider, G., & Wüthrich, K. (1997). Attenuated T2 relaxation by mutual cancellation of dipole-dipole coupling and chemical shift anisotropy indicates an avenue to NMR structures of very large biological macromolecules in solution. *Proceedings of the National Academy of Sciences of the United States of America*, *94*(23), 12366–12371.

Ponnalagu, D., Gururaja Rao, S., Farber, J., Xin, W., Hussain, A. T., Shah, K., Tanda, S., Berryman, M., Edwards, J. C., & Singh, H. (2016). Molecular identity of cardiac mitochondrial chloride intracellular channel proteins. *Mitochondrion*, *27*, 6–14.

Ponnalagu, D., Rao, S. G., Farber, J., Xin, W., Hussain, A. T., Shah, K., Tanda, S., Berryman, M. A., Edwards, J. C., & Singh, H. (2016). Data supporting characterization of CLIC1, CLIC4, CLIC5 and DmCLIC antibodies and localization of CLICs in endoplasmic reticulum of cardiomyocytes. *Data in Brief*, *7*, 1038–1044.

Qian, Z., Okuhara, D., Abe, M. K., & Rosner, M. R. (1999). Molecular cloning and characterization of a mitogen-activated protein kinase-associated intracellular chloride channel. *Journal of Biological Chemistry*, *274*(3), 1621–1627.

Qu, H., Chen, Y., Cao, G., Liu, C., Xu, J., Deng, H., & Zhang, Z. (2016). Identification and validation of differentially expressed proteins in epithelial ovarian cancers using quantitative proteomics. *Oncotarget*, *7*(50), 83187–83199.

Quintero-Fabián, S., Arreola, R., Becerril-Villanueva, E., Torres-Romero, J. C., Arana-Argáez, V., Lara-Riegos, J., Ramírez-Camacho, M. A., & Alvarez-Sánchez, M. E. (2019). Role of Matrix Metalloproteinases in Angiogenesis and Cancer. In *Frontiers in Oncology*, Frontiers, 9, 1370

Ranjbar, B., & Gill, P. (2009). Circular dichroism techniques: Biomolecular and nanostructural analyses- A review. In *Chemical Biology and Drug Design*, 101-120

Rao, S. G., Ponnalagu, D., Sukur, S., Singh, H., Sanghvi, S., Mei, Y., Jin, D. J., & Singh, H. (2017). Identification and Characterization of a Bacterial Homolog of Chloride Intracellular Channel (CLIC) Protein. *Scientific Reports*, *7*(1), 1–13.

Sakai, T., Tochio, H., Tenno, T., Ito, Y., Kokubo, T., Hiroaki, H., & Shirakawa, M. (2006). In-cell NMR spectroscopy of proteins inside Xenopus laevis oocytes. *Journal of Biomolecular NMR*, *36*(3), 179–188.

Sakakibara, D., Sasaki, A., Ikeya, T., Hamatsu, J., Hanashima, T., Mishima, M., Yoshimasu, M., Hayashi, N., Mikawa, T., Wälchli, M., Smith, B. O., Shirakawa, M., Güntert, P., & Ito, Y. (2009). Protein structure determination in living cells by in-cell NMR spectroscopy. *Nature*, *458*(7234), 102–105.

Schanda, P., & Brutscher, B. (2005). Very fast two-dimensional NMR spectroscopy for real-time investigation of dynamic events in proteins on the time scale of seconds. *Journal of the American Chemical Society*, *127*(22), 8014–8015.

Schievella, A. R., Regier, M. K., Smith, W. L., & Lin, L. L. (1995). Calcium-mediated translocation of cytosolic phospholipase A2 to the nuclear envelope and endoplasmic reticulum. *Journal of Biological Chemistry*, *270*(51), 30749–30754.

Schirrmacher, V. (2019). From chemotherapy to biological therapy: A review of novel concepts to reduce the side effects of systemic cancer treatment (Review). *International Journal of Oncology*, *54*(2), 407–419.

Scipion, C. P. M., Ghoshdastider, U., Ferrer, F. J., Yuen, T.-Y., Wongsantichon, J., & Robinson, R. C. (2018). Structural evidence for the roles of divalent cations in actin polymerization and activation of ATP hydrolysis. *Proceedings of the National Academy of Sciences*, *115*(41), 10345 LP – 10350.

Selenko, P., Serber, Z., Gadea, B., Ruderman, J., & Wagner, G. (2006). Quantitative NMR analysis of the protein G B1 domain in Xenopus laevis egg extracts and intact oocytes. *Proceedings of the National Academy of Sciences of the United States of America*, *103*(32), 11904–11909.

Serber, Z., Keatinge-Clay, A. T., Ledwidge, R., Kelly, A. E., Miller, S. M., & Dötsch, V. (2001). High-resolution macromolecular NMR spectroscopy inside living cells. In *Journal of the American Chemical Society* 123(10), 2446-2447.

Serber, Z., Ledwidge, R., Miller, S. M., & Dötsch, V. (2001). Evaluation of parameters critical to observing proteins inside living Escherichia coli by in-cell NMR spectroscopy. *Journal of the American Chemical Society*, *123*(37), 8895–8901.

Serber, Z., Straub, W., Corsini, L., Nomura, A. M., Shimba, N., Craik, C. S., De Montellano, P. O., & Dötsch, V. (2004). Methyl groups as probes for proteins and complexes in in-cell NMR experiments. *Journal of the American Chemical Society*, *126*(22), 7119–7125.

Setti, M., Osti, D., Richichi, C., Ortensi, B., Bene, M. Del, Fornasari, L., Beznoussenko, G., Mironov, A., Rappa, G., Cuomo, A., Faretta, M., Bonaldi, T., Lorico, A., & Pelicci, G. (2015). Extracellular vesicle-mediated transfer of CLIC1 protein is a novel mechanism for the regulation of glioblastoma growth. *Oncotarget*, *6*(31), 31413–31427.

Setti, M., Savalli, N., Osti, D., Richichi, C., Angelini, M., Brescia, P., Fornasari, L., Carro, M. S., Mazzanti, M., & Pelicci, G. (2013). Functional role of CLIC1 ion channel in glioblastoma-derived stem/progenitor cells. *Journal of the National Cancer Institute*, 105(21), 1644-1655

Shaulian, E. (2010). AP-1 - The Jun proteins: Oncogenes or tumor suppressors in

disguise? In *Cellular Signalling*, Cell Signal, 22(6), 894-899
Sheehan, D., Meade, G., Foley, V. M., & Dowd, C. A. (2001). Structure, function and evolution of glutathione transferases: Implications for classification of non-mammalian members of an ancient enzyme superfamily. *Biochemical Journal*, *360*(1), 1–16.
Sheng, S., Perry, C. J., & Kleyman, T. R. (2004). Extracellular Zn2+ activates epithelial Na+ channels by eliminating Na+ self-inhibition. *Journal of Biological Chemistry*, *279*(30), 31687–31696.
Silvius, J. . (1982). Thermotropic Phase Transitions of Pure Lipids in Model Membranes and Their Modifications by Membrane Proteins,. In *Lipid-Protein Interactions*. John Wiley & Sons, Ltd.
Simon, H. U., Haj-Yehia, A., & Levi-Schaffer, F. (2000). Role of reactive oxygen species (ROS) in apoptosis induction. *Apoptosis*, *5*(5), 415–418.
Singh, H., & Ashley, R. H. (2006). Redox Regulation of CLIC1 by Cysteine Residues Associated with the Putative Channel Pore. *Biophysical Journal*, *90*(5), 1628–1638.
Singh, H., Cousin, M. A., & Ashley, R. H. (2007). Functional reconstitution of mammalian "chloride intracellular channels" CLIC1, CLIC4 and CLIC5 reveals differential regulation by cytoskeletal actin. *FEBS Journal*, *274*(24), 6306–6316.
Singha, B., Harper, S. L., Goldman, A. R., Bitler, B. G., Aird, K. M., Borowsky, M. E., Cadungog, M. G., Liu, Q., Zhang, R., Jean, S., Drapkin, R., & Speicher, D. W. (2018). CLIC1 and CLIC4 complement CA125 as a diagnostic biomarker panel for all subtypes of epithelial ovarian cancer. *Scientific Reports*, *8*(1), 14725.
Slepchenko, K. G., Lu, Q., & Li, Y. V. (2017). Cross talk between increased intracellular zinc (Zn 2+) and accumulation of reactive oxygen species in chemical ischemia. *American Journal of Physiology-Cell Physiology*, *313*(4), C448–C459.
Smith, D. B., & Johnson, K. S. (1988). Single-step purification of polypeptides expressed in Escherichia coli as fusions with glutathione S-transferase. *Gene*, *67*(1), 31–40.
Sohlenkamp, C., & Geiger, O. (2016). Bacterial membrane lipids: diversity in structures and pathways. *FEMS Microbiology Reviews*, *40*(1), 133–159.
Solcan, N., Kwok, J., Fowler, P. W., Cameron, A. D., Drew, D., Iwata, S., & Newstead, S. (2012). Alternating access mechanism in the POT family of oligopeptide transporters. *EMBO Journal*, *31*(16), 3411–3421.
Sprangers, R., & Kay, L. E. (2007). Quantitative dynamics and binding studies of the 20S proteasome by NMR. *Nature*, *445*(7128), 618–622.
Stadmiller, S. S., & Pielak, G. J. (2018). The Expanding Zoo of In-Cell Protein NMR. In *Biophysical Journal*, Biophysical Society, 115(9), 1628-1629.
Stakaityte, G., Nwogu, N., Lippiat, J. D., Blair, G. E., Poterlowicz, K., Boyne, J. R., MacDonald, A., Mankouri, J., & Whitehouse, A. (2018). The cellular chloride channels CLIC1 and CLIC4 contribute to virus-mediated cell motility. *Journal of Biological Chemistry*, *293*(12), 4582–4590.
Stoychev, S. H., Nathaniel, C., Fanucchi, S., Brock, M., Li, S., Asmus, K., Woods, V. L., & Dirr, H. W. (2009). Structural dynamics of soluble chloride intracellular channel protein CLIC1 examined by amide hydrogen-deuterium exchange mass spectrometry. *Biochemistry*, 48(35), 8413-8421

Stray, S. J., Ceres, P., & Zlotnick, A. (2004). Zinc ions trigger conformational change and oligomerization of hepatitis B virus capsid protein. *Biochemistry*, 43(31), 9989-98

Suh, K. S., Crutchley, J. M., Dumont, R. A., Levy, J. M., & Yuspa, S. H. (2004). CLIC4, a proapoptotic chloride channel protein, has potential as a novel molecular target for tumor therapy. *Cancer Research*, *64*(7 Supplement), 1240 LP – 1240.

Suh, K. S., Crutchley, J. M., Koochek, A., Ryscavage, A., Bhat, K., Tanaka, T., Oshima, A., Fitzgerald, P., & Yuspa, S. H. (2007). Reciprocal modifications of CLIC4 in tumor epithelium and stroma mark malignant progression of multiple human cancers. *Clinical Cancer Research*, *13*(1), 121–131.

Suh, K. S., Malik, M., Shukla, A., Ryscavage, A., Wright, L., Jividen, K., Crutchley, J. M., Dumont, R. A., Fernandez-Salas, E., Webster, J. D., Simpson, R. M., & Yuspa, S. H. (2012). CLIC4 is a tumor suppressor for cutaneous squamous cell cancer. *Carcinogenesis*, *33*(5), 986–995.

Tamimi, A. F., & Juweid, M. (2017). Epidemiology and Outcome of Glioblastoma. *Glioblastoma*, 143–153.

Tang, T., Lang, X., Xu, C., Wang, X., Gong, T., Yang, Y., Cui, J., Bai, L., Wang, J., Jiang, W., & Zhou, R. (2017). CLICs-dependent chloride efflux is an essential and proximal upstream event for NLRP3 inflammasome activation. *Nature Communications*, *8*, 202.

Terpe, K. (2006). Overview of bacterial expression systems for heterologous protein production: From molecular and biochemical fundamentals to commercial systems. *Applied Microbiology and Biotechnology*, *72*(2), 211–222.

Thain, A., Gaston, K., Jenkins, O., & Clarke, A. R. (1996). A method for the separation of GST fusion proteins from co-purifying GroEL. *Trends in Genetics : TIG*, *12*(6).

Theillet, F. X., Binolfi, A., Bekei, B., Martorana, A., Rose, H. M., Stuiver, M., Verzini, S., Lorenz, D., Van Rossum, M., Goldfarb, D., & Selenko, P. (2016). Structural disorder of monomeric α-synuclein persists in mammalian cells. *Nature*, *530*(7588), 45–50.

Thuringer, D., Chanteloup, G., Winckler, P., & Garrido, C. (2018). The vesicular transfer of CLIC1 from glioblastoma to microvascular endothelial cells requires TRPM7. *Oncotarget*, *9*, 33302–33311.

Tian, Y., Guan, Y., Jia, Y., Meng, Q., & Yang, J. (2014). Chloride intracellular channel 1 regulates prostate cancer cell proliferation and migration through the MAPK/ERK pathway. *Cancer Biotherapy & Radiopharmaceuticals*, *29*(8), 339–344.

Tolde, O., Rösel, D., Veselý, P., Folk, P., & Brábek, J. (2010). The structure of invadopodia in a complex 3D environment. *European Journal of Cell Biology*, *89*(9), 674–680.

Tonini, R., Ferroni, A., Valenzuela, S. M., Warton, K., Campbell, T. J., Breit, S. N., & Mazzanti, M. (2000). Functional characterization of the NCC27 nuclear protein in stable transfected CHO-K1 cells. *Faseb J*, *14*(9), 1171–1178.

Townsend, D. M., & Tew, K. D. (2003). The role of glutathione-S-transferase in anti-cancer drug resistance. *Oncogene*, *22*(47), 7369–7375.

Tugarinov, V., Kanelis, V., & Kay, L. E. (2006). Isotope labeling strategies for the study of high-molecular-weight proteins by solution NMR spectroscopy.

Nature Protocols, *1*(2), 749–754.
Tugarinov, V., & Kay, L. E. (2003). Ile, Leu, and Val Methyl Assignments of the 723-Residue Malate Synthase G Using a New Labeling Strategy and Novel NMR Methods. *Journal of the American Chemical Society*, *125*(45), 13868–13878.
Tulk, B. M., Kapadia, S., Edwards, J. C., Al-Awqati, Q., Alberts, B., Bray, D., Lewis, J., Raff, M., Roberts, K., Watson, J., Armitage, P., Berryman, M., Bretscher, A., Columbini, M., Dulhunty, A., Gage, P., Curtis, S., Chelvanayagam, G., Board, P., … Breit, S. (2002). CLIC1 inserts from the aqueous phase into phospholipid membranes, where it functions as an anion channel. *American Journal of Physiology - Cell Physiology*, *282*(5), C1103-12.
Tulk, B. M., Schlesinger, P. H., Kapadia, S. A., & Edwards, J. C. (2000). CLIC-1 Functions as a Chloride Channel When Expressed and Purified from Bacteria. *Journal of Biological Chemistry* , *275*(35), 26986–26993.
Tung, J. J., & Kitajewski, J. (2010). Chloride intracellular channel 1 functions in endothelial cell growth and migration. *Journal of Angiogenesis Research*, *2*(1), 23.
Ulmasov, B., Bruno, J., Woost, P. G., & Edwards, J. C. (2007). Tissue and subcellular distribution of CLIC1. *BMC Cell Biology*, *8*, 8.
Valenzuela, S. M., Alkhamici, H., Brown, L. J., Almond, O. C., Goodchild, S. C., Carne, S., Curmi, P. M. G., Holt, S. A., & Cornell, B. A. (2013). Regulation of the Membrane Insertion and Conductance Activity of the Metamorphic Chloride Intracellular Channel Protein CLIC1 by Cholesterol. *PLoS ONE*, *8*(2).
Valenzuela, S. M., Martin, D. K., Por, S. B., Robbins, J. M., Warton, K., Bootcov, M. R., Schofield, P. R., Campbell, T. J., & Breit, S. N. (1997). Molecular cloning and expression of a chloride ion channel of cell nuclei. *Journal of Biological Chemistry*, *272*(19), 12575–12582.
Valenzuela, S. M., Mazzanti, M., Tonini, R., Qiu, M. R., Warton, K., Musgrove, E. A., Campbell, T. J., & Breit, S. N. (2000). The nuclear chloride ion channel NCC27 is involved in regulation of the cell cycle. *Journal of Physiology*, *529*(3), 541–552.
Van Wazer, J. R., & Callis, C. F. (1958). Metal Complexing By Phosphates. *Chemical Reviews*, *58*(6).
Varela, L., Hendry, A. C., Medina-Carmona, E., Cantoni, D., & Ortega-Roldan, J. L. (2019). Membrane insertion of soluble CLIC1 into active chloride channels is triggered by specific divalent cations. *BioRxiv*.
Veatch, S. L. (2007). Electro-formation and fluorescence microscopy of giant vesicles with coexisting liquid phases. *Methods in Molecular Biology*, *398*, 59–72.
Verduci, I., Carlini, V., Raciti, F. M., Conti, M., Barbieri, F., Florio, T., & Mazzanti, M. (2017). *CLIC1 membrane insertion is a pivotal regulator of glioblastoma stem cell G1-S transition by promoting an increase of chloride permeability*. *77*, 304–304.
Wang, J. W., Peng, S. Y., Li, J. T., Wang, Y., Zhang, Z. P., Cheng, Y., Cheng, D. Q., Weng, W. H., Wu, X. S., Fei, X. Z., Quan, Z. W., Li, J. Y., Li, S. G., & Liu, Y. Bin. (2009). Identification of metastasis-associated proteins involved in gallbladder carcinoma metastasis by proteomic analysis and functional exploration of chloride intracellular channel 1. *Cancer Letters*, *18*(281), 71–81.
Wang, L., He, S., Tu, Y., Ji, P., Zong, J., Zhang, J., Feng, F., Zhao, J., Zhang, Y., & Gao,

G. (2012). Elevated expression of chloride intracellular channel 1 is correlated with poor prognosis in human gliomas. *Journal of Experimental and Clinical Cancer Research*, *31*(1), 44.

Wang, P., Zeng, Y., Liu, T., Zhang, C., Yu, P. W., Hao, Y. X., Luo, H. X., & Liu, G. (2014). Chloride intracellular channel 1 regulates colon cancer cell migration and invasion through ROS/ERK pathway. *World Journal of Gastroenterology*, *20*(8), 2071–2078.

Wang, P., Zhang, C., Yu, P., Tang, B., Liu, T., Cui, H., & Xu, J. (2012). Regulation of colon cancer cell migration and invasion by CLIC1-mediated RVD. *Molecular and Cellular Biochemistry*, *365*(1–2), 313–321.

Wang, W., Xu, X., Wang, W., Shao, W., Li, L., Yin, W., Xiu, L., Mo, M., Zhao, J., He, Q., & He, J. (2011). The expression and clinical significance of CLIC1 and HSP27 in lung adenocarcinoma. *Tumour Biology : The Journal of the International Society for Oncodevelopmental Biology and Medicine*, *32*(6), 1199–1208.

Wang, Z., Ling, S., Rettig, E., Sobel, R., Tan, M., Fertig, E. J., Considine, M., El-Naggar, A. K., Brait, M., Fakhry, C., & Ha, P. K. (2015). Epigenetic screening of salivary gland mucoepidermoid carcinoma identifies hypomethylation of CLIC3 as a common alteration. *Oral Oncology*, *51*(12), 1120–1125.

Warton, K., Tonini, R., Douglas Fairlie, W., Matthews, J. M., Valenzuela, S. M., Qiu, M. R., Wu, W. M., Pankhurst, S., Bauskin, A. R., Harrop, S. J., Campbell, T. J., Curmi, P. M. G., Breit, S. N., & Mazzanti, M. (2002). Recombinant CLIC1 (NCC27) assembles in lipid bilayers via a pH-dependent two-state process to form chloride ion channels with identical characteristics to those observed in Chinese hamster ovary cells expressing CLIC1. *Journal of Biological Chemistry*, *277*(29), 26003–26011.

Wei, Z., & Liu, H. T. (2002). MAPK signal pathways in the regulation of cell proliferation in mammalian cells. In *Cell Research*, Nature Publishing Group, 12(1), 9-18.

Witham, S., Takano, K., Schwartz, C., & Alexov, E. (2011). A missense mutation in CLIC2 associated with intellectual disability is predicted by in silico modeling to affect protein stability and dynamics. *Proteins: Structure, Function and Bioinformatics*, *79*(8), 2444–2454.

Xu, Y., Xu, J., Feng, J., Li, J., Jiang, C., Li, X., Zou, S., Wang, Q., & Li, Y. (2018). Expression of CLIC1 as a potential biomarker for oral squamous cell carcinoma: A preliminary study. *OncoTargets and Therapy*, *11*, 8073–8081.

Xu, Y., Zhu, J., Hu, X., Wang, C., Lu, D., Gong, C., Yang, J., & Zong, L. (2016). CLIC1 inhibition attenuates vascular inflammation, oxidative stress, and endothelial injury. *PLoS ONE*, *11*(11).

Yang, J. Y., Jung, J. Y., Cho, S. W., Choi, H. J., Kim, S. W., Kim, S. Y., Kim, H. J., Jang, C. H., Lee, M. G., Han, J., & Shin, C. S. (2009). Chloride intracellular channel 1 regulates osteoblast differentiation. *Bone*, *45*(6), 175–185.

Yu, W., Cui, R., Qu, H., Liu, C., Deng, H., & Zhang, Z. (2018). Expression and prognostic value of CLIC1 in epithelial ovarian cancer. *Experimental and Therapeutic Medicine*, *15*(6), 4943–4949.

Yu, W., Qu, H., Cao, G., Liu, C., Deng, H., & Zhang, Z. (2017). MtHsp70-CLIC1-pulsed dendritic cells enhance the immune response against ovarian cancer. *Biochemical and Biophysical Research Communications*, *494*(1), 13–19.

Yue, X., Cui, Y., You, Q., Lu, Y., & Zhang, J. (2019). MicroRNA-124 negatively regulates chloride intracellular channel 1 to suppress the migration and invasion of liver cancer cells. *Oncology Reports*, *42*(4), 1380–1390.

Zhang, J., Li, M., Song, M., Chen, W., Mao, J., Song, L., Wei, Y., Huang, Y., & Tang, J. (2015). Clic1 plays a role in mouse hepatocarcinoma via modulating Annexin A7 and Gelsolin in vitro and in vivo. *Biomedicine and Pharmacotherapy*, *69*, 416–419.

Zhao, W., Lu, M., & Zhang, Q. (2015). Chloride intracellular channel 1 regulates migration and invasion in gastric cancer by triggering the ROS-mediated p38 MAPK signaling pathway. *Molecular Medicine Reports*, *12*(6), 8041–8047.

Zhu, J., Xu, Y., Ren, G., Hu, X., Wang, C., Yang, Z., Li, Z., Mao, W., & Lu, D. (2017). Tanshinone IIA Sodium sulfonate regulates antioxidant system, inflammation, and endothelial dysfunction in atherosclerosis by downregulation of CLIC1. *European Journal of Pharmacology*, *815*, 427–436.

Appendix

Classification : Biological Sciences, Biochemistry

Title: Membrane insertion of soluble CLIC1 into active chloride channels is triggered by specific divalent cations.

Authors: Lorena Varela[&], Alex C. Hendry[&], Encarnacion Medina-Carmona, Diego Cantoni and Jose L. Ortega-Roldan[*]

Author information:

School of Biosciences. University of Kent. CT2 7NJ. Canterbury. United Kingdom.

[&]Lorena Varela and Alex C. Hendry contributed equally to this work.

[*] corresponding author/Lead contact: j.l.ortega-roldan@kent.ac.uk

Keywords: Membrane protein, Membrane insertion, ion channels, CLIC.

ABSTRACT

The CLIC family of proteins display the unique feature of altering their structure from a soluble form to a membrane-bound chloride channel. CLIC1, a member of this family, can be found in the cytoplasm or in nuclear, ER and plasma membranes, with membrane overexpression linked to tumour proliferation. The molecular switch promoting CLIC1 membrane insertion has been related to environmental factors, but still remains unclear. Here, we use solution NMR studies to confirm that both the soluble and membrane bound forms are in the same oxidation state. Our data from fluorescence assays and chloride efflux assays indicate that Ca^{2+} and Zn^{2+} trigger association to the membrane into active chloride channels. We use fluorescence microscopy to confirm that an increase of the intracellular Ca^{2+} leads to re-localisation of CLIC1 to both plasma and internal membranes. Finally, we show that soluble CLIC1 adopts an equilibrium of oligomeric species, and Ca^{2+}/Zn^{2+} mediated membrane insertion promotes the formation of a tetrameric assembly. Thus, our results identify Ca^{2+} and Zn^{2+} binding as the molecular switch promoting CLIC1 membrane insertion.

SIGNIFICANCE STATEMENT

CLIC1, a member of the CLIC family of proteins, is expressed as a soluble protein in cells but can insert in the membrane forming a chloride channel. This chloride channel form is upregulated in different types of cancers including glioblastoma and promote tumour invasiveness and metastasis. The factors promoting CLIC1 membrane insertion nor the mechanism of this process are yet understood. Here, we use a combination of solution NMR, biophysics and fluorescence microscopy to identify Ca^{2+} and Zn^{2+} binding as the switch to promote CLIC1 insertion into the membrane to form active chloride channels. We also provide a simple mechanism how such transition to the membrane occurs. Such understanding will enable subsequent studies on the structure of the chloride channel form and its inhibition.

INTRODUCTION

The Chloride Intracellular Channel (CLIC) family consists of a group of highly homologous human proteins with a striking feature, their ability to change their structure upon activation from a soluble form into a membrane bound chloride channel, translocating from the cytoplasm to intracellular membranes (1, 2). CLIC1 is the best characterised of the CLIC protein family. It is expressed intracellularly in a variety of cell types, being especially abundant in heart and skeletal muscle (2). CLIC1's integral membrane form has been found to be localised mostly in the nuclear membrane, although it is present in the membranes of other organelles and transiently in the plasma membrane. It has also been shown to function as an active chloride channel in phospholipid vesicles when expressed and purified from bacteria, showing clear single channel properties (3, 4).

CLIC1 has been implicated in the regulation of cell volume, electrical excitability (5), differentiation (6), cell cycle (7) and cell growth and proliferation (8). High CLIC1 expression has been reported in a range of malignant tumours, including prostate (9), gastric (10), lung (6) and liver (11) cancers, with evidence of CLIC1 promoting the spread and growth of glioblastoma cancer stem/progenitor cells (12, 13).

The activity and oncogenic function of CLIC1 is modulated by its equilibrium between the soluble cytosolic form and its membrane bound form. Only CLIC1 in its channel form has been shown to have oncogenic activity, and specific inhibition of the CLIC1 channel halts tumour progression (13). However, to date very little and conflicting information is available for the membrane insertion mechanism, and the structure of the channel form is unknown. Oxidation with hydrogen peroxide causes a conformational change due to the formation of a disulphide bond between Cys24 and the non-conserved Cys59, exposing a hydrophobic patch that promotes the formation of a dimer (14), in a process that has been proposed to lead to membrane insertion (15). However, numerous studies have shown that oxidation does not promote membrane insertion(16); with evidence pointing at pH (17, 18) or cholesterol (19) as the likely activation factors. Thus, long standing inconsistencies in the data surrounding the molecular switch that unusually transforms CLIC1 from its soluble form into a membrane bound channel has prevented further advances in the understanding of CLIC1 function. In this study, we have explored the membrane insertion mechanism of CLIC1. We used NMR experiments on CLIC1 extracted from the soluble and

in the spectrum (Figure S1). In contrast, oxidation with H_2O_2 resulted in large chemical shift differences for a subset of resonances in both spectra, indicating that CLIC1 is inserted in *E. coli* membranes in the reduced state, and therefore the membrane association process is not triggered by oxidation.

Divalent cations trigger CLIC1 membrane insertion

Since our data indicates that oxidation does not induce membrane insertion, we screened for different conditions that could trigger membrane insertion. A membrane insertion assay was developed, in which CLIC1 was mixed with the lipid mixture asolectin. The mixture was subsequently ultra-centrifuged to separate the soluble and membrane bound components. Native tryptophan fluorescence experiments were collected from the initial mixture, the supernatant and membrane pellets fractions. Using phosphate buffer, which forms insoluble complexes with divalent cations, no insertion could be detected even in the presence of oxidizing conditions. (Figure 2A). A simple change in the buffer composition to HEPES resulted in an increase in the tryptophan fluorescence emission spectrum for the membrane fraction. Since phosphate is known to form insoluble complexes with divalent cations, we explored whether the lipid insertion could be triggered by binding of divalent cations. A series of membrane insertion assays were conducted in the presence of Zn^{2+}, Ca^{2+} and Mg^{2+} to identify the effect of 2+ metals (Figure 2A). A significant increase in the overall intensity in the emission fluorescence spectra of the membrane fractions of CLIC1 was found in samples incubated with Zn^{2+}, and in a lower extent with Ca^{2+}, suggesting that CLIC1 membrane insertion is driven by binding to Zn^{2+} and/or Ca^{2+}. In a further series of experiments, tryptophan emission fluorescence spectra were measured at increasing concentrations of Zn^{2+} in the presence and absence of asolectin vesicles. In the absence of lipids, a decrease in the overall intensity of fluorescence is observed, consistent with aggregation of the protein that eventually lead to the appearance of a precipitate. In the presence of lipid vesicles, a blue shift of the fluorescence maximum is observed which was consistent with a lack of aggregation, confirming that divalent cations trigger membrane insertion or association and ruling out any interference of protein aggregation in our membrane insertion assay (Figure S2). To confirm this interaction with lipid bilayers, fluorescence microscopy images were taken in mixtures of GFP-labelled CLIC1 and giant unilamellar vesicles (GUVs) labelled with Nile red dye. While in the absence of divalent cations no co-localisation of CLIC1 and vesicles was found

membrane fraction of *E. coli* to show that membrane bound CLIC1 is in a reduced state. We demonstrate that CLIC1 exists in an equilibrium between monomers, dimers and higher-order oligomers, and that oligomerisation of CLIC1 is required for membrane insertion. Finally, we use membrane binding assays to show that divalent cations enhance CLIC1 membrane insertion, and fluorescence microscopy and chloride efflux assays to confirm that 2+ cation-triggered membrane insertion results in the formation of active chloride channels.

RESULTS

Membrane insertion is not driven by oxidation.

CLIC1 has previously been successfully expressed in *E. coli*, purified and assayed for chloride conductance (1). To assess if recombinant CLIC1 is able to insert in *E. coli* membranes, we expressed a C-terminal GFP tagged construct in *E. coli* and isolated both the cytosolic and membrane fractions. GFP fluorescence measurements for both the soluble fraction and membranes resuspended in similar volumes indicate that the majority of recombinant CLIC1 inserts in the *E. coli* membrane (Figure 1A). CLIC1 is a human protein, but it has been observed to possess chloride efflux activity in mixtures of lipids containing Phosphatidyl Serine (PS) (4). Given the high proportion of PS lipids in *E. coli* membranes, it is not surprising that CLIC1 can insert into bacterial membranes.

Oxidation has been proposed as the key trigger for membrane insertion, through the formation of a disulphide bridge between the conserved Cysteine 24 to the non-conserved Cysteine 59, although more recent studies do not reconcile with this mechanism (16, 19). To test the oxidation state of both soluble and membrane fractions, ^{15}N-labelled CLIC1 was expressed recombinantly in *E. coli* and purified from the membrane and soluble fractions independently. 2D ^{15}N TROSY or ^{15}N-SOFAST-HMQC experiments were collected for each fraction. ^{1}H and ^{15}N chemical shifts were measured, as the chemical shifts of NH moieties are very sensitive to dynamics, as well as the local and global structure of the protein. Any structural changes resulting from disulphide bond formation would have a big impact in the chemical shifts of a large subset of NH resonances. An overlay of spectra from both fractions shows that the CLIC1 proteins they contain are nearly indistinguishable (Figure 1B), indicating that both forms are in the same oxidation state. Reduction of both samples with 5 mM DTT did not cause significant alterations

(Figure 2C), addition of Zn^{2+} resulted in complete co-localisation of CLIC1 and the GUVs (Figure 2C and Figure S3A,B). Ca^{2+} ions also promote CLIC1 membrane association, with a lower level of co-localisation (Figure 2C and Figure S3C,D).

To test if membrane bound CLIC1 possess chloride transport properties, chloride efflux was recorded upon addition of Valinomycin using CLIC reconstituted in asolectin vesicles in the presence of Zn^{2+} and Ca^{2+}. While CLIC1 shows chloride efflux activity in the presence of Zn^{2+} (Figure 2B) or Ca^{2+} (Figure S4), incubation with EDTA leads to the complete repression of chloride efflux, confirming that efflux observed with divalent cations is due to the formation of active CLIC1 channels.

We sought to examine the influence of the increase of these metal cations on mammalian cell lines in the presence of CLIC1 and whether *in vivo*, CLIC1 would localise to the plasma or internal membranes. To investigate this, we stained endogenous CLIC1 in HeLa cells with CLIC1-specific antibodies, and treated with 5 mM extracellular Ca^{2+} or 10μM Ionomycin to increase the intracellular Ca^{2+} concentrations. The intracellular calcium levels were monitored using a Fluo4 reporter system. A moderate increase of intracellular Ca^{2+} levels could be observed upon stimulation with extracellular Ca^{2+}, and a marked increase was found upon stimulation with Ionomycin (Figure S5). Fluorescence microscopy demonstrated that CLIC1 localisation changes in HeLa cells upon increasing intracellular calcium levels (Figure 4 and Figure S6). Control cells with no addition of Ca^{2+} show a cytoplasmic localisation of CLIC1 with little observable membrane localisation. Contrastingly, an increase in the intracellular Ca^{2+} levels results in CLIC1 re-localisation to internal membranes and the plasma membrane and a notable decrease of CLIC1 concentration in the cytoplasm, demonstrating the effect of 2+ metal cations on CLIC1 localisation in cells. Together with our previous findings, these images show that metal cations are imperative to CLIC1's mechanism of insertion into the membrane and control of where it is localised.

Dynamics of CLIC1 in solution shows oligomerization in equilibrium.

The formation of the CLIC1 channel has been shown to involve oligomerisation in the membrane to large complexes containing six to eight subunits (20). In light of this, we explored if CLIC1 oligomerisation also occurs in solution, and if it was modulated by divalent cation binding. Size exclusion chromatography (SEC) in reducing and not-reducing conditions indicates the presence of at least three species with different molecular weight and some minor high-order

oligomers that are not dependent on the formation of disulphide bonds (Figure 4 and S7). To assess the stability of the monomers and oligomers both species was then subjected to a second SEC step. Again, two peaks were obtained, indicating that CLIC1 exists in a non-covalent equilibrium between the two species (Figure 4A). This was confirmed by multiangle light scattering (MALS). SEC-MALS analysis indicates that the main peaks correspond to monomeric, dimeric and tetrameric species. Treatment with Zn^{2+} resulted in strong interactions with the Superdex200 matrix, and no elution peak could be detected.

CLIC1 samples were also subjected to interferometric scattering mass photometry (iSCAMS). Due to the limit of detection being in the range of 40KDa no monomers could be observed, and only dimers and tetramers and hexamers were detected (Figure 4B). Treatment with equimolar concentrations of Zn^{2+} did not significantly alter the equilibrium between oligomeric species in solution, ruling out that CLIC1 oligomerisation occurs as a consequence of divalent cation activation (Figure 4C). To study the oligomeric state of CLIC1 in the membrane bound form, soluble CLIC1 was incubated with asolectin vesicles in the presence of Zn^{2+}, and the lipid fraction was treated with SMAs to form nano-discs. Mass photometry measurements with empty and CLIC1 containing discs indicated a shift in the average mass of around 100KDa, consistent with a tetrameric assembly in the chloride channel state in nano-discs (Figure 4D-E). A similar shift is observed upon incubation of empty nano-discs with 1μM Zn^{2+}.

DISCUSSION

A model for CLIC1 membrane insertion

Combining our data we can propose a new mechanism of CLIC1 membrane insertion (Figure 5) whereby soluble CLIC1 exists as a mixture of oligomeric states, mainly monomers, dimers and tetramers, exploring the oligomeric state of the membrane-bound form. Upon intracellular Ca^{2+} release (or release of other divalent cations), CLIC1 alters it structure likely exposing a hydrophobic segment and inserts in the membrane in a tetrameric assembly, forming active chloride channels. The propensity to oligomerise in solution, exploring the same tetrameric association than in the membrane bound form, contributes to diminish the entropic penalty of this assembly. CLIC1 binding to divalent cations, on the other hand, does not contribute to the oligomerisation process, and likely contribute to the exposure of a hydrophobic region on the N-terminus of the protein. Previous work (20) using FRET and oxidation suggested an oligomeric

model comprising hexamers or octamers. While the formation of SMALPs could impact the oligomeric state of the chloride channel, the direct detection of mass by interferometric scattering mass spectrometry on native, unoxidized CLIC1 prepared inserting CLIC1 in vesicles or directly in SMALPs give us confidence in the validity of our measurements

While Zn^{2+} triggers a more pronounced insertion of CLIC1 in the membrane than Ca^{2+}, a rise in intracellular Ca^{2+} is sufficient for CLIC1 re-localisation to the membrane. An increase in the concentration of both cations has been linked upstream and downstream of the ROS signalling pathway (21, 22), explaining why CLIC activity has previously been related to ROS production and oxidative stress. Further work is required to address this cation selectivity, but one could hypothesise that maximal membrane insertion of CLIC1 could be detrimental for the cells. Ca^{2+} on the other hand would enable a better regulated equilibrium between soluble and membrane bound CLIC1.

Calcium has been related to the membrane insertion properties of proteins of the annexin family (23), as well as the E1 membrane protein of rubella virus (24) and the amyloidogenic peptide amylin (25), promoting the interactions of the soluble forms of these proteins with negatively charged lipids. The extract of soy bean lipids asolectin, which is rich in the lipid classes PE, PC and the negatively charged PI, has been shown to promote maximal CLIC1 chloride efflux activity (4), supporting the role of divalent cations in CLIC1 membrane insertion. Annexin membrane association is expected to occur due to the exposure of an otherwise buried amphipathic segment upon binding to calcium ions. CLIC1 contains a region (residues 24-41) with moderate hydrophobicity and a moderate hydrophobic moment that could, in a similar mechanism, detach from the protein's globular structure upon divalent cation binding, become exposed to the solvent and mediate association with the membranes, likely forming a helix. The hydrophobicity of this segment would also explain the aggregation of the protein at higher concentrations of calcium and zinc ions in the absence of lipids. Interestingly, the same region in the structurally homologous Glutathione S-transferase is not hydrophobic, suggesting that this helix plays a different role in the CLIC family.

While the structural rearrangements involved in this process are not yet fully understood, the molecular switch between the soluble and membrane bound forms and the changes in

oligomerisation state required to generate the chloride channel assembly are now elucidated. This provides a clear mechanism for this unusual and clinically important channel formation process.

METHODS

Protein Expression and Purification

The Human CLIC1 gene (clone HsCD00338210 from the Plasmid service at HMS) was cloned into a pASG vector (IBA) containing an N-terminal twin strep tag and into a pWaldo (26) vector containing a C-terminal GFP. CLIC1 was expressed recombinantly in the C43 *E.coli* strain (Lucigen). The cells were lysed by sonication, and the membrane and soluble fractions were separated by ultracentrifugation at 117734 g. Membrane-bound CLIC1 can be extracted using a mixture of 1% DDM (Glycon) and 1% Triton X-100. Both fractions were purified separately in the absence of any detergent using affinity chromatography with a Strep-Tactin XT column and a subsequent step of gel filtration using a Superdex200 Increase column (GE) in either 20 mM HEPES buffer with 20 mM NaCl at pH 7.4 or 20 mM Potassium Phosphate buffer with 20 mM NaCl at pH 7.4. SEC-MALS experiments were run in similar conditions injecting 5 mg/mL CLIC1 samples.

NMR Spectroscopy

Purified ^{15}N-labelled CLIC1 from both the membrane and soluble fractions were subjected to ^{15}N-SoFast HMQC(27) or BEST ^{15}N-Trosy experiments (28) at 30°C on a Bruker Avance3 spectrometer operating at a ^{1}H frequency of 600 MHz or 800 MHz equipped with a TCI-P cryo-probe. High-field spectra were collected at the MRC Biomedical NMR Centre. Spectra were uniformly collected with 256 increments in the ^{15}N dimension.

Fluorescence Assays

Asolectin, a lipid extract from soybean, was solubilised in chloroform, dried under a stream of nitrogen and solubilised in HEPES or in phosphate buffer. 10 μM CLIC1 was incubated at 30 °C with 3 mM Asolectin lipids and was treated with 2 mM $ZnCl_2$ or $CaCl_2$ or left untreated, all in 50 mM HEPES 50 mM NaCl pH 7.4 buffer, or with H_2O_2 in phosphate buffer. Intrinsic protein fluorescence was recorded by excitation at 280 nm and emission was measured between wavelengths of 300 nm to 400 nm on a Varian Cary Eclipse fluorimeter, and between 400 to 500

nm with an excitation of 395 nm for the GFP-labelled samples. The samples were then spun at 208000 g for 30 minutes in an ultracentrifuge at 25 °C. Immediately after centrifugation, the soluble fraction was separated from the membrane pellet and the pellet was resuspended to similar volume as the supernatant. Tryptophan fluorescence was then carried out with the same methodology as described above for both the soluble and membrane protein fractions. All fluorescence data was normalised with subtraction of any background buffer or lipids.

Chloride Efflux Assays

CLIC1 chloride channel activity was assessed using the chloride selective electrode assay described previously (4). Unilamellar Asolectin vesicles were prepared at 50 mg/mL in 200 mM KCl, 50 mM HEPES (pH 7.4). CLIC1 protein at 11 μM final concentration was mixed with the vesicles, incubated during 5 minutes and then 1 mM $Ca(OH)_2$ or 1 mM $ZnSO_4$ was added to a 2.5 mL final volume mixture and incubated again for 10 minutes. The lipid mixture was then applied to a PD-10 desalting column previously equilibrated in 400 mM Sucrose, 50 mM HEPES (pH 7.4) and collected in 3.5 mL of the same buffer. 500 μL of the lipid mixture were then added to a cup with 4 mL of 400 mM Sucrose, 50 mM HEPES, 10 μM KCl (pH 7.4) and the free chloride concentration was continuously monitored. 60 seconds after the addition of the lipid mix, 10 μM Valinomycin in ethanol was added and 60 seconds later, 1% TRITON X-100 was also added to release the remaining intra-vesicular chloride.

Fluorescence Microscopy

Giant unilamellar vesicle formation was carried out using a protocol adapted from (29, 30). An Asolectin lipid stock was prepared in 50 mM HEPES, 50 mM NaCl pH 7.4 buffer. 2 μl/cm^2 of 1 mg/ml lipid mixed with 1 mM Nile red lipophilic stain (ACROS Organic) was applied to two ITO slides and dried under vacuum for 2 hours. 100 mM Sucrose, 1 mM HEPES pH 7.4 buffer was used to rehydrate the lipids in the described chamber. 10 Hz frequency sine waves at 1.5 V were applied to the chamber for 2 hours. Liposomes were recovered and diluted into 100 mM glucose, 1 mM HEPES, pH 7.2 buffer. For all four assays 90 nM CLIC1-GFP was incubated with the GUVs with either 0.5 mM $ZnCl_2$, 0.5 mM $CaCl_2$, or were left untreated and incubation at room temperature for ten minutes followed. Microscopy for each assay was performed in an 8 well Lab-

Tek Borosilicate Coverglass system (Nun) with a Zeiss LSM-880 confocal microscope using 488 nm and 594 nm lasers. All images were processed with Zen Black software.

HeLa cells were kindly provided by Chris Toseland laboratory, University of Kent. HeLas were maintained in DMEM media supplemented with 10% FBS and 1% Penicillin/Streptomycin at 37°C, 95% humidity and 5% CO_2.

For immunofluorescence assays HeLa cells were seeded into 24 well plates onto sterile microscopy slides for next day treatment. 24 hours post seeding cells were washed with Tris- buffered saline (TBS), transferred to phosphate free media and treated with 5 mM $CaCl_2$ or 10 μM ionomycin as required. Fixation with 4% formaldehyde for 15 minutes was carried out at two hours post treatment. The cells were then washed and permeabilised for 10 minutes with 0.1% Triton in TBS and washed twice with TBS to remove any detergent. The cells were then stained with CellMask Deep Red plasma membrane stain (Invitrogen) at 1.5X concentration for 15 minutes. Following a TBS wash step the cells were blocked at room temperature with 2% BSA for 1 hour. Primary incubation was carried out overnight at 4 °C with a 1:50 dilution of monoclonal mouse CLIC1 antibody (Santa Cruz Biotechnology, clone 356.1). After primary incubation, 3 wash steps were carried out, prior to 1 hour incubation with secondary antibody at a 1:1000 dilution (Alexa Fluor 488 donkey anti-mouse, Life Technologies). A further 3 washes followed, then nucleus staining with NucBlu Live Cell Stain (Invitrogen) for 20 minutes. The slides were washed a final time and mounted with ProLong Gold Antifade (Invitrogen). All microscopy slides were viewed with a Zeiss LSM-880 confocal microscope using 405 nm, 488 nm, 633 nm lasers. All images were processed with Zen Black and Zen Blue software.

The fluo4 experiment was carried out from the same HeLa stock. The cells were seeded into 96 well plates and 24 hours later were treated with identical $CaCl_2$ or ionomycin concentrations to the immunofluorescence assay, to verify intracellular calcium levels. Fluo-4 Direct (Invitrogen) was added to the cells at 1X dilution according to manufacturers' protocol and visualised using a LS620 Etaluma microscope at the same time point as CLIC1 assay cells were fixed. Contrast and brightness were adjusted equally for all images and pseudo colouring was applied for intensity reading, using ImageJ.

Mass Photometry

10μL of the protein/nanodisc was applied to 10 μL buffer on a cover slip resulting in a final concertation of 100nM. The data was collected on a Refeyn OneMP (Refeyn Ltd, UK) mass photometry system. Movies were acquired for 60 seconds. The mass was calculated using a standard protein calibration curve.

ACKNOWLEDGEMENTS

We thank Dr N. Fili and Dr. J. Rossman for help with confocal imaging, Dr C. Toseland for providing HeLa cells, and Dr G.S. Thompson and Dr. D.A.I. Mavridou for feedback on the manuscript. We thank Refeyn Ltd for enabling us to collect our mass photometry data. We acknowledge the use of the MRC Biomedical NMR Centre, which is supported by Cancer Research UK (FC001029), the UK Medical Research Council (FC001029), and the Wellcome Trust (FC001029), via the Francis Crick Institute. We acknowledge support from the Wellcome Trust Seed Award (207743/Z/17/Z).

CONTRIBUTIONS

JLOR, LV and ACH designed experiments. LV performed NMR data acquisition, fluorescence assays and chloride efflux measurements. ACH performed fluorescence assays, GUV experiments and cell imaging. EMC collected the mass photometry experiments. DC provided assistance with cell imaging experiments. JLOR, LV and ACH prepared figures. JLOR supervised the project and prepared the manuscript. JLOR, LV, ACH and DC edited the manuscript. LV and ACH contributed equally to the work.

COMPETING INTERESTS

The authors declare no competing interests.

REFERENCES

1. Tulk BM, Schlesinger PH, Kapadia SA, Edwards JC (2000) CLIC-1 Functions as a Chloride Channel When Expressed and Purified from Bacteria. *Journal of Biological Chemistry* 275(35):26986–26993.

2. Valenzuela SM, et al. (1997) Molecular cloning and expression of a chloride ion channel of cell nuclei. *Journal of Biological Chemistry* 272(19):12575–12582.

3. Tulk BM, Schlesinger PH, Kapadia SA, Edwards JC (2000) CLIC-1 functions as a chloride channel when expressed and purified from bacteria. *Journal of Biological Chemistry* 275(35):26986–26993.

4. Tulk BM, Kapadia S, Edwards JC (2002) CLIC1 inserts from the aqueous phase into phospholipid membranes, where it functions as an anion channel. *American Journal of Physiology - Cell Physiology* 282(5):C1103–C1112.

5. Averaimo S, Gritti M, Barini E, Gasparini L, Mazzanti M (2014) CLIC1 functional expression is required for cAMP-induced neurite elongation in post-natal mouse retinal ganglion cells. *J Neurochem* 131(4):444–456.

6. Wang W, et al. (2011) The expression and clinical significance of CLIC1 and HSP27 in lung adenocarcinoma. *Tumour Biol* 32(6):1199–1208.

7. Valenzuela SM, et al. (2000) The nuclear chloride ion channel NCC27 is involved in regulation of the cell cycle. *J Physiol (Lond)* 529 Pt 3(3):541–552.

8. Tung JJ, Kitajewski J (2010) Chloride intracellular channel 1 functions in endothelial cell growth and migration. *Journal of Angiogenesis Research* 2(1):23.

9. Tian Y, Guan Y, Jia Y, Meng Q, Yang J (2014) Chloride intracellular channel 1 regulates prostate cancer cell proliferation and migration through the MAPK/ERK pathway. *Cancer Biother Radiopharm* 29(8):339–344.

10. Zhao W, Lu M, Zhang Q (2015) Chloride intracellular channel 1 regulates migration and invasion in gastric cancer by triggering the ROS-mediated p38 MAPK signaling pathway. *Mol Med Rep* 12(6):8041–8047.

11. Zhang J, et al. (2015) Clic1 plays a role in mouse hepatocarcinoma via modulating Annexin A7 and Gelsolin in vitro and in vivo. *Biomed Pharmacother* 69:416–419.

12. Gritti M, et al. (2014) Metformin repositioning as antitumoral agent: selective antiproliferative effects in human glioblastoma stem cells, via inhibition of CLIC1-mediated ion current. *Oncotarget* 5(22):11252–11268.

13. Setti M, et al. (2015) Extracellular vesicle-mediated transfer of CLIC1 protein is a novel mechanism for the regulation of glioblastoma growth. *Oncotarget* 6(31):31413–31427.

14. Littler DR, et al. (2004) The intracellular chloride ion channel protein CLIC1 undergoes a redox-controlled structural transition. *Journal of Biological Chemistry* 279(10):9298–9305.

15. Goodchild SC, et al. (2009) Oxidation promotes insertion of the CLIC1 chloride intracellular channel into the membrane. *Eur Biophys J* 39(1):129–138.

16. Singh H, Ashley RH (2006) Redox Regulation of CLIC1 by Cysteine Residues Associated with the Putative Channel Pore. *Biophys J* 90(5):1628–1638.

17. Fanucchi S, Adamson RJ, Dirr H (2008) Formation of an Unfolding Intermediate State of Soluble Chloride Intracellular Channel Protein CLIC1 at Acidic pH†. *Biochemistry* 47(44):11674–11681.

18. Stoychev SH, et al. (2009) Structural Dynamics of Soluble Chloride Intracellular Channel Protein CLIC1 Examined by Amide Hydrogen−Deuterium Exchange Mass Spectrometry. *Biochemistry* 48(35):8413–8421.

19. Hossain KR, Khamici Al H, Holt SA, Valenzuela SM (2016) Cholesterol Promotes Interaction of the Protein CLIC1 with Phospholipid Monolayers at the Air-Water Interface. *Membranes (Basel)* 6(1):15.

20. Goodchild SC, Angstmann CN, Breit SN, Curmi PMG, Brown LJ (2011) Transmembrane Extension and Oligomerization of the CLIC1 Chloride Intracellular Channel Protein upon Membrane Interaction. *Biochemistry* 50(50):1–9.

21. Slepchenko KG, Lu Q, Li YV (2017) Cross talk between increased intracellular zinc (Zn2+) and accumulation of reactive oxygen species in chemical ischemia. *American Journal of Physiology - Cell Physiology* 313(4):C448–C459.

22. Görlach A, Bertram K, Hudecova S, Krizanova O (2015) Calcium and ROS: A mutual interplay. *Redox Biol* 6:260–271.

23. Rosengarth A, Luecke H (2003) A calcium-driven conformational switch of the N-terminal and core domains of annexin A1. *Journal of Molecular Biology* 326(5):1317–1325.

24. Dubé M, Etienne L, Fels M, Kielian M (2016) Calcium-Dependent Rubella Virus Fusion Occurs in Early Endosomes. *J Virol* 90(14):6303–6313.

25. Sciacca MFM, et al. (2013) Cations as Switches of Amyloid-Mediated Membrane Disruption Mechanisms: Calcium and IAPP. *Biophys J* 104(1):173–184.

26. Drew DE, Heijne von G, Nordlund P, de Gier JW (2001) Green fluorescent protein as an indicator to monitor membrane protein overexpression in Escherichia coli. *FEBS Lett* 507(2):220–224.

27. Schanda P, Kupče Ē, Brutscher B (2005) SOFAST-HMQC Experiments for Recording Two-dimensional Deteronuclear Correlation Spectra of Proteins within a Few Seconds. *J Biomol NMR* 33(4):199–211.

28. Schanda P, Van Melckebeke H, Brutscher B (2006) Speeding Up Three-Dimensional Protein NMR Experiments to a Few Minutes. *J Am Chem Soc* 128(28):9042–9043.

29. Veatch SL (2007) Electro-formation and fluorescence microscopy of giant vesicles with coexisting liquid phases. *Methods Mol Biol* 398(1):59–72.

30. Manley S, Gordon VD (2008) Making giant unilamellar vesicles via hydration of a lipid film. *Curr Protoc Cell Biol* Chapter 24(1):Unit 24.3–24.3.13.

FIGURES

Figure 1. CLIC1 membrane insertion in *E. coli* is not driven by oxidation. (A) - Quantification of CLIC1 extracted from the membrane (green) or the soluble fraction (red)**.** (B) – Overlay of ^{15}N Trosy HSQC or SoFAST HMQC spectra of CLIC1 extracted and purified from the *E. coli* membrane fraction (green), or cytosol (red) and oxidised with 50 mM H_2O_2 (black).

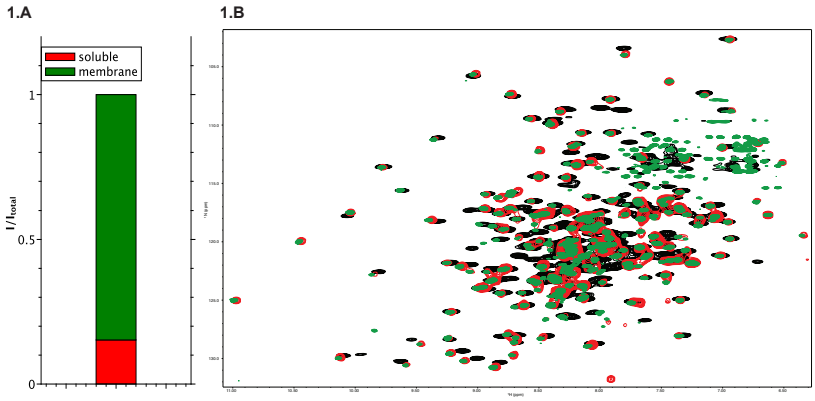

Figure 2. Divalent cations trigger CLIC1 membrane insertion. A - Native tryptophan fluorescence emission spectra of the membrane fraction of asolectin samples incubated with CLIC1 in the presence of H_2O_2 (magenta), no divalent cations (black), Ca^{2+} (blue), Zn^{2+} (red) and Mg^{2+} (green). B - CLIC1 chloride conductance monitored in Asolectin vesicles in presence of Zn^{2+} (blue) or EDTA (red). A control experiment without the addition of CLIC1 is represented in black. The first arrow indicate the addition of Valinomycin, and the second arrow indicates the addition of Triton X-100. C – Fluorescent microscopy images of Asolectin GUVs labelled with Nile red dye incubated with GFP-labelled CLIC1 in the absence of metals (top) and in the presence of 500 µM of Zn^{2+} (middle) or Ca^{2+} (bottom). The left panel shows images exciting Nile red, and the left panel shows images exciting GFP.

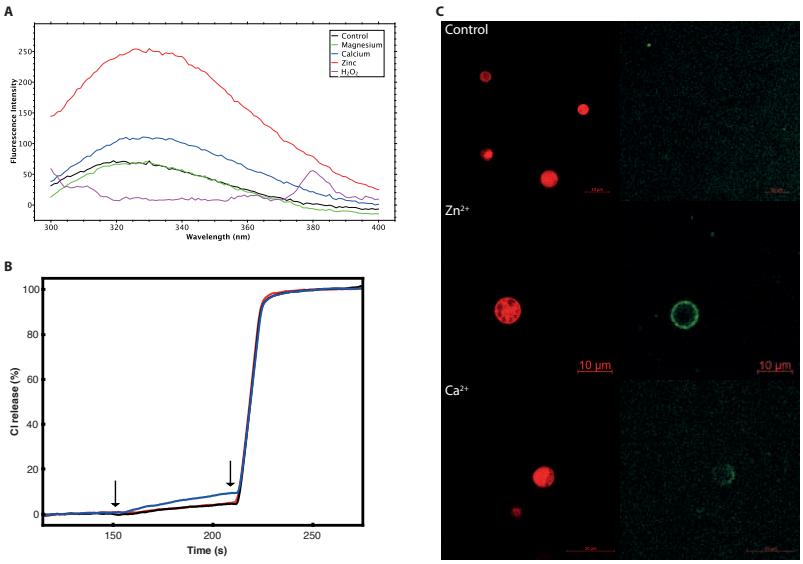

Figure 3. Ca^{2+} driven re-localisation of CLIC1 in HeLa cells. Fluorescence microscopy images of HeLa cells stained with a CLIC1 antibody (green), a membrane marker (red) and DAPI (blue) in the absence (A-D) and presence (E-H) of 5 mM Ca^{2+} in the media or upon treatment with 10 μM Ionomycin (I-L). Images in D, H and L show a merge of the three different channels for the three conditions.

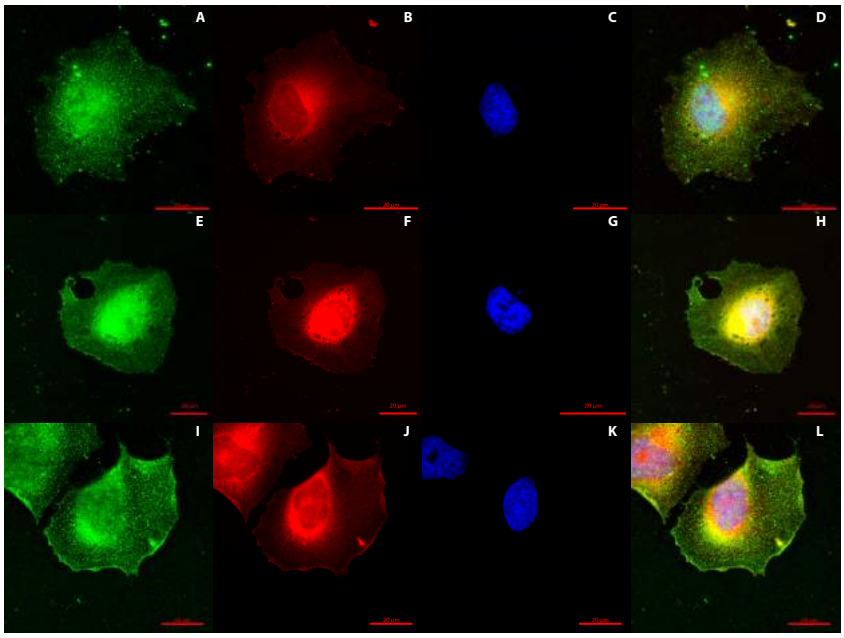

Figure 4. CLIC1 oligomeric states in solution and in the chloride channel form. SEC-MALS traces of non-treated CLIC1 (black). CLIC1 samples corresponding to the dimeric form were subjected for a second SEC-MALS run (red). The molecular weights calculated for the monomer, dimer and tetramer peaks are shown in blue. B,C – Mass Photometry histograms for 100nM CLIC1 samples in the absence and presence of an equimolecular concentration of Zn^{2+}. D,E – Mass Photometry histograms of empty and CLIC1-containing nanodiscs.

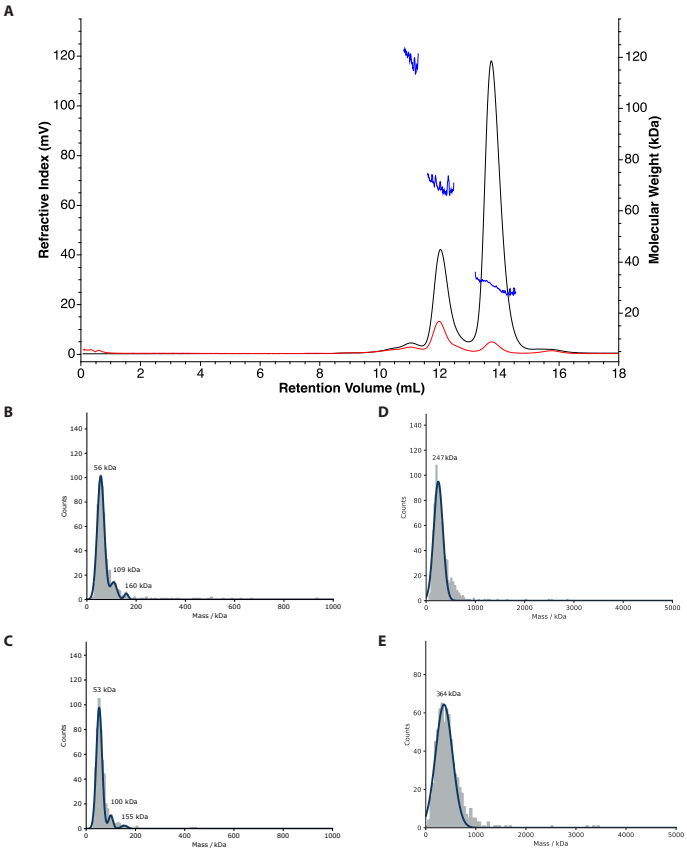

Figure 5. A model of the membrane insertion mechanism of CLIC1. Cytosolic CLIC1 exists in solution (Structural model from PDB 1k0m). With an increase in the intracellular Ca^{2+} (or Zn^{2+}) levels, CLIC1 changes its structure, associates and insert in the membrane, forming active chloride channels.

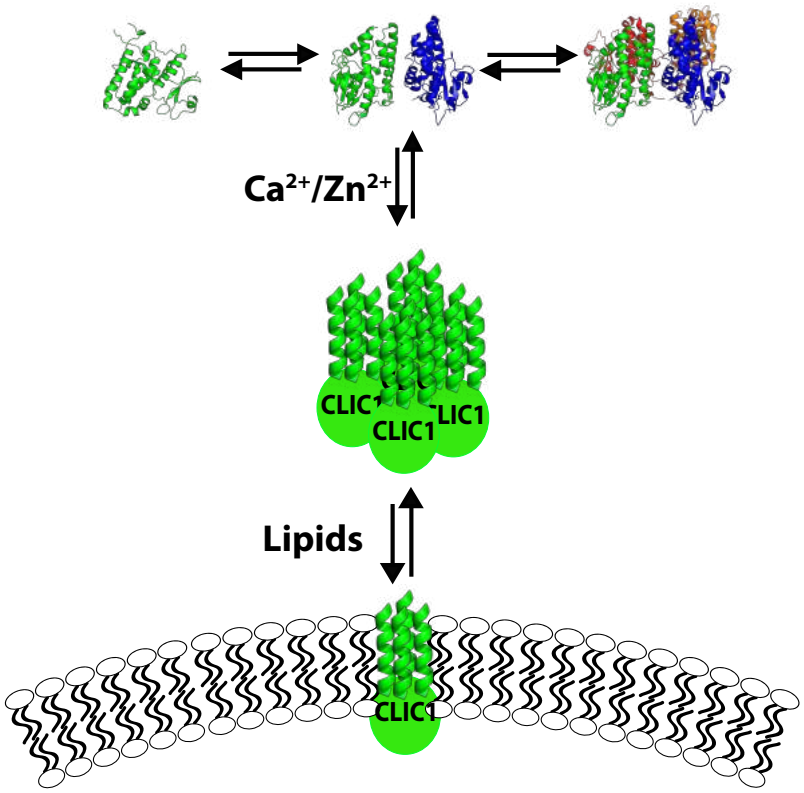

SUPPLEMENTAL FIGURES.

Figure S1. CLIC1 membrane insertion in *E. coli* is not driven by oxidation. Overlay of ^{15}N Trosy HSQC spectra of soluble CLIC1 non-treated (red) and reduced with 5 mM DTT (blue).

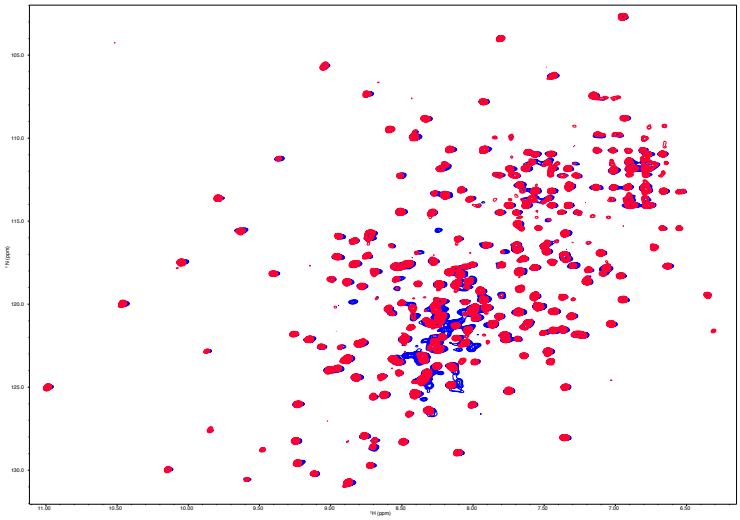

Figure S2. CLIC1 association with lipids in the presence of divalent cations. Native tryptophan fluorescence emission spectra of soluble CLIC1 (black) and the membrane fractions of CLIC1 incubated with asolectin in the presence of Zn^{2+} (red).

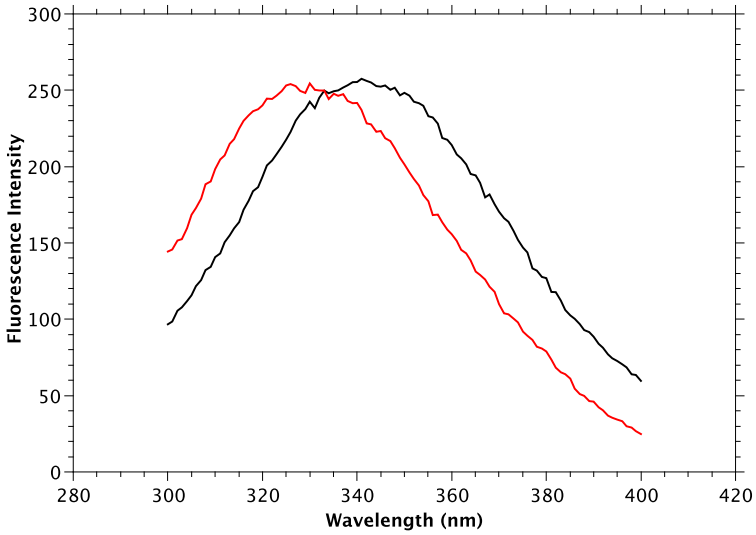

Figure S3. Divalent cations trigger CLIC1 membrane insertion. Widefield fluorescence microscopy images of Asolectin GUVs labelled with Nile red dye incubated with GFP-labelled CLIC1 in the presence of 500 μM of Zn^{2+} (A,B) or Ca^{2+} (C,D). The left panel shows images exciting Nile red, and the left panel shows images exciting GFP.

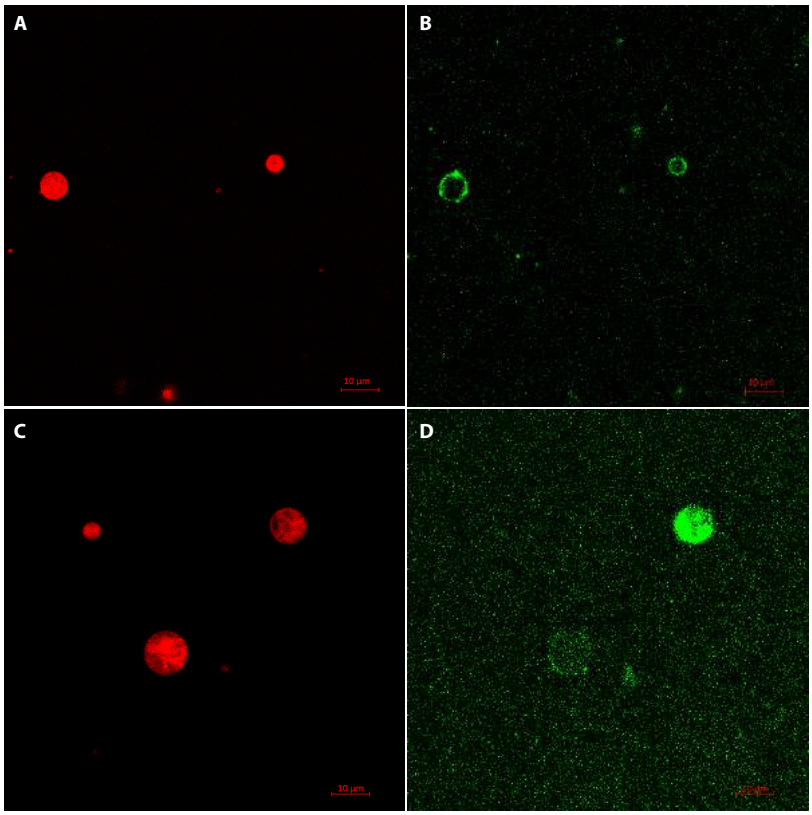

Figure S4. Chloride efflux assay of CLIC1 channel activity. CLIC1 chloride conductance monitored in Asolectin vesicles in presence of Ca^{2+} (blue) or EDTA (red). A control experiment without the addition of CLIC1 is represented in black. The arrows indicate the addition of Valinomycin and Triton X-100.

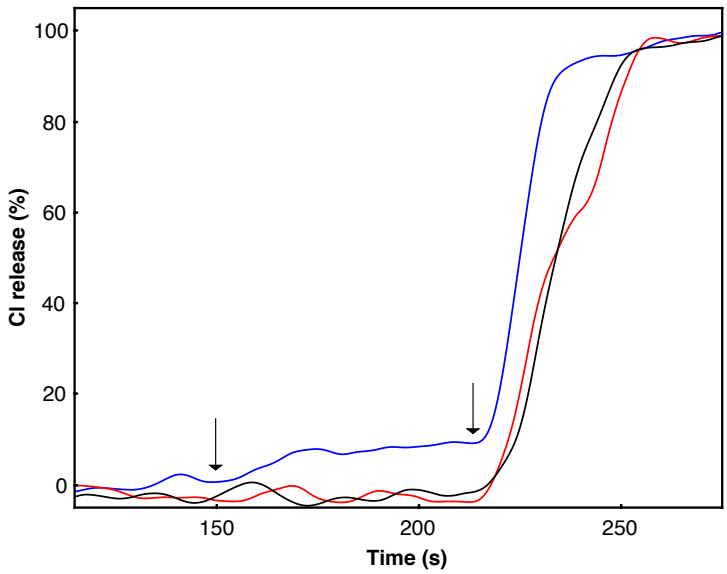

Figure S5. Increasing the intracellular calcium levels in HeLa cells. Intracellular calcium levels monitored following Fluo4 fluorescence (blue) in the absence (A) and presence of 5 mM Ca^{2+} (B) and upon treatment of HeLa cells with 10 μM Ionomycin (C).

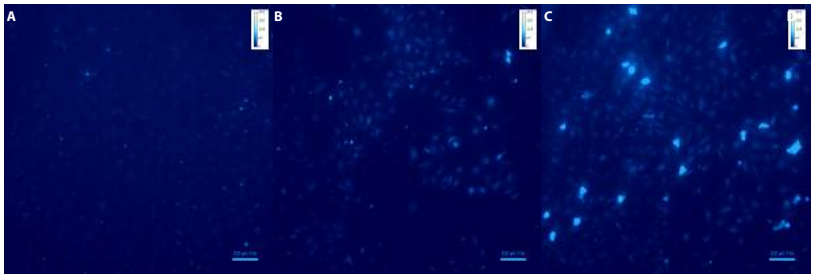

Figure S6. Ca^{2+} driven re-localisation of CLIC1 in HeLa cells. Widefield fluorescence microscopy images indicating Ca^{2+} driven re-localisation of CLIC1 in HeLa cells. Fluorescence microscopy images of HeLa cells stained with a CLIC1 antibody (green), a membrane marker (red) and DAPI (blue) in the absence (A-D) and presence (E-H) of 5 mM Ca^{2+} in the media or upon treatment with 10μM Ionomycin (I-L). Images in D, H and L show a merge of the three different channels for the three conditions.

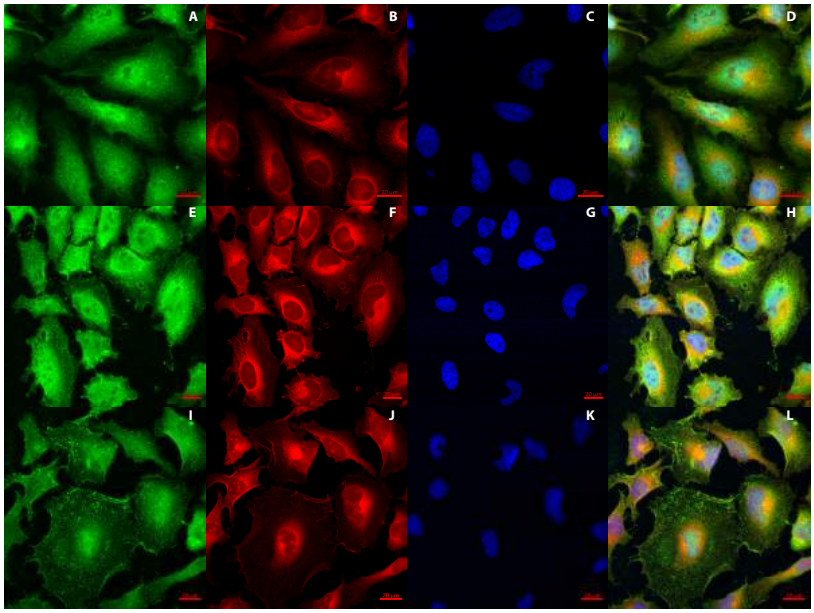

Figure S7. CLIC1 oligomeric species are not dependent on cysteine oxidation. SEC traces of non-reduced (black) and reduced (red) CLIC1.

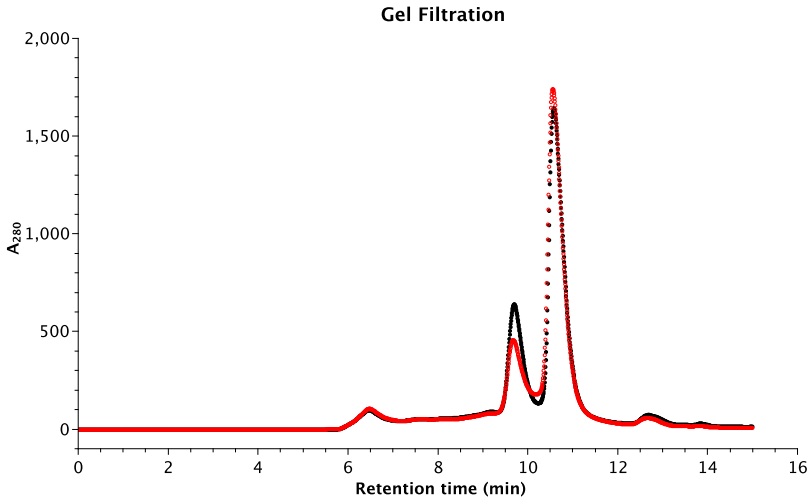

Title: Membrane insertion of soluble CLIC1 into active chloride channels is triggered by Zn^{2+} binding.

Authors: Lorena Varela[&], Alex C. Hendry[&], Joseph Cassar, Ruben Martin-Escolano, Diego Cantoni, John C Edwards, Vahitha Abdul-Salam and Jose L. Ortega-Roldan[*]

Author information:

School of Biosciences. University of Kent. CT2 7NJ. Canterbury. United Kingdom.

[&]Lorena Varela and Alex C. Hendry contributed equally to this work.

[*] corresponding author/Lead contact: j.l.ortega-roldan@kent.ac.uk

Running Title: CLIC1 membrane insertion is triggered by divalent cations.

Keywords: Membrane protein, chloride channel, channel activation, lipid-protein interaction, biophysics.

ABSTRACT

The CLIC protein family displays the unique feature of altering its structure from a soluble form to a membrane-bound chloride channel. CLIC1, a member of this family, is found in the cytoplasm or in internal membranes, with membrane overexpression linked to tumour proliferation. The molecular switch promoting CLIC1 membrane insertion remains unclear. Here, cellular chloride efflux assays and immunofluorescence studies have identified Zn2+ intracellular release as the trigger for CLIC1 activation and membrane relocalisation. Biophysical assays with recombinant CLIC1 confirmed specific binding to Zn2+, inducing membrane association to vesicles and enhancing chloride efflux at low pH. Thus, our results identify Zn^{2+} binding as the molecular switch promoting CLIC1 membrane insertion and activation as a chloride channel.

INTRODUCTION

The Chloride Intracellular Channel (CLIC) family consists of a group of highly homologous human proteins with a striking feature, their ability to change their structure upon activation from a soluble form into a membrane bound chloride channel, translocating from the cytoplasm to intracellular membranes (1, 2). CLIC1 is the best characterised of the CLIC protein family. It is expressed intracellularly in a variety of cell types, being especially abundant in heart and skeletal muscle (2). CLIC1's integral membrane form has been found to be localised mostly in the nuclear membrane, although it is present in the membranes of other organelles and transiently in the plasma membrane. It

has also been shown to function as an active chloride channel in phospholipid vesicles when expressed and purified from bacteria, showing clear single channel properties (3, 4).

CLIC1 has been implicated in the regulation of cell volume, electrical excitability (5), differentiation (6), cell cycle (7) and cell growth and proliferation (8). High CLIC1 expression has been reported in a range of malignant tumours, including prostate (9), gastric (10), lung (6) and liver (11) cancers, with evidence of CLIC1 promoting the spread and growth of glioblastoma cancer stem/progenitor cells (12, 13).

The activity and oncogenic function of CLIC1 is modulated by its equilibrium between the soluble cytosolic form and its membrane bound form. Only CLIC1 in its channel form has been shown to have oncogenic activity, and specific inhibition of the CLIC1 channel halts tumour progression (13). However, to date very little and conflicting information is available for the membrane insertion mechanism, and the structure of the channel form is unknown. In-vitro Oxidation with hydrogen peroxide causes a conformational change due to the formation of a disulphide bond between Cys24 and the non-conserved Cys59, exposing a hydrophobic patch that promotes the formation of a dimer (14), in a process that has been proposed to lead to membrane insertion (15). However, numerous studies have shown that oxidation does not promote membrane insertion(16); with evidence pointing at pH (17, 18) or cholesterol (19) as the likely activation factors. Thus, long standing inconsistencies in the data surrounding the molecular switch that unusually transforms CLIC1 from its soluble form into a membrane bound channel has prevented further advances in the understanding of CLIC1 function.

In this study, we have explored the membrane insertion activation mechanism of CLIC1. We have discovered the activation of CLIC1 chloride efflux by intracellular Zn^{2+} release in Glioblastoma cells, which also causes CLIC1 relocalisation to the plasma membrane. Finally, in-vitro studies with purified CLIC1 shows Zn^{2+} driven activation of chloride efflux, membrane association, as well as CLIC1 specific binding to both Zn^{2+} and Ca^{2+}.

RESULTS

There isn't yet a clear understanding of the mechanism behind CLIC1 activation and insertion in the membrane. Divalent cation binding, specifically Ca^{2+}, is involved in the membrane interactions of other protein families (REF). Interestingly, the CLIC homologs *exc*-4 and DmCLIC1 both contain a calcium ion bound trapped during the expression and purification process. We therefore sought understand if divalent cations may have a role in CLIC1 activation as a chloride channel.

The effect of divalent cation-driven membrane localisation on the chloride efflux activity of CLIC1 was tested in U87G cells using MQAE as a fluorescent reporter or the intracellular concentration of Cl^-. Ionomycin, an ionophore shown to increase both Ca^{2+} and Zn^{2+} intracellular concentrations, induced a

significant increase of the Cl- efflux that was reversed upon treatment with the Zinc chelator TPEN or with the commonly used CLIC1 inhibitor IAA-94 (Figure 1). Interestingly, TPEN inhibits the chloride conductance of the control cells to a level similar to IAA-94, suggesting the involvement of Zn^{2+} in the activation of CLIC1 chloride efflux activation.

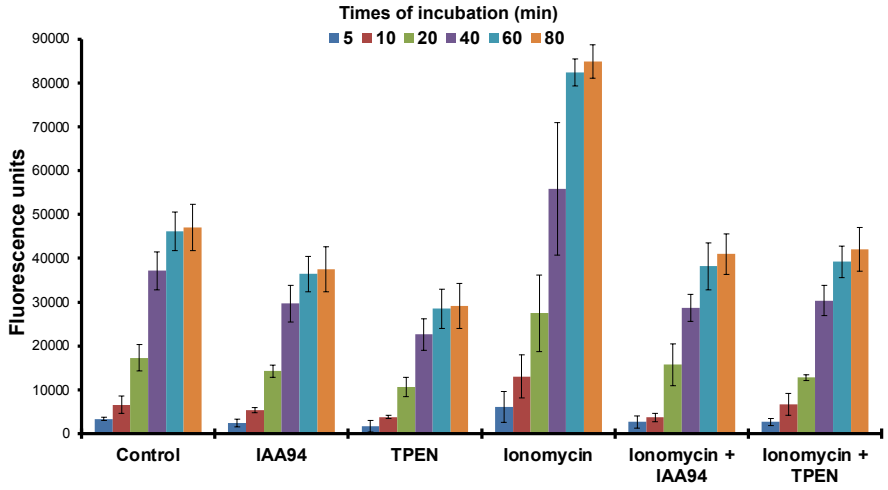

Figure 1. Effect of different treatments on chloride efflux (measured as fluorescence intensity units of the dye MQAE) in MQAE-stained U87 cells exposed to IAA94 (10 µM), TPEN (5 µM) and/Ionomycin (10 µM) for 80 min. Values constitute means of three separate determinations ± standard deviation.

In light of these results, we questioned if Zn^{2+} could trigger CLIC1 membrane relocalisation in cells. Endogenous CLIC1 localisation was monitored in Human Umbilical Vein Endothelial Cells (HUVEC) and Glioblastoma using immunostaining. CLIC1 typically exists in the cytosol in untreated HUVEC cells, and the addition of external $ZnCl_2$ promoted the presence of CLIC1 at the plasma membrane. This effect was reversed with the treatment of TPEN or a chloride channel inhibitor (NPPB)(Figure 2A-D). A similar effect was observed in HeLa cells. Addition of Ionomycin increased the degree of CLIC1 plasma membrane localisation (Figures E-L), in line with our findings in HUVEC cells and confirming that Zn2+ triggers the activation and membrane relocalisation of CLIC1.

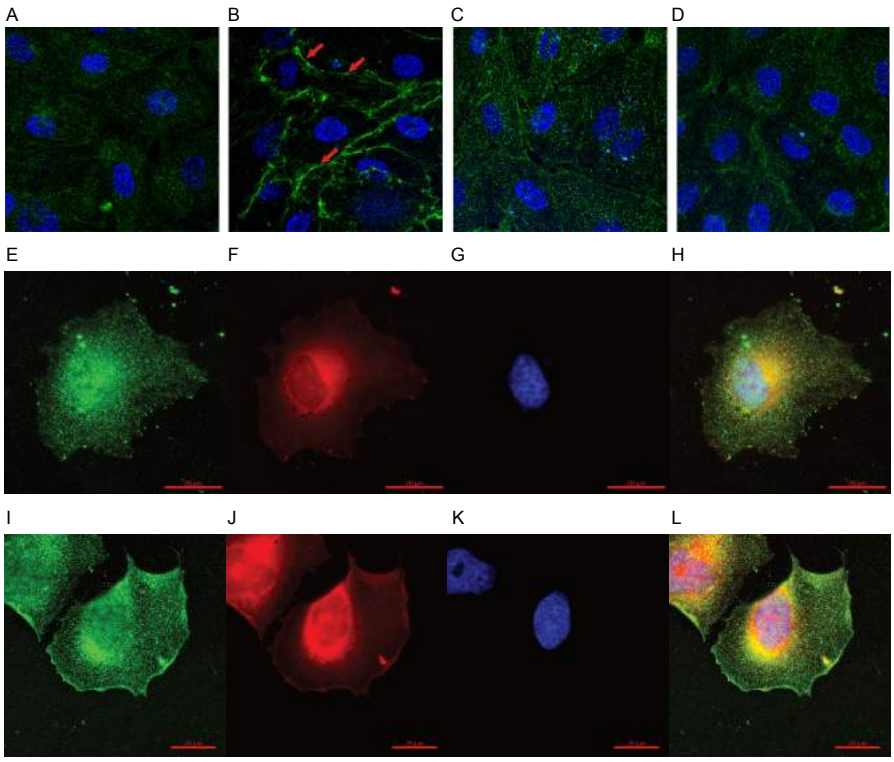

Figure 2: Divalent cations promote membrane insertion. **A-D** - CLIC1 localisation in Human Umbilical Vein Endothelial Cells (HUVEC). HUVECs were either untreated (A) or treated for 3 hours with (B) 10mM ZnCl2, (C) 10mM ZnCl2 with 5mM N,N,N′,N-tetrakis(2-pyridylmethyl) ethylenediamine (TPEN) and (C) 10mM with 10mM 5-nitro-2-(3-phenylpropyl-amino) benzoic acid (NPPB). CLIC1 typically exists in the cytosol and the addition of $ZnCl_2$ promoted the presence of CLIC1 at plasma membrane (shown in red arrows). This effect was reversed with the treatment a zinc chelator (TPEN) or a chloride channel inhibitor (NPPB). **E-L** - Fluorescence microscopy images of HeLa cells stained with a CLIC1 antibody (green), a membrane marker (red) and DAPI (blue) in the absence (E-H) and upon treatment with 10 μM Ionomycin (I-L). Images in H and L show a merge of the three different channels for the three conditions.

Previous studies have indicated the importance of low pH for CLIC1 chloride efflux. To understand the effect of pH and divalent cation biding on CLIC1 chloride efflux properties, chloride efflux was recorded upon addition of Valinomycin using recombinantly expressed CLIC1 reconstituted in asolectin vesicles in the presence and absence of Zn^{2+} at pH 7.4 and 5.5 (Figure 3A). As previously shown, CLIC1 only possess chloride efflux activity at low pH values (Breit reference). While the addition of Zn^{2+} at pH 7.4 had no effect on the chloride efflux rate, equimolar concentrations of Zn^{2+}

significantly increased the chloride efflux at pH 5.5. CLIC1 showed significant chloride efflux activity in vitro at pH 5.5 even in the absence of Zn2+, which we hypothesise is related to the inability to sequester all divalent cations from the media.

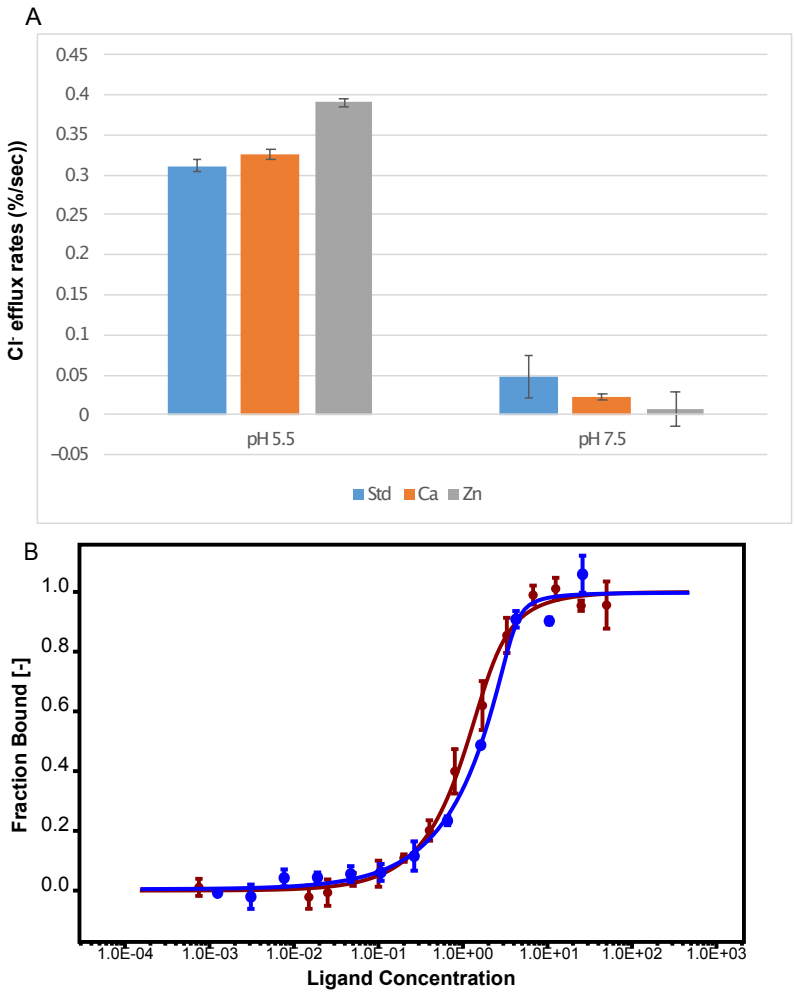

Figure 3. A- Chloride efflux rate of untreated CLIC1 (blue) or CLIC1 treated with 1 molar equivalent of Ca^{2+} (orange) or Zn^{2+} (gray). **B** – MST binding curves of CLIC1 titrations with Ca^{2+} (red) or Zn^{2+} (blue), displaying a Kd of 0.3mM ± XXX..

We subsequently attempted to separate activation of the CLIC1 chloride channel from its insertion in the membrane. To this end, we explored the effect of Zn^{2+} and pH on membrane association on

recombinantly expressed and purified GFP-tagged CLIC1. Fluorescence microscopy images collected in fluorescently labelled giant unilamellar vesicles (GUVs) showed CLIC1 co-localisation in the membrane only in the presence of Zn^{2+} irrespective of the pH value, indicating that Zn^{2+} has a direct effect on CLIC1 triggering its membrane insertion (Figure 4) and identifying pH as a likely activating or gating mechanism of the channel form. Calcium on the other hand only induced partial insertion in the membrane at the same protein and cation concentrations, in agreement with its neglectable effect on CLIC1 chloride efflux (Figure SX).

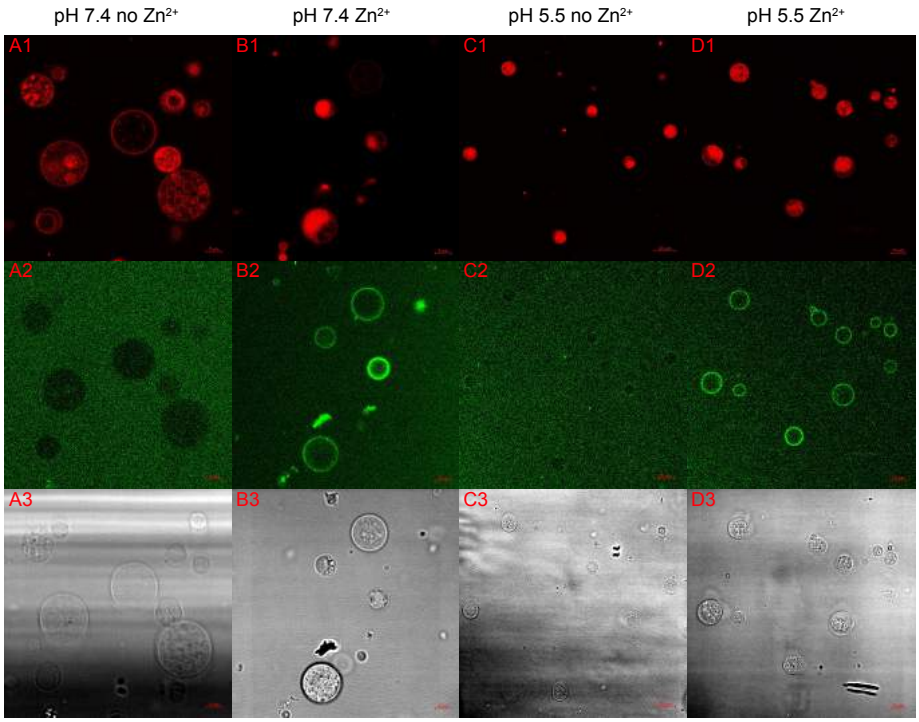

Figure 4. Fluorescent microscopy images of Asolectin. GUVs labelled with Nile red dye incubated with GFP-labeled CLIC1 in giant unilamellar vesicles at pH 7.4 (columns A and B) and pH 5.5 (columns C and D) in the absence (Coluns A and C) and presence (Columns B and D) of Zn^{2+}. Row 1 displays the fluorescence images of lipid. Row 1 displays Red Nile fluorescence, row 2 GFP fluorescence and row 3 shows the brighfield images of the GUVs.

Microscale Thermophoresis (MST) can be used to identify specific divalent cation binding on CLIC1. We used GFP tagged CLIC1 to compare its binding affinities of Ca^{2+} and Zn^{2+} ions in the presence of asolectin vesicles, as CLIC1 can aggregate at molar ratios of Ca^{2+} and Zn^{2+} higher than 1 in the absence of lipids. CLIC1 showed specific binding to both ions, with Zn^{2+} and Ca^{2+}having a similar apparent affinity of 0.3mM (Figure 3B). The higher activation potential of Zn^{2+} over Ca^{2+} must therefore be a result of a higher degree of structural changes resulting from the interaction with Zn^{2+}.

DISCUSSION

A model for CLIC1 membrane insertion

In this study, we demonstrate that CLIC1 binds to Zn^{2+}, promoting membrane insertion in both model membranes and in cellular environment. Once inserted, chloride efflux is only activated at low pH values. Combining our data, we propose a new mechanism of CLIC1 membrane insertion whereby CLIC1 exists in a soluble state, and upon intracellular Zn^{2+} release CLIC1 alters its structure and inserts into the membrane. The channel is only activated at low pH, suggesting either a pH gating mechanism or a conformational rearrangement within the membrane at low pH values. CLIC1 has been shown to regulate phagosomal acidification , supporting the role of pH in the activation of the channel.

An increase in the cellular Zn^{2+} concentration has been linked upstream and downstream of the ROS signalling pathway (21), explaining previous studies on the relationship between CLIC activity with ROS production and oxidative stress. Ionomycin is known to increase both intracellular levels of Zn^{2+} and Ca^{2+}. We show that although ionomycin treatment can result in binding of both Zn^{2+} and Ca^{2+} to CLIC1 with similar affinity, only Zn^{2+} is able to induce membrane association (Figure SX) and chloride efflux (Figure 3A). This is further supported by treatment with zinc chelators (TPEN), that is able to suppress CLIC1 membrane relocalisation.

Divalent cations have been related to the membrane insertion properties of proteins of the annexin family (23), as well as the E1 membrane protein of rubella virus (24) and the amyloidogenic peptide amylin (25), promoting the interactions of the soluble forms of these proteins with negatively charged lipids. The extract of soy bean lipids asolectin, which is rich in the lipid classes Phosphatidylethanolamine (PE), Phosphatidylcholine (PC) and the negatively charged Phosphatidylinositol (PI), has been shown to promote maximal CLIC1 chloride efflux activity (4), supporting the role of divalent cations in CLIC1 membrane insertion. Annexin membrane association is expected to occur due to the exposure of an otherwise buried amphipathic segment upon binding to calcium ions. CLIC1 contains a region (residues 24-41) with moderate hydrophobicity and a moderate hydrophobic moment that could, in a similar mechanism, detach from the protein's globular structure upon divalent cation binding, become exposed to the solvent and mediate association with the membranes, likely forming a helix. The hydrophobicity of this segment would also explain the

aggregation of the protein at higher concentrations of calcium and zinc ions in the absence of lipids. Interestingly, the same region in the structurally homologous Glutathione S-transferase is not hydrophobic, suggesting that this helix plays a different role in the CLIC family.

While the structural rearrangements involved in this process are not yet fully understood, the molecular switch between the soluble and membrane bound forms is now elucidated. This enables, for the first time, the manipulation of CLIC1 localisation in cellular systems and provides a clear mechanism for the channel formation process of this unusual and clinically important protein.

METHODS

Protein Expression and Purification

The Human CLIC1 gene (clone HsCD00338210 from the Plasmid service at HMS) was cloned into a pASG vector (IBA) containing an N-terminal twin strep tag and a TEV cleavage site, and into a pWaldo (26) vector containing a C-terminal GFP and a TEV cleavage site. CLIC1 was expressed recombinantly in the C43 *E.coli* strain (Lucigen). The cells were lysed by sonication, and the membrane and soluble fractions were separated by ultracentrifugation at 117734 g. Membrane-bound CLIC1 can be extracted using a mixture of 1% DDM (Glycon) and 1% Triton X-100, resulting in solutions with CLIC1 soluble form. Both fractions were purified separately in the absence of any detergent using affinity chromatography with a Strep-Tactin XT column. The elutions were pooled and cleaved with TEV protease, and subsequently gel filtrated using a Superdex200 Increase column (GE) in either 20 mM HEPES buffer with 20 mM NaCl at pH 7.4 or 20 mM Potassium Phosphate buffer with 20 mM NaCl at pH 7.4. SEC-MALS experiments were run in similar conditions injecting 5 mg/mL CLIC1 samples.

Chloride efflux assays

U87 cells were maintained in DMEM media supplemented with 10% FBS and 1% Penicillin/Streptomycin at 37°C, 95% humidity and 5% CO_2.

For MQAE (*N*-(Ethoxycarbonylmethyl)-6-Methoxyquinolinium Bromide) (ThermoFisher) assays U87 cells were seeded into dark 96-well microtiter flat-bottom plates at 4×10^4 cells·well^{-1} in 100 µL volumes DMEM media supplemented with 10% FBS and 1% Penicillin/Streptomycin and incubated overnight at 37°C, 95% humidity and 5% CO_2. Cells were then stained with 8 mM MQAE for 2 h (10.1016/S0006-291X(03)01436-0), and subsequently washed three times with PBS. Non-stained cells were also included. A variety of conditions were evaluated after MQAE loading. In conditions where inhibitors were used, these – 5 µM TPEN or 10 µM IAA-94 – were added and incubated for 10 min. Finally, 10 µM ionomycin were added and repetitive fluorescence measurements (every 1 min for 80 min) were initiated immediately using an Omega fluorescence plate reader (excitation, 355 nm;

emission, 460 nm). Three separate wells were used for each group. Mean and standard deviations were calculated for each condition and time.

Chloride Efflux Assays with purified protein.

CLIC1 chloride channel activity was assessed using the chloride selective electrode assay described previously (4). Unilamellar Asolectin vesicles were prepared at 50 mg/mL in 200 mM KCl, 50 mM HEPES (pH 7.4). CLIC1 protein at 11 μM final concentration was mixed with the vesicles, incubated during 5 minutes and then 1 mM $Ca(OH)_2$ or 1 mM $ZnSO_4$ was added to a 2.5 mL final volume mixture and incubated again for 10 minutes. The lipid mixture was then applied to a PD-10 desalting column previously equilibrated in 400 mM Sucrose, 50 mM HEPES (pH 7.4) and collected in 3.5 mL of the same buffer. 500 μL of the lipid mixture were then added to a cup with 4 mL of 400 mM Sucrose, 50 mM HEPES, 10 μM KCl (pH 7.4) and the free chloride concentration was continuously monitored. 60 seconds after the addition of the lipid mix, 10 μM Valinomycin in ethanol was added and 60 seconds later, 1% TRITON X-100 was also added to release the remaining intra-vesicular chloride.

Fluorescence Microscopy

Giant unilamellar vesicle formation was carried out using a protocol adapted from (29, 30). An Asolectin lipid stock was prepared in 50 mM HEPES, 50 mM NaCl pH 7.4 buffer. 2 μl/cm^2 of 1 mg/ml lipid mixed with 1 mM Nile red lipophilic stain (ACROS Organic) was applied to two ITO slides and dried under vacuum for 2 hours. 100 mM Sucrose, 1 mM HEPES pH 7.4 buffer was used to rehydrate the lipids in the described chamber. 10 Hz frequency sine waves at 1.5 V were applied to the chamber for 2 hours. Liposomes were recovered and diluted into 100 mM glucose, 1 mM HEPES, pH 7.2 buffer. For all four assays 90 nM CLIC1-GFP was incubated with the GUVs with either 0.5 mM $ZnCl_2$, 0.5 mM $CaCl_2$, or were left untreated and incubation at room temperature for ten minutes followed. Microscopy for each assay was performed in an 8 well Lab-Tek Borosilicate Coverglass system (Nun) with a Zeiss LSM-880 confocal microscope using 488 nm and 594 nm lasers. All images were processed with Zen Black software.

HeLa cells were kindly provided by Chris Toseland laboratory, University of Kent. HeLa cells were maintained in DMEM media supplemented with 10% FBS and 1% Penicillin/Streptomycin at 37°C, 95% humidity and 5% CO_2.

For immunofluorescence assays HeLa cells were seeded into 24 well plates onto sterile microscopy slides for next day treatment. 24 hours post seeding cells were washed with Tris- buffered saline (TBS), transferred to phosphate free media and treated with 5 mM $CaCl_2$ or 10 μM ionomycin as required. Fixation with 4% formaldehyde for 15 minutes was carried out at two hours post treatment. The cells were then washed and permeabilised for 10 minutes with 0.1% Triton in TBS and washed twice with

TBS to remove any detergent. The cells were then stained with CellMask Deep Red plasma membrane stain (Invitrogen) at 1.5X concentration for 15 minutes. Following a TBS wash step the cells were blocked at room temperature with 2% BSA for 1 hour. Primary incubation was carried out overnight at 4 °C with a 1:50 dilution of monoclonal mouse CLIC1 antibody (Santa Cruz Biotechnology, clone 356.1). After primary incubation, 3 wash steps were carried out, prior to 1 hour incubation with secondary antibody at a 1:1000 dilution (Alexa Fluor 488 donkey anti-mouse, Life Technologies). A further 3 washes followed, then nucleus staining with NucBlu Live Cell Stain (Invitrogen) for 20 minutes. The slides were washed a final time and mounted with ProLong Gold Antifade (Invitrogen). All microscopy slides were viewed with a Zeiss LSM-880 confocal microscope using 405 nm, 488 nm, 633 nm lasers. All images were processed with Zen Black and Zen Blue software.

The fluo4 experiment was carried out from the same HeLa stock. The cells were seeded into 96 well plates and 24 hours later were treated with identical $CaCl_2$ or ionomycin concentrations to the immunofluorescence assay, to verify intracellular calcium levels. Fluo-4 Direct (Invitrogen) was added to the cells at 1X dilution according to manufacturers' protocol and visualised using a LS620 Etaluma microscope at the same time point as CLIC1 assay cells were fixed. Contrast and brightness were adjusted equally for all images and pseudo colouring was applied for intensity reading, using ImageJ.

ACKNOWLEDGEMENTS

We thank Dr N. Fili and Dr. J. Rossman for help with confocal imaging, Dr C. Toseland for providing HeLa cells, and Dr G.S. Thompson and Dr. D.A.I. Mavridou for feedback on the manuscript. VAS is supported by Barts Charity's Rising Star programme. We acknowledge support from the Wellcome Trust Seed Award (207743/Z/17/Z).

CONTRIBUTIONS

JLOR, LV and ACH designed experiments. LV performed protein expression and purification, preliminary biophysical assays and chloride efflux measurements. ACH performed fluorescence assays, GUV experiments and cell imaging. JC measured the MST binding experiments. RME collected the chloride efflux assays in cells. VAS performed fluorescence imaging experiments in HUVEC cells. DC provided assistance with cell imaging experiments at Kent. JLOR, LV and ACH prepared figures. JLOR supervised the project and prepared the manuscript. JLOR, LV and ACH edited the manuscript. LV and ACH contributed equally to the work.

COMPETING INTERESTS

The authors declare no competing interests.

REFERENCES

1. Tulk, B. M., Schlesinger, P. H., Kapadia, S. A., and Edwards, J. C. (2000) CLIC-1 Functions as a Chloride Channel When Expressed and Purified from Bacteria. *Journal of Biological Chemistry*. 275, 26986–26993
2. Valenzuela, S. M., Martin, D. K., Por, S. B., Robbins, J. M., Warton, K., Bootcov, M. R., Schofield, P. R., Campbell, T. J., and Breit, S. N. (1997) Molecular cloning and expression of a chloride ion channel of cell nuclei. *Journal of Biological Chemistry*. 272, 12575–12582
3. Tulk, B. M., Schlesinger, P. H., Kapadia, S. A., and Edwards, J. C. (2000) CLIC-1 functions as a chloride channel when expressed and purified from bacteria. *Journal of Biological Chemistry*. 275, 26986–26993
4. Tulk, B. M., Kapadia, S., and Edwards, J. C. (2002) CLIC1 inserts from the aqueous phase into phospholipid membranes, where it functions as an anion channel. *American Journal of Physiology - Cell Physiology*. 282, C1103–C1112
5. Averaimo, S., Gritti, M., Barini, E., Gasparini, L., and Mazzanti, M. (2014) CLIC1 functional expression is required for cAMP-induced neurite elongation in post-natal mouse retinal ganglion cells. *J. Neurochem.* 131, 444–456
6. Wang, W., Xu, X., Wang, W., Shao, W., Li, L., Yin, W., Xiu, L., Mo, M., Zhao, J., He, Q., and He, J. (2011) The expression and clinical significance of CLIC1 and HSP27 in lung adenocarcinoma. *Tumour Biol.* 32, 1199–1208
7. Valenzuela, S. M., Mazzanti, M., Tonini, R., Qiu, M. R., Warton, K., Musgrove, E. A., Campbell, T. J., and Breit, S. N. (2000) The nuclear chloride ion channel NCC27 is involved in regulation of the cell cycle. *J. Physiol. (Lond.)*. 529 Pt 3, 541–552
8. Tung, J. J., and Kitajewski, J. (2010) Chloride intracellular channel 1 functions in endothelial cell growth and migration. *Journal of Angiogenesis Research*. 2, 23
9. Tian, Y., Guan, Y., Jia, Y., Meng, Q., and Yang, J. (2014) Chloride intracellular channel 1 regulates prostate cancer cell proliferation and migration through the MAPK/ERK pathway. *Cancer Biother. Radiopharm.* 29, 339–344
10. Zhao, W., Lu, M., and Zhang, Q. (2015) Chloride intracellular channel 1 regulates migration and invasion in gastric cancer by triggering the ROS-mediated p38 MAPK signaling pathway. *Mol Med Rep*. 12, 8041–8047
11. Zhang, J., Li, M., Song, M., Chen, W., Mao, J., Song, L., Wei, Y., Huang, Y., and Tang, J. (2015) Clic1 plays a role in mouse hepatocarcinoma via modulating Annexin A7 and Gelsolin in vitro and in vivo. *Biomed. Pharmacother.* 69, 416–419
12. Gritti, M., Würth, R., Angelini, M., Barbieri, F., Peretti, M., Pizzi, E., Pattarozzi, A., Carra, E., Sirito, R., Daga, A., Curmi, P. M. G., Mazzanti, M., and Florio, T. (2014) Metformin repositioning as antitumoral agent: selective antiproliferative effects in human glioblastoma stem cells, via inhibition of CLIC1-mediated ion current. *Oncotarget*. 5, 11252–11268
13. Setti, M., Osti, D., Richichi, C., Ortensi, B., Del Bene, M., Fornasari, L., Beznoussenko, G., Mironov, A., Rappa, G., Cuomo, A., Faretta, M., Bonaldi, T., Lorico, A., and Pelicci, G. (2015) Extracellular vesicle-mediated transfer of CLIC1 protein is a novel mechanism for the regulation of glioblastoma growth. *Oncotarget*. 6, 31413–31427
14. Littler, D. R., Harrop, S. J., Fairlie, W. D., Brown, L. J., Pankhurst, G. J., Pankhurst, S., DeMaere, M. Z., Campbell, T. J., Bauskin, A. R., Tonini, R., Mazzanti, M., Breit,

S. N., and Curmi, P. M. G. (2004) The intracellular chloride ion channel protein CLIC1 undergoes a redox-controlled structural transition. *Journal of Biological Chemistry*. 279, 9298–9305
15. Goodchild, S. C., Howell, M. W., Cordina, N. M., Littler, D. R., Breit, S. N., Curmi, P. M. G., and Brown, L. J. (2009) Oxidation promotes insertion of the CLIC1 chloride intracellular channel into the membrane. *Eur. Biophys. J.* 39, 129–138
16. Singh, H., and Ashley, R. H. (2006) Redox Regulation of CLIC1 by Cysteine Residues Associated with the Putative Channel Pore. *Biophys. J.* 90, 1628–1638
17. Fanucchi, S., Adamson, R. J., and Dirr, H. (2008) Formation of an Unfolding Intermediate State of Soluble Chloride Intracellular Channel Protein CLIC1 at Acidic pH†. *Biochemistry*. 47, 11674–11681
18. Stoychev, S. H., Nathaniel, C., Fanucchi, S., Brock, M., Li, S., Asmus, K., Virgil L Woods, J., and Dirr, H. (2009) Structural Dynamics of Soluble Chloride Intracellular Channel Protein CLIC1 Examined by Amide Hydrogen−Deuterium Exchange Mass Spectrometry. *Biochemistry*. 48, 8413–8421
19. Hossain, K. R., Khamici, Al, H., Holt, S. A., and Valenzuela, S. M. (2016) Cholesterol Promotes Interaction of the Protein CLIC1 with Phospholipid Monolayers at the Air-Water Interface. *Membranes (Basel)*. 6, 15
20. Goodchild, S. C., Angstmann, C. N., Breit, S. N., Curmi, P. M. G., and Brown, L. J. (2011) Transmembrane Extension and Oligomerization of the CLIC1 Chloride Intracellular Channel Protein upon Membrane Interaction. *Biochemistry*. 50, 1–9
21. Slepchenko, K. G., Lu, Q., and Li, Y. V. (2017) Cross talk between increased intracellular zinc (Zn2+) and accumulation of reactive oxygen species in chemical ischemia. *American Journal of Physiology - Cell Physiology*. 313, C448–C459
22. Görlach, A., Bertram, K., Hudecova, S., and Krizanova, O. (2015) Calcium and ROS: A mutual interplay. *Redox Biol*. 6, 260–271
23. Rosengarth, A., and Luecke, H. (2003) A calcium-driven conformational switch of the N-terminal and core domains of annexin A1. *Journal of Molecular Biology*. 326, 1317–1325
24. Dubé, M., Etienne, L., Fels, M., and Kielian, M. (2016) Calcium-Dependent Rubella Virus Fusion Occurs in Early Endosomes. *J. Virol.* 90, 6303–6313
25. Sciacca, M. F. M., Milardi, D., Messina, G. M. L., Marletta, G., Brender, J. R., Ramamoorthy, A., and La Rosa, C. (2013) Cations as Switches of Amyloid-Mediated Membrane Disruption Mechanisms: Calcium and IAPP. *Biophys. J.* 104, 173–184
26. Drew, D. E., Heijne, von, G., Nordlund, P., and de Gier, J. W. (2001) Green fluorescent protein as an indicator to monitor membrane protein overexpression in Escherichia coli. *FEBS Lett.* 507, 220–224
27. Schanda, P., Kupče, Ē., and Brutscher, B. (2005) SOFAST-HMQC Experiments for Recording Two-dimensional Deteronuclear Correlation Spectra of Proteins within a Few Seconds. *J. Biomol. NMR*. 33, 199–211
28. Schanda, P., Van Melckebeke, H., and Brutscher, B. (2006) Speeding Up Three-Dimensional Protein NMR Experiments to a Few Minutes. *J. Am. Chem. Soc.* 128, 9042–9043
29. Veatch, S. L. (2007) Electro-formation and fluorescence microscopy of giant vesicles with coexisting liquid phases. *Methods Mol. Biol.* 398, 59–72
30. Manley, S., and Gordon, V. D. (2008) Making giant unilamellar vesicles via hydration of a lipid film. *Curr Protoc Cell Biol*. Chapter 24, Unit 24.3–24.3.13

ChemComm

COMMUNICATION

View Article Online
View Journal | View Issue

Check for updates

Cite this: *Chem. Commun.*, 2020, **56**, 11665

Received 20th May 2020,
Accepted 25th August 2020

DOI: 10.1039/d0cc03612a

rsc.li/chemcomm

A quantitative assay to study the lipid selectivity of membrane-associated systems using solution NMR†

Encarnacion Medina-Carmona,[ab] Lorena Varela,[a] Alex C. Hendry,[a] Gary S. Thompson,[a] Lisa J. White,[c] Jessica E. Boles,[c] Jennifer R. Hiscock[c] and Jose L. Ortega-Roldan*[a]

The activity of membrane proteins and compounds that interact with the membrane is modulated by the surrounding lipid composition. However, there are no simple methods that determine the composition of these annular phospholipids in eukaryotic systems. Herein, we describe a simple methodology that enables the identification and quantification of the lipid composition around membrane-associated compounds using SMA-nanodiscs and routine ^{1}H–^{31}P NMR.

The structure and function of membrane proteins, synthetic channels and any membrane-associated compound can be influenced by the lipid environment, yet the precise composition of lipids surrounding them is often difficult to discern.[1,2] Additionally, understanding lipid specificity in biological membranes is crucial for the understanding of the modulation of membrane protein activity in cells as well as for the design and development of chemical molecules that interact with biological membranes such as antimicrobials, carriers, or synthetic channels.[3,4]

Two different classes of lipids can be identified around membrane-embedded systems: (1) non-annular lipids are those tightly bound to cavities in the hydrophobic regions of the protein (or compound) and are non-exchangeable. Non-annular lipids can be resistant to membrane solubilisation by harsh treatment with detergent micelles and, in the case of integral membrane proteins, could be subsequently detected by co-crystallisation or native mass spectrometry.[5,6] (2) Annular lipids constitute the first layer of lipids surrounding the membrane-bound system and have restricted mobility compared to bulk lipids, but may exchange with the bulk lipids of the membrane. The detection of annular lipids is not possible for membrane-bound systems extracted in detergent micelles, and their influence is commonly assayed using reconstituted vesicles of different lipid compositions.[6,7] It is generally assumed that membrane-bound systems will be surrounded by those lipids that render their maximal activity.[5] However, this approach does not enable the study of lipid selectivity by membrane proteins or membrane-interacting compounds in their host biological membranes, and is not sensitive to alterations in the specific lipid composition of the annular and non-annular lipids surrounding membrane-bound compounds.

The development of native styrene–maleic acid copolymer (SMA) nanodiscs has enabled the extraction of membrane-associated compounds from native membranes.[8,9] SMA nanodiscs have been shown to maintain many desirable physical properties of the membrane bilayer, such as lipid phase transition temperatures and lipid bilayer thickness.[10,11] Recently, new families of SMA have also been developed expanding the range of conditions in which this type of membrane mimetic can be utilised.[12] In addition, the use of nanodiscs has been shown to be a useful tool for studying the chemical interactions between small molecules and the phospholipid bilayer, which is of great importance for the development of novel pharmaceuticals, drug delivery systems, synthetic membrane transporters or ion channel technologies.[13] The combination of SMA solubilisation with thin layer chromatography and mass spectrometry has allowed the identification of lipids co-extracted with different membrane proteins, in bacterial systems and simple lipid mixtures.[14–16] However, such approaches are not easily applicable to eukaryotic membranes due to the complexity of their phospholipid composition, also they do not allow for lipid quantification without the addition of non-natural lipid internal standards for each lipid analysed.

Herein, we present an easily accessible solution state NMR methodology that allows the identification and quantification of the specific phospholipid headgroup composition around membrane-associated systems in their natural lipid environment.

[a] *School of Biosciences, University of Kent, Canterbury, CT2 7NJ, UK. E-mail: J.L.Ortega-Roldan@kent.ac.uk; Tel: +44 (0)1227 824730*
[b] *Departamento de Quimica-Fisica, Facultad de Ciencias, Universidad de Granada, Granada 18010, Spain*
[c] *School of Physical Sciences, University of Kent, Canterbury, CT2 7NJ, UK*

† Electronic supplementary information (ESI) available: This includes experimental details and NMR spectroscopy data. See DOI: 10.1039/d0cc03612a

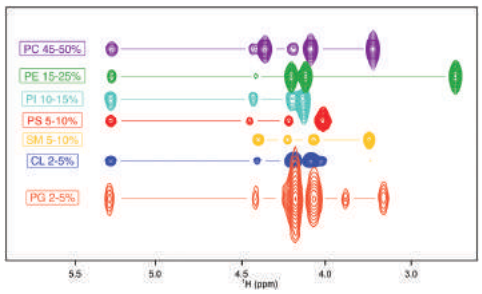

Fig. 1 Overlay of ^{1}H fingerprints of standard mammalian phospholipids from ^{1}H–^{31}P HSQC spectra arranged by abundance[1] from the most abundant (top) to the least (bottom). PC (purple), PE (green), PI (cyan), PS (red), SM (yellow), CL (dark blue) and PG (orange). The spectra were collected in in 75% $CDCl_3$, 25% MeOD, and 0.05% TMS.

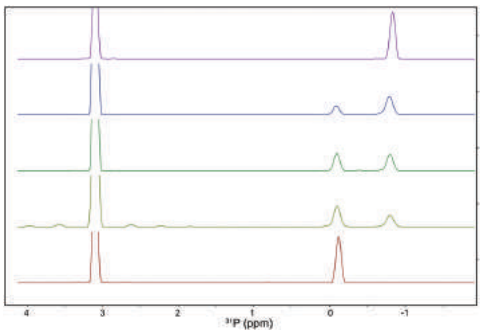

Fig. 2 ^{31}P 1D skyline projections from ^{1}H–^{31}P HSQC spectra of samples containing mixtures PC : PE in the ratios 100 : 0% (top), 72 : 28%, 50 : 50%, 33 : 66%, and 0 : 100% (bottom).

This can be applied to both membrane-associated and transmembrane proteins, synthetic channels, or generally to any compounds tightly associated to any phospholipid membrane.

This methodology combines an extraction step using SMA-nanodiscs with a simple ^{1}H–^{31}P NMR experiment that allows both the identification and quantification of lipid headgroups present in the mixture (including annular lipids). Phosphorus NMR is routinely used for determination and quality control of phospholipids. However, ^{31}P NMR experiments are insensitive and display a narrow dispersion of the lipid NMR resonances. To alleviate both problems, we turned to a proton start ^{1}H–^{31}P HSQC (ESI†).

Firstly, we collected ^{1}H–^{31}P HSQC spectra of the most common lipids that form the biological membranes (Fig. S1, ESI†) and which have at least one phosphorus molecule in their headgroup (dimyristoyl phosphatidyl choline (PC), palmitoyloleoyl phosphatidyl ethanolamine (PE), dipalmitoyl phosphatidyl serine (PS), soy phosphatidyl inositol (PI), brain sphingomyelin (SM), egg phosphatidyl glycerol (PG) and cardiolipin (CL) (Fig. S2–S8 respectively, ESI†). Each lipid shows a unique ^{1}H resonance pattern irrespective of its acyl chain (Fig. 1) that allows for the correct headgroup identification.

Phosphorus chemical shifts have already been used for phospholipid identification,[17–19] however we detected a linear dependence of ^{31}P chemical shifts of each individual lipid with the total lipid concentration. This is likely due to crowding effects which prevents lipid identification based solely on ^{31}P chemical shifts in complex lipid mixtures (Fig. S9–S12, ESI†). The combination of both ^{1}H and ^{31}P resonances provide unique patterns that enable the identification of all the lipids in our library by comparison with the ^{1}H resonances and the expected ^{31}P chemical shifts in complex phospholipid mixtures, such as eukaryotic membranes (Fig. S13, ESI†).

Relative lipid quantification was then carried out using the ^{31}P 1D skyline projection of the ^{1}H–^{31}P HSQC spectra, where every point has the highest intensity of all points of the corresponding orthogonal ^{1}H traces in the 2D spectrum, used due to its high sensitivity and ease of use. Absolute areas were calculated and normalised against the integral of trimethyl phosphate (TMP) as an internal standard, enabling the quantification of the relative proportions of each phospholipid component in the mixture. To validate this method, five samples with known concentrations of PC and PE lipids were prepared and the relative concentrations of both phospholipids were determined (Fig. 2). Linear fitting of the data showed excellent accuracy, with a slope of 0.9966 and a correlation coefficient (R) of 0.9999 (Fig. S20, ESI†). We verified our NMR-based identification and quantification with a commercial *Escherichia coli* (*E. coli*) lipid extract and with eukaryotic lipid mixtures extracted from Colo-680N cell lines (Fig. S13 and S14, ESI†). In all cases, our calculated compositions correlate well with experimentally derived compositions.[1]

To study the lipid selectivity of membrane-associated systems, we devised a strategy where purified proteins or membrane-associated compounds are incorporated into lipid vesicles from their host cell type or containing lipid mixtures of a desired composition and extracted using SMA. For SMA extraction, the vesicles are incubated with 2% SMA, dialysed and purified using a native chromatography technique. Size exclusion chromatography was used to separate empty or loaded SMA-nanodiscs and any free SMA (Fig. S15, ESI†). Moreover, we observed that in the presence of an excess of membrane-associated compound the SMA nanodiscs eluted at a lower retention volume, suggesting that they are predominantly loaded. The relevant empty or loaded SMA nanodisc fractions are then subjected to the Folch lipid extraction method,[20] with the lipids then dried under a nitrogen stream. The dried lipids were then resuspended in a 1 : 1 $CDCl_3$: MeOD-d_4 solvent mixture, with the reference compound TMP. A ^{1}H–^{31}P-HSQC spectrum was then collected. To rule out any influence of SMAs on the lipid composition, we compared the lipid composition of empty SMA nanodiscs against the original vesicles. No significant differences were observed, confirming the suitability of our approach (Fig. S16, ESI†).

For this proof of principle study, we studied the lipid composition surrounding a membrane-associated protein, the

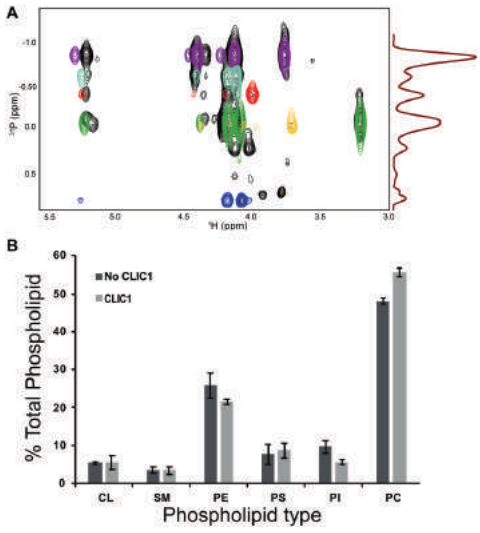

Fig. 3 (A) Overlay of ^{31}P HSQC spectra of phospholipids extracted from CLIC1-containing SMA nanodiscs formed with COLO-680N cells lipid extract (black) and the reference lipids overlaid based on the ^{1}H patterns (PC = purple, PE = green, PI = light blue, PS = red, SM = yellow, cardiolipin = dark blue). (B) Differences in total phospholipid composition between samples with and without CLIC1 (n = 3).

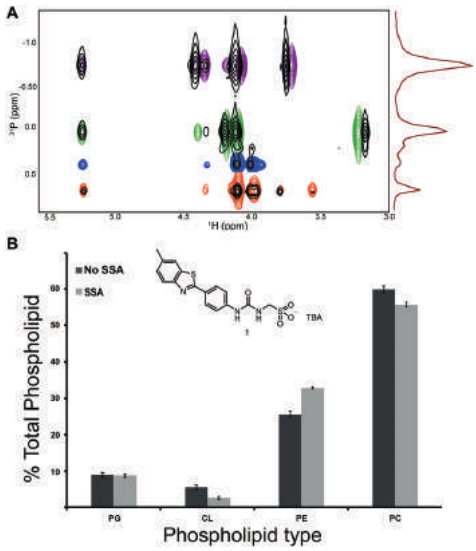

Fig. 4 (A) Overlay of ^{31}P HSQC spectra of phospholipids extracted from SSA compound 1-containing SMA nanodiscs formed with *E. coli* lipid extract mixed with DMPC (2 : 3) (black) and the reference lipids overlaid based on the ^{1}H patterns (PC = purple, PE = green, PI = light blue, PS = red, SM = yellow, cardiolipin = dark blue). (B) Differences in total phospholipid composition between samples with and without SSA (ESI†) (n = 3). The chemical structure of SSA compound 1 is included. TBA = tetrabutylammonium.

chloride intracellular channel-1 (CLIC1) and a membrane-associated compound, a representative compound from a novel class of supramolecular self-associating amphiphile (SSA) with antimicrobial activity.[21] CLIC1, a member of the CLIC family of proteins, is expressed as a soluble protein in human cells, but inserts in the membrane through interaction with divalent cations, forming a chloride channel.[22–24] This chloride channel form is upregulated in different types of cancers including glioblastoma and promotes tumour invasiveness and metastasis.[25,26] The chloride efflux activity has been shown to be modulated by the lipid composition, with maximum chloride efflux in soybean lipid extract, enriched with PC and PE lipids.[23] A high chloride efflux activity of CLIC1 in the plasma membrane has been associated with disease states, and therefore we questioned if the cells would tune CLIC1 to give maximal activity or would rather regulate it to lower levels.[27]

We assayed the lipid selectivity of CLIC1 in eukaryotic membranes. The vesicles formed with lipids extracted from eukaryotic membranes were incubated with purified CLIC1 or buffer, and subsequently extracted with SMAs. The empty and protein containing SMA-nanodiscs were purified as described above. The lipids contained in the discs were extracted and assayed by ^{1}H–^{31}P HSQC NMR. The analysis of these samples showed differences in the total distribution of lipids due to the presence of CLIC1 (Fig. 3). These results provide an indication of the lipid selectivity of CLIC1 close to physiological conditions, with a 7.5% change in PC and 4% change in PE and PI, which supports the idea that CLIC1 is not regulated to its maximum activity despite its lipid selectivity. Furthermore, the sensitivity of the method allows the detection of a small preference for certain types of phospholipids by CLIC1.

We then applied this novel assay to ascertain the selectivity of non-protein compounds for different types of phospholipid headgroups. We previously showed a compound from the antimicrobial agent SSA library to have higher affinity towards SMA nanodiscs derived from *E. coli* phospholipids over those derived from DMPC-mimicking a general human cell surface.[13] Following an analogous approach to that described previously, but instead incubating this SSA with a mixture of *E. coli* total lipid extract and DMPC in a 2 : 3 ratio, followed by SMA extraction. Phospholipid headgroup analysis indicated an enrichment of 6% in PE lipids at the cost of a decrease in the content of DMPC (Fig. 4), in agreement with previous results. It is hypothesised that quantifying these molecular level interactions will enable the tuning of this SSA technology towards bacterial, over eukaryotic cell membranes, reducing the potential for these SSAs to illicit toxic effects when supplied to a system *in vivo*.

In summary, we present a simple methodology that enables, for the first time, the identification and quantification of small differences in the phospholipid composition of any type of biological membrane, including complex eukaryotic phospholipid mixtures, induced by the lipid selectivity of either

membrane-associated proteins or synthetic compounds. Due to the sensitivity of the ^{1}H–^{31}P-HSQC, sub-milligram amounts of proteins or chemical compounds and lipids are sufficient. This method also allows the identification of other types of phospholipids, provided that the ^{1}H–^{31}P resonances are known, although is insensitive to different acyl chains or to lipids not containing phosphorus groups. Furthermore, this strategy can be an excellent resource for the design and development of chemical molecules that interact with biological membranes such as antimicrobials, carriers, or synthetic channels.

The authors would like to acknowledge Dr Timothy Knowles (University of Birmingham) for his assistance with this work. The authors would also like to thank the following organisations for funding this work: the Wellcome Trust (207743/Z/17/Z), the Royal Society (RGS\R1\191414) and Public Health England (JEB PhD studentship).

Conflicts of interest

There are no conflicts to declare.

Notes and references

1 P. V. Escribá, X. Busquets, J. Inokuchi, G. Balogh, Z. Török, I. Horváth, J. L. Harwood and L. Vígh, *Prog. Lipid Res.*, 2015, **59**, 38–53.
2 A. Laganowsky, E. Reading, T. M. Allison, M. B. Ulmschneider, M. T. Degiacomi, A. J. Baldwin and C. V. Robinson, *Nature*, 2014, **510**, 172–175.
3 P. Maturana, M. Martinez, M. E. Noguera, N. C. Santos, E. A. Disalvo, L. Semorile, P. C. Maffia and A. Hollmann, *Colloids Surf., B*, 2017, **153**, 152–159.
4 M. Zhang, P.-P. Zhu, P. Xin, W. Si, Z.-T. Li and J.-L. Hou, *Angew. Chem., Int. Ed.*, 2017, **56**, 2999–3003.
5 C. Schölz, D. Parcej, C. S. Ejsing, H. Robenek, I. L. Urbatsch and R. Tampé, *J. Biol. Chem.*, 2011, **286**, 13346–13356.
6 J. A. Poveda, A. M. Giudici, M. L. Renart, M. L. Molina, E. Montoya, A. Fernández-Carvajal, G. Fernández-Ballester, J. A. Encinar and J. M. González-Ros, *Biochim. Biophys. Acta, Biomembr.*, 1838, **2014**, 1560–1567.
7 A. G. Lee, *Biochim. Biophys. Acta, Biomembr.*, 2004, **1666**, 62–87.
8 K. S. Simon, N. L. Pollock and S. C. Lee, *Biochem. Soc. Trans.*, 2018, **46**, 1495–1504.
9 J. M. Dörr, S. Scheidelaar, M. C. Koorengevel, J. J. Dominguez, M. Schäfer, C. A. van Walree and J. A. Killian, *Eur. Biophys. J.*, 2016, **45**, 3–21.
10 P. Angelisová, O. Ballek, J. Sýkora, O. Benada, T. Čajka, J. Pokorná, D. Pinkas and V. Hořejší, *Biochim. Biophys. Acta, Biomembr.*, 1861, **2019**, 130–141.
11 M. Jamshad, V. Grimard, I. Idini, T. J. Knowles, M. R. Dowle, N. Schofield, P. Sridhar, Y. Lin, R. Finka, M. Wheatley, O. R. T. Thomas, R. E. Palmer, M. Overduin, C. Govaerts, J.-M. Ruysschaert, K. J. Edler and T. R. Dafforn, *Nano Res.*, 2014, **8**, 774–789.
12 T. Ravula, N. Z. Hardin, S. K. Ramadugu, S. J. Cox and A. Ramamoorthy, *Angew. Chem., Int. Ed.*, 2018, **57**, 1342–1345.
13 G. Townshend, G. S. Thompson, L. J. White, J. R. Hiscock and J. L. Ortega-Roldan, *Chem. Commun.*, 2020, **56**, 4015–4018.
14 V. Schmidt, M. Sidore, C. Bechara, J.-P. Duneau and J. N. Sturgis, *Biochim. Biophys. Acta, Biomembr.*, 2019, **1861**, 431–440.
15 A. C. K. Teo, S. C. Lee, N. L. Pollock, Z. Stroud, S. Hall, A. Thakker, A. R. Pitt, T. R. Dafforn, C. M. Spickett and D. I. Roper, *Sci. Rep.*, 2019, **9**, 1–10.
16 I. Prabudiansyah, I. Kusters, A. Caforio and A. J. M. Driessen, *Biochim. Biophys. Acta, Biomembr.*, 2015, **1848**, 2050–2056.
17 B. Gouilleux, N. V. Christensen, K. G. Malmos and T. Vosegaard, *Anal. Chem.*, 2019, **91**, 3035–3042.
18 Y. B. Monakhova and B. W. K. Diehl, *Anal. Bioanal. Chem.*, 2018, **410**, 7891–7900.
19 J. Schiller and K. Arnold, *Med. Sci. Monit.*, 2002, **8**, MT205-22.
20 J. Folch, M. Lees and G. H. Sloane Stanley, *J. Biol. Chem.*, 1957, **226**, 497–509.
21 L. J. White, J. E. Boles, N. Allen, L. S. Alesbrook, J. M. Sutton, C. K. Hind, K. L. F. Hilton, L. R. Blackholly, R. J. Ellaby, G. T. Williams, D. P. Mulvihill and J. R. Hiscock, *J. Mater. Chem. B*, 2017, **8**, 7620–7630.
22 B. M. Tulk, P. H. Schlesinger, S. A. Kapadia and J. C. Edwards, *J. Biol. Chem.*, 2000, **275**, 26986–26993.
23 B. M. Tulk, S. Kapadia and J. C. Edwards, *Am. J. Physiol. Cell Physiol.*, 2002, **282**, C1103–C1112.
24 L. Varela, A. C. Hendry, D. Cantoni and J. L. Ortega-Roldan, *bioRxiv*, 2019, **275**, 638080.
25 M. Gritti, R. Würth, M. Angelini, F. Barbieri, M. Peretti, E. Pizzi, A. Pattarozzi, E. Carra, R. Sirito, A. Daga, P. M. G. Curmi, M. Mazzanti and T. Florio, *Oncotarget*, 2014, **5**, 11252–11268.
26 M. Setti, D. Osti, C. Richichi, B. Ortensi, M. Del Bene, L. Fornasari, G. Beznoussenko, A. Mironov, G. Rappa, A. Cuomo, M. Faretta, T. Bonaldi, A. Lorico and G. Pelicci, *Oncotarget*, 2015, **6**, 31413–31427.
27 T. Tang, X. Lang, C. Xu, X. Wang, T. Gong, Y. Yang, J. Cui, L. Bai, J. Wang, W. Jiang and R. Zhou, *Nat. Commun.*, 2017, **8**, 1–12.